

LIMITED SLIP BOLTED JOINTS - A DEVICE TO CONTROL
THE SEISMIC RESPONSE OF LARGE PANEL STRUCTURES

Avtar Singh Pall.

A Thesis
in
The Faculty
of
Engineering

Presented in Partial Fulfillment of the Requirements
for the Degree of Doctor of Philosophy

Centre for Building Studies
Concordia University
Montreal, Quebec, Canada
September, 1979

© Avtar Singh Pall, 1979

ABSTRACT

ABSTRACT

LIMITED SLIP BOLTED JOINTS - A DEVICE TO CONTROL
THE SEISMIC RESPONSE OF LARGE PANEL STRUCTURES

Avtar Singh Pall, Ph.D., Eng.
Concordia University, 1979

Large panel precast concrete structures offer many technical and economical advantages over conventional building methods. In seismic regions the construction of such structures is viewed with suspicion due to the serious problems posed by traditional jointing procedures. This can be overcome by the use of joints devised to dissipate energy. During severe seismic excitations, the limited slippage in the joints provides a potential for considerable energy dissipation and by locating these connections in the vertical joints only, serious deformations and damage can be avoided.

The present study is devoted to the development of limited slip bolted joints and the investigation of the seismic response of buildings using such joints. The results of nonlinear time history analyses have shown that energy dissipated by limited slip bolted joints can provide an improved solution to the problems engendered by severe ground motions. By using such joints the building can be "tuned" so as to obtain optimum seismic response. This is conveniently possible by selecting the appropriate slip load of the joint.

The concept of energy dissipating slipping joints can be easily extended to improve the seismic response of cast-in-place shear walled

structures and framed structures clad with precast architectural curtain walls. In effect, the proposed joints act as structural dampers and safety valves. In this manner the basic philosophy of building earthquake resistant structures can be raised from the present level of protecting human life by preventing collapse to that of minimum structural and secondary damage.

ACKNOWLEDGEMENTS

ACKNOWLEDGEMENTS

This research project was made possible through grants from Natural Sciences and Engineering Research Council of Canada, and La Formation de Chercheurs et d'Action Concertée du Québec. Thanks to Dr. Paul Fazio, Director of Centre for Building Studies, for arranging the financial support and for his continued interest and encouragement.

The author is especially grateful to Professor Cedric Marsh for accepting the task of supervising the direction, organization and scope of this investigation and wishes to sincerely thank him for his guidance, criticism, corrections and willingness to contribute to this research.

The author also wishes to thank Dr. Zenon A. Zielinski, Dr. Oscar A. Pekau and Prof. William F. Dawson of Concordia University and Dr. James M. Becker of Massachusetts Institute of Technology for their interest in this study.

Coöperation of the local industries in the fabrication of test specimens, and assistance of M/s. J. Zilka and A. Clarke during experimental work is gratefully acknowledged. Thanks are also due to Mrs. Laila Hussein for the typing of this thesis.

A special thanks is extended to my understanding wife, Tripat, for her encouragement, interest and psychological support, and finally to my children, Rashmi and Sonu for their extreme patience.

In Memory of My Father, Dr. Shamsher Singh Pall.

TABLE OF CONTENTS

TABLE OF CONTENTS	PAGE
ABSTRACT	i
ACKNOWLEDGEMENTS	iii
LIST OF TABLES	x
LIST OF FIGURES	xif
NOMENCLATURE	xvii
I INTRODUCTION	1
1.1 Large Panel Concrete Structures	2
1.2 Structural Behaviour	3
1.3 Seismic Implications	5
1.4 Energy Dissipation Mechanism	7
1.5 Object of the Research Project	10
1.6 Organisation of the Text	10
II DEVELOPMENT OF THE LIMITED SLIP BOLTED JOINT	14
2.1 Structural Functions of a Vertical Joints	14
2.2 Design Criteria	15
2.3 State-of-Art, Vertical Joint	17
2.3.1 Wet Joints	17
2.3.1.1 Plain Joints	17
2.3.1.2 Grooved Joints	18
2.3.1.3 Keyed Joints	18
2.3.2 Dry Joints	19
2.3.3 Discussion of Performance	20
2.3.4 Descon-Concordia Mechanical Joints	21
2.4. Design Approach	22

	PAGE
2.5 Limited Slip Bolted Joints	23
2.6 Extension of Concept	24
2.6.1 Cast-in-place Shear Walls	24
2.6.2 Framed Buildings clad with Architectural Curtain Walls	25
2.7 Summary	26
 III LABORATORY TESTS AND RESULTS	 32
3.1 Past Research	32
3.2 Test Program	34
3.3 Details of Test Specimen	35
3.3.1 Description of Specimen	35
3.3.2 Materials	36
3.3.3 Surface Finishes	36
3.3.4 Assembly	38
3.4.1 Load Calibration of Bolt	38
3.4.2 Loading Machine	40
3.4.3 Static Tests	41
3.4.4 Dynamic Cyclic Tests	41
3.5 Analysis of Experimental Results	42
3.5.1 Static Tests	42
3.5.2 Dynamic Cyclic Tests	44
3.5.3 Creep in Brake Lining Pads	48
3.6 Practical Considerations in Application	49
3.6.1 Surface Finish	49
3.6.2 Installation Procedures	50
3.6.3 Inspection	53

	PAGE
3.6.4 Losses in Bolt tension	53
3.6.5 Reuse of Bolts	54
3.6.6 Use of Washers	55
3.6.7 Evaluation of Slip Load	56
3.6.8 Joint Stiffness	56
3.7 Summary	57
IV MODELING PROCEDURE AND ANALYSIS	75
4.1 Methods of Structure Idealization	76
4.1.1 Beam Model	76
4.1.2 Continuous Medium Method	77
4.1.3 Frame Analogy Method	78
4.1.4 Finite Element Method	79
4.2 Choice of Model	80
4.3 Seismic Analysis	82
4.3.1 Nonlinear Time History Dynamic Analysis ..	82
4.3.2 Time Step	84
4.3.3 Damping	84
4.3.4 Input Motion	85
4.4 Computer Program	87
4.5 Modeling	87
4.5.1 Selection of a Building	87
4.5.2 General Modeling Assumptions	82
4.5.3 Modeling of Panel Walls	90
4.5.4 Modeling of Limited Slip Bolted Joints ...	91
4.5.5 Seismic Input	93

	PAGE
4.6 Preliminary Analysis	94
4.7 Summary	97
V PARAMETRIC STUDIES AND OPTIMIZATION	105
5.1 Factors Affecting Seismic response	105
5.2 Parametric Studies	108
5.3 Effect of Restricted Slot Length	109
5.3.1 10 Story Building	109
5.3.2 20 Story Building	110
5.4 Effect of Initial Stiffness of the Joint	111
5.5 Effect of Slip Load on Building Response	112
5.5.1 5 Story Building	113
5.5.2 10 Story Building	114
5.5.3 15 Story Building	114
5.5.4 20 Story Building	115
5.6 Comparison of LSB Jointed Walls with Isolated and Monolithic Walls	115
5.6.1 Story Shears	115
5.6.2 Bending Stresses in Panels	116
5.6.3 Building Deflections	116
5.6.4 Time Histories	117
5.7 Summary	118
VI APPROXIMATE APPROACH TO NONLINEAR ANALYSIS	173
6.1 Reserve Energy Technique	173
6.2 Energy Approach for Optimum Slip Load of Joint..	176

	PAGE
6.3 Analysis Using the Reserve Energy Technique	180
6.4 Discussion of Results	181
6.5 Equivalent Ductility	182
6.6 Summary	183
VII CONCLUSIONS AND RECOMMENDATIONS	189
7.1 Conclusions	189
7.2 Recommendations for Future Studies	194
REFERENCES	197
APPENDIX A.1 Properties of Wall and LSB Joint	204
A.2 Listing of Modified Subroutines	205
A.3 Print out of Beam Column Specifications	217
A.4 Description of Input Data for LSB Joint	218
A.5 Print out of LSB Joint Specifications	219
A.6 Output Results of LSB Joint	220
A.7 Quasi Static Analysis for Seismic Forces	226
APPENDIX B.1 Magnification Factor for Work Capacity of a Story in Reserve Energy Technique	230
B.2 Member Stiffness Matrices	232
B.3 Equivalent Ductility of LSB Jointed Walls.....	233

LIST OF TABLES

LIST OF TABLES

NUMBER	DESCRIPTION	PAGE
3.1	Test Specimens	59
3.2	Slip Coefficients, Static Test, Specimen type A ..	60
3.3	Slip Loads, Static Tests, Specimen type B & C	61
3.4	Dynamic Slip Coefficients, Specimen type A	62
3.5	Energy Dissipation, Specimen type A	64
3.6	Average Slip Coefficients	66
3.7	Average Dynamic Slip Loads of LSB Joints	67
5.1	Effect of Restricted Slip Length and Initial Joint Stiffness on Building Response, 0.25 g	119
5.2	Bending Moments, Axial Coupling Force, Maximum Stresses - 5 Story Building	120
5.3	Bending Moments, Axial Coupling Force, Maximum Stresses - 10 Story Building	122
5.4	Bending Moments, Axial Coupling Force, Maximum Stresses - 15 Story Building	124
5.5	Bending Moments, Axial Coupling Force, Maximum Stresses - 20 Story Building	126
5.6	Building Deflection, Connection Slippage and Story Shears - 5 Story Building	128
5.7	Building Deflection, Connection Slippage and Story Shears - 10 Story Building	130
5.8	Building Deflection, Connection Slippage and Story Shears - 15 Story Building	132
5.9	Building Deflection, Connection Slippage and Story Shears - 20 Story Building	134

NUMBER	DESCRIPTION	PAGE
5.10	Net Stresses at Base, 0.33 g	136
5.11	Fundamental Periods of Vibration	137
7.1	Reduction in Response Using LSB Joints	196

LIST OF FIGURES

LIST OF FIGURES

FIGURE	DESCRIPTION	PAGE
1.1	Structural System - Large Panel Construction	12
1.2	Types of Joints in Large Panel Buildings	13
1.3	Modes of Deformation	13
2.1	Forces on Vertical Joints	27
2.2	Influence of Joint on Wall Behaviour	27
2.3	Ideal Behaviour of Vertical Joint	28
2.4	Details of Wet Vertical Joints	28
2.5	Effect of Castellations on Ultimate Strength	28
2.6	Hysteresis Loop of Lock Joint	28
2.7	Dry Vertical Joints	29
2.8	Hysteresis Loop, Welded Headed Stud Connection	29
2.9	Load-Displacement Curve, Slab-to-Slab Joint of Descon System	29
2.10	Wall-to-Wall Joint	30
2.11	Corner Wall-to-Wall Joint	30
2.12	Details of Location Pin	31
2.13	LSB Joints for Cast-in-place Shear Walls	31
3.1	Details of Test Specimen	68
3.2	Bolt Calibration Cell	69
3.3	Bolt Calibration Procedure	69
3.4	Load Calibration Curve for Bolt of Specimen-A	69
3.5	Instron Machine, Testing Specimen type A	70

FIGURE	DESCRIPTION	PAGE
3.6	Reaction Frame	70
3.7	Testing Specimen Type B Using Reaction Frames	70
3.8	Load-Displacement Curve, Wall-to-Wall Joint	71
3.9	Behaviour of Specimen type B	71
3.10	Hysteresis Loops, Wall-to-Wall Joint	72
3.11	Load-Displacement Curve, Specimen types B & C	73
3.12	Surface Condition after 20 Cycles	73
3.13	Joint Stiffness	74
4.1	Structural Idealization	98
4.2	Peaking type and Broad Band Spectrums	99
4.3	Relative Velocity Response Spectra for Different Normalized Input Motions	99
4.4	Typical Panelized Apartment Building	100
4.5	Structure Idealization	100
4.6	Load-Deformation of LSB Joint	100
4.7	Equivalent Truss Element Properties	101
4.8	Decomposition of Trilinear Relationship into Three Components	101
4.9	Story Shear Envelopes	102
4.10	Forces in Joints	102
4.11	Building Deflection Envelopes	103
4.12	Stresses in Panels	103
4.13	Ground Motion History, El Centro, 1940 N.S Component (First Seven Seconds only)	104

FIGURE	DESCRIPTION	PAGE
4.14	Typical Time Histories, Top Story, 10 Story Building	104
4.15	Typical Time Histories, Top Story, 15 Story Building	104
5.1	Natural Frequency of LSB Jointed Wall	138
5.2	Effect of Slip Load on Load-Deformation Characteristics of Coupled Walls	138
5.3	Effect of Slip Load on Hysteretic Behaviour of Coupled Walls	138
5.4	El Centro Response Spectrum, N.S Component	139
5.5	Slip Load - Stress Relation, 5 Story Building	140
5.6	Slip Load - Stress Relation, 10 Story Building	141
5.7	Slip Load - Stress Relation, 15 Story Building	142
5.8	Slip Load - Stress Relation, 20 Story Building	143
5.9	Effect of Slip Load on Stresses, 0.33g	144
5.10	Effect of Slip Load on Building Deflection, 0.33g ..	145
5.11	Story Shear Envelope, 5 Story Building	146
5.12	Story Shear Envelope, 10 Story Building	147
5.13	Story Shear Envelope, 15 Story Building	148
5.14	Story Shear Envelope, 20 Story Building	149
5.15	Stresses in Panels, 5 Story Building	150
5.16	Stresses in Panels, 10 Story Building	151

FIGURE	DESCRIPTION	PAGE
5.17	Stresses in Panels, 15 Story Building	152
5.18	Stresses in Panels, 20 Story Building	153
5.19	Deflection Envelope, 5 Story Building	154
5.20	Deflection Envelope, 10 Story Building	155
5.21	Deflection Envelope, 15 Story Building	156
5.22	Deflection Envelope, 20 Story Building	157
5.23	Effect of LSB Joint on Bending Stress, 0.33g	158
5.24	Effect of LSB Joint on Building Deflection, 0.33g ...	158
5.25	Effect of Slip Load on Overturning Moments, 0.33g	159
5.26	Net Stresses at Base, 0.33g	160
5.27	Time History, 10 Story Building, Top Deflection, 0.25g	161
5.28	Time History, 10 Story Building, Top Deflection, 0.33g	162
5.29	Time History, 10 Story Building, Top Deflection, 0.5g	163
5.30	Time History, 15 Story Building Top Deflection, 0.25g	164
5.31	Time History, 15 Story Building, Top Deflection, 0.33g	165
5.32	Time History, 15 Story Building, Top Deflection, 0.5g	166
5.33	Time History, 20 Story Building, Top Deflection, 0.25g	167
5.34	Time History, 20 Story Building, Top Deflection, 0.33g	168

FIGURE	DESCRIPTION	PAGE
5.35	Time History, 20 Story Building, Top Deflection 0.5g	169
5.36	Time Histories, Top Connection, 10 Story Building ...	170
5.37	Time Histories, Top Connection, 15 Story Building	171
5.38	Time Histories, Top Connection, 20 Story Building	172
6.1	Conceptual Model, Reserve Energy Technique	184
6.2	General Construction of Force-Deformation Diagram of a Story	184
6.3	Optimization of Slip Load, Simple Walls	185
6.4	Story Shear Envelope, 15 Story Building	185
6.5	Typical Load-Displacement Diagram, 15 Story Building for 11th Story	186
6.6	Energy Reconciliation at 1st Story, 15 Story Building	186
6.7	Deflection Envelopes	187
6.8	Energy Dissipation by Joints at Different Stories....	188
6.9	Total Energy Dissipated by Joints	188
6.10	Deformation in Joints, 0.25g, for 15 Story Building..	188

NOTATIONS

NOTATIONS

a, b	Dimensions of the member
A	Cross-sectional area
A_b	Nominal cross-sectional area of bolt
A_s	Effective shear area
C	Damping coefficient
E	Modulus of elasticity; Energy
E_k	Kinetic energy
E_s	Strain energy
E_d	Energy dissipated by viscous damping; total energy demand in reserve energy technique
E_D	Energy dissipated by hysteretic damping
g	Acceleration due to gravity
G	Shear modulus
h	Height of member
H	Area of hump in Load-deformation Curve of reserve energy technique.
$[H]$	Transformation matrix
I	Moment of inertia
k	Member stiffness
k_d	Dynamic slip coefficient
k_s	Static slip coefficient
$[K]$	Stiffness matrix
l	Length of member
m	Number of slip planes
M	Moment; Mass

[M]	Mass matrix
n	Number of bolts; number of stories
P	Total force or load
P_d	Dynamic slip load
P_s	Slip load
P_y	Yield load
P_u	Ultimate Load
Prime	Denotes differentiation
q	Shear per unit length
R	Resistance of each bolt
S	Shear load
t	Thickness; time
T	Tension in bolt; natural period of vibration
u	Nodal displacement relative to ground
U	Strain energy; area of load - deformation curve in reserve energy technique
v	Spectral velocity
V	Volume of member; story shear
W	Weight of member
x	Ground displacement
α	Ratio of dynamic slip coefficient to static slip coefficient; acceleration
β	Degradation factor as applied to joints
α, β	Mass, stiffness dependent factors of damping
ℓ	Effective span length
Δ	Deformation
λ	Critical damping ratio
ω	Angular velocity or undamped natural circular frequency

γ	Deterioration factor as applied to reserve energy technique
Ω	Participation factor as applied to reserve energy technique
σ_b	Bending stress
σ_t	Stress due to coupling action of the joint
σ_o	Combined stress

CHAPTER I
INTRODUCTION

CHAPTER I

INTRODUCTION

Ground motions arising during earthquakes create oscillating lateral loads on the buildings, thereby causing them to sway back and forth with an amplitude proportional to the energy input. If some of this energy can be dissipated during the building motion, then the distress can be considerably reduced and structural collapse avoided during catastrophic earthquakes. In conventional buildings reliance is placed on the ductility of the structure, i.e. ability to dissipate energy while undergoing inelastic deformation. This is not available in large panel structures. Hence, the use of this popular building system is viewed with suspicion in seismic regions. The problems mainly converge to the role of joints, which are considered as planes of weakness in the structure. If these very planes of weakness are properly harnessed, they can be advantageously used in dissipating seismic energy for improving the seismic response of large panel buildings.

This chapter begins with a brief introduction to large panel structures, followed by the role of connections in structural behaviour and their seismic implications. Then, the energy dissipation mechanism is discussed with a possible solution to the problem. Finally, the objectives of the research project and the organization of the text are described.

1.1 LARGE PANEL CONCRETE STRUCTURES

Major developments in prefabricated concrete building systems occurred in Europe after World War II [1]. The severe housing shortage, lack of skilled labour and materials prompted the switch to industrialized housing. Short construction time is probably the most important advantage of prefabrication. By precasting the main parts of the structure, the amount of site labour is greatly reduced. Most of the work is done in a factory where it can be carried out more efficiently and independently of climatic conditions.

Large panel concrete construction is one of the most important areas in which industrialized building techniques have proved advantageous and has been the most popular form of construction for high rise apartment type buildings in Europe and the Soviet Union [2]. Encouraged by "Operation Breakthrough" 1969, in the United States, interest is now steadily growing in large panel structures in North America. Increasing labour and material costs are other factors likely to change the climate in favour of panelized buildings.

Briefly, in large panel construction, the structural system is composed of precast wall panels and precast floor or roof panels which are factory manufactured and assembled at site. The wall panels, 4 - 8 m. long, are of full story height, and the floor panels are 2 - 3 m. wide by 4 - 10 m. long. In this construction, there are basically three different arrangements differentiated by the layout of load bearing wall panels, namely, the cross wall system, the long wall system and the mixed wall system [3].

The cross wall system (Fig. 1.1a) offers greater freedom and variety in the architectural façade and is the most successful configuration. This form of construction however restricts the open plan and is most typically suited for multistory apartment housing, hotels, etc. where permanent partitions and the lack of flexibility for future modifications can be tolerated. The long wall system (Fig. 1.1b) on the other hand is more suitable for uses in hospitals, schools, offices, etc. The mixed wall system or two-way system is used for small-size apartments and is not very popular. The American panelized buildings differ from the European system to the extent that they use larger panels and thus have fewer joints.

1.2 STRUCTURAL BEHAVIOUR

In large panel structures, the interconnected floor and wall panels perform the dual function of carrying vertical loads as well as bracing the building against lateral loads arising from wind or seismic loads. The main structural difference between the precast large panel buildings and cast in place concrete buildings is the presence of joints. Under normal service load conditions, the behaviour of large panel structures is no different from cast in place structures as all parts of the structure are expected to be within the elastic range. The existence of many large panel structures have evidences that performance can be satisfactory under such conditions and they have not been a matter of any concern. At ultimate loads, however, there are radical behavioural differences due to cracking and yielding of connections. Quoting from Despeyroux :

"The connections constitute a large number of special points in a structure, and it has to be considered, on the one hand,

under what conditions their strength is ensured and, on the other, what deformations are produced when this strength is utilized. Obviously, the end restraints to which the structural members are subjected depend on the behaviour of the connections, and the slight deformations which the latter may allow are liable to produce considerable redistribution of forces and moments in all other parts of the structure. Thus the behaviour of the structure as a whole may turn out to be quite different from that of a monolithic system". [4]

This, however, contradicts the provisions of ACI-ASCE Committee 512 "Suggested Design of Joints and Connections in Precast Structural Concrete", which states :

"The strength of a partially completed or completed structure should be governed by the strength of the structural members rather than by the strength of the connections; the connections should not be weak links in the structure.

The ultimate strength capacity of the joints and connections should be at least 10% in excess of that required of the members connected". [5]

These provisions while not differentiating between precast large panel structural elements and framed type columns or beams are in reality applicable to only the latter category. In actual practice, the strength of the joint seldom exceeds the strength of the panel and in some cases it is as low as 50% of the panel strength [4, 6, 7, 8]. At ultimate loads, the overall behaviour of the panelized buildings is, therefore, mainly

dependent on the strength and stiffness of the joints which represent the weakest structural elements.

The gravity type joints, relying solely on compression and friction, may be satisfactory for normal service loads and moderate earthquakes but could shake apart under the dynamic action of severe earthquakes or abnormal loads. The jointing details and the importance of tensile continuity in large panel structures had not received much attention until 1968 when a gas explosion on the 18th floor of a 22-story apartment building triggered the progressive collapse of an entire corner of the Ronan Point building in London [9].

The design of connections, therefore, plays an important role and the success of any large panel building system can largely be measured by the successful performance of its connections.

1.3 SEISMIC IMPLICATIONS

During severe seismic excitations, the amount of energy fed into the structure may exceed its elastic strain energy capacity. To survive, the structure must, without undue damage, absorb all the energy imparted to it. The reconciliation of energy is achieved by mobilizing the energy absorbing capacity available through the process of inelastic deformations in ductile structures.

One of the main causes of hesitation in the adoption of large panel structures in certain regions had been the fear of their performance under severe seismic action. The fear stems from the fact that development of flexural ductility, as available to other steel or cast in place structures, is extremely difficult to achieve in panelized structures. Ductility

is considered to be an essential prerequisite for the survival of a structure in a major earthquake. Present seismic codes are based on the premise of ductility and lay penalties on structures not possessing adequate ductility, thus they are not directly applicable to the seismic analysis of large panel structures.

The development of panelized construction originally started in essentially non-seismic regions and in severe seismic regions their use was limited to low rise construction [7, 8]. On the other hand, such structures have been constructed in earthquake zones in the Soviet Union, Rumania, Cuba, Japan and their use is gradually spreading to other places [10, 11, 12]. This calls for a thorough theoretical and experimental investigation to understand the behaviour of large panel buildings so as to substantiate their seismic suitability.

Several full scale and large scale models of panelized buildings have been tested under simulated earthquake loads using explosions or shaking tables [6, 13, 14, 15]. All these tests have demonstrated that joints between the panels are the only locations to crack. Inspection of recent destructive earthquakes in Rumania, Venezuela and the Soviet Union [10, 16] has provided evidence that large panel buildings, designed for earthquake resistance, experience minimum distress. While other brick and framed building failed or were severely damaged, the joints between the panel were the only locations to develop cracks in the case of panelized buildings.

Large panel structures are thus seen to be capable of meeting the requirement of safety and damage control. The question then arises as to how these buildings, in which development of flexural ductility

is limited, could perform so well in catastrophic earthquakes. It would appear that it is the overall energy dissipating capability of the structure which is the key factor for its survival rather than merely the presence or absence of ductility. In the words of Despeyroux :

"At higher loads, prefabricated walls are found to be less rigid than monolithic walls because of the small additional deformations which occur in the joints; and associated with this, the prefabricated walls have a greater damping capacity, in as much as these deformations and the attendant frictional phenomena help to dissipate the energy. The degree of damping is about twice as high as that of monolithic walls.

Prefabricated walls are therefore to be considered better than monolithic walls as far as earthquakes are concerned" [4].

1.4 ENERGY DISSIPATION MECHANISM

The joints in large panel buildings are usually the weakest links and during actual and simulated earthquakes the damage has always been along the joints with little damage in the panels. Cracking and slipping along these planes of weakness is associated with energy dissipation, a process similar to energy absorption during inelastic yielding in ductile structures. Also, these natural planes of weakness are mainly responsible for introducing a nonlinear behaviour to the overall building system, the large panels themselves remaining in the elastic range. Thus

the connections are the main source of an energy dissipating mechanism and hence, these very planes of weakness if properly engineered, can be advantageously used for improving the seismic resistance of large panel buildings.

The challenge therefore lies not only in providing joints of sufficient strength but in maximizing the energy dissipating mechanism. In large panel construction there are basically three locations for the joints. These are the joints between floor panels, the horizontal joints between wall panels, and the vertical joints between wall panels (Fig.1.2).

As the forces within the floor diaphragms are small there is little probability of slippage or energy dissipation in the floor joints.

The horizontal joints between wall panels are not desirable locations for energy dissipation because sliding movements necessary for energy dissipation will cause inevitable destruction of the interfaces thus jeopardizing the structural integrity of this load carrying joint. Moreover, the deformations at the horizontal joint are of a permanent nature and may render the structure unserviceable following the earthquake (Fig.1.3b). A pure rocking type motion, i.e. opening and closing of joints, in a typical horizontal connection, even if post-tensioned, does not cause energy dissipation [7, 17]. Furthermore, the concentration of vertical and lateral forces at the corners of the panel (Fig.1.3c), associated with a rocking motion may cause failure in either the connection or the panel [8, 18].

The vertical joints between wall panels (Fig.1.3d), appear to be the most suitable source of energy dissipation. Unlike horizontal joints, the vertical joints after necessary slippage to dissipate energy,

will come back almost to their original alignment with little or no permanent deformations [19]. Also, when the vertical joints yield, the overall building rigidity reduces thereby lengthening the apparent fundamental period of the building. This uncoupling effect may be beneficial in certain cases in reducing lateral forces on the building. Even in extreme loading cases, the failure of a few joints is not likely to threaten the stability of the building as these are not the gravity load carrying joints.

The possible locations of these joints are : (a) continuous vertical joints in the end wall panels, (b) connections between corridor lintels, (c) at vertical right angle joints between panels eg. I or T sections, around elevator shafts and staircases. In North America, most of the apartment buildings use the so called American system which does not have vertical joints. This system not only loses the opportunity of energy dissipation through joint motion but is also undesirable from the point of view of resistance against progressive collapse. However, even with the American system, plans can be developed to introduce vertical joints, by means of which seismic energy can be dissipated.

Other researchers have also concluded that the vertical joints are the most logical choice. Muto's "slitted" shear walls, creating artificial joints in the otherwise rigid concrete infill panels [20], and energy dissipation through inelastic yielding of concrete lintel beams in coupled shear walls as proposed by Paulay [21] are based on a similar philosophy. As a result of extensive analytical studies carried out at MIT, Mueller and Becker [22] have also proposed the

philosophy of "strong horizontal joints and weak vertical joints" for large panel buildings, which is similar to the strong column, weak girder seismic design philosophy advocated for framed buildings.

1.5 OBJECT OF THE RESEARCH PROJECT

For the vertical joints to function as an efficient means of energy dissipation :

- (1) they must possess a nearly elasto-plastic behaviour;
- (2) they must possess reasonably stable hysteretic characteristics over a number of cycles of reversal as expected in a severe earthquake;
- (3) they must dissipate sufficient energy to relieve the structure from distress;
- (4) no permanent damage should be incurred.

A study of the different jointing systems being used presently indicates that none of them can meet all the above requirements. There is therefore a need to develop a jointing system which, while meeting the normal design criteria and functions, can provide a reliable means of energy dissipation during severe ground shakings. The necessity of developing such a joint has also been stressed by Mueller and Becker [22].

It is towards the development of such a jointing system that the present research project is directed.

1.6 ORGANIZATION OF TEXT

The thesis has been organized in the following manner :

In Chapter II, the state of the art and performance of existing jointing systems are discussed in relation to the desirable criteria for

an energy dissipating joint and a design approach is suggested to simulate an ideal elasto-plastic joint. Finally the details of the proposed limited slip joints are described.

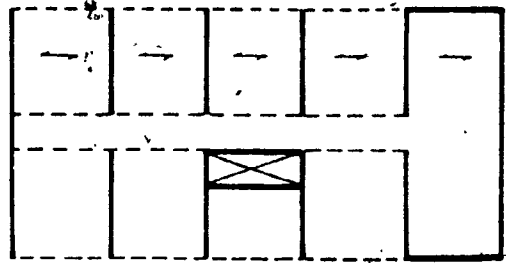
Chapter III deals with the laboratory tests conducted on specimens of Limited Slip Bolted (LSB) joints. The results and their applications are discussed.

Chapter IV is directed towards the mathematical modeling and seismic analysis of a typical panelized building using limited slip bolted joints. Results of preliminary analyses are discussed.

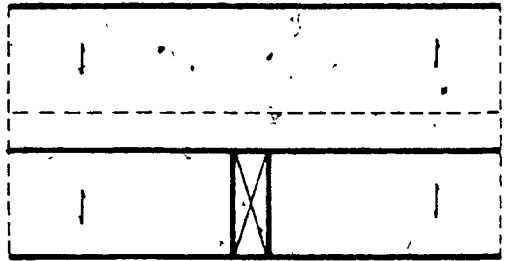
Chapter V deals with the important aspect of optimization of the joints to obtain minimum response. Results of parametric studies on 5, 10, 15 and 20 story buildings for seismic levels of 0.15, 0.25, 0.33 and 0.5 of gravity are reported in the form of curves and tables.

Chapter VI describes the approximate approach for nonlinear seismic analysis and for obtaining the optimum connection design.

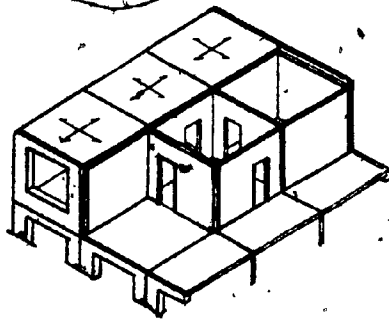
Finally, the conclusions of the investigation are summarized in Chapter VII. Recommendations for future studies are also suggested.



a) Cross Wall System



b) Long Wall or Spine Wall System



c) Two-way System

FIG. 1.1- STRUCTURAL SYSTEMS, LARGE PANEL CONSTRUCTION

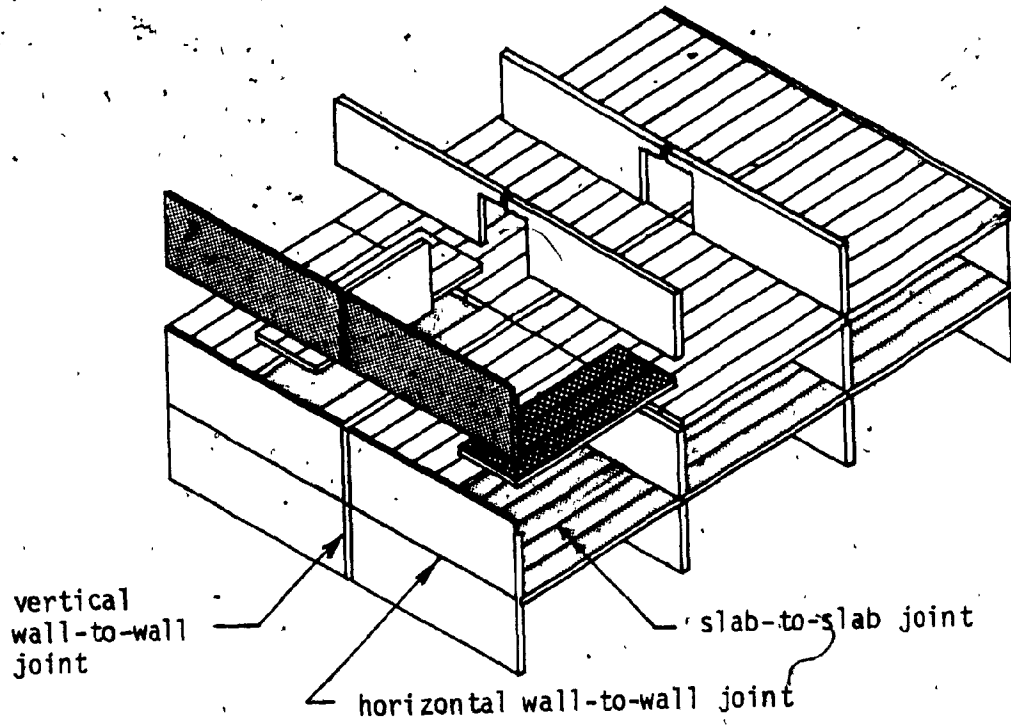


FIG. 1.2 - TYPES OF JOINTS IN LARGE PANEL BUILDING

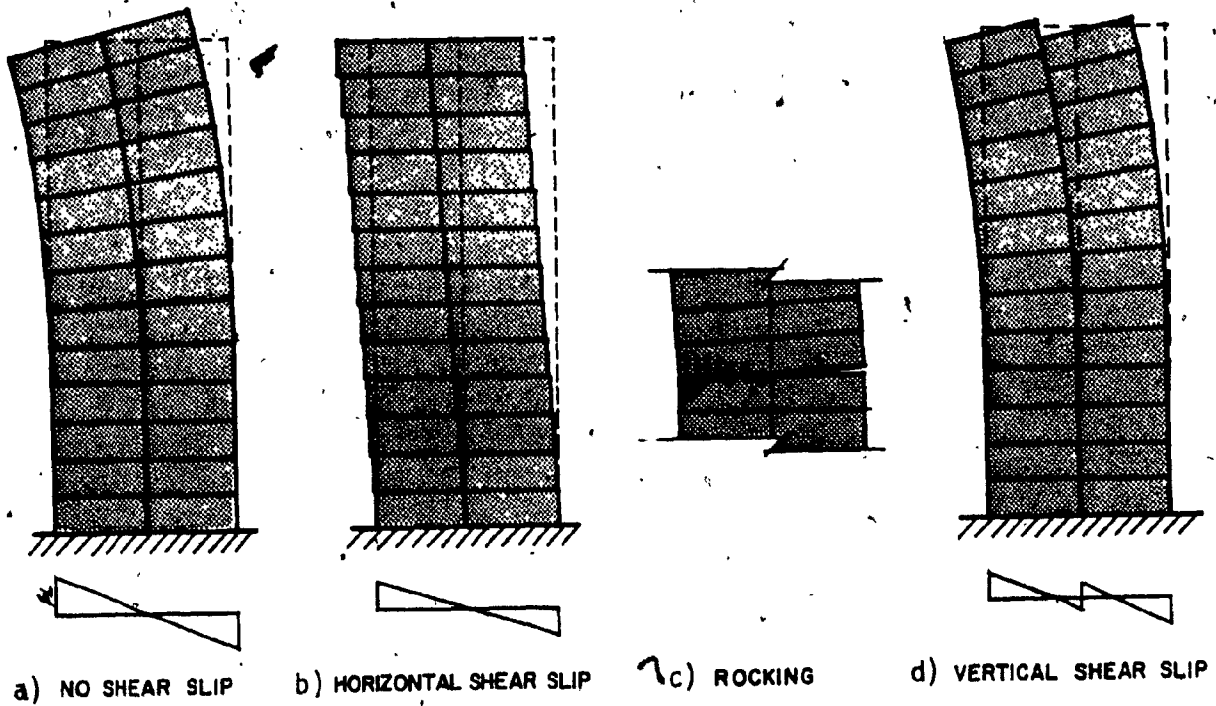


FIG. 1.3 - MODES OF DEFORMATION

CHAPTER II
DEVELOPMENT OF THE LIMITED SLIP BOLTED JOINT

CHAPTER II

DEVELOPMENT OF THE LIMITED SLIP BOLTED JOINT

Properly conceived and designed joints are essential to assure the satisfactory performance of panelized buildings. The three principal design considerations are : 1) structural purpose and expected performance; 2) strength and deformability; 3) economy in fabrication and erection procedures. The primary object of this study was to develop a vertical joint to provide an efficient source of energy dissipation, during severe seismic excitations, but not conflicting with the other requirements of a successful joint.

This chapter begins with an introduction to the nature of the forces and the structural functions of a vertical joint, and the criteria for the design of the joint. The existing systems for vertical joints are then reviewed in respect to these design criteria and finally the design philosophy and details of the proposed joint are described.

2.1 STRUCTURAL FUNCTIONS OF A VERTICAL JOINT

Before attempting to design any joint it is important to understand the nature of the forces which act and the influence of such actions on the behaviour of the structure. The forces acting at a vertical joint are shown in Fig. 2.1. These are :

- i) vertical shear forces as a result of lateral forces or due to differential movement or unequal loading of adjoining components (Fig. 2.1a);
- ii) horizontal tensile and tangential forces due to the buckling tendencies of adjoining walls, or to shrinkage and temperature

variations, or to wind suction (Figs. 2.1b and 2.1c);

iii) transverse shear due to lateral loads (Fig. 2.1d).

Of all of these forces the vertical shear at the joint, caused by lateral wind, seismic or abnormal loads, governs the design.

Under normal loads the structure and the joint are expected to remain within the elastic stage with a sufficient margin of safety. Under abnormal lateral loads, the strength and stiffness of the vertical joint significantly affect the behaviour of the walls. With joints of little stiffness, the wall will act as a series of individual cantilevers; with very stiff joints the wall becomes a single monolithic cantilever. The influence of varying the joint stiffness on stress distribution and deflections is shown in Fig. 2.2.

2.2 DESIGN CRITERIA

The criteria for an efficient energy dissipating vertical joint are discussed below:

- i) **Elasto-plastic behaviour :** This implies that the joint should yield at a known force level so that it can be designed for a predictable force without causing any damage to its anchors or surrounding concrete. An ideal load deformation curve for the joint is shown in Fig. 2.3a. The area of the hysteresis loop represents the energy dissipated per cycle. For a given maximum force in the connection, the energy dissipation is maximum when it is perfectly elasto-plastic (Fig. 2.3b).
- ii) **Stable hysteretic character :** During several cycles of load reversals, as expected in a severe earthquake, the joint should

show a reasonably stable, predictable behaviour. An appreciable degradation in strength and stiffness can adversely affect the seismic response of the building.

- iii) Ductility demands : The joint material should be able to undergo large displacements to meet seismic demands for energy dissipation.
- iv) No permanent damage : The joint which undergoes inelastic deformations to dissipate energy should not be damaged or should at least be repairable to face future earthquakes.

In addition to the above criteria, the following considerations should also be kept in mind :

- i) The ability to accommodate changes resulting from creep, shrinkage, and temperature variations.
- ii) Tensile continuity to ensure resistance against progressive collapse.
- iii) Ability to provide the necessary structural strength.
- iv) All weather construction.
- v) Feasibility of construction by moderately skilled personnel and use of minimum specialized equipment.
- vi) Economy in fabrication and erection.
- vii) Speed of erection.
- viii) Field quality control and admittance of effective inspection and rectification.

2.3 STATE-OF-ART, VERTICAL JOINT

There are numerous connection methods for vertical joints but these may be broadly classified into two categories, namely a) wet joints and b) dry joints. These are briefly described below.

2.3.1 Wet Joints

In wet joints, in-situ concrete or grout is used to fill the gap between the adjoining panels. This method is the most popular in Europe and the Soviet Union. The greatest advantage of these joints is that they do not require the panels to have highly accurate dimensioning as the gap in any case is going to be filled up at site. The grouted joints can be plain or reinforced. However, due to abnormal load requirements, the existence of unreinforced joints is disappearing. In reinforced vertical joints, horizontal wires project from the panels into the joint. These wires are normally bent to form loops and interwoven with vertical bars. Sometimes, the projecting dowels are welded together at site. In fact, the effort in these joints had been to provide a monolithic character to the assembly. The provision of a narrow joint width is not desirable as it is difficult to fill and compact grout in a congestion of reinforcing steel. At the same time the width should not be too large as shrinkage is proportional to the volume of the joint.

Wet joints may be further broken down to the following types based on the geometry of panel edges :

2.3.1.1 Plain Joints

This is the simplest form of vertical joint (Fig. 2.4a). In an unreinforced plain joint the load transfer capacity depends on the

strength of the grout and the bond with the panels. This is not dependable due to shrinkage in both the panels and the joint. Test results [23, 24] indicate a wide disparity in shear capacity. Such joints are subject to brittle failure. Plain reinforced concrete joints are relatively ductile and can develop considerable ultimate shear resistance through dowel action and shear friction.

2.3.1.2 Grooved Joints

The unreinforced grooved joints shown in Fig. 2.4b can exhibit great rigidity because the groove increases the bond surface. However, as in the case of unreinforced plane joints, such resistance is not very dependable. Reinforced groove joints exhibit higher elastic resistance than plain reinforced joints while their ultimate shear resistance is the same.

2.3.1.3 Keyed Joints

Keyed joints as shown in Fig. 2.4c are the most commonly used wet joints. The elastic resistance against slip is provided by interlocking rather than by bond. Once the principal tensile stress in the joint exceeds the tensile resistance of cast-in-place grout, the cracks develop and shear resistance decreases drastically. In reinforced sections, after cracking the shear force is transferred across the joint through diagonal strut action. The role of reinforcement then is to resist the tensile stresses while the concrete is resisting the compressive component. This type of joint is more ductile as compared to the other two types.

The effect of castellations on the joint strength are shown in Fig. 2.5. Under monotonic load the ultimate strength of keyed joints may be 3 to 4 times greater than of plain ones. The residual strengths,

which are based on shear friction mechanism, are, however, identical. The greater difference between the ultimate strength and residual strength represents brittle failure and is not desirable.

Sometimes the reinforcement of the vertical joint is concentrated at the floor level in the horizontal joint [23, 25]. This results in economy in fabrication and construction. Hysteretic behaviour of such a joint called "locking joint" [26] using a 150 x 150 mm cross sectional concrete beam to resist the vertical shear force is shown in Fig. 2.6.

To summarize, 1) the wet joints may present some difficulty in grouting or in-situ concreting; 2) quality control, especially during inclement weather, is questionable, and to compensate for this, the joints are often designed with larger factors of safety. While this does not present any problem under service load conditions, it is not desirable from the seismic aspect when predictable and stable behaviour is the main consideration for predictable response; 3) for seismic design, it is necessary to consider the behaviour of the joint under load reversals, and although the experimental results available for such loadings are quite limited [27], substantial degradation of the joint is anticipated during load reversals, which could result in poor seismic response; 4) the capacity of the joint to deform is limited.

2.3.2. Dry Joints

In dry joints, the steel sections are either welded or bolted to inserts cast within the panels (Fig. 2.7). The advantages of this system are that the joint develops strength immediately on completion which increases the speed of erection. According to Koncz [28], the use of dry joints results in saving 30-40% in construction time over that for

wet joints. On the other hand, the disadvantages are that if the dimensional accuracy of the members is not good, the assembly of the connection may be extremely difficult.

Field welding of inserts develops temperature stresses causing expansion of the inserts and disturbance of the bond with the concrete, and also causing staining and cracking of the concrete due to the excessive heating. Field welding may also present quality control problems. For these reasons bolted connections are seen to be more desirable for future joints [29, 30].

Spencer and Neille [31] have conducted a series of cyclic load tests on typical embedded connections. A typical hysteresis loop from such a test is shown in Fig. 2.8. Although the design strength required by the codes [32] was exceeded by up to 30% in the initial cycle, the strength began to fall as the number of load cycles increased and finally at failure the capacity was only 40% of that experienced at the first cycle.

The main shortcoming of dry joints is their excessive rigidity resulting in concentration of stresses on relatively small areas of panel which may result in failure of its anchors or crushing of adjacent concrete [8]. Failure of the bolt or weld is also a brittle mode of failure.

2.3.3 Discussion of Performance

The study of existing vertical jointing systems in terms of their performance under seismic loading shows that they are not satisfactory for the following reasons :

- i) The difference between the ultimate load and the residual load is large, thus the behaviour is more brittle than elasto-plastic. The size of the hysteresis loops is very small.
- ii) The results of limited tests under load reversals show that the joints undergo rapid deterioration in strength and stiffness.
- iii) The deformability is limited and the connections or their anchors may fail at deformations needed to meet the seismic demand.
- iv) The damage to the joint may require major repair.

2.3.4 Descon-Concordia Mechanical Joints

One of the successful examples of bolted joints, although not for vertical joints, is the Descon-Concordia system [33] which used bolted joints for horizontal wall-to-wall and slab-to-slab joints for their panelized buildings constructed for "Operation Breakthrough" in the United States in 1973. Slotted holes were used to accommodate dimensional tolerances in panels. Strength evaluation static tests of their prototype specimens were conducted at the U.S. National Bureau of Standards [34]. A load-deformation curve of a typical slab-to-slab joint under monotonic loading is shown in Fig. 2.9. It is seen that the capacity continues to increase after initial slip. In this respect, the performance is ductile. However, no tests were conducted to see the performance of this connection under reversals of load beyond slip capacity or the nature of joint degradation after several cycles of reversal.

Basically, the system was used to facilitate and speed up the construction operation rather than as an energy dissipating source for severe ground shakings. This is evident from :

- a) The nature of tests conducted at NBS were only static in nature to determine the slip resistance capacity of friction bolted joints. Since the design was of the friction resistance type, determination of performance during slip therefore does not arise.
- b) These joints were used at locations where the concept of energy dissipation is either not available or not desirable.
- c) The lengths of the slots were designed to accommodate tolerances and could be entirely consumed, with some bolts at the extreme ends of their slot, thereby leaving no room for slippage during extreme earthquakes.

The above system however rates high in meeting all the other good qualities of a successful joint.

2.4 DESIGN APPROACH

The static tests of Descon-Concordia joints shown in Fig. 2.9 are encouraging to the extent that by the use of slotted holes there exists a potential to obtain the desired deformations in the joint without causing yielding of the materials. Frictional movement of the joint as it slips could provide necessary energy dissipation.

With proper design and detailing, a slipping bolted connection can be developed for a vertical joint to simulate ideal elasto-plastic behaviour. Provision of proper surface treatment of the sliding

mechanism can ensure stable hysteretic characteristics. The possibility of obtaining these properties in any other jointing system seems limited. Using this approach, the drawback of force concentration can be eliminated by allowing the slip to occur at an appropriate level before damage occurs to the panel, connection or its anchors. Since there will be no built up of forces beyond slip capacity, redistribution of forces takes place until they are uniform over the full height of the vertical joint line.

Also, since the energy dissipation results from slipping rather than inelastic deformations, no damage is caused.

2.5 LIMITED SLIP BOLTED JOINTS

Limited slip bolted joints consist of steel plates or sections with slotted holes which are friction bolted to steel inserts anchored into concrete panels. Figs. 2.10 and 2.11 show details for some of the wall-to-wall vertical joints. The length of the slot accommodates the normal fabrication and erection tolerances with an additional clearance to absorb energy by slipping. Provision of controlled slippage in the joint on either side of the bolt is the main feature of limited slip bolted joints. This is ensured by simply using a special location pin, shown in Fig. 2.12. At the same time, the length of the slip is not to be so large as to allow the distortion of the structure beyond acceptable limits.

The horizontal slots in the connecting plates are provided only to aid in initial lining up of the connector plate in position and bolted temporarily to assist in the erection procedure. Once the plate is in position, the plate on this side of the joint is welded to provide

a permanent fixture. This avoids any rotation of the plate which might interfere with the free slippage along the vertical slots on the other side.

The load at which the joint starts to slip is determined by the coefficient of friction and the clamping force of the bolts. By varying one or other of these components, the connection can be designed for the desired slip load.

Since seismic response of the building is mainly dependent on the stiffness and energy dissipating capability of the structure, optimization of both of these parameters can be conveniently done by appropriately adjusting the slip load of the connections.

As the vertical joints are the ones expected to slip under severe seismic action, these joints will not be grouted but sealed by other appropriate means. Using this system, the wall panels have plane edges without castellations or projecting reinforcing loops, thus the fabrication of panels is simplified.

Limited slip bolted connections in the vertical joints may be used with any other jointing system for horizontal wall-to-wall and slab-to-slab joints, but is more attractive for those systems which use bolted joints for the other locations as then the construction operation is industrialized.

2.6 EXTENSION OF CONCEPT

2.6.1 Cast-in-place Shear Walls

Solid walls being very stiff could be subjected to destructively large seismic forces. In order to increase the flexibility of such walls

and thereby its ductility or energy dissipating capacity, concepts of sectionalizing, like coupled shear walls have been suggested [21]. The potential of this transformed structure as an efficient earthquake resistant construction stems from its ability to dissipate energy within this shear transfer or coupling system over its full height.

Paulay has shown that by properly detailing the reinforcement in the coupling beams, large ductilities could be obtained [35]. During severe earthquakes, considerable energy could be dissipated by the coupling system, involving yielding and consequent damage before damage would occur to the main walls, thereby reducing the ductility demands on the walls. This results in an improved earthquake resistant structure.

Energy dissipation through in-plane coupling in coupled shear walls is comparable to that of limited slip bolted joints in the vertical joints. By introducing limited slip bolted joints in cast-in-place solid shear walls or even in the coupling beams proposed by Paulay, the inelastic deformations and permanent damage to coupling beams, can be avoided. Limited slip bolted joints can be conveniently incorporated in solid shear walls by inserting them in the forms before pouring the concrete. Some of the typical details of such a joint are shown in Fig. 2.13. Floor slabs, roof and other finishes will however have to be so detailed as to accomodate the differential slippage in the walls.

2.6.2. Framed Buildings Clad with Architectural Curtain Walls

The use of precast concrete architectural panels in combination with concrete or steel framed buildings is becoming increasingly popular for all types of buildings. These panels are tied to the frame using bolts embedded in the panels. The panels do not carry any vertical load and

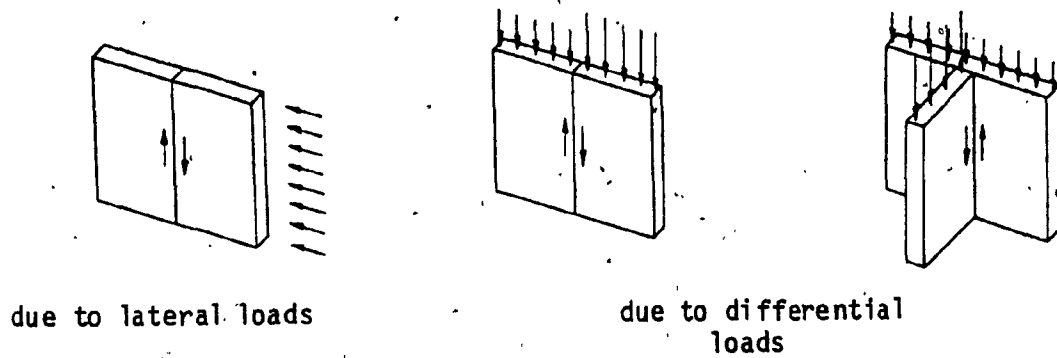
often serve only as weather enclosure. It has been shown earlier [89] that when such rigid cladding panels are connected to the frames, the panels and frame will interact resulting in increased lateral stiffness of the structure and thus reduced deformations. While this is advantageous from the point of view of wind loading, it may not be desirable from seismic considerations where increased stiffness could mean an invitation to higher seismic forces.

By using energy dissipating limited slip bolted joints for tying such panels to the frame of the building, the dual advantage of increased stiffness for wind type loading and flexible character during severe ground shakings, when all the joints are slipping, can be achieved. As large amounts of fed-in seismic energy can be dissipated during slipping the overall seismic response of the framed building is considerably improved. In this case since horizontal joints are not gravity load carrying joints, the slipping of the joint can be permitted horizontally as well as vertically.

An important consideration in such buildings is that as the elastic strain energy of the frame is relatively small compared to panelized structures, the slip load of the joint should neither be large enough to hinder the recovery of the deflected frame back to its original alignment nor be low enough to slip under wind loads.

2.7 SUMMARY

Limited slip bolted joints are proposed to provide the "elasto-plastic" behaviour of an ideal energy dissipating vertical joint. The proposed joints extend the existing benefits of mechanical connections to give additional security during severe earthquakes.



a) Vertical Shears

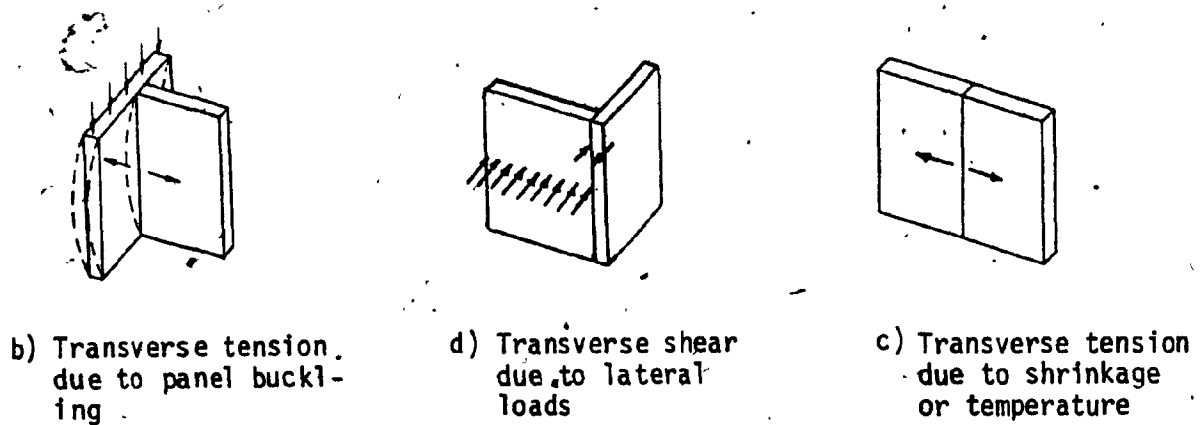


FIG. 2.1 FORCES ON VERTICAL JOINT

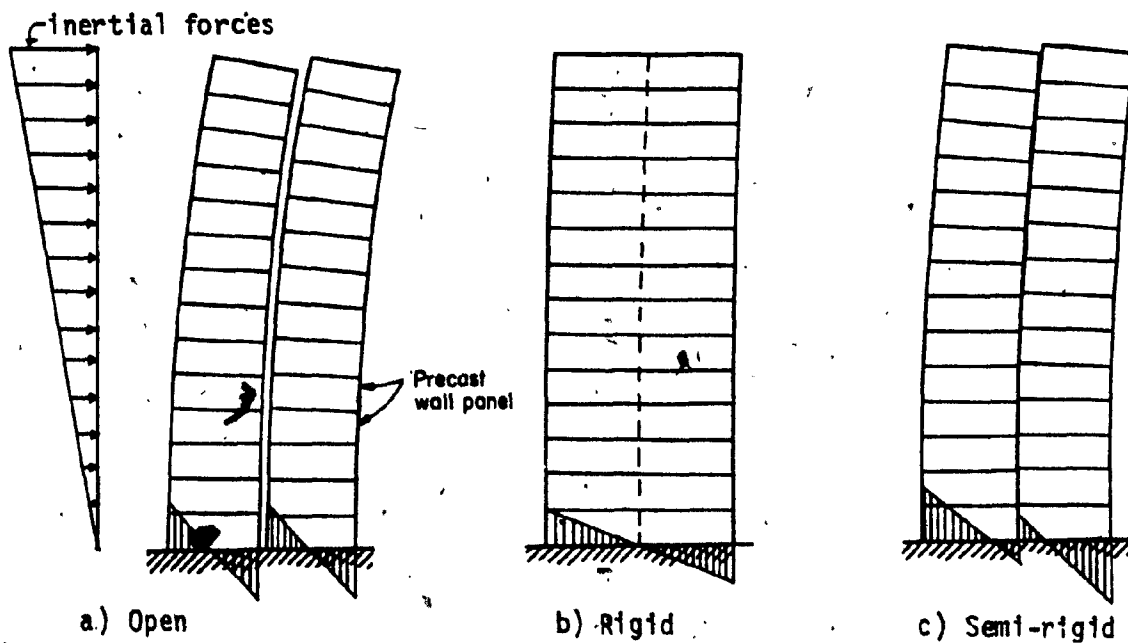


FIG. 2.2 INFLUENCE OF JOINT ON WALL BEHAVIOUR

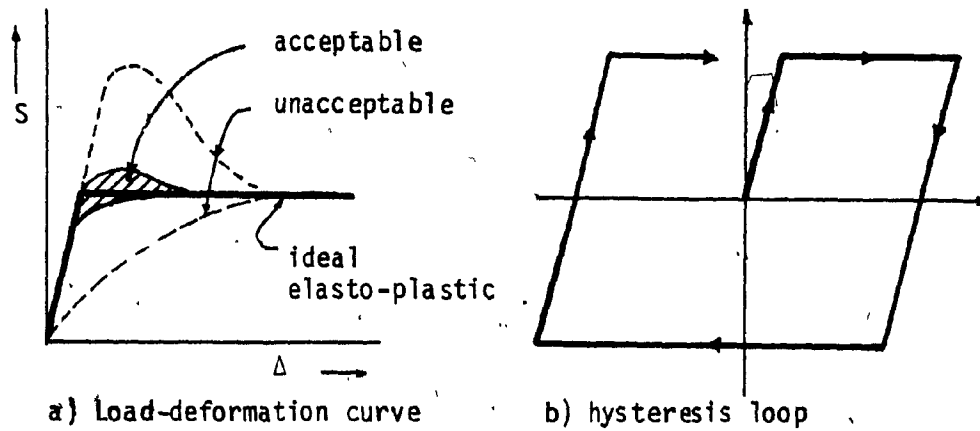


FIG. 2.3 IDEAL BEHAVIOUR OF VERTICAL JOINT

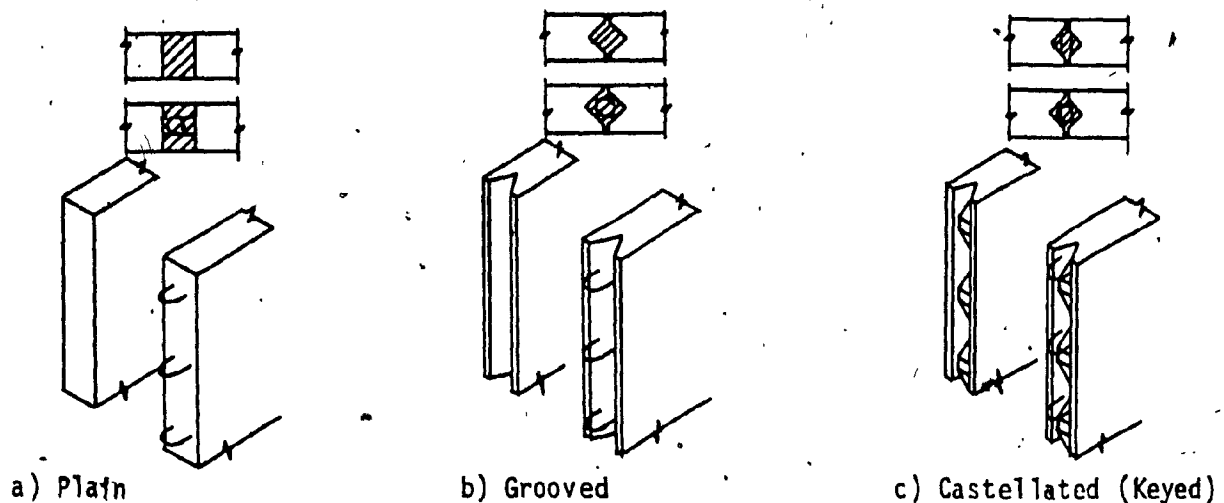


FIG. 2.4 DETAILS OF WET VERTICAL JOINTS [23]

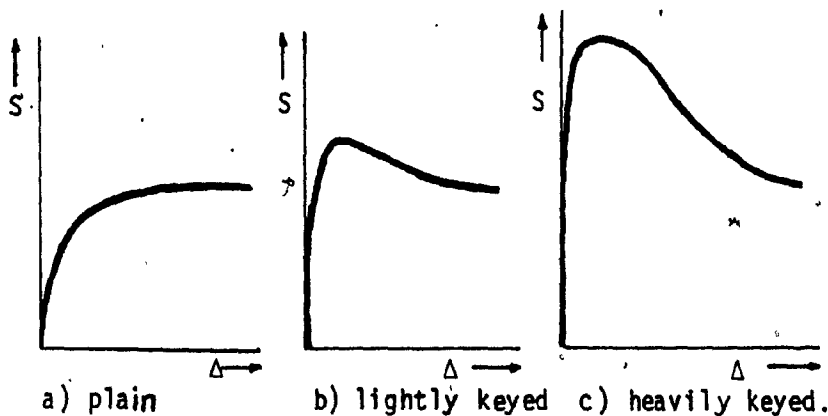


FIG. 2.5 EFFECT OF CASTELLATIONS ON ULTIMATE STRENGTH [27]

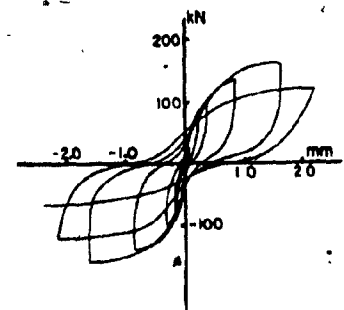
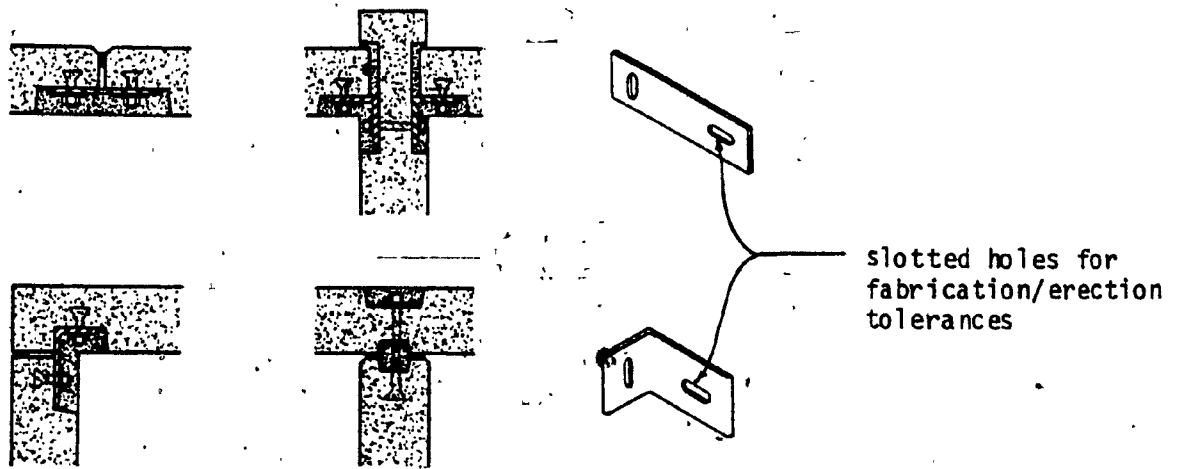


FIG. 2.6 HYSTERESIS LOOP OF LOCK JOINT [26]



a) Bolted Joints



b) Welded Joints

FIG. 2.7 DRY VERTICAL JOINTS

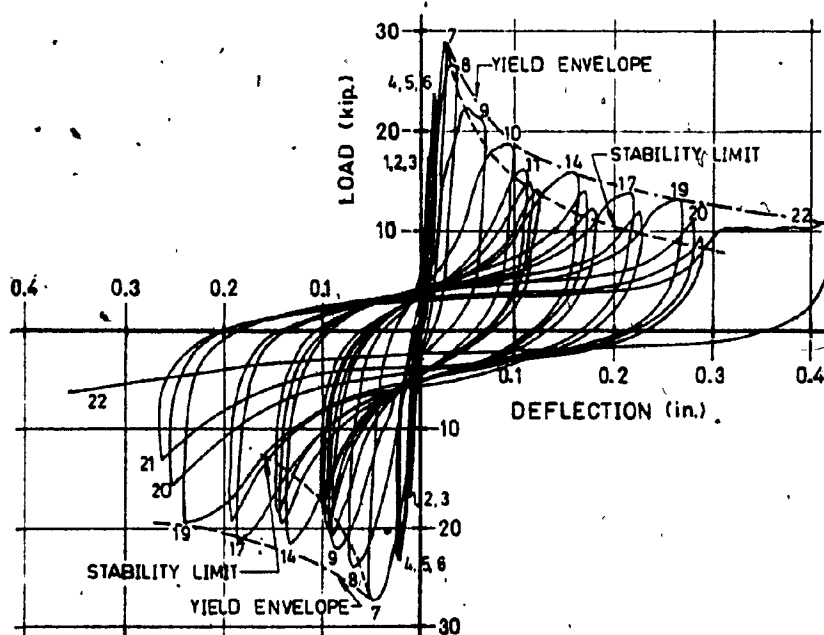


FIG. 2.8 HYSTERESIS LOOP, WELDED HEADED STUD CONNECTION [31]

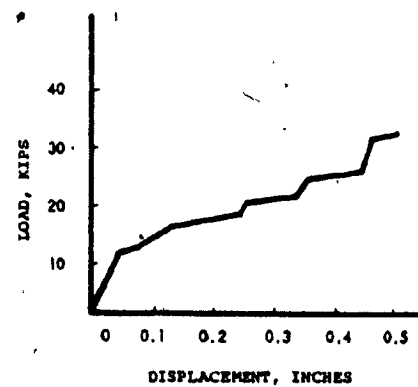


FIG. 2.9 LOAD-DISPLACEMENT CURVE, SLAB-TO-SLAB JOINT OF DESCON SYSTEM [34]

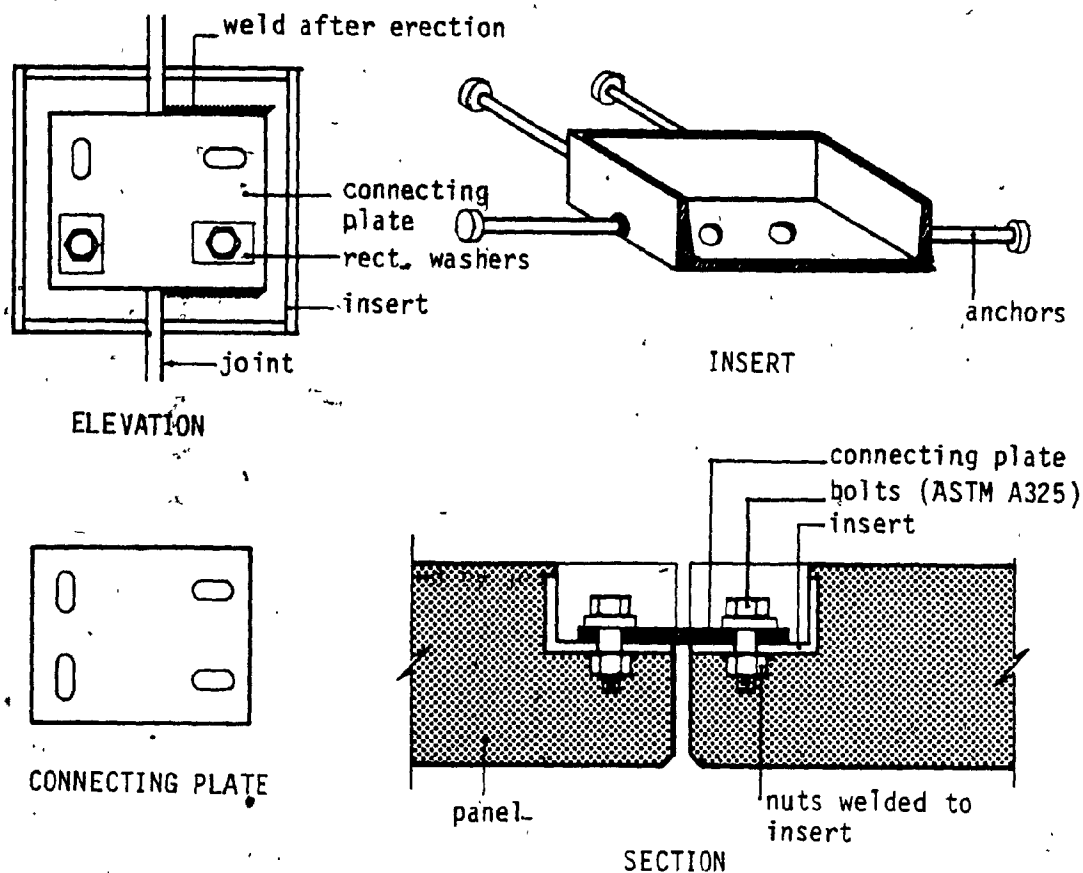


FIG. 2.10 - WALL-TO-WALL JOINT

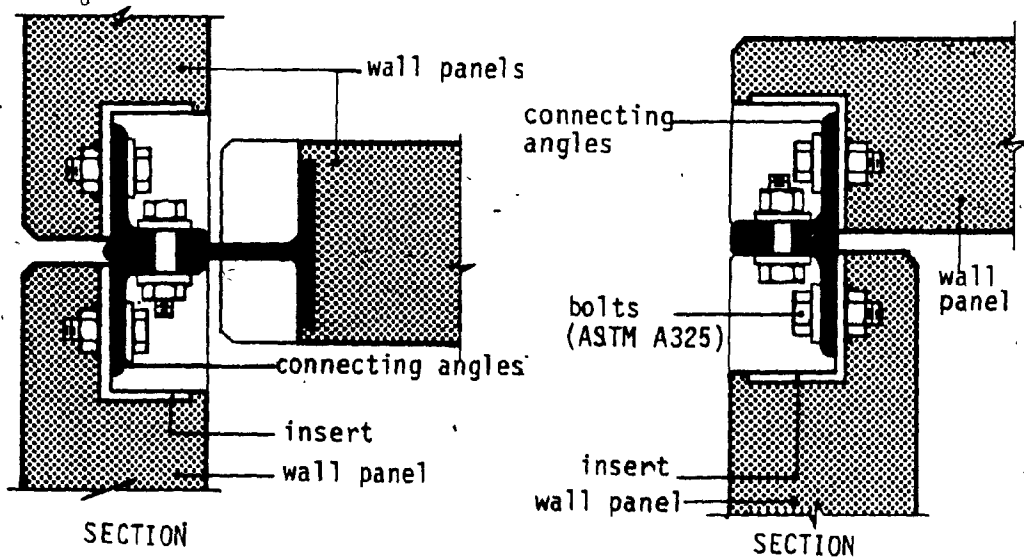
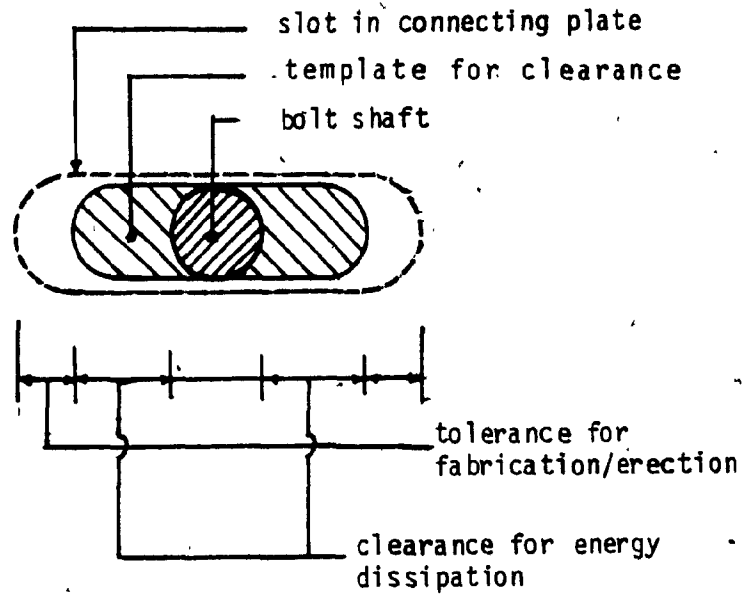
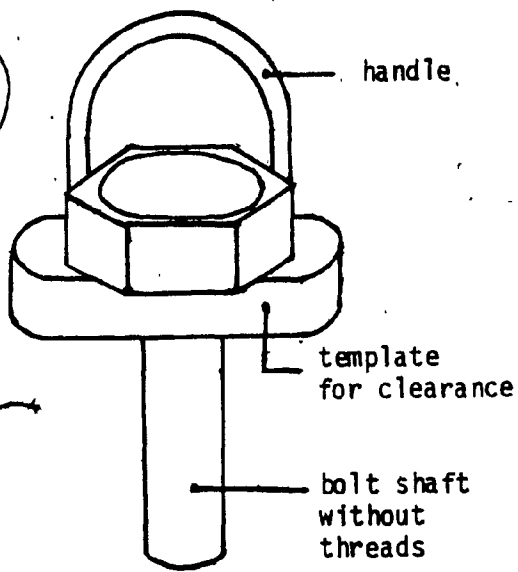


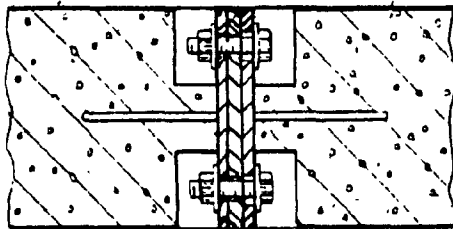
FIG. 2.11 - CORNER WALL-TO-WALL JOINT



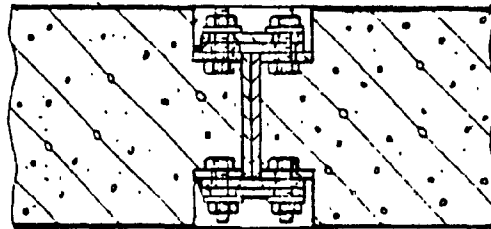
Isometric view

Plan

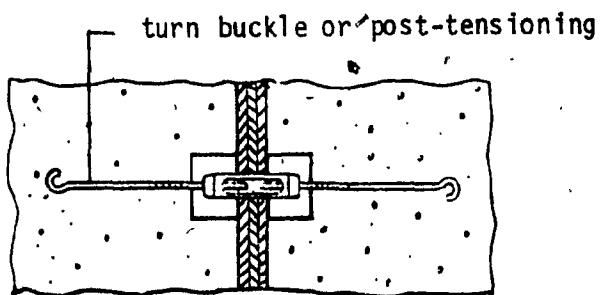
FIG. 2.12 DETAILS OF LOCATION PIN



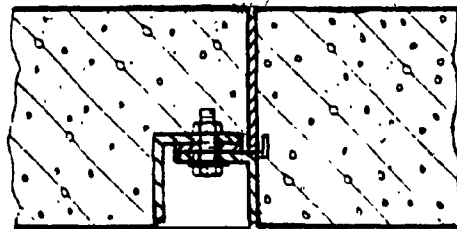
a)



b)



c)



d)

FIG. 2.13 LSB JOINTS FOR CAST-IN-PLACE SHEAR WALLS (TYPICAL)

CHAPTER III

LABORATORY TESTS AND RESULTS

CHAPTER III

LABORATORY TESTS AND RESULTS

Based on the philosophy presented in Chapter II, the proposed limited-slip bolted joints appear to be the answer to simulate elastoplastic behaviour in vertical joints. Design data and behaviour of such joints during repeated cycles of reversals were not available, hence the first task was to conduct experiments on specimens of typical joints to obtain the basic design data so that a realistic response of the structure could be studied. This chapter begins with a review of past research, followed by the test program, description of test specimens, test procedures, and analysis of test results. Then the practical considerations and recommendations in the application of test results are discussed, and design data is presented in tabular form.

3.1 PAST RESEARCH

Batho and Bateman were the first to suggest the use of high strength bolts for the assembly of steel structures. In 1934, they reported to the Steel Structures Committee of Great Britain, that these could be tightened sufficiently to provide enough margin of safety against slippage of connected parts. Since then, much research has been performed on bolted structural connections with respect to the installation procedures, use of different surface treatments, behaviour under static, sustained and repeated loading within slip capacity, losses in bolt tension due to creep, and the effect of oversize and slotted holes [36]. The design specifications for friction type and bearing type structural joints using high strength bolts are well documented in RCRBSJ Specifications [37]. The Guide by

Fisher et al. [38] provides a state-of-the-art summary of the experimental and theoretical studies and is a comprehensive source of information on bolted structural joints.

To the author's knowledge, the only published work so far reported on the dynamic behaviour of connected assemblies using treated faying surfaces and high strength bolts is reported by Vitelleschi et al. [39]. In this case, holes 1.5 mm (1/16 in.) larger than the bolt diameter were used to study the effect of damping due to finite slip.

In conventional buildings, the satisfactory performance of the structure depends upon the joints not moving, and any slippage is considered to be a failure of the structural assembly. The research in bolted assemblies, therefore, remained restricted to the slip capacity of the joint or to a very finite slip which was followed by bearing type behaviour.

The first use of bolted joints for large panel structures was by Descon-Concordia of Montreal in their projects for Operation Breakthrough in the United States in 1973 [34]. Static tests to evaluate the strength of their prototype connection assemblies, built out of tubular steel sections with mill scale surfaces were performed by the U.S. National Bureau of Standards [40]. A total of 25 tests were performed on specimens for slab-to-slab and horizontal wall-to-wall joints representing inplane shear, out of plane shear and pull-out tests. Overcoming the frictional resistance, as identified by initial slip, defined shear failure of the connector. Only two specimens were subjected to repeated cycles of load within the slip resistance capacity of the connection which showed no slip failure or distress.

3.2 TEST PROGRAM

In the present study, limited-slip bolted joints, having long slotted holes, are provided as a means to dissipate energy by friction during the repeated cycles experienced in a severe earthquake. As no design data was available on the performance of such joints after several reversals of slipping, the first priority in the present research was to conduct tests on specimens of such joints to obtain the basic design data.

The past research has shown that surface coatings on mating surfaces change the characteristics of bolted joints to a varying degree [41]. One of the main variables in the present tests was, therefore, the use of different surface treatments. The performance of slip resistant design of structural joints for most of these surface finishes is known. Brake lining pads, made up of asbestos fibre reinforced with metallic particles, have excellent frictional and wearing resistance qualities against moving metallic surfaces. These are widely used in automobiles and the heavy engineering industry. The pressures on brake linings in these cases normally do not exceed 2 MPa and hence the test data for pressures exceeding this value are not available. In our case the loads on the brake lining pads could be of the order of 15-50 MPa. It was, therefore, important to study the performance of this material including the effect of its long term creep on losses in bolt tension.

The earlier load tests conducted at NBS were for connections between inserts embedded in small concrete panels with grouted as well as ungrouted joints. Two observations were apparent from these tests. Firstly that the insert anchors in the concrete panel if properly designed in accordance with code provisions, showed no sign of distress

before bolt failure. Secondly, grouted joints increase the initial slip load by only 8-10% over ungrouted joints and the ultimate load capacity remained unchanged.

Based on the above observations, it was decided to carry out tests on the connection assemblies without the panels as it is assumed that the ultimate strength of the panels and the assembly anchors will exceed the ultimate strength of the connections. Since we are mainly interested in the behaviour during slipping of the connection, it is assumed that there is no inelastic behaviour of the concrete or anchors up to the slip load. This was also evident from the tests conducted at NBS.

3.3 DETAILS OF TEST SPECIMEN

3.3.1 Description of Specimen

Details of various test specimens are shown in Fig. 3.1. Specimen type A, 35 in number, consists of one central plate of 175x125x12.7 mm with a slotted hole of 13x32 mm, and two cover plates of 200x125x9.5 mm having holes of 14.3 mm dia., which are bolted together with a 12.7 mm dia. x 50 mm long bolt. In 10 specimens, brake lining pads of 750x750x3 mm with a 13.5 mm dia. hole were used. Two pads, one on either side of the central plate were inserted under the cover plates.

Specimen type B, 10 in number, consists of two end pieces and a central piece fabricated out of standard rolled steel channel C200x19.6 kg/m (C8x13.2). These pieces are tied together by two connecting plates with 8 bolts of 12.7 mm dia. x 500 mm. Connecting plates are of 130x170x12.7 mm having slotted holes of dimensions shown in the sketch. The nuts for the bolts are already welded to the back of channel pieces. Rectangular washers of 50x28x8 mm with 13.5 mm dia. holes, which are sufficient to completely cover the slotted holes, were used.

Specimen type C is similar to type B except that the connecting plates are welded to the central piece.

3.3.2 Materials

The steel used for fabrication of the test specimens was conventional structural steel with a specified minimum yield stress of 300 MPa (44 ksi) conforming to Grade 44W of CSA G40.21. High-strength medium carbon steel bolts with a minimum tensile strength of 830 MPa (120 ksi), conforming to ASTM A325 were used. Brake lining pads of ordinary quality (black) and heavy duty quality (woven flat sheet, type 628), manufactured by Raybestos-Manhattan, Peterborough, Ontario, Canada were used. The brake lining pads are made up of asbestos fibre which is reinforced with brass particles.

Fabrication and supply of the steel specimens was made by the Dominion Bridge Company of Montreal. Brake lining pads were supplied by the J.C. McLaren Belting Company Ltd., Montreal.

3.3.3 Surface Finishes

(a) Mill Scale : The steel plates were in the as received condition. The plates had tight mill scale with patches of light rust representing normal field condition.

(b) Grit Blasted : The metal surfaces were grit blasted, completely removing mill scale and rust, using crushed grit of cast iron of maximum particle size no larger than that passing through a 16 mesh screen, U.S. screen series as per SSPC-SP6-63 "commercial blast cleaning".

(c) Sand Blasted : The surfaces were cleaned to near white metal surface by dry sand blasting using compressed air blast nozzles

and dry sand of maximum particle size no larger than that passing through a 16 mesh screen, all as per SSPC-SP5-63, "white metal blast cleaning".

(d) Zinc-Rich Paint : After the metal surfaces were commercial blast cleaned, a coat of inorganic zinc base primer (Carbo-Zinc 11) was applied with a brush as per SSPC PS-1200. This was allowed to cure at room temperature for a period of 7 days before testing. This primer protects the steel galvanically and has excellent abrasion resistance. The average thickness of a single coat was measured to be 95 microns against the specified value of 50-100 microns.

(e) Metalized : The metal surfaces were blast cleaned to white metal and sprayed with a layer of hot zinc as per CSA standard G-189. The average thickness of coating was measured to be 215 microns against the specified value of 50-100 microns.

(f) Hot-Dip Galvanizing : All mill scale from the plates was removed prior to the coating application. The plates were then coated with a metallic layer by dipping into a bath of hot metal, following a standard factory procedure. The thickness of the coating was measured to be 100 microns.

(g) Polyethylene Coating : Pellets of low density polyethylene were melted at about 140°C and applied over prewarmed sand blasted steel plates. This was allowed to cure for 48 hours at room temperature. The thickness of film was measured to be 90 microns.

(h) PVC Coating : Pellets of PVC (Polyvinylchloride) were dissolved in a solution of cyclohexanon and a coating was applied on the sand blasted surface of the steel plates. Average thickness was measured to be 95 microns. This was allowed to cure at room temperature for 48 hours.

The thickness of coatings were measured with an "Elcometer Inspector" Thickness Gauge (Scale 1E, 0-25 thous).

The surface finishes type (b) through (e) were made by the Dominion Bridge Company of Montreal. Surface finish type (f) was made by Locweld Forge & Co. of Montreal. Polyethylene pellets were provided by Union Carbide (Canada) Ltd., Montreal.

3.3.4 Assembly

Before assembling the components all contact surfaces were cleaned of dust, oil and grease by using vaporized chlorinated hydrocarbon solvent (Chlorothene NU degreaser).

Assembly of all the connections was made with bolts at the centre of the slot. All bolts were tightened by the turn-of-nut method to $1/3$ turn from snug tight position, as required for bolts of grip length to diameter ratio of 4 or less [37, 42]. The bolt tension was then determined by measuring the change in bolt length with a micrometer and reading bolt load from calibration curves to be described later. In all cases the tension in the bolt was in the yield range and about 30% greater than the minimum specified value of 53 kN or the proof load of the bolt which is 70% of the minimum tensile strength.

The specimens were tested, on average, 3 days after bolting up. The plates were coated about a week earlier.

3.4 TEST EQUIPMENT AND PROCEDURE

3.4.1 Load Calibration of Bolt

Tightening of high strength bolt is not an exact science. It has been noted that normal installation procedures will furnish only

approximate results. Slip load of a friction bolted joint assembly is related to the clamping force caused by tightening the nut. So, determination of actual tension in the bolt is very important for research work. Calibration of the bolt to establish its load elongation relationship is done by adopting the following procedure.

Special load cells shown in Fig. 3.2, consisted of small hollow cylindrical steel pieces of length equal to the grip length of the test specimens. Two precision strain gauges (Type CEA-06-125UW-350, manufactured by $\equiv M \equiv M \equiv$), were bonded at right angles to each other to eliminate any error due to temperature variation and to increase the sensitivity by taking advantage of Poisson's ratio. The load cells were then calibrated by loading them in an "Instron" machine and recording the strain readings versus load.

These cells were then placed on a bolt and used to establish the relationship between bolt load and extension during the tightening of the nut. This was done by first turning the bolt to snug tight position and then tightening by turning the nut in increments of 30° . Changes in length of the bolt and strain readings were recorded for each increment of turn. The bolts were machined on both ends to ensure accurate readings of the changes in length which were measured by a micrometer (0.0025 mm). Changes in bolt length during unloading process were also recorded in order to establish losses in bolt tension.

Because of different grip lengths, different cells were required to calibrate specimen type A (with and without brake lining pads), and for specimen type B. Fig. 3.3 shows the set up for bolt calibration. Fig. 3.4 shows the load calibration curves for specimen type A and type

B. The lower yield level in the calibration curve for the bolts used with brake lining pads (Fig. 3.4b) was due to the fact that the longer bolts required for this grip length were not locally available, and the bolts used had an insufficient number of threads engaged in the nut and yielded prematurely.

3.4.2 Loading Machine

Instron Universal Testing Machine; Model 1125 (Fig. 3.5) was used as a loading and recording device. This incorporates an electronic load weighing system with load cells that use strain gauges for detecting tensile or compressive loads. A tension-compression load cell of 100 kN capacity was used for the present tests.

The specimen is mechanically attached to the load cell and the compressive or tensile loads are applied by the moving cross head. Digitally commanded crosshead speeds are push button selectable. Direction and sequence of crosshead movements may be manually or automatically controlled. In order to measure accurate relative displacements between the parts of the test assemblage, the Instron strain gauge extensometer was used and connected directly to the Servo Chart Drive system which gave a continuous load/displacement record. Before mounting the extensometer on the specimen, it was calibrated on a high magnification extensometer calibrator (0.0005 mm).

For specimen type B and type C, two reaction frames (Fig. 3.6) were fabricated to hold the outer parts of the connection. Fig. 3.7 shows the two frames installed in the machine. Dial gauges were used to detect possible rotation of the joint as full fixity is difficult to ensure.

3.4.3 Static Tests

These tests were carried out in order to determine the slip loads, the coefficient of friction and assembly stiffness. After the connection had slipped and the bolt come into bearing, the tests were continued until reaching the full capacity of the machine i.e. 100 kN. The ultimate shear capacity of the bolts exceeded 100 kN. All the static tests were carried out in tension. Since the loading was transmitted to the specimen by the moving crosshead, displacement rather than load, was controlled (10 mm/min).

3.4.4 Dynamic Cyclic Tests

These tests gave the elastic behaviour up to slip, the energy dissipation capacity during slip, the loss in the coefficient of friction, the loss in bolt tension, the deterioration of the contact surface conditions and the stiffness degradation after load cycling. The specimens were initially subjected to progressively increasing load amplitude starting from 50% of the slip load until slip occurred. After slip, the mode of cycling was changed to controlled displacement amplitude between the slot extremities i.e. ± 10 mm and -10 mm, except for specimen type B in which case load cycling was continued up to ± 100 kN, as displacement cycling was not possible due to the jamming of the bolts in the slots. In each case the speed of moving crosshead was so adjusted to keep the frequency of cycling to about 0.1 Hz, which is limited by the maximum operative speed of the crosshead (250 mm/min.) and length of travel in a slot (40 mm). The specimens were each subjected to about 20 cycles. The limit of 20 cycles is considered reasonable since in any extreme earthquake the number of cycles of actual slippage in a connection are not likely to be more than 4 or 5. Bolt lengths were measured after 1 and 5 cycles, and at the end of cycling to determine any losses in bolt tension.

Table 3.1 gives the various static and cyclic tests for the different types of specimen.

3.5 ANALYSIS OF EXPERIMENTAL RESULTS

3.5.1 Static tests

Specimen Type A : Bolt tensions and slip loads for specimen type A are shown in Table 3.2. From these values, the coefficient of friction, hereafter called the slip coefficient, was obtained by using the equation

$$k_s = \frac{P_s}{m \sum_{i=1}^n T_i} \quad (3.1)$$

where k_s = static slip coefficient; P_s = static slip load (kN);
 m = number slip planes; and $\sum_{i=1}^n T_i$ is the sum of the tensions in n bolts.

In case of specimen type A, the slip coefficient $k_s = \frac{P_s}{2T}$.

Comparison with results obtained by others [38] indicates about 25% lower slip coefficients for mill scale, grit blasted, sand blasted, and inorganic zinc-rich paint. It was also noticed by Allan and Fisher [43] that joints with slotted holes showed a 22-33% decrease in slip coefficients when compared to test specimens with holes with a clearance of 1.5 mm (1/16 in.). It is explained by them that the reduced contact area in the case of slotted holes causes higher contact pressures adjacent to the hole which tend to flatten the surface irregularities thereby reducing the slip load. For this reason the code specifications [37, 42] require 1/3 more bolts in the case of long slotted holes. A much smaller difference in slip coefficient was observed for the metallized surface.

Study of this surface after the tests revealed that the width of contact area offering frictional resistance was in this case (see specimen T-22 on Fig. 3.12) nearly double that observed for other finishes which was normally within a width of 3 to 4 times the bolt diameter. Test results by others for brake lining pads are not available at high contact pressures, but from data obtained from the manufacturers, the coefficient of friction of heavy duty brake lining pads (Style 628) is 0.5 @ 350 kPa (50 psi).

Load displacement curves for specimen type A are shown in Fig. 3.8. In general, up to the point of slipping the connection behaves elastically after which it slides simulating "elasto-plastic" behaviour. As the bolt reaches the end of the slotted holes, it goes into bearing giving an ultimate load much higher than that causing slip.

Specimen Type B : The total slip load for the two connections of specimen type B, using the slip coefficients for specimen type A from Table 3.2 and referring to Fig. 3.9a, is given by the equation:

$$P = \frac{4R}{\left[1 + \left(\frac{a}{b}\right)^2\right]^{1/2}} \quad (3.2)$$

where P = total slip load acting on the two connections, R = slip resistance of one bolt, a and b = spacing of bolts.

For a and b equal to 127 mm and 76 mm respectively (Fig. 3.9a), the slip load $P = 2.05R$.

During the tests on specimen type B, after a small slip, the slip load of which agreed with that calculated, the connecting plates rotated and bolts jammed against the walls of the slot with no further slipping

(Fig. 3.9b). Rotation of the plates during slipping was experienced in all the tests on specimen type B.

Specimen Type C : To prevent rotation and jamming in specimen type C, one half of the connecting plate was welded after bolting up thereby allowing free movement in the vertical slots. The calculated slip load for the two connections of specimen type C will now be $P = 4R$ against the total slip value of $2.05 R$ for specimen type B. Therefore, with nominal additional cost of welding, the slip load of type B is doubled.

The slip loads of each of the two connections of specimen type C will be similar to the slip loads of specimen type A, since specimen type A has two contact planes and a single bolt whereas specimen type C has a single contact plane but two bolts for each connection. Values of calculated and measured slip loads of specimen type B and type C are shown in Table 3.3 and are seen to be in close agreement.

Load displacement curves of specimen type B and type C are shown in Fig. 3.11.

Grouted specimen : One of the specimens type B (T-31) was filled with grout of $f'_c = 15$ MPa, a strength expected under actual field conditions, and tested. It showed only a nominal increase in the slip load (9%) over the ungrouted specimen, after which the grout did not contribute much. This is in agreement with the results of NBS according to which an increase of 8-10% in initial slip load value was observed.

3.5.2 Dynamic Cyclic Tests

Specimen Type A : Hysteresis loops for different faying surfaces of specimen type A are shown in Fig. 3.10. Dynamic slip coefficients for

the first half cycle and static slip coefficients are shown in Table 3.4. It is seen that dynamic slip coefficients vary between 2/3 and 3/4 of the static slip coefficients except for zinc-rich paint in which case they are approximately equal.

The area enclosed within an hysteresis loop represents the energy dissipated in a particular cycle. The shape and area of hysteresis loops of slipping joints indicate a far greater energy dissipation than those exhibited by concrete members as discussed in Chapter II. The areas of the loops were measured by means of a planimeter and then converted to energy units (Joules). In order to have a better comparison of energy dissipation performance, the values obtained for different loops were normalized for a common bolt tension of 75 kN and a slip length of ± 9.5 mm. The ratio of energy dissipated in a particular cycle to the first cycle represents the degradation factor β . Normalized values of energy dissipation and degradation factors for different surfaces are shown in Table 3.5.

Total losses in bolt tension due to normal relaxation after installation and including those due to cycling were up to a maximum of 10% of the initial bolt tension for mill scale, sand blasted, zinc-rich paint, brake lining pads, and 5% for metalized surfaces.

It is seen from the hysteresis loops (Fig. 3.10 and Table 3.5) that specimen type A treated with zinc-rich paint showed continuous degradation and finally stabilized near cycle 17 at 50% of the initial slip load. The metalized surface showed an increase in slip load for each cycle up to 24 cycles with a total increase of 50%. Mill scale and sand blasted surfaces showed degradation in slip load in the first few cycles and then increased in the next few cycles after which it diminished again and repeated the rise and fall in resistance. The loops did not stabilize up to 20 cycles.

The phenomenon can be attributed to the friction mechanism suggested by Bowden et al. [44]. It states that when two metal surfaces slide on one another, distortion of the metal penetrates to some depth beneath the surface and that the friction cannot be regarded as a purely surface effect. It has been suggested that the frictional resistance is primarily due to shearing of the metallic junctions formed by adhesion and cold welding at these points of contact and to the work of dragging and ploughing the surface irregularities. With the increase in volume of debris, the ploughing effect dominates over the shearing action.

On completion of tests, the examination of the surface conditions for mill scale and sand blasted surfaces showed that at some points the penetration, ploughing and tearing of metal had occurred and at some points the surface of the metal was raised above its normal surface. In the case of metalized surfaces, it was more of a ploughing and dragging of the coating. A small force was required to separate the plates when disassembling.

Brake lining pads (heavy duty) when used with mill scale surface showed reasonably high slip load and very stable hysteresis with almost no degradation. Deterioration in slip load was noticed when brake lining pads were used in contact with sand blasted surfaces and galvanized surfaces. This was due to the formation of a fine powder which worked in contact with the sand blasted surface and acted as a lubricant, and by polishing of the soft galvanized surfaces. Polyethylene coated surfaces and PVC coated surfaces had very low initial slip loads. In the case of the Polyethylene coated surfaces there was a continuous drop in slip load due to the formation of powder whereas the PVC coated surfaces

showed an increase of slip load and then a falling and rising in further cycles. The behaviour in the latter case was similar to that observed in sand blasted surfaces. Surface condition of the PVC coated surface revealed that this coating was completely torn out, perhaps during the first cycle, thereby exposing the sand blasted surfaces in contact. The loss in bolt tension in the case of the Polyethylene and PVC coated surfaces was high (20%) due to wearing out of the coating thickness.

Surface condition after 20 cycles for different surfaces of specimen type A are shown in Fig. 3.12.

Specimen type B : Cyclic tests on specimen type B indicated jamming of the bolt in the slots similar to the static tests. Under repeated cyclic loading, a slight rotation (about 0.5 degree) of the clamping arrangement was noticed. This enabled the bolt to slip further in subsequent cycles giving a variable quantity of energy per cycle, but in any case it was still a small fraction of that obtained from specimen type A. It was concluded that specimen type B is not a suitable arrangement for an efficient connection because of its low initial slip load and low energy dissipation.

Specimen type C : By welding the connecting plates on one side as in specimen type C, the initial slip load and the energy dissipation of the connection are doubled. Energy dissipation in each connection of specimen type C is similar to that of specimen type A.

Energy dissipation : Energy dissipation in one cycle of a long slotted hole is given by the product of dynamic slip load and relative displacement and can be written in the following form :

$$\begin{aligned}
 E_d(av) &= 4 \Delta P_d(av) \\
 &= 4 \Delta \beta k_d m \sum_{i=1}^n T_i \\
 &= 4 \Delta \alpha \beta k_s m \sum_{i=1}^n T_i \quad (3.3)
 \end{aligned}$$

where E_d = energy dissipated per cycle; α = ratio of dynamic slip coefficient to static slip coefficient as per Table 3.4; β = degradation factor as per Table 3.5; Δ = amplitude of the relative displacement.

3.5.3 Creep in Brake Lining Pads

In order to determine the additional losses in bolt tension due to long term creep of brake lining pads under high pressure, two specimens were tested. Brake lining pads (heavy duty) of size 750x750x3 mm with a circular hole of 13.5 mm dia. were placed between the central and outer plates of specimen type A, bolted together with a 12.7 mm. dia. bolt of A325. The nut was tightened by 1/3 turn after snug tightness and the change in bolt length and thus the load on the bolt was recorded.

One hour after tightening, the loss in bolt tension was 11.5% in contrast to normal 2-3% when only steel plates are used. The total loss in bolt tension after one week was about 16.5% compared to about 6% when no pads are used. It was observed that virtually all the additional losses in bolt tension due to the use of brake lining pads occurred within a short period of 1 hour or so after which further losses were negligible and were substantially the same with and without pads. The reason for this is that the commercially available brake linings are not designed to be used at these high pressures. One of the test assemblies was reopened

after one week and reassembled with a new bolt but using the same pad. The loss in bolt tension, one hour after tightening was only 3.5% compared to 11.5% observed earlier.

Therefore, to eliminate the effect of losses in bolt tension due to use of brake lining pads, the situation can be remedied by using precompressed pads, done by the manufacturer, or by retightening the bolts after 2 hours or so of initial tightening. It is desired to continue these tests for a period of at least one year.

3.6 PRACTICAL CONSIDERATIONS IN APPLICATION

3.6.1 Surface Finish

A surface finish which offers a high, stable and predictable slip load, after repeated reversals of cycles, is desired. Variations in initial and dynamic slip load lead to an unpredictable seismic response.

Metalized surfaces offer the highest amount of energy dissipation but are not desirable as the performance of the joint is far from predictable. In fact, all metal surfaces having externally applied coatings can be eliminated in view of the criteria of predictable behaviour. This is so because of the ploughing and dragging effect of debris which gets deposited between the moving plates and the resulting deterioration in surface condition of the coatings.

Of all the surface finishes tested, brake lining pads on mill scale surfaces best meet the two criteria, exhibiting nearly "elasto-plastic" behaviour with minimum degradation. Sand blasted faying surfaces are the second choice.

At this point, it should be mentioned that panels when manufactured are likely to be exposed for some time to the weather until assembled in the building. During this time, the bare steel components of the joint cast with the concrete panels are likely to rust. This rust can act like a lubricating powder and may alter the expected performance. Wire brushing and dusting off the surfaces just before assembly or use of some other means of eliminating rust should be kept in mind.

3.6.2 Installation Procedures

The slip load in a friction joint is directly related to the tension force in the bolts. LSB joints require a knowledge of the true slip load rather than the conservative values normally adopted for conventional friction type joints. So the selection of the proper field methods of tightening is important to produce uniform results.

The current RCRBSJ Specifications [37] permit high strength bolts to be tightened by using calibrated wrenches, by the turn-of-nut method, and by the use of direct tension indicators. In the calibrated wrench method the wrench is calibrated or adjusted to stall when the desired tension in the bolt is reached. Tests performed by Pauw and Howard [45] showed the great variability of the torque-tension relationship. Bolts from the same lot yielded extreme values of bolt tension $\pm 30\%$ from the mean tension desired. The average variation was in general $\pm 10\%$. This variation was mainly caused by the variability of the threaded conditions, surface conditions under the turned part, lubrication, tolerance on wrench, etc. Experience in field use of

high-strength bolts also confirmed the erratic nature of the torque-tension relationship. For this reason, the calibrated wrench method of tightening is no longer permitted by Canadian specifications [42] for use in Canada.

Controlling tension by the turn-of-nut method is primarily a strain control, and effectiveness of the method depends on the starting point and accuracy of the rotational measurements. In this method, the bolts are first brought to "snug tight" condition to ensure that the parts of the joint are brought into good contact with each other. Snug tight is defined as the tightness attained by a few impacts of an impact wrench or the full effort of a man using an ordinary spud wrench. In the inelastic region, the load elongation curve of a bolt is relatively flat (Fig. 3.4) so that any variations in snug tightness or accuracy in turning the nut gives only a minor variation in bolt tension. For short grip lengths (less than 4 bolt diameters), one-third turn of nut is specified, and if the grip length exceeds 4 bolt diameters but does not exceed 8 bolt diameters, one-half turn of nut is sufficient from snug tight condition to produce the minimum specified tensile force in the bolt (proof load or 70% of minimum specified tensile strength).

In practice, the bolt tension using the turn-of-nut method may exceed substantially the required minimum tension specified in the codes. In a large number of tests conducted at Lehigh University [38], it was noted that the average bolt tension in these joints was about 20% and 26% greater than the required minimum tension specified for A325 and A490 bolts respectively. The bolts used in these tests were purposely ordered to minimum tensile strength requirements applicable to ASTM

Specifications. Since the average tensile strength of A325 bolt is about 18% higher than the minimum specified strength in the specifications and that the average clamping force is about 80% of the actual tensile strength, it follows that the actual bolt tension is about 95% of the specified minimum tensile strength. Hence, the average bolt tension will likely exceed the specified bolt tension by approximately 35% when the turn-of-nut method is used to install the bolt. A value of about 30% over the specified value was also noted in our tests. Considering field tightening conditions and future losses in bolt tension, it is reasonable to assume the predictable bolt tension as 80% instead of 70% of the minimum tensile strength.

The latest RCRBSJ and CSA Specifications [37, 42] permit high-strength bolts to be tightened by use of a direct tension indicator, provided that it can be demonstrated by an accurate direct measurement procedure that the bolt has been tightened to the specified tension value. A direct tension indicator is any device which provides characteristics which can be measured and related to bolt tension. Several systems which fall into this category have been developed such as the "Swedge-bolt" [46] and load indicating washers [47] which are commercially available.

As the turn-of-nut method has been found to produce uniform control of bolt tension in the simplest manner [48] this method is recommended to be used for LSB joints.

Powered wrenches can be conveniently used for turn-of-nut tightening. Adequate wrenches, of reasonable weight, are now available which will easily tighten bolts requiring tension of 650 kN or enough for a 36 mm dia. bolt of A490M. Wrench sockets should be marked on the outer

periphery for each 60 degrees to enable the operator to easily measure nut rotation. Many erectors still use torque-control electric driven or pneumatic impact wrenches. These wrenches can be used to tighten by the turn-of-nut method by simply eliminating the torque cut-off device. Field gangs and supervisory staff can be easily educated about this simple procedure [52].

3.6.3 Inspection

In order to ensure that the bolts have the desired preload, field inspection, especially for LSB joints, is essential.

Bolts tightened by the turn-of-nut method may have the outer face of the turned element match-marked with the reference element after snug tightening. This affords the inspector a visual means of noting the actual nut rotation. Such marks can be made by the wrench operator with a crayon or dab of paint, after the bolts have been brought up snug tight.

Although visual inspection is an important part of the inspection procedure, the use of calibrated torque wrenches as a measure of tension in the tightened bolt is still the basic final test available to the Inspector. The inspection procedure using calibrated torque wrench is contained in RCRBSJ and CSA Specifications [37, 42].

3.6.4 Losses in Bolt tension

Immediately after a bolt is tightened, a loss in bolt tension occurs. This is thought to result from creep in the threaded portions and plastic flow in the steel plates under the head and the nut. Relaxation studies on assemblies with high strength bolts performed in Japan

[49] have shown that the major portion of losses in bolt tension occurred in the first few days of installation. By extrapolating the test data it was concluded that the relaxation after 100,000 hours (11.4 years) could be estimated at about 6% of the bolt tension immediately after tightening. Similar studies were carried out on over-size and slotted holes at Lehigh University [43]. It was observed that virtually all of the losses occurred within one week after installation. The loss in bolt tension was observed to be about 8% of the initial preload.

According to the tests conducted on LSB joints, it was seen that the total losses in bolt tension due to normal relaxation after 3 days of installation and including those due to additional relaxation on completion of cyclic tests were up to a maximum of 10%. In the case of brake lining pads it is, however, recommended to retighten the bolts after one or two hours of the initial tightening to recover the loss due to compression of the pad. It is also desirable to consider 5% additional loss over and above normal loss when using these pads.

3.6.5 Reuse of Bolts

Since the tension in the bolt exceeds the elastic limit of the threaded portion, reuse of the bolts once tightened may be undesirable. The earlier research at Lehigh University [50], has shown that cumulative plastic deformations caused a decrease in the A325 bolt deformation capacity after each succeeding turn. In the case of A490 bolts, subsequent reuses showed a sharp decrease in induced bolt tension.

Considering the meager cost of the bolt and importance of the desired preload in the bolt, reuse of bolts is not recommended in the case of LSB joints.

3.6.6 Use of Washers

Earlier tests [51] showed that a hardened washer makes no difference in the value of the bolt relaxation resulting from the high stress concentration under the bolt head or nut in connections assembled with A325 bolts. Such relaxations were less than 5% for standard size holes. The losses took place within hours of bolt tightening, after which further loss of tension was negligible. These tests also showed that any galling which takes place when nuts for A325 bolts are tightened directly against the connected parts is not detrimental to the static or fatigue strength of the joint. However, to minimize irregularity in torque-tension ratio when the bolts are tightened by the calibrated wrench method, a hardened washer is still required under the turned element. The washers are also required with A490 bolts in steel parts having a specified minimum yield point less than 275 MPa (40 ksi) to reduce galling of these parts. Without a hardened washer under the turned element, the galling may be of such a magnitude that if a torque wrench is used, before the required rotation or minimum tension is achieved, resistance to turning may be very high. Because of this, some erectors always prefer to use a hardened washer under the turned element regardless of the tightening method specified.

When oversize or short slotted holes are used in outside plies of connected parts, standard hardened washers are required to provide adequate bearing area. When long slotted holes are used, experimental evidence has shown that a rectangular washer or a continuous plate of at least 8 mm plate with standard holes is necessary to provide adequate bearing. This washer or plate is of structural grade material, not

necessarily hardened, and has a size sufficient to cover completely the slot after installation. Since the inspection of the assembly for bolt tension is to be finally made with a calibrated torque wrench, it is preferable to use a hardened washer over the outer surface of the plate washer.

3.6.7 Evaluation of Slip Load

The average dynamic slip load of LSB joints can be expressed in the following equation :

$$\begin{aligned} P_{d(av)} &= K_s \alpha \beta m n T_i \\ &= K_{d(av)} m n T_i \end{aligned} \quad (3.4)$$

Table 3.6 gives the average dynamic slip coefficients, $K_{d(av)}$, for sand blasted and brake lining surfaces. Assuming that the tension in the bolt is 80% of the minimum specified tension strength and that the net area of a threaded bolt is on an average 0.75 of the nominal shank area (actually it varies from 0.74 for 16 mm dia. to 0.77 for 24 mm dia.), the equation 3.4 can be rewritten as :

$$\begin{aligned} P_{d(av)} &= K_{d(av)} . m . n . 0.8 \sigma_u . 0.75 A_b \\ &= 0.6 K_{d(av)} . m . n . \sigma_u . A_b \end{aligned} \quad (3.5)$$

Table 3.7 gives the average dynamic slip loads for different bolt sizes of grade A325M and A490M for sand blasted and brake lining surfaces.

3.6.8 Joint Stiffness

Load-displacement relationship of LSB joints is shown in Fig. 3.13. The initial joint stiffness, K_0 , is basically in the elastic range and is made up of the stiffness of the connecting plates. It is assumed that

up to this load, the deformations in the inserts and its anchors in the concrete panels are insignificant. The deformation Δ_i of the connecting plate is given by the equation :

$$\Delta_i = \frac{P\ell^3}{3EI} + \frac{P\ell}{G.A_s} \quad (3.6)$$

in which the first term on the right hand side is the flexural component and the second is the shear component, G = shear modulus and A_s = effective shear area which is $\frac{1}{1.2}$ of the rectangular sectional area.

The deformations obtained with this equation agree closely to those obtained from actual experimental results.

$$\text{Stiffness } K_0 = \frac{P}{\Delta_i} = \frac{1}{\frac{\ell^3}{3EI} + \frac{1.2\ell}{G.A}} \quad (3.7)$$

As the connection slips, K_1 is zero. On reaching the end of the slot the bolt goes into bearing. At this stage deformations are due to the bolt in shear, the plate in bearing and for the inserts anchored in the concrete. It is difficult to compute the deformations due to these influences, but from experimental results, it is reasonable to assume the stiffness K_2 as one-half of the stiffness K_0 . In any case, this stage is not of much importance as it is avoided except in extreme loading situations.

3.7 SUMMARY

The laboratory tests have demonstrated that the proposed slipping joints, designed to exhibit "elasto-plastic" behaviour possessing reasonably stable hysteretic behaviour, are an efficient means of energy dissi-

pation . Moreover, the process of energy dissipation by LSB joints is through friction only without yielding or structural damage, thus no repairs are necessary after the event.

The tests have demonstrated the performance of different faying surface treatments under cyclic load reversals in long slotted holes. The commonly known externally applied surface treatments, although they may possess high static slip coefficients, are not suitable for cyclic loads as they undergo wide variations in behaviour. A predictable and repeatable load is an important requirement to ensure a known response of the structure during several ground motion and is difficult to achieve with most surfaces. The use of brake lining pads, inserted between the moving steel plates, gives the most desirable characteristic.

Surface Finish	Specimen Type A		Specimen Type B		Specimen Type C	
	Static	Cyclic	Static	Cyclic	Static	Cyclic
Mill Scale	2	2	-	-	-	-
Grit Blasted	4	-	3	3	-	1
Sand Blasted	2	2	-	-	-	-
Zinc-rich paint	4	2	2	2	-	-
Metalized	2	2	-	-	-	-
PVC Coating	-	1	-	-	-	-
Polyethylene Coating	-	2	-	-	-	-
Brake Lining Pads	3	7	-	-	-	-
Total	17	18	5	5	-	1 / 46

TABLE 3.1 - TEST SPECIMENS

Surface Finish	Test Specimen	Bolt Tension, T (kN)	Slip Load, P _s (kN)	Slip Coeff. k _s	Results by Others [38]
Mill Scale	T-13	78	41	0.26	0.322
	T-14	78	49	0.31	
	Average	78	45	0.29	
Grit Blasted	T-1	78	87	0.56	0.527
	T-2	76	66	0.43	
	T-3	78	58	0.37	
	T-4	78	70	0.56	
	Average	77	70	0.45	
Sand Blasted	T-11	78	75	0.48	0.603
	T-12	74	70	0.47	
	Average	76	72	0.47	
Zinc-Rich Paint	T-5	75	68	0.45	0.607
	T-6	78	76	0.49	
	T-9	76	74	0.49	
	T-10	76	66	0.43	
	Average	76	71	0.47	
Metalized	T-7	73	112	0.77	0.78
	T-8	73	104	0.71	
	Average	73	108	0.74	
Brake Lining Pads (H-D) in contact with sand blasted plates	T-34	55	76	0.69	--
Brake Lining Pads (H-D) in contact with mill scale surface on plates	T-36	55.5	50	0.45	--
Brake Lining Pads (H-D) in contact with galvanized plates	T-42	55.5	44	0.40	--

TABLE 3.2 - SLIP COEFFICIENTS, STATIO TESTS, SPECIMEN TYPE A

Surface Finish	Test Specimen (type)	Actual Slip Load, P_s (kN)	Estimated Slip Load, P (kN)	Variation
Grit Blasted	T-23 (B)	65	71	7%
	T-24 (B)	68		
	Average	66		
Grit Blasted and filled with grout	T-31 (B)	72	--	About 9% higher than ungrouted specimen
Zinc-rich paint	T-25 (B)	71	72	3%
	T-26 (B)	69		
	Average	70		
Grit Blasted and connecting plates welded on one side	T-33 (C)	125	116	7.8%

TABLE 3.3 - SLIP LOADS, STATIC TESTS - SPECIMEN TYPE B & C

Surface Finish	Test Specimen	Bolt Tension, T (kN)	Initial Dy. slip Load, P _d	Dy. Slip Coeff., k_d	Static Slip Coeff., k_s (from Table 3.2)	$\frac{k_d}{k_s} = \alpha$	Dynamic Slip Load after Major Slip	Ratio of Initial Slip Load to Major Slip Load
Mill Scale	T-15	73	32	0.20			28	
	T-16	74	30	0.20			28	
	Average	76	31	0.20	0.29	0.71	28	0.9
Sand Blasted	T-17	76	44	0.29			40	
	T-18	71	51	0.36			44	
	Average	73	47	0.32	0.47	0.68	42	0.91
Zinc-rich Paint	T-19	73	77	0.53			60	
	T-20	76	70	0.46			67	
	Average	74	73	0.49	0.47	1.06	63	0.88
Metalized	T-21	74	100	0.67			100	
	T-22	77	52	0.33			46	
	Average	75	76	0.50	0.74	0.68	73	0.98
Brake Lining Pads (H-d) in contact with sand blasted surface	T-35	55	32	0.29	0.69	0.42	30	0.93

TABLE 3.4 - DYNAMIC SLIP COEFFICIENT, SPECIMEN TYPE A

Surface Finish	Test Specimen	Bolt Tension, T (kN)	Initial Dy. Slip Load, P _d	Dy. Slip Coeff., k_d	Static Slip Coeff., k_s (from Table 3.2)	$\frac{k_d}{k_s} = \alpha$	Dynamic Slip Load after Major Slip	Ratio of Initial Slip Load to Major Slip Load
Brake Lining Pads (H-D) in contact with mill scale surface	T-37	55	40	0.36			40	
	T-46	55	40	0.36			39.5	
	Average	55	40	0.36	0.45	0.80	40	1.0
Brake Lining Pads (H-D) in contact with galvanized surface	T-43	55	42	0.38			20	
	T-44	55	49	0.42			25	
	Average	55	45	0.40	0.40	1.0	22	0.5
Brake Lining Pads (ordinary) in contact with mill scale surface	T-38	55	30	0.27			28	
	T-39	55	26	0.24			26	
	Average	55	28	0.25	--	--	27	1.0
P.V.C. Coating on sand blasted surface	T-45	77	11	0.07	--	--	15	1.42
Polyethylene coating on sand blasted surface	T-40	78	12	0.08			12	
	T-41	77	15	0.10			15	
	Average	78	13	0.09	--	--	13	1.0

TABLE 3.4 - DYNAMIC SLIP COEFFICIENT, SPECIMEN TYPE A (CONT'D)

Surface Finish	Energy dissipated per cycle (Joules)										Degradation factor, β compared to first cycle			Predictability ratio $(\frac{j}{h})$
	cycle 1	cycle 3	cycle 5	cycle 10	cycle 15	cycle 20	Min. (cycle)	Av.	Max. (cycle)	Min. $(\frac{h}{b})$	Av. $(\frac{i}{b})$	Max. $(\frac{j}{b})$		
a	b	c	d	e	f	g	h	i	j	k	l	m	n	
Mill Scale	1020	760	690	990	1040	880	640 (7)	900	1200 (22)	0.62	0.88	1.17	1.88	
Sand Blasted	1600	1520	1530	1520	1770	1550	1520 (11)	1580	1770 (15)	0.95	0.98	1.10	1.16	
Zinc-rich Paint	2180	1670	1430	1190	1120	1080	1080 (20)	1450	2180 (1)	0.50	0.66	1.00	2.00	
Metallized	1680	2000	2110	2220	2370	2480	1680 (1)	2140	2510 (24)	1.00	1.27	1.49	1.49	
Brake Lining Pads over mill scale surface	2120	2100	2080	2070	2050	2050	2050 (20)	2070	2120 (1)	0.97	0.98	1.00	1.03	
Brake Lining Pads over sand blasted surface	1400	1100	1150	1150	1150	1030	1030 (20)	1160	1400 (1)	0.73	0.82	1.00	1.37	

TABLE 3.5 - ENERGY DISSIPATION, SPECIMEN TYPE A

Surface Finish	Energy dissipated per cycle (Joules)										Degradation factor, β compared to first cycle			Predictability ratio $(\frac{1}{h})$
	cycle 1	cycle 3	cycle 5	cycle 10	cycle 15	cycle 20	Min. (cycle)	Av.	Max. (cycle)	Min. $(\frac{h}{b})$	Av. $(\frac{1}{b})$	Max. $(\frac{1}{b})$		
a	b	c	d	e	f	g	h	i	j	k	l	m	n	
Brake Lining Pads over galvanized surface	1300	1120	950	950	925	925	925 (20)	1025	1300 (1)	0.71	0.78	1.00	1.41	
P.V.C. Coating on blasted surface	750	1140	1500	1650	1550	1520	750 (1)	1350	1650 (10)	1.00	1.8	2.20	2.20	
Polyethylene coating over sand blasted surface	460	640	550	500	450	420	420 (20)	500	640 (3)	0.91	1.08	1.39	1.53	

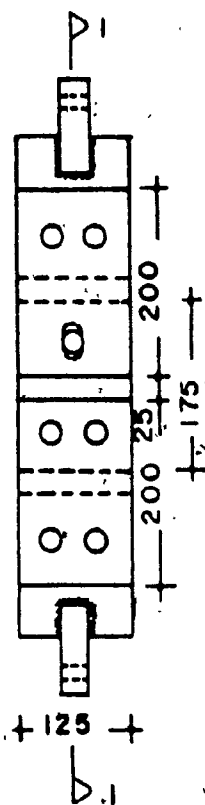
TABLE 3.5 - ENERGY DISSIPATION, SPECIMEN TYPE A. (CONT'D)

Description	Sand Blasted Surface	Brake Lining Pads with Mill Scale Surface
Static slip coefficient, K_s	0.47	0.45
Ratio of dynamic slip load to static slip load, α	0.68	0.80
Degradation factor, β (average)	0.98	0.98
Dynamic slip coefficient, $K_d(av) = K_s \cdot \alpha \cdot \beta$	0.31	0.35

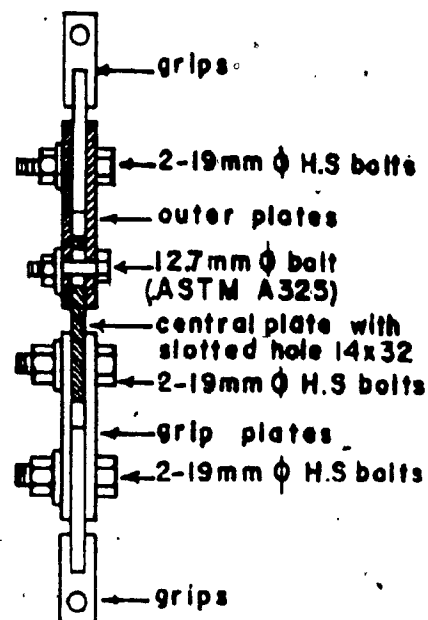
TABLE 3.6 - AVERAGE DYNAMIC SLIP COEFFICIENTS

Bolt Size (metric)	m x n	Average Dynamic Slip Load, kN			
		Sand Blasted Surface		Brake Lining Pads on Mill Scale Surface	
		A325M	A490M	A325M	A490M
M16	1	31	38	35	43
	2	62	77	70	87
	4	124	155	140	175
M20	1	48	60	54	68
	2	97	121	109	137
	4	194	243	219	274
M22	1	59	74	66	83
	2	118	148	133	167
	4	236	296	266	334
M24	1	70	88	80	100
	2	141	177	160	200
	4	282	354	320	400

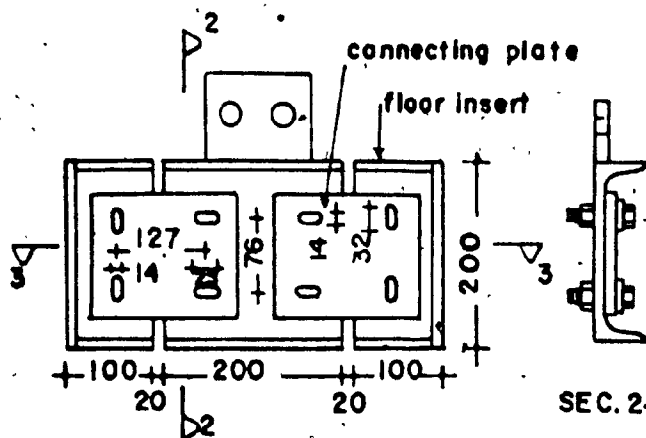
TABLE 3.7 - AVERAGE DYNAMIC SLIP LOADS OF LSB JOINTS



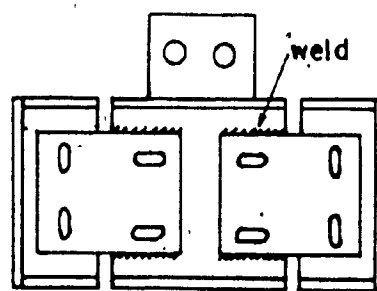
Test specimen type A



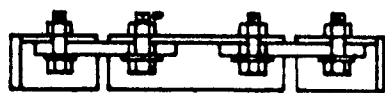
SEC.1-1



SEC.2-2



Test specimen type C



SEC.3-3

Test specimen type B

FIG. 3.1 - DETAILS OF TEST SPECIMEN

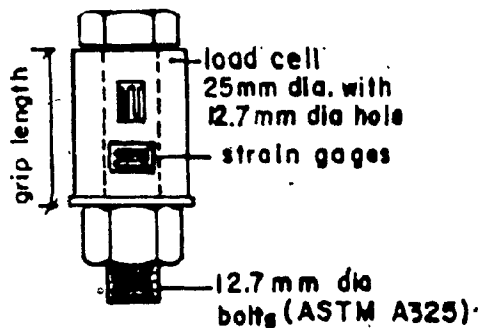


FIG. 3.2 BOLT CALIBRATION CELL



FIG. 3.3 BOLT CALIBRATION PROCEDURE

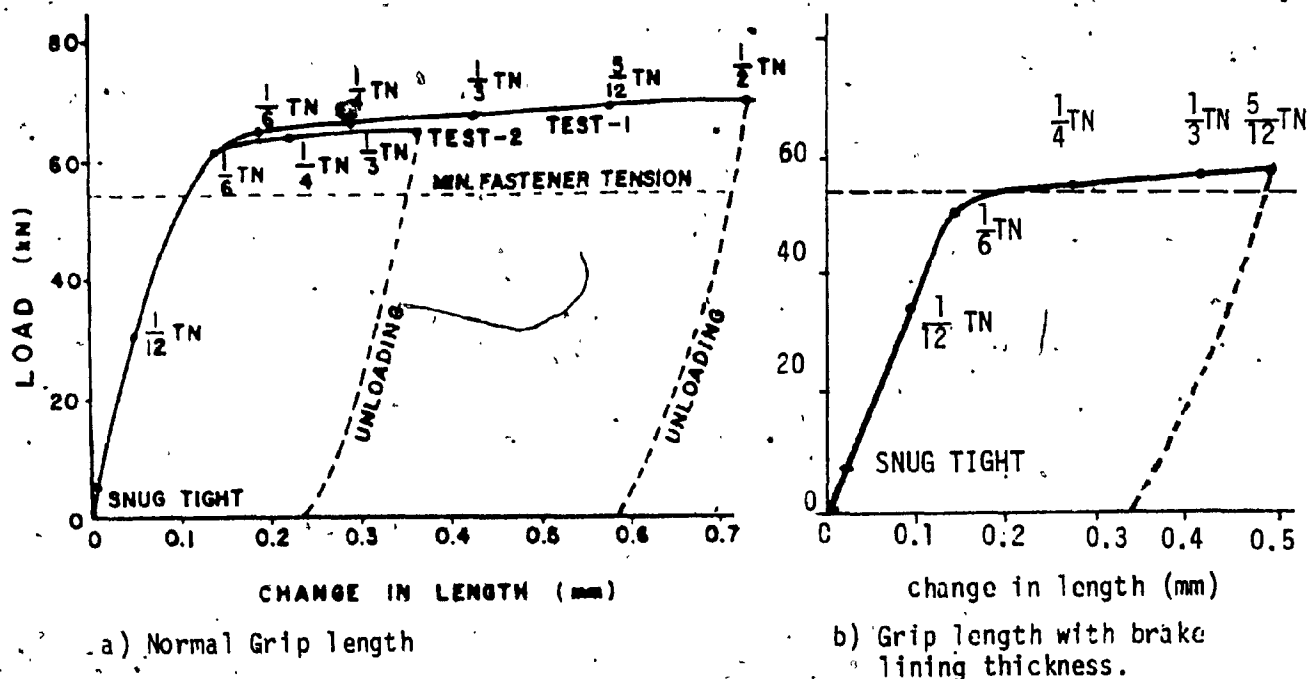


FIG. 3.4 LOAD CALIBRATION CURVE FOR BOLT OF SPECIMEN TYPE A



FIG. 3.5 INSTRON MACHINE, TESTING SPECIMEN TYPE A.

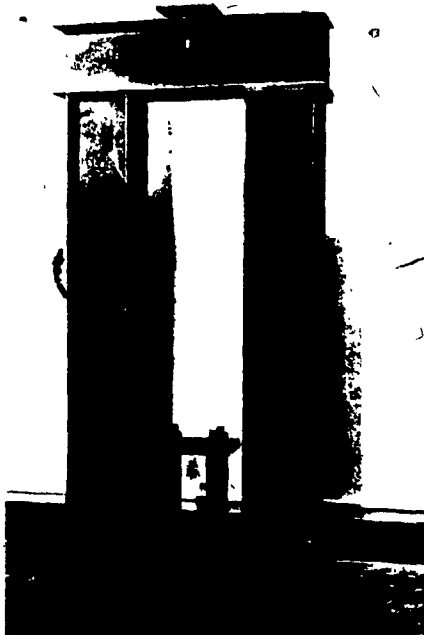


FIG. 3.6 REACTION FRAME



FIG. 3.7 TESTING SPECIMEN TYPE-B USING REACTION FRAMES

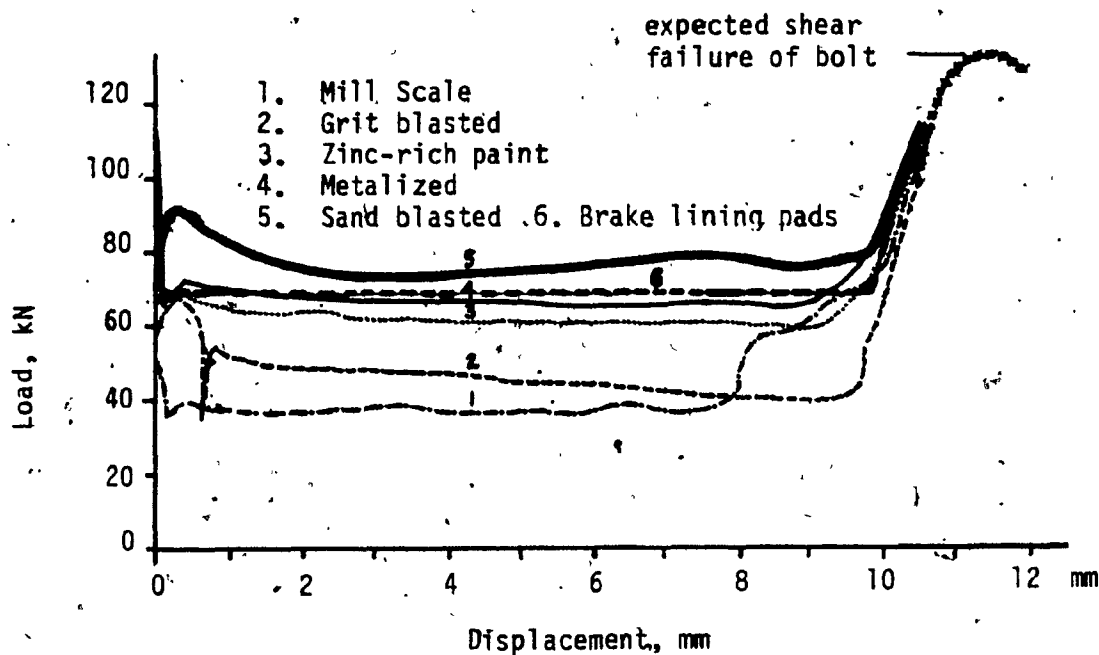


FIG. 3.8 LOAD DISPLACEMENT CURVE, WALL-TO-WALL JOINT

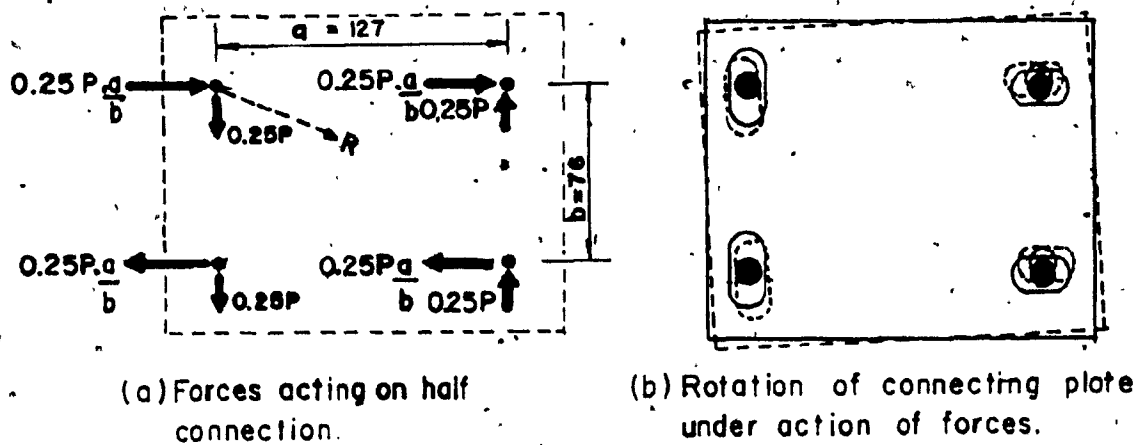
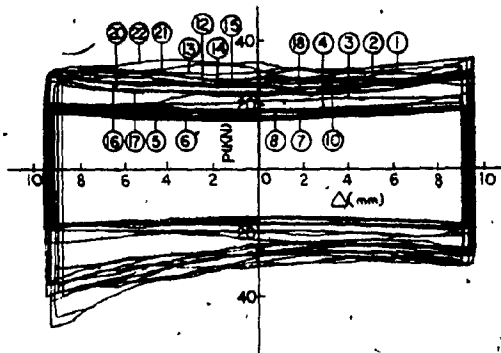
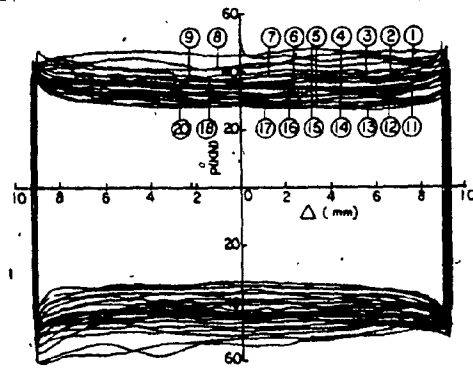


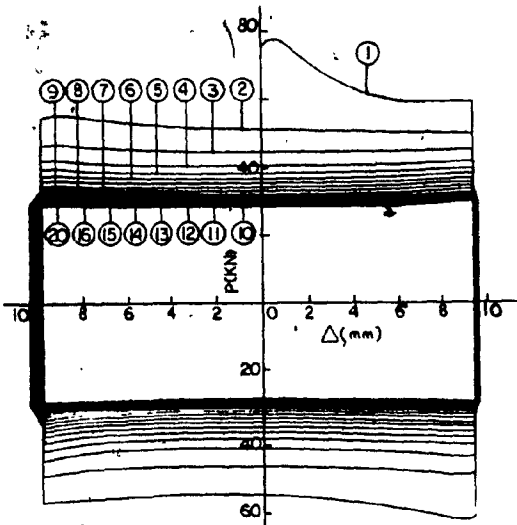
FIG. 3.9 - BEHAVIOUR OF SPECIMEN TYPE 'B'



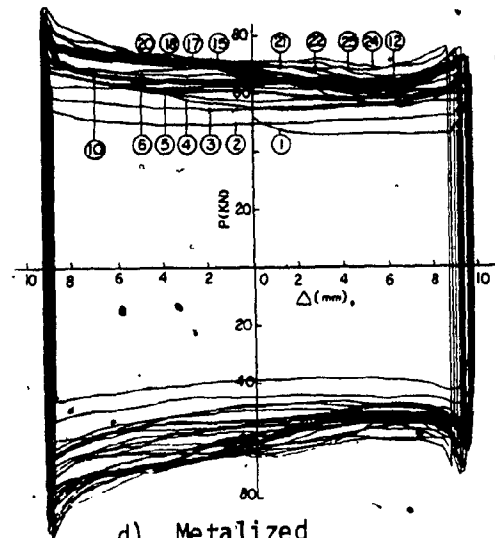
a) Mill Scale



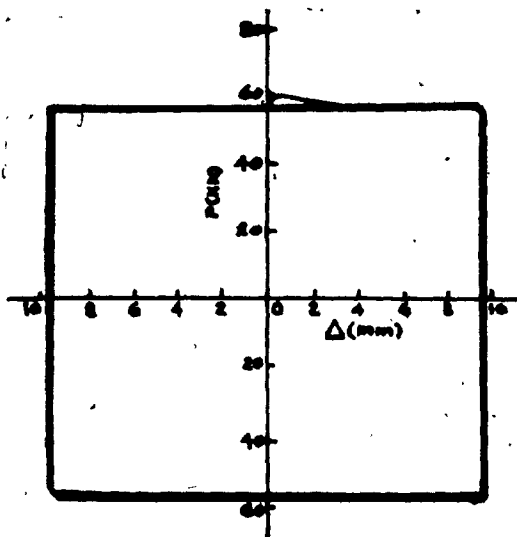
b) Sand Blasted



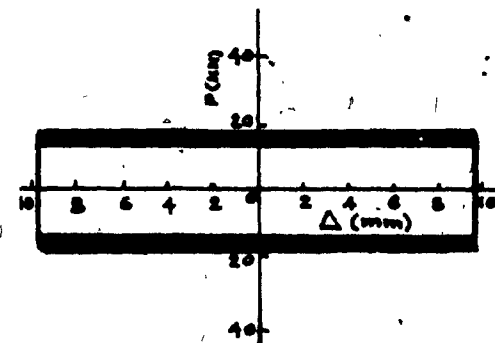
c) Inorganic Zinc-Rich Paint



d) Metalized



e) Brake Lining Pads



f) Polyethylene Coating

FIG. 3.10 - HYSTERESIS LOOPS, WALL-TO-WALL JOINT

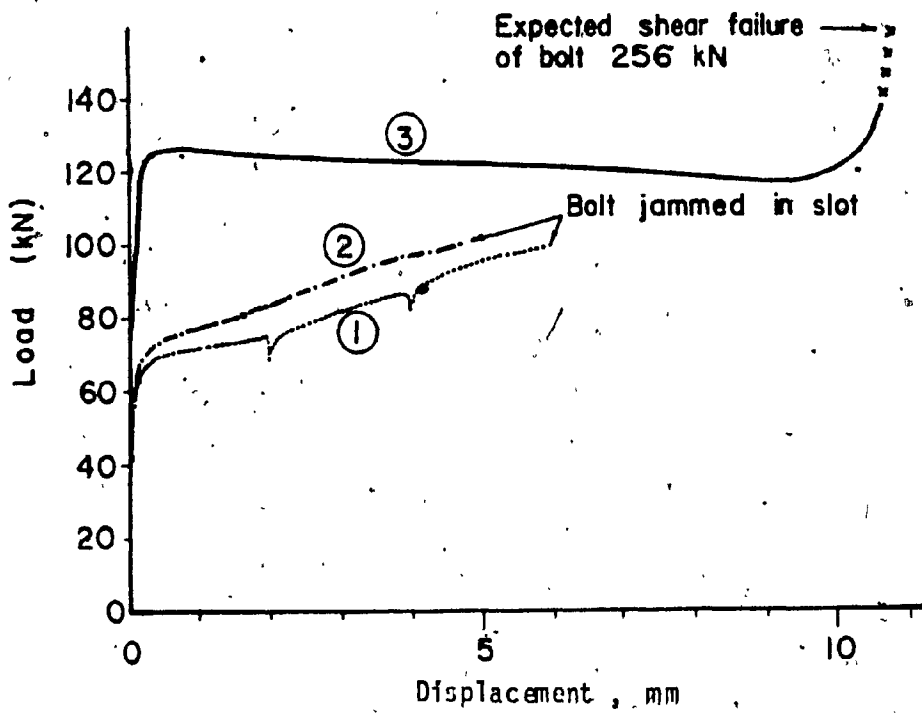
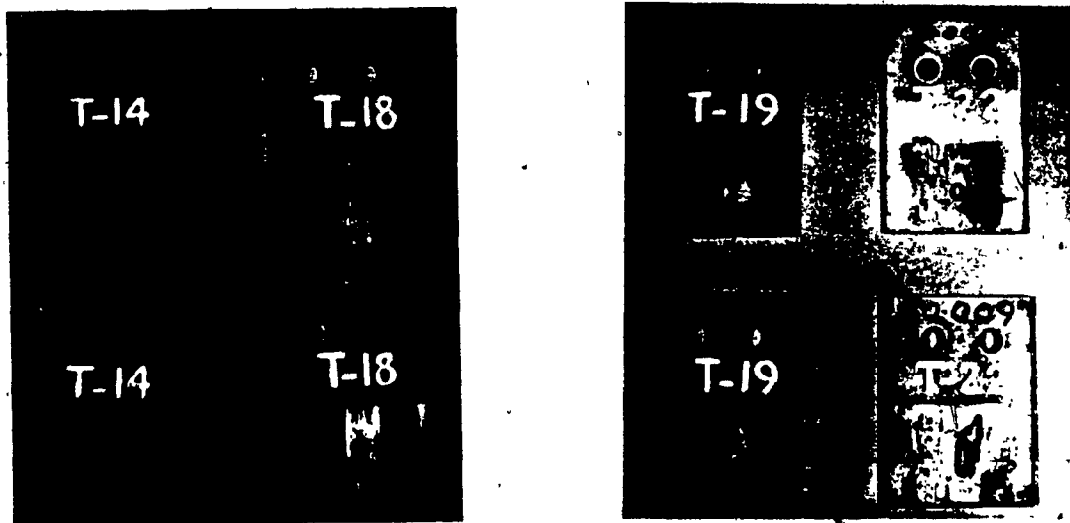


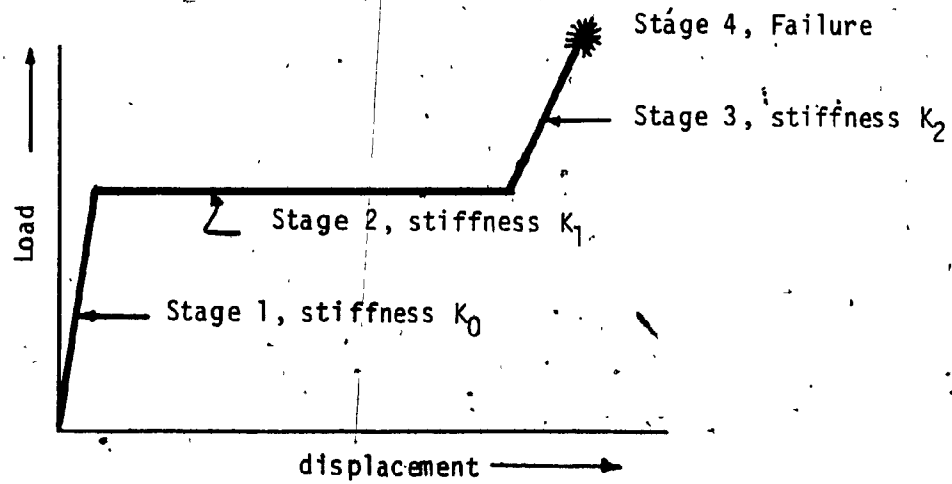
FIG. 3.11 LOAD-DISPLACEMENT CURVE, SPECIMEN TYPES B&C



T-14 Mill Scale, T-18 Sand blasted

T-19 Zinc rich paint, T-22 Metalized

FIG. 3.12 SURFACE CONDITION AFTER 20 CYCLES OF REVERSALS



Load-Displacement Curve, LSB Joint

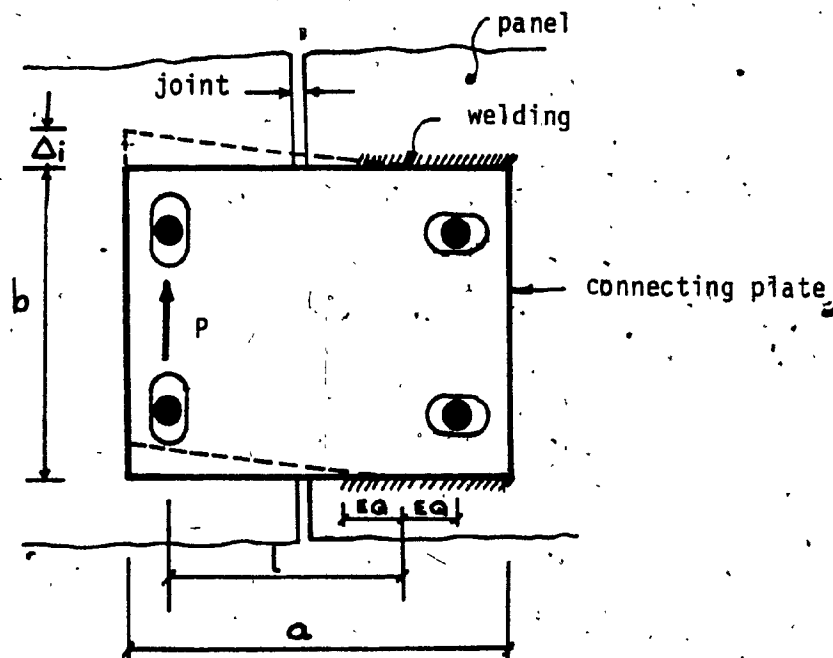


FIG. 3.13 JOINT STIFFNESS

CHAPTER IV
MODELING PROCEDURE AND ANALYSIS

CHAPTER IV

MODELING PROCEDURE AND ANALYSIS

In large panel construction the structural system resisting the lateral forces consists of the wall panels connected along horizontal and vertical joints forming shear walls. The floor system, also made of panels, ties together various walls and provides necessary horizontal diaphragm action. For normal service loads, wind forces, and low amplitude ground motions the response of large panel buildings is basically linear elastic and analysis for them is no different from that for conventional buildings with cast in place shear walls. During severe seismic excitations, there may be slip along the joints between the panels giving rise to considerable redistribution of forces, moments and change in response. Thus, the structural behaviour of the large panel shear wall system is predominantly influenced by the characteristics of the joints.

The primary concern in this project is to study the participation of limited-slip bolted joints in improving the seismic response of large panel structures. With this in mind, the chapter begins with the review of different structure idealization techniques in regard to their suitability for dynamic modeling of panelized structures. This is followed by the selection of a model, method of seismic analysis, and the description of the computer program. Then, the modeling of a typical apartment building and preliminary analysis including the results obtained are described.

4.1 METHODS OF STRUCTURE IDEALIZATION

An important first step in the analysis of a structure is the selection of an appropriate idealized model which can include all the working elements and their significant role. A concise survey of literature on methods of analyses for shear wall structures was presented by Coull and Stafford-Smith [53]. Methods of analysis, which are based on some form of idealization, have also been summarized in tabular form by McLeod [54]. Basically there are four types of modeling techniques for analysis of shear walled structures which are equally applicable to panelized structures. These are the beam model, the continuous medium method, the frame analogy method and the finite element method. A vast literature is available that describes these analytical techniques but mostly these are addressed to static elastic behaviour. An update of current dynamic research, as applicable to large panel structures, is provided by Becker et al. [7]. The choice of a particular method is based on the required accuracy, the time factor, cost of analysis and above all suitability to tackle a particular problem. Structural idealization using different approaches are shown in Fig. 4.1. A brief summary of these methods, along with their suitability for nonlinear dynamic modeling of panelized structures, is discussed below.

4.1.1 Beam Model

This is the most inexpensive model and is ideally suitable for hand calculations. For a fairly regular structure, as is normally the case with panelized structures in which mass and stiffness are well distributed over the full height, a single degree of freedom behaviour

as a cantilever beam is approximated. This provides an easy and quick means of estimating the fundamental period, mode shapes and forces. For higher levels of accuracy, effects of shear deformations and rotational degrees of freedom could be incorporated. It is not, however, very effective as an analytical tool in predicting nonlinear response.

4.1.2 Continuous Medium Method

In this method, the individual connecting beams or linkage connections can be effectively treated as an equivalent continuous medium in pure shear Fig. 4.1b. Under horizontal loading, the walls deflect and induce shear forces in the medium. A single second order differential equation is set up and solved to give shear forces, moments and deformations throughout the wall. The technique appears to have been used first by Chitty [55] and further developed by Beck [56], Rosman [57] and Coull [58]. Several papers use this approach with differing choice of variables, all essentially yielding the same results. Solutions are available in the form of curves and tables for uniformly distributed loads, triangularly distributed loads and for concentrated point loads [59, 60].

In its basic form the theory assumes that the elastic structural properties of the coupled wall system remains constant throughout, that walls are founded on a common stiff footing, and that the points of contraflexure of all the connecting beams are at mid span. Noticeable error can be introduced through coupling of rigid and flexible walls. Within these limitations, this method has proved to be effective and is relatively simple to use.

The method is equally applicable to panelized buildings with vertical joints, and in fact more accurate since the width of joint is closer than the coupling girder span and the assumption of replacing the girders with continuous shear medium is more closely represented. Experiments on model structures made of plastic have yielded results in good agreement with values given by the theory [61]. This method has been extensively used for the analysis of large panel buildings [3, 22, 61, 62]. Dynamic analysis, although not commonly done can be performed using the continuous medium method by discretizing the system in a manner similar to that in the beam method [22].

4.1.3 Frame Analogy Method

In this method, more popularly called Wide Column Frame Analogy, the walls and beams are represented by line members of corresponding stiffness along their centroidal axis, the influence of the finite width of the wall being incorporated by a stiff arm connecting the ends of the beam to the centroidal axis of the wall as shown in Fig. 4.1c. The flexible line elements can be deformed axially, in bending and in shear. This method can be more easily adapted to deal with general systems of walls and can take into account changes in dimensions and properties of the walls, and different types of connecting beams. Analyses can be carried out using a standard plane frame computer program and is a convenient design tool since the output comes out in the form of forces, shears and moments.

A very versatile modeling technique which has been extensively used for modeling panelized structures [3, 8, 84], this method can handle most types of linear and nonlinear aspects and can be easily

adapted for dynamic analysis.

4.1.4 Finite Element Method

The framework elements as proposed by Hrennikoff [63], McHenry [64], and McCormick [65] for lattices and by Grinter [66] for grids were forerunners of the finite element method. In the framework method the continuum of the structure is replaced by an equivalent framework of elements which are made up of a number of bars arranged in a pattern governed by the size and nature of the elements. The weakness of this method is its difficulty in developing higher order elements. Furthermore, the solution requires a considerable amount of computation. The main advantages of framework elements over finite elements is that these can be used over with a standard plane frame program. However, the latter method gives more accurate results for the same computational effort.

In the finite element method, the continuum of the structure is represented by finite regions which are all interconnected at the nodes. There exists a large variety of elements which can be selected for a specified problem. In panelized structures, the partitioning will generally correspond to the panels. In this approach, the internal degrees of freedom of each substructure are eliminated through static condensation. The static condensation thus allows the creation of super elements that correspond to actual panels and the main structure can be analyzed as an assemblage of these super elements in a manner directly analogous to the actual structure.

The accuracy of the analysis depends on the fineness of the mesh or the use of a refined element which contains a complex strain distribution, both of which affect cost. It is therefore often necessary to make some sort of compromise between the desired level of accuracy and the computational costs. The output is given in the form of stresses.

The finite element method is the most versatile and also the most rigorous of the modeling techniques used in analyzing the behaviour of structural system. This method has been extensively used in modeling the static and dynamic behaviour of shear walls and panelized structures [17, 18, 67, 68, 69, 70, 71, 72, 73, 74].

This technique can handle static and dynamic analysis in both linear and nonlinear stages.

4.2 CHOICE OF MODEL

The modeling techniques discussed in the foregoing section present a wide spectrum of available methods. Each one of the methods has relative merits over the other and has its own limitations to tackle the problem. The cost of analysis and degree of accuracy desired are the other important parameters to be considered. For example, one should not choose a highly refined finite element model where a simple beam model would suffice. Nor would one choose a continuum model to analyze a structure with irregular properties.

The main object of the analysis in the present research project is to investigate the participation of LSB joints in improving the seismic performance of large panel structures rather than pursue an elaborate comparison of methods of analysis. Knowing that nonlinear dynamic behaviour of panelized buildings is inevitable, only two methods,

namely frame analogy and finite element method, are considered to be appropriate modeling techniques. The next question is whether it is necessary to use a finite element method when a simple frame analogy could be sufficient without sacrifice of any accuracy.

An earlier study was made by Unemori [75] to assess the suitability of two methods of analysis for coupled cross wall systems. To evaluate the accuracy involved in using the frame analogy as a function of height, as well as to substantiate the claim that reverse bending, that apparently arises in the wide column analogy, does not lead to any inaccuracy, static analysis of planar coupled walls with 5, 10 and 15 story heights were run using the two techniques. The average top deflection agreed within 1% for all the three heights. Results using a frame analogy, including shear deformations, were in good agreement with those obtained with finite element models. In fact, unless a relatively fine mesh, with a very large number of degrees of freedom, is used for the finite element idealization, the results provided by this more expensive model would be less accurate than those by an equivalent frame. Using a relatively coarse mesh, the static deflections resulting from the finite element model differed from those of the frame by about 15% leading to a variation of about 7% in fundamental period.

A large scale model of a 10 story large panel building, excited on a shaking table, was tested in Rumania [6]. It was concluded that "by comparing the results of various methods of analysis used in elastic behaviour range to the experimental data, it was found that the most suitable method is that of an equivalent frame, whose stiffnesses are determined by considering both bending and shear deformations".

Based on the earlier analytical and experimental studies, it was decided to use the wide column frame analogy for studying the participation of LSB joints in improving the seismic resistance of panelized buildings.

4.3 SEISMIC ANALYSIS

As already stated, the panelized buildings will invariably behave in a nonlinear manner when subjected to severe seismic action, the nonlinearity being introduced by the joints which are weaker and less stiff than the panels themselves. The method of dynamic response analysis based on linear elastic assumption, although convenient and economical, does not provide information on the nonlinear behaviour of the structure or its components.

4.3.1 Nonlinear Time History Dynamic Analysis

The only generally applicable method for the analysis of nonlinear systems is the numerical step-by-step integration of coupled equations of motion. The response history is divided into short equal time increments and the response is calculated during each increment for a linear system having the properties determined at the beginning of the interval. At the end of the interval, the properties are modified to conform to its state of deformation and stress at that time; thus the nonlinear analysis is approximated as a sequence of analyses of successively changing linear systems.

The dynamic equilibrium equation of a system of structural elements can be expressed in the following matrix form :

$$[M]\{\ddot{u}_t\} + [C]\{\dot{u}_t\} + [K]\{u_t\} = \{P_t\} \quad (4.1)$$

where $\{u_t\}$, $\{\dot{u}_t\}$ and $\{\ddot{u}_t\}$ are vectors of nodal point displacement, velocity and acceleration, respectively, at time 't'. In the case of earthquake forces, the load vector $\{P_t\}$ is a function of the mass matrix and ground acceleration \ddot{x} at time 't'. $[M]$ is the mass matrix and $[C]$ and $[K]$ are the tangent values of the damping and stiffness matrices for the structure in its current state. For a finite time step Δt , the following equation is approximately satisfied :

$$[M]\{\Delta\ddot{u}_t\} + [C]\{\Delta\dot{u}_t\} + [K]\{\Delta u_t\} = \{\Delta P_t\} = -[M]\{\Delta\ddot{x}_t\} \quad (4.2)$$

where $\{\Delta u_t\}$, $\{\Delta\dot{u}_t\}$, $\{\Delta\ddot{u}_t\}$ and $\{\Delta P_t\}$ are the finite increments of displacement, velocity, acceleration and force vector respectively. Damping and stiffness matrices correspond to the state of the structure at the beginning of the time step.

During the time step, changes in the state of the structure may take place and the new state obtained by solving Eq. 4.2 may not exactly satisfy equilibrium. Corrective forces are therefore applied during succeeding time steps to compensate for these errors.

With regard to response history, the assumption of linear variation of acceleration provides an efficient step-by-step integration procedure so long as short enough time increments are used. The method is known to be unstable in the presence of vibration modes with periods less than approximately three times the time step. Modifications [76] to the basic method which eliminate stability problems tend to introduce damping in the higher frequencies of the system. Another approach, suggested by Newmark [77], is to adopt constant acceleration within the time step. This method has the advantage of being stable for all periods and time steps and of not introducing damping into the system.

For vibration modes with longer periods, the response computed by the constant acceleration method may be slightly less accurate than by linear acceleration method but is sufficiently accurate for practical purposes.

4.3.2 Time Step

In general, time increments must be short enough to permit the realistic representation of the forcing function (seismic record) and response of the system i.e. period of vibration of the structure. Greater accuracy can be expected as the integration time step is reduced. To minimize the computation effort, however, it is desirable to select as long a time step as possible.

In general, the increment Δt may not be larger than one-tenth of the fundamental period [78]. For seismic records, in which the high frequency content of the acceleration is important, a time step increment of the order of a hundredth of a second is considered adequate. In case of any doubt, a second analysis can be made having a new time increment to see if the results are appreciably changed.

4.3.3 Damping

The viscous damping matrix $[C]$ in the elastic elements of the structure can be considered to result from mass and stiffness dependent effects known as Rayleigh's damping, and is given by the following matrix equation :

$$[C] = \alpha[M] + \beta[K] \quad (4.3)$$

where α and β are constants to be determined from two given critical damping ratios that correspond to two frequencies of vibration [79].

From the relationship

$$C_i = 2\lambda_i \omega_i M_i$$

and

$$K_i = \omega_i^2 M_i$$

We get

$$2\omega_i \lambda_i = \alpha + \beta \omega_i^2$$

or

$$\lambda_i = \frac{1}{2} \left(\frac{\alpha}{\omega_i} + \beta \omega_i \right)$$

or

$$\begin{Bmatrix} \lambda_i \\ \lambda_j \end{Bmatrix} = \frac{1}{2} \begin{bmatrix} \frac{1}{\omega_i} & \omega_i \\ \frac{1}{\omega_j} & \omega_j \end{bmatrix} \begin{Bmatrix} \alpha \\ \beta \end{Bmatrix}$$

or

$$\begin{Bmatrix} \alpha \\ \beta \end{Bmatrix} = \frac{2\omega_i \omega_j}{\omega_j^2 - \omega_i^2} \begin{bmatrix} \omega_j - \omega_i \\ -\frac{1}{\omega_i} & \frac{1}{\omega_j} \end{bmatrix} \begin{Bmatrix} \lambda_i \\ \lambda_j \end{Bmatrix} \quad (4.4)$$

For panelized buildings, the viscous damping normally varies from 3-5% in the elastic stage [6, 68, 80]. Since the response is mostly in the lower modes, the damping ratio λ chosen is that for the first mode in Rayleigh's method. In addition to the viscous damping, the analysis must include the effect of hysteretic energy dissipation due to the nonlinear behaviour of the elements.

4.3.4 Input Motion

The principal ground motion characteristic affecting dynamic structural response are intensity, duration and frequency content. Intensity is used as a characteristic measure of the amplitude of the acceleration pulses in a record. Duration refers to the length of the record during which relatively large amplitude pulses occur with

due allowance made for a reasonable build up time. The importance of frequency characteristics of a given input motion lies in the phenomenon of resonance or quasi resonance which occurs when the frequency of the exciting motion approaches the natural frequency of the structure experiencing the motion.

The choice of a suitable ground motion is probably the most difficult and important part of the seismic analysis. Variability in the character of the ground motion at a site makes it desirable to consider a number of representative input motions when determining the likely maximum response of a particular structure. Different records, even though of the same intensity may give widely varying structural responses and design values obtained by using a single record may not be useful.

P.C.A. [81] has carried out a study to classify accelerograms into fairly broad categories according to certain basic properties. Such classification allows reasonably good choice in the estimation of maximum response of structures to potential earthquakes. For linear structures or a structure that experiences only limited yielding under ground excitations, a peaking accelerogram is likely to produce stronger response than a broad-band motion of the same intensity and duration. A peaking accelerogram is one with a velocity spectrum that has its peak approximately centered at the initial fundamental period of the structure considered, Fig. 4.2. In structures where yielding significantly increases the period of vibration, the effect of the dominant frequency in a peaking accelerogram diminishes as the period of the structure moves beyond the peaking range. For such

structures, a broad-band accelerogram of the same intensity is more likely to produce the critical response. Relative velocity response spectra for some ground motions are shown in Fig. 4.3.

4.4 COMPUTER PROGRAM

A general purpose computer program "Drain-2D" [82], developed at the University of California, was selected for nonlinear time history dynamic analysis of the equivalent wide column frame model of large panel structures.

The program consists of a series of subroutines which carry out a step-by-step integration of the dynamic equilibrium equations utilizing a constant acceleration algorithm within any time step. The accuracy of this algorithm is enhanced by the use of a corrector which applies the out of balance loads from the last time step to the present one. The earthquake excitation is defined by time histories of ground accelerations. Analysis is by direct stiffness method with nodal displacements as the unknowns. The structure mass is assumed to be lumped at the nodes so that the mass matrix is diagonal. Subroutines for common types of elements are available. The subroutine for truss elements was modified to represent the LSC joint behaviour. This is described in the next section.

4.5 MODELING

4.5.1 Selection of a Building

A typical apartment building plan, as shown in Fig. 4.4, was chosen for study. The dimensions are representative of a popular cross wall system in large concrete panel construction. The building

is fairly regular in plan and wall/floor panels are of uniform thickness throughout the height. Four buildings of 5, 10, 15 and 20 story height, following the same plan, were considered in the present study.

The two end cross walls are coupled together using two LSB joints per story height whereas interior cross walls are considered coupled at the corridor beam with a single LSB joint. Gravity loads (dead plus live loads) are in accordance with NBC [83]. Details of loads and other properties of wall panels and LSB joints are given in Appendix A.1.

In order to investigate the participation of LSB joints, the analysis is carried out for exterior end walls, which represent the extremely loaded case.

4.5.2 General Modeling Assumptions

Dynamic behaviour of a complete panelized building is an extremely complex problem. To reduce the size of the problem, the following assumptions were made to isolate and examine the most important behavioural mechanism of the vertical joints. Although these assumptions may not be entirely true, they are considered reasonable enough for this type of analysis.

a) Vertical panel walls are considered as continuous elastic cantilevers. Although each cantilever wall includes horizontal joints, in the present analysis it is assumed that gravity loads (or post tensioning if necessary) produce sufficient friction to prevent any shear slip or rocking and the softening of walls due to this is neglected.

b) The floor diaphragms are infinitely rigid in their own planes and distribute the lateral forces on the building between different walls in proportion to their stiffnesses. Based on the research carried

out at MIT [75], the validity of this assumption has been questioned for low-rise panelized structures in which the stiffness of cross walls is often as large as that of panelized floor diaphragms. The assumption of rigid diaphragms is however reasonably valid for crosswall buildings of 10 stories and above.

c) During extreme seismic ground motions when all the joints are in the state of slipping, the exterior end wall is assumed to share approximately one-fourth of the total lateral forces in the short direction of the building (Appendix A-1).

d) Mass and stiffness dependent type viscous damping has been assumed corresponding to 5% of critical damping for elastic panel members. Energy dissipation due to hysteretic behaviour of LSB joints is looked after in the computer program.

e) The panels are assumed to remain in the linear elastic range.

f) Nonlinear behaviour of the structure is limited to the joints only. The stiffness of the joint is a function of the load and the relative displacement of the connected parts.

g) P- Δ effects, i.e action of vertical loads on deflected shape, are insignificant in panelized structure and are neglected.

h) The foundations are rigid and soil structure interaction is ignored. In fact, panelized buildings being very stiff are more sensitive to soil structure interaction. The overall effect of which may be beneficial from the point of view of prolonged primary period and added damping. This assumption is made so as to reduce the complexity of the problem and to concentrate the study on the role of the connections.

4.5.3 Modeling of Panel Walls

The two vertical panel walls forming the end wall are coupled together along the vertical joints by two LSB joints in each story height. Sectional properties of each wall element are shown in Fig. 4.5. The coupled walls are idealized as an equivalent wide column frame. The walls for every story height are represented by line columns of corresponding properties along their centroidal axis and the influence of the finite width of the wall is incorporated by rigid arms which connect the ends of LSB joints to the centroidal axis of the walls. Effects of flexural, axial and shear deformations for the column elements are taken into account by specifying the properties of wall panels. The effect of the rigid arm is incorporated by arbitrarily substituting very high values to the sectional areas and moments of inertia. Sectional properties of beam and column elements used as input data for the computer program, are shown in Appendix A.3. The structure stiffness matrix is assembled by the program from the given data.

Structure idealization for a typical 10 story wall is shown in Fig. 4.5, and is similar for other walls except for the number of stories. Translational displacements for all the nodes at a floor level are assigned identical values since axial deformations in the floor diaphragm are assumed to be negligible. Also due to the assumption that rigid arms are of infinite stiffness and that the two panel walls are of equal dimension, rotational displacement of all the nodes at a floor level are identical. This reduces the number of degrees of freedom and the computation time is greatly reduced. Story masses are assumed to be lumped at the column nodes only.

4.5.4 Modeling of Limited Slip Bolted Joints

There are two LSB joints in each story height and for modeling purpose these are considered as lumped at each floor level. This is done by simply doubling the load and stiffness values of each connection, displacement values remaining unchanged.

The load deformation relationship of a single LSB joint is shown in Fig. 4.6.

These joints are modeled as axial elements (truss elements) yielding both in tension and compression in the vertical direction. The joint behaviour is simulated by specifying fictitious geometric and material properties of the axial element. In order to avoid any numerical problem, a very small length of one centimeter is given to the axial element. This is provided by shifting the centre line of rigid arms. This small difference is not likely to affect the overall results.

In the existing program, only two modes of behaviour, as shown in Fig. 4.7a, can be specified in the truss element, i.e. for the elastic stage and the yielding stage. In the case of elasto-plastic behaviour, infinitely small values of strain hardening ratio $\frac{E_s}{E}$ (say 0.00001) may be specified to avoid any numerical difficulties.

Fictitious truss member properties may be substituted in the following manner to simulate LSB joints. Referring to Fig. 4.7, we get

$$\frac{EA}{L} = k_o = 1.28 \times 10^3 \text{ MN/m}$$

Assigning arbitrary values to E and L of 10 MN/m and 0.01 m respectively, we get

$$\text{Equivalent element area, } A = \frac{1.28 \times 10^3 \times 0.01}{10} = 1.28 \text{ m}^2$$

$$\text{Yield stress of element} = \frac{P_y = P_s}{A} = \frac{320}{1.28} = 250 \text{ kPa}$$

Stages 1 and 2 of LSB joints can thus be modeled using the truss element in the program. In the case of unexpectedly severe earthquakes, the bolts in the connection could go in bearing and eventually fail in shear. Study of the behaviour of the joint in these two stages is necessary to understand the following effects :

- a) Effectiveness in controlling the excessive drift of the building;
- b) Effectiveness in forcing uniform slippage in other connections and thereby utilizing their full energy dissipation capacity;
- c) Effect of impact loading when the bolt hits against the end of the slot;
- d) In the event of failure of a connection as a consequence of impact, will there be a propagation of the failure?
- e) Influence on overall seismic response.

The subroutine of truss element was modified to incorporate stages 3 and 4 of the LSB joint.

The modifications are affected by considering that for stages 1 and 2, the joint consists of two parallel components as shown in Fig. 4.8a, which is the same as that for the existing truss element. On the termination of stage 2, a third elastic component becomes

effective and acts in parallel with the previous two components. In the event of failure of the joint, i.e. stage 4, the unbalanced load is transmitted as a shock load at that point. The load deformation path during each cycle is as shown in Fig. 4.8b. Listing of the relevant 4 subroutines which have been modified to incorporate the above changes are given in Appendix A.2. The description of the input data for the LSB joint is shown in Appendix A.4. The print-out of the element specifications for the LSB joint comes out in terms of the initial stiffness k_0 , slip load, slip length, stiffness ratio for stages 2 and 3 as related to initial stiffness, and failure load. This is shown in Appendix A.5. The modified element for the LSB joint can still be used as a truss element by giving a specific command in the control card as shown in the input data in Appendix A.4. Typical output results for the LSB joint are shown in Appendix A.6. As already indicated on the output results, it may be stated here that the term "accumulated plastic extension" does not apply to LSB joints since there is no actual yielding of the materials. These columns in the output are however kept to be used for the truss element.

4.5.5 Seismic Input

For large panel structures, which have a relatively high yield level, the peaking accelerogram produces the most severe response. El Centro 1940 (N.S.) ground motion, which is of the peaking type was therefore used in the present study. Moreover, this accelerogram is reasonably symmetric and renders it particularly useful for nonlinear studies.

Alternately, it may be preferable to use some form of an average earthquake which is free of any particular bias. The use of an artificial earthquake record, generated at MIT to match the Newmark-Blume-Kapur response spectrum for 2% damping, was also attempted but proved to be very expensive for a 10 story building for a time step of 0.01 seconds and for 15 seconds duration. Using this earthquake record the duration cannot be reduced since the peaking acceleration occurs at 10.3 seconds. This dictated the use of El Centro, 1940 (N.S) ground motion throughout the study. In this study, the duration was limited to the first seven seconds only, which includes the most severe motion, and is followed by fictitious zero accelerations for the next two seconds to allow the structure to come to rest, Fig. 4.13. This is considered to be sufficient to determine the important features of the structural response for panelized structures where the effect of cumulative deformations during a longer duration is not a problem.

For probabilities exceeding 0.01 and 0.005 in 1 year, the peak ground acceleration in seismic zone 3 in Canada, are only 0.08g and 0.25g respectively [83]. In order to make this study broader based rather than regional, the analyses were carried out for peak ground accelerations scaled to intensities of 0.15, 0.25, 0.33 and 0.5 of gravity.

4.6 PRELIMINARY ANALYSIS

In the preliminary study, two walls of 10 and 15 story height were analyzed for peak ground accelerations of 0.25g and 0.08g. A time step of 0.01 second was used for both buildings. To check the accuracy with this time step, a second run was made using a time step of 0.005

seconds for a 10 story wall which gave a difference of only 5%. Considering the savings in computation cost, the accuracy is reasonable enough.

Analyses were also made for walls with stiff elastic joints and for isolated walls, i.e. with no joints. This was done by assigning a very high slip-load value for the first case and zero slip load for the second case. These analyses were made so that a comparison showing the effectiveness of LSB joints could be made.

Results of time histories and maximum envelopes were obtained for displacements, shears, and axial forces for panels and connections.

Quasi-static analyses, as given in NBC [83], were also made for peak ground accelerations of 0.08g (Zone III). Details of these analyses are given in Appendix A.7.

The results of the above studies are summarized below.

- i) It is seen from the analysis that both walls remain within linear elastic stage up to seismic level of 0.08g.
- ii) The quasi-static analysis yields shears which are much less than those which would actually develop in these structures for a seismic level of 0.08g, Fig. 4.9. This is so because for this seismic level, the structures are still within the elastic range rather than in the inelastic range assumed in the code for other buildings. However, the structure has sufficient resistance for higher seismic forces.
- iii) As the connections slip, redistribution of forces in the joints take place until they become almost uniform throughout the

height. One of the advantages of the slipping joints is, therefore, to provide a limit to the load, which is a predetermined value and is independent of seismic intensity. It also allows the full capacity of all the connections to be utilized.

Had the connections been elastic, the distribution of forces would be as shown by the dotted lines in Fig. 4.10. The force level in these joints increases with an increasing severity of earthquake. In fact, the stiff connections or their anchorages under the action of concentrated reactions, might fail even before reaching the depicted force levels.

- iv) During severe shaking, the joints slip and dissipate considerable energy resulting in an overall improved seismic response. This is clearly apparent from the envelopes for story shears, building deflections and bending stresses, as shown in Figs. 4.9, 4.11 and 4.12.

The response of 15 story walls with LSB joints is considerably less than for walls with either very stiff joints or without joints. In this particular case (building period - 0.6 seconds), the advantages of softening the structure and energy dissipation during slipping are complimentary to each other. In the case of 10 story walls with LSB joints, the response is considerably reduced when compared to isolated walls, but it is almost the same when compared to stiff elastic joints. The reason is attributed to the fact that any prolongation in the period of building (period 0.3 seconds), in this particular case, means amplification of building motions or higher forces which override

the beneficial effects of energy dissipation.

- iv) After the earthquake, the stored elastic strain energy of the panels will restore the connections nearly to their original position and the building will be ready to face future earthquakes with the same efficiency. This is clearly seen from typical time-histories of the displacements of the panels and connections (Figs. 4.14 and 4.15).
- v) It may however be noted that since maximum permissible stresses in panelized walls are most often governed by the limiting stresses at horizontal joints, the values of stresses and forces shown in the diagrams are only for comparison purposes and are not the design values.

4.7 SUMMARY

The results of preliminary analyses have demonstrated that the use of the proposed energy dissipating LSB joints can significantly improve the seismic response of panelized buildings. In effect, the proposed joints act as structural dampers in arresting seismic forces.

The primary building period, upon which depends the seismic forces, is affected by the value of the slip load of the joints. In order to maximize the benefits resulting from softening and energy dissipation, there is a need to optimize the slip load values of the joints for different story heights of the building. This important aspect of optimization will be discussed in the next chapter.

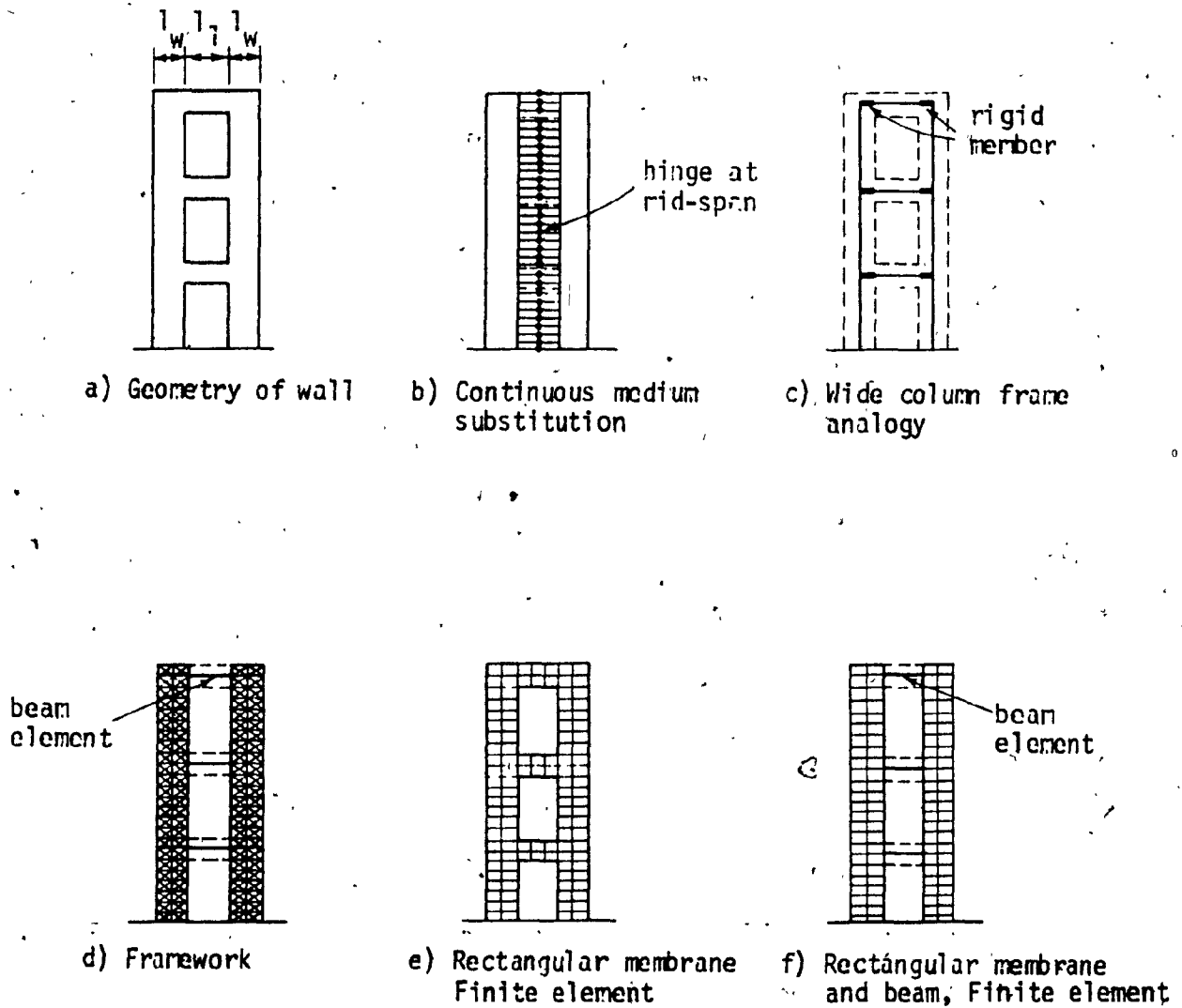


FIG. 4.1 - STRUCTURAL IDEALIZATION

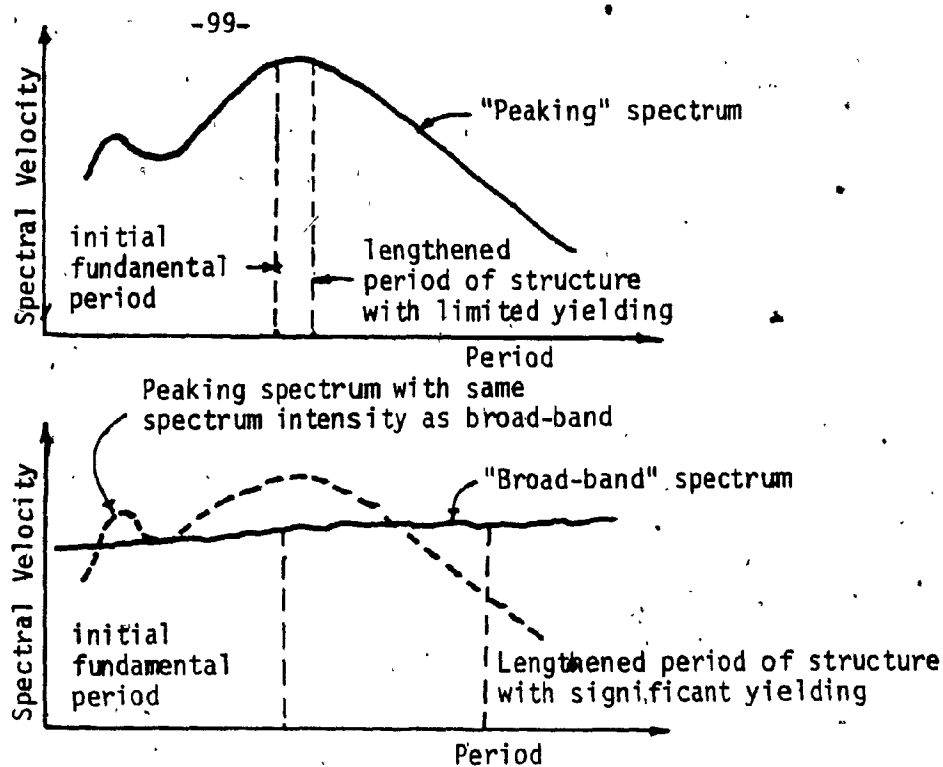


FIG. 4.2 - PEAKING TYPE AND BROAD BAND SPECTRUM

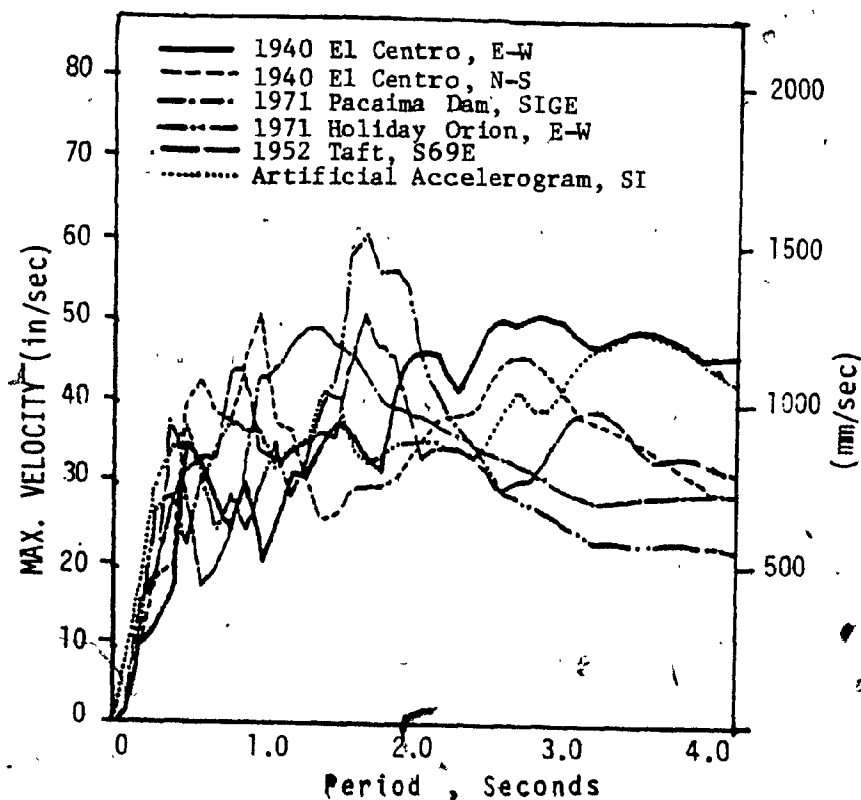


FIG. 4.3 - RELATIVE VELOCITY RESPONSE SPECTRA FOR DIFFERENT NORMALIZED INPUT MOTIONS, 5% DAMPING

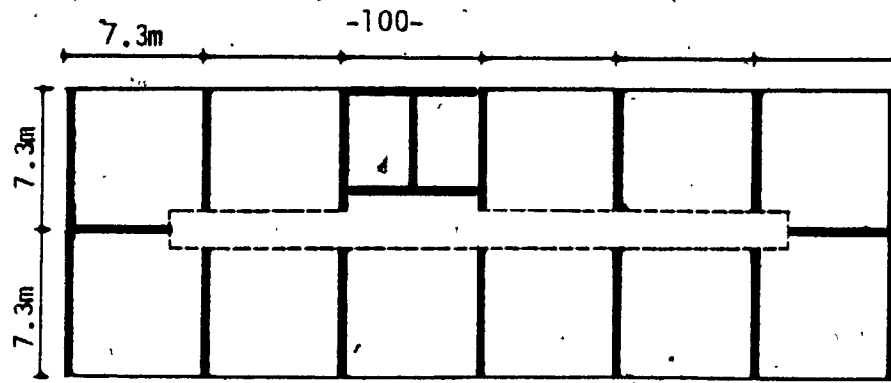
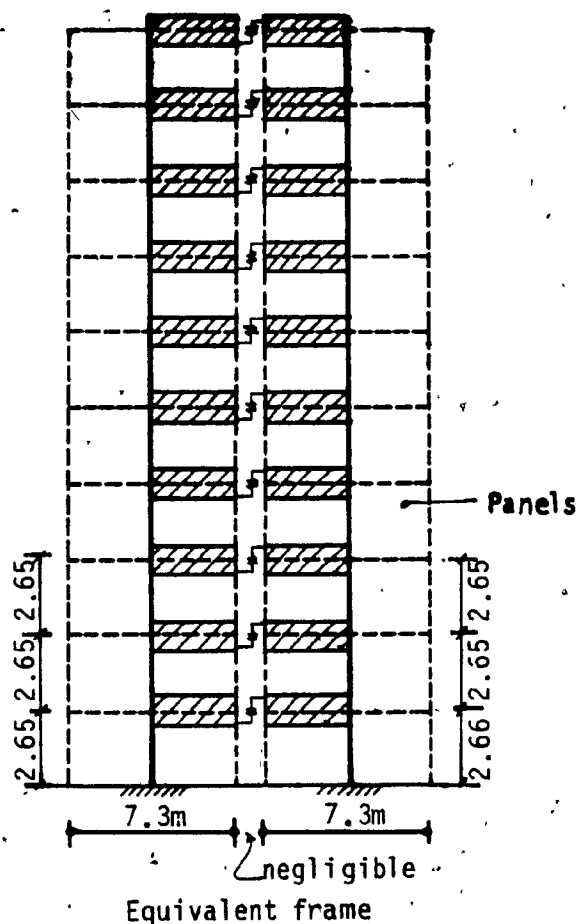


FIG. 4.4- TYPICAL PANELIZED APARTMENT BUILDING



Properties of each Panel Wall

Area	= 1.46 m^2
Moment of Inertia	= 6.48 m^4
Modulus of Elasticity	= $2.92 \times 10^7 \text{ kPa}$
Gravity Load per Story	= 245 kN
Mass for Lateral Forces per Story	= 64 tonnes

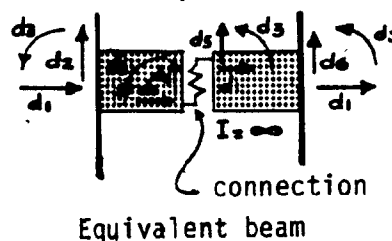
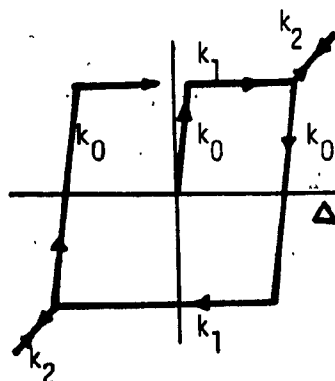
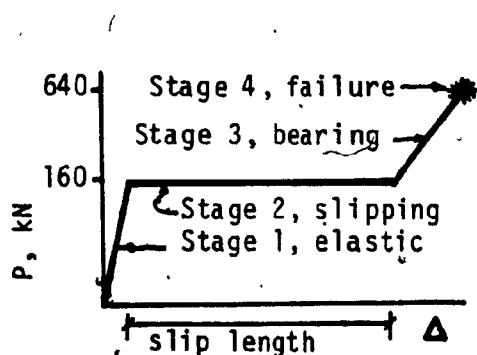


FIG. 4.5 - STRUCTURE IDEALIZATION



Stiffness of each Connection

Stage 1 (k_0)	= $64 \times 10^4 \text{ kN/m}$
Stage 2 (k_1)	= 0
Stage 3 (k_2)	= $32 \times 10^4 \text{ kN/m}$
(Two connections used for each story)	

FIG. 4.6 - LOAD DEFORMATIONS OF LSB JOINT

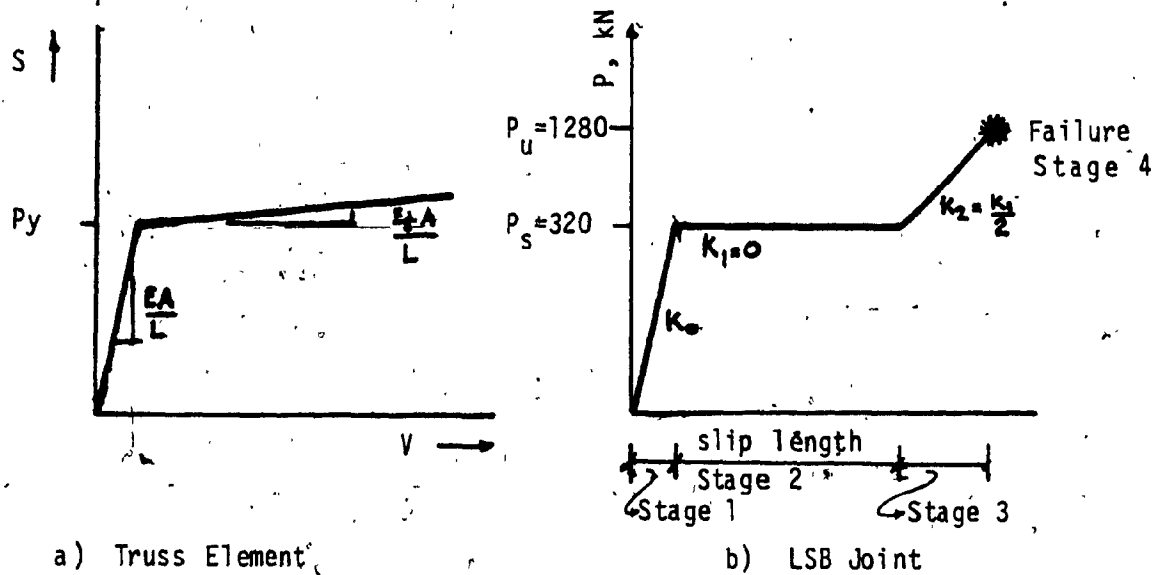


FIG. 4.7 - EQUIVALENT TRUSS ELEMENT PROPERTIES

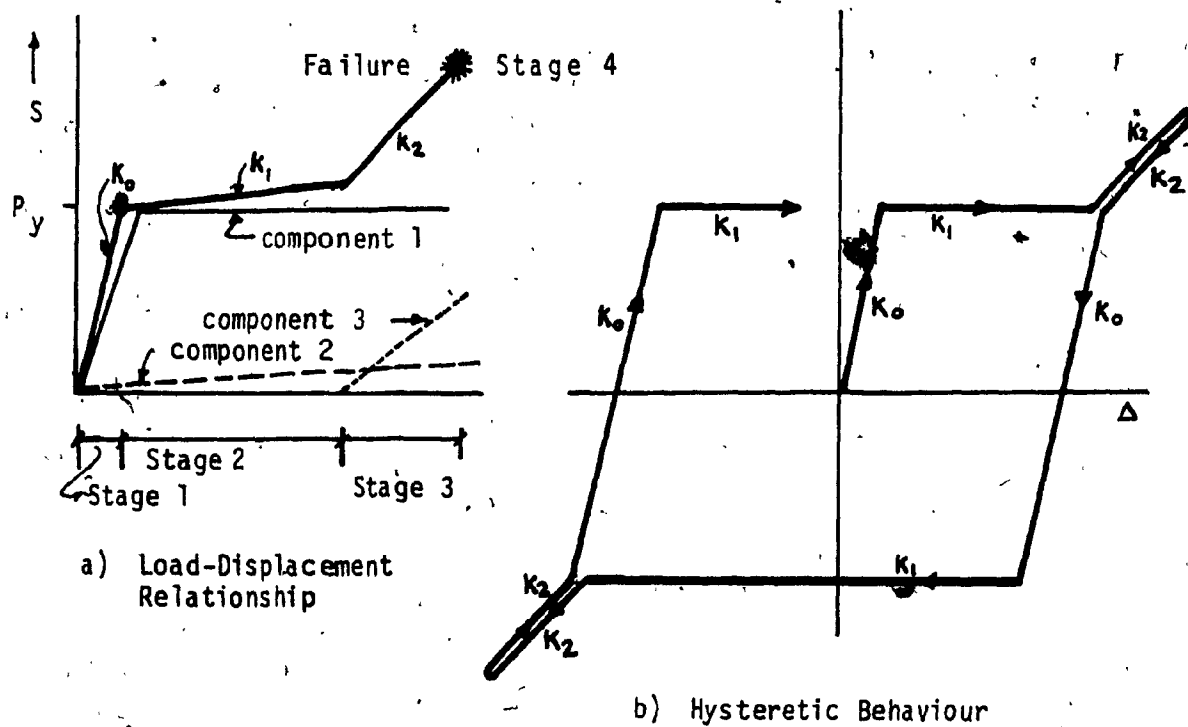


FIG. 4.8 - DECOMPOSITION OF TRILINEAR RELATIONSHIP INTO THREE COMPONENTS

Legend
 LSB Joint 0.25 g
 LSB Joint 0.08 g
 Stiff elastic 0.25 g

Legend
 LSB Joint 0.25 g
 LSB Joint 0.08 g
 Quasi static 0.08 g
 Isolated walls 0.25 g
 Stiff elastic 0.25 g

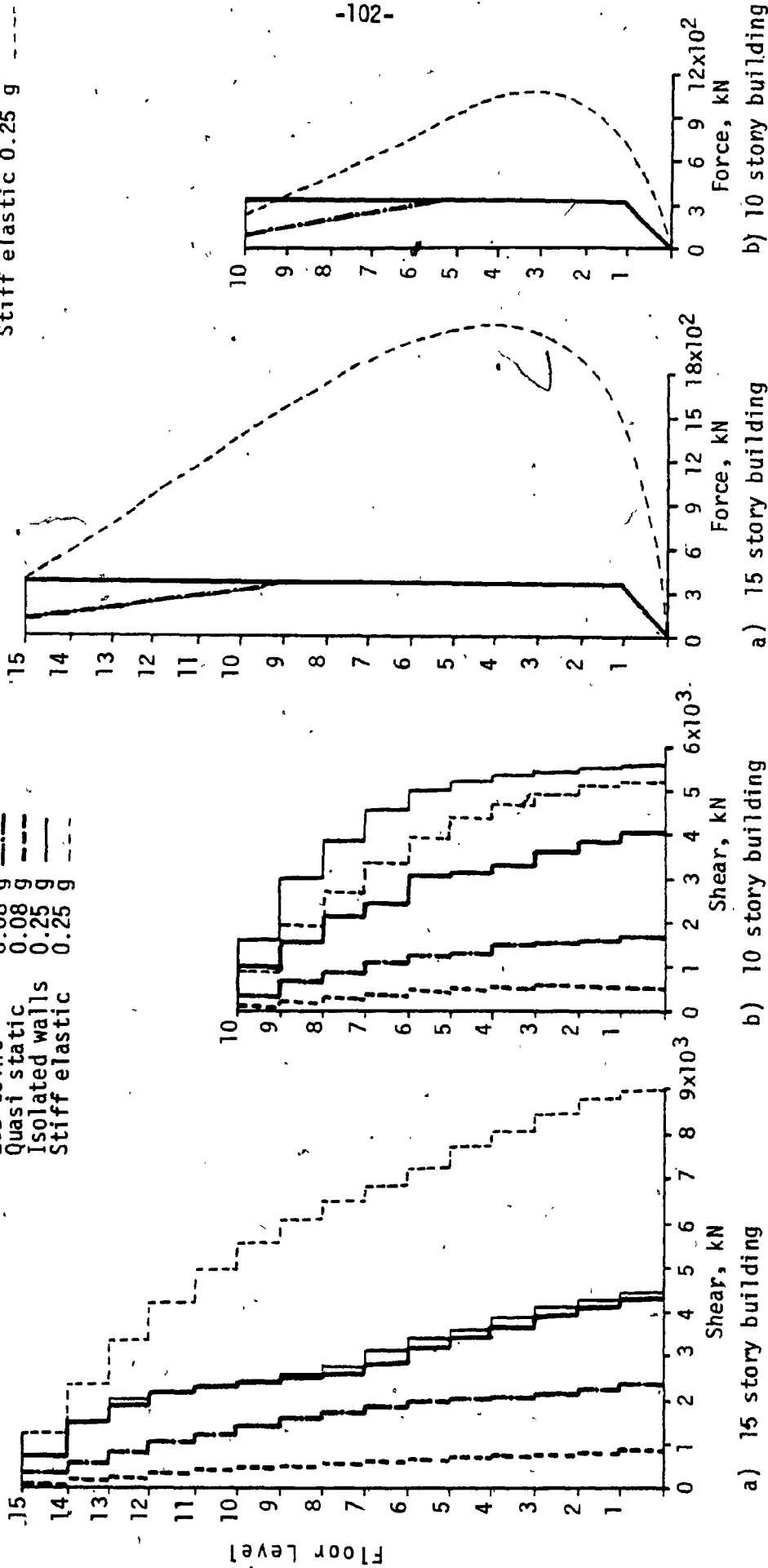


FIG. 4.10 - FORCES IN JOINTS

FIG. 4.9 - STORY SHEAR ENVELOPE

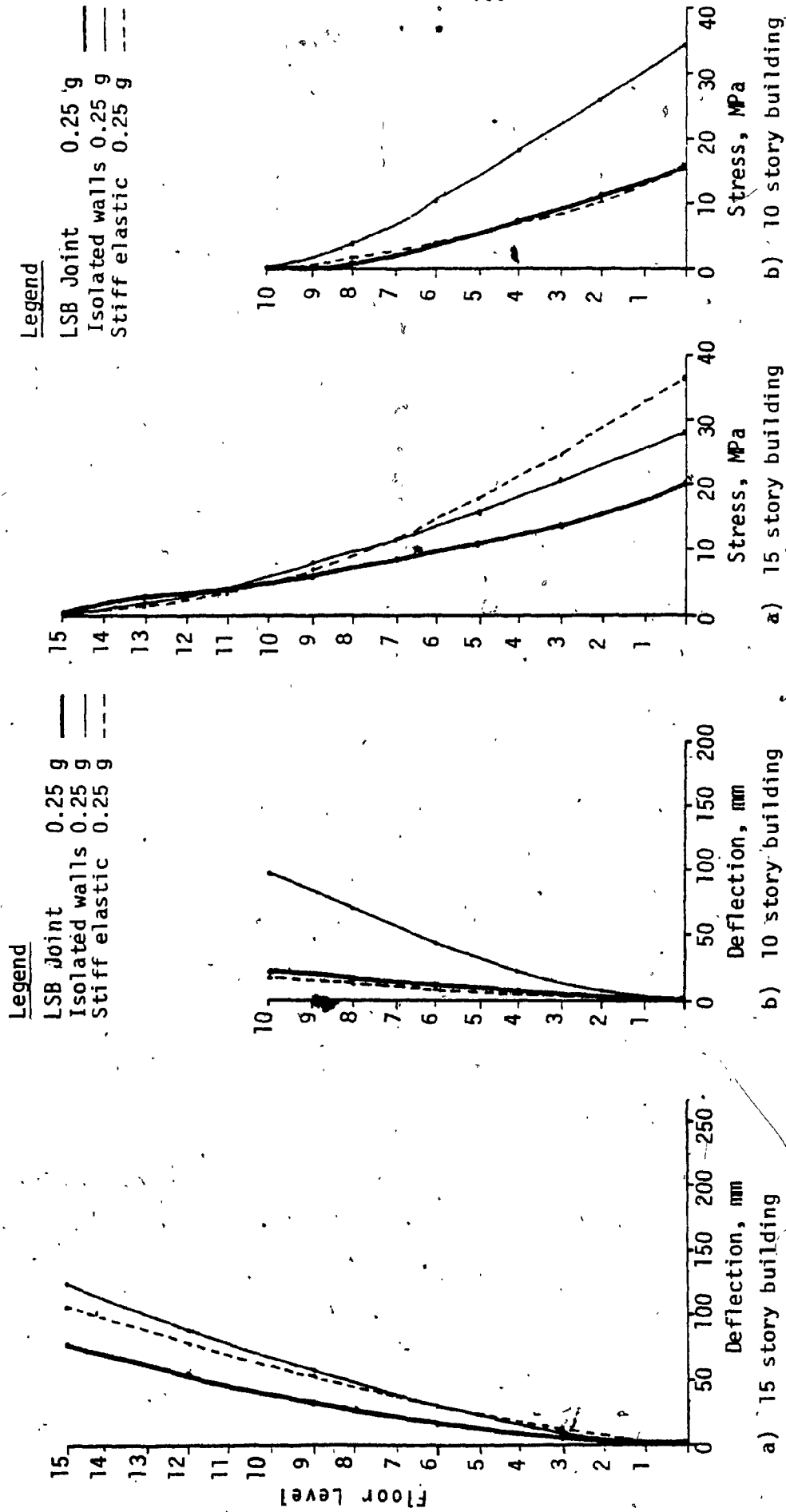
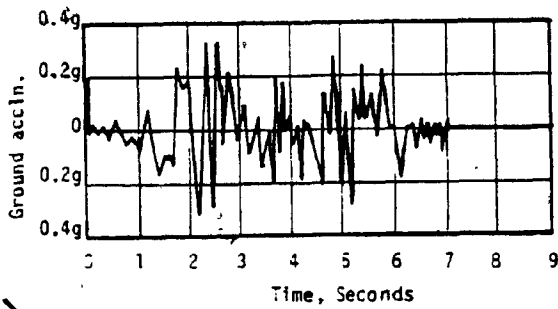


FIG. 4.11 - BUILDING DEFLECTION ENVELOPE

FIG. 4.12 - STRESSES IN PANELS



4.13-GROUND MOTION HISTORY
EL CENTRO, 1940 NS, FIRST SEVEN SECONDS.

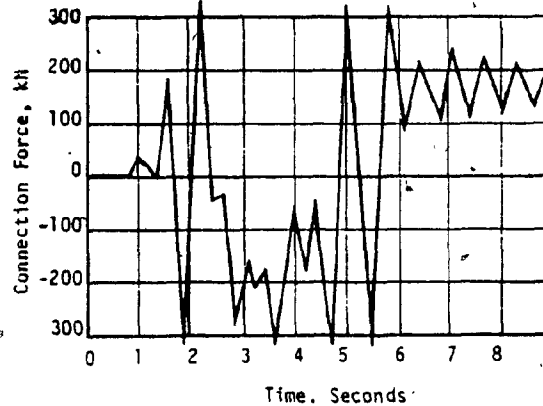
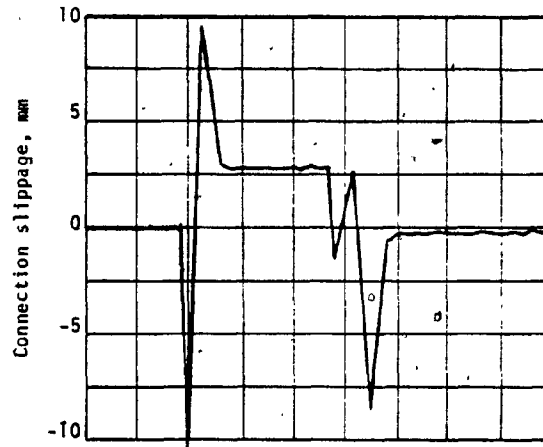
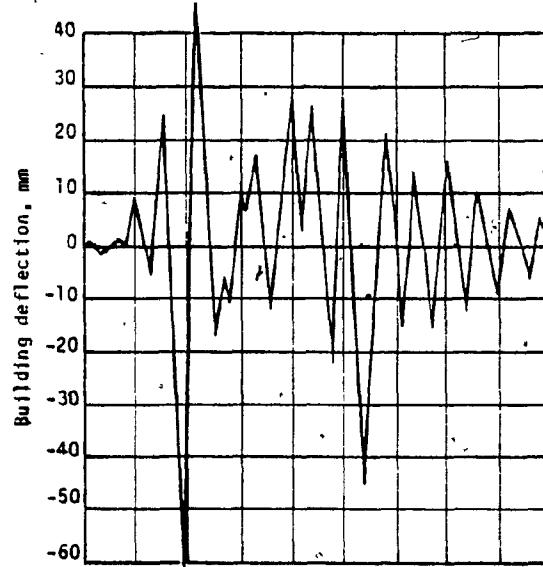
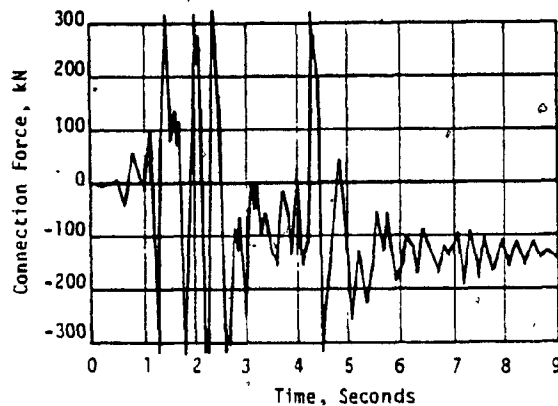
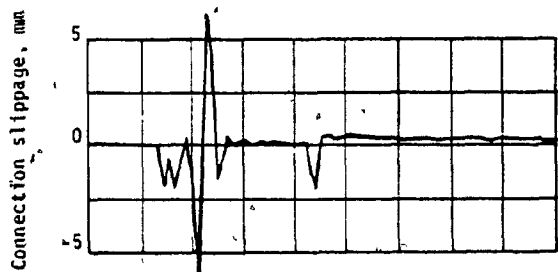
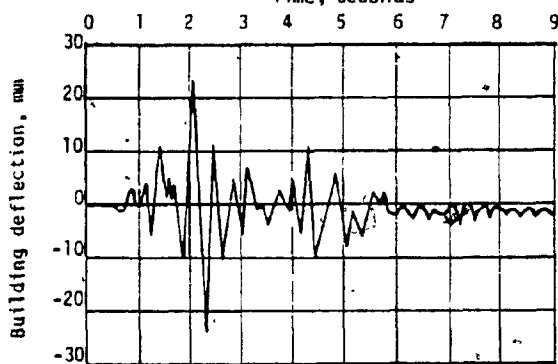


FIG.4.14-TYPICAL TIME HISTORIES, TOP STOREY, FIG.4.15-TYPICAL TIME HISTORIES, TOP STOREY,
10 STOREY BUILDING 15 STOREY BUILDING

CHAPTER V

PARAMETRIC STUDIES AND OPTIMIZATION

CHAPTER V

PARAMETRIC STUDIES AND OPTIMIZATION

Ground motions arising during earthquakes create oscillating lateral loads on the buildings, thereby causing them to sway back and forth with an amplitude proportional to the energy input. If some of this energy can be dissipated during the building motion, then the distress can be considerably reduced. The optimization of seismic response of the structure therefore depends on the technique of minimization of input energy and maximization of energy dissipation. In this chapter, the influence of various parameters affecting these two factors are studied and optimum seismic response is obtained using LSB joints. Results are compared with those of isolated and monolithic walls.

5.1 FACTORS AFFECTING SEISMIC RESPONSE

The basic equation of motion for a single degree of freedom system is given as [78]:

$$M\ddot{u} + C\dot{u} + Ku = -M\ddot{x} \quad (5.1)$$

or, $\ddot{u} + 2\lambda\omega\dot{u} + \omega^2 u = -\ddot{x}$

where \ddot{x} is the ground acceleration, ω is the undamped natural frequency of the structure and u is the displacement relative to ground given by the equation [78]:

$$u(t) = -\frac{1}{\omega_d} \int_0^t \ddot{x}(\tau) e^{-\lambda\omega(t-\tau)} \sin \omega_d(t-\tau) d\tau \quad (5.2)$$

multiplying Eqn. 5.1 by \dot{u} and integrating from time t to $t+\Delta t$, we get the incremental energy per unit mass as follows :

$$\int_t^{t+\Delta t} (\ddot{u}\dot{u} + 2\lambda\omega\dot{u}^2 + \omega^2 u\dot{u}) dt = - \int_t^{t+\Delta t} \ddot{x}\dot{u} dt \quad (5.13)$$

or $\Delta E_k + \Delta E_d + \Delta E_s = E_i \quad (5.4)$

When there is energy dissipation by hysteretic damping, as with the LSB joint, Eqn. 5.4 can be written as

$$\Delta E_k + \Delta E_d + \Delta E_D + \Delta E_s = \Delta E_i \quad (5.5)$$

where E_k is kinetic energy, E_d is energy dissipated by viscous damping, E_D is energy dissipated by hysteretic damping, E_s is recoverable strain energy and E_i is total energy input.

Since elastic strain energy is often a small part of the total energy, the two factors determining the maximum amplitude of a structure are :

- a) Energy input
- b) Energy dissipation.

As seen from Eqn. 5.2 and 5.3, the seismic energy fed into the structure depends upon the amplitude, characteristics and duration of the ground motion and on the dynamic characteristics of the structure. For a given earthquake motion, the energy input is basically dependent on the natural frequency of the structure which in turn is dependent upon the stiffness of the structure as given in the equation

$$\omega = \sqrt{\frac{K}{M}} \quad \text{and} \quad T = \frac{2\pi}{\omega} \quad (5.6)$$

where K , M and T are stiffness, mass and period of the structure respectively.

The overall stiffness of a coupled wall depends upon the strength and stiffness of the vertical joint. With strong joints between two walls, creating a monolith, the natural period of vibration will be t_1 , as shown in Fig. 5.1. Isolated walls will have a longer period, t_2 . The introduction of LSB joints will produce a periodicity, t_3 of an intermediate value between t_1 and t_2 , which is dependent on amplitude. By selecting the appropriate strength and stiffness of the LSB joint, the required value of t_3 can be obtained to minimize the energy input. It is known that for a particular ground motion, certain oscillation frequencies give more desirable response than others by avoiding the phenomenon of resonance or quasi resonance. Fundamental periods of vibration of the 5, 10, 15 and 20 story buildings studied are shown in Table 5.11.

Energy dissipated in a vertical joint is proportional to the product of slip load and slip travel during each excursion, the latter being inversely proportional to the value of slip load. The effect of joint slip load on a single story wall deformation is shown in Fig. 5.2. Fig. 5.3 shows its effect on hysteretic behaviour. For very high slip loads, the energy dissipation tends to zero as there may not be any slippage in the joint. If the slip load is very low, the amount of energy dissipated will again be negligible. Obviously the slip load has to be of an intermediate value for maximizing energy dissipation. This is clearly seen in Fig. 5.3c.

As soon as the forces in the joints exceed their slip load value, the joints start slipping and in the extreme case when all the joints over the full height of the wall are slipping, the behaviour approaches that of two individual walls. Softening of the structure can mean an invitation to either higher or lower seismic forces, depending upon its relation with the ground motion. The beneficial effects of energy dissipation may then combine with the positive or negative effects of the prolonged period of vibration.

Hence, input energy and energy dissipation have to be balanced so as to obtain the optimum response. For a given building geometry and earthquake motion this can be achieved by the appropriate selection of the strength and stiffness of the joint. In the case of the LSB joints, the strength of joint means its slip load value.

5.2 PARAMETRIC STUDIES

In order to understand the phenomenon of optimization, the following parametric studies were carried out to see their effect on the overall seismic response :

- a) wall height
- b) assembly stiffness of the joint
- c) restricted slot length of the joint
- d) slip load of the joint
- e) seismic intensity.

Although the parametric studies should include the effect of different earthquake records, as it is not only the intensity but also the frequency content of the earthquake which affects the response of a structure. The choice of only one earthquake record, i.e. El Centro

1940 (N.S.), was kept for reasons of economy in computation efforts and also since the object of the analysis is to demonstrate the overall participation of the slipping joint in improving the seismic response of the structure rather than looking at the figures of the output. Seismic accelerations of intensity 0.15 g, 0.25 g, 0.33 g and 0.5 g were considered.

Variables a) to d) affect the overall building stiffness and its period of vibration and, thereby, the input of seismic energy. The same variables also affect the rate of energy dissipation. The wall heights were varied for 5, 10, 15 and 20 stories keeping the same sectional and material properties. Slip load values were varied for 160, 320, 640 and 2560 kN, the last case representing a non-slipping elastic joint. Analyses were also carried out assuming zero slip load to represent isolated individual walls and for monolithic walls so that the effectiveness of the use of LSB joints could be compared with these two types of construction.

5.3 EFFECT OF RESTRICTED SLOT LENGTH

In order to study the effect of restricted slot length of the LSB joint on the overall building response, 10 and 20 story buildings were analyzed using a modified computer program for LSB joints. All the analyses were made using the same seismic intensity, slip load and stiffness of joint, the only variable being the slot length. The results of the study are shown in Table 5.1 and are discussed below.

5.3.1 10 Story Building

The maximum joint deformation in the case of the unrestricted slipping joint was 6.74 mm. so the slot length was restricted to 6 mm. By doing so, 5 out of 10 connections came in bearing, i.e. 3rd

stage, and the other 5 connections remained in stages 1 and 2. No connection failed. As the slipping joint comes in bearing, the effective stiffness of the coupled walls increases thereby shortening its effective period of vibration. For this building (fundamental period 0.3 second), any decrease in period of vibration means, in general, downward shift in the acceleration spectrum which means reduced forces on the structure. The unsmoothed response spectrum of the N.S. component of El Centro 1940 is shown in Fig. 5.4. But restricted slippage also means smaller energy dissipation. From the study of the results in Table 5.1, we find that the maximum joint deformation is reduced by 6%, base moments are reduced by 4% whereas the internal coupling forces due to increased reactions in bearing have increased by 3%.

Next, the slot length was further reduced from 6 mm. to 5.5 mm. With this small reduction, 8 connections out of 10 failed. The shear failure of the connection is transmitted as a shock load on the neighbouring joints and panels resulting in a sharp increase in force levels. As a consequence, the base shear, base moment and axial coupling forces increased by 20%, 90% and 175% respectively over unrestricted slipping joints. The overall building deflection also increased by 165%.

5.3.2 20 Story Building

The maximum joint deformation in the case of unrestricted slip length was 10.16 mm., so the slot length was restricted to 9 mm. This brought 14 connections in the 3rd stage of bearing while the remaining 6 connections were still in stages 1 and 2. No connection failed. In this case, not much variation was noticed in the base shear, base moments and axial coupling forces. However, there is an

18% increase in building deflection but a 5% reduction in joint deformation.

By further reducing the slip length to 8.5 mm., all the 20 connections broke. The shock load tremendously increased the forces, moments and deflections in the wall and are far more than if the walls were initially unjoined.

From the above studies, it is seen that no advantage is derived from the restricted slot length but on the contrary this could result in permanent damage to joints and consequent damage to panels due to a sudden increase in force levels caused by shock loading. If the slip length of the joint requires to be limited to avoid excessive deformations, it could be more economically done by increasing the slip load value of the joint rather than shortening the slot lengths of the joint. It is desirable to keep some margin of safety while deciding on the slot lengths as the nature of future earthquake motion could be far different from that used in the analysis.

5.4 EFFECT OF THE INITIAL STIFFNESS OF THE JOINT

Under service load conditions and during moderate earthquakes, the initial stiffness of the joint itself affects the stiffness of the coupled wall and its fundamental period of vibration, but during severe excitations, when the connections are slipping throughout the height, it has little influence on the overall wall stiffness.

In this study, 10 and 20 story walls with unrestricted slip lengths were analyzed by varying the joint stiffness. The stiffness of the joint was doubled by simply using a 20 mm. plate instead of the 10 mm. plate used in the previous studies. This is the maximum variation which

could be practically encountered in such joints. The results of analyses are shown in columns e and i of Table 5.1.

The results are somewhat comparable to those obtained by the use of restricted slot lengths shown in columns c and g of Table 5.1. Slight variations in forces and moments are attributed to the same reasoning as given in previous sections. The only difference between the two cases is that in the earlier case, the overall stiffness of the structure increases towards the end of the cycle when the joints come into bearing while in the present case, the stiffness of the structure is more at the beginning. The change in response is insignificant.

For these values of stiffness changes, $k_0 = (128-256)10^4 \text{ kN/m}$, the response is likely to be insensitive even during service loads (22,70).

5.5 EFFECT OF SLIP LOAD ON BUILDING RESPONSE

As discussed earlier, the slip load is the main variable which influences the effective period of vibration, thus the input seismic energy, and the energy dissipation. In this study, the slip loads of 160, 320, 640 and 2560 kN were used for each of the four walls of 5, 10, 15 and 20 story heights and four seismic intensities of 0.15 g, 0.25 g, 0.33 g and 0.5 g.

The results of these parametric studies in respect to bending moments and coupling forces at different story heights are shown in Tables 5.2 to 5.5. Maximum stresses in the panels due to lateral forces were evaluated and are shown in the same tables. Shear forces, building deflections and joint deformations are shown in Tables 5.6 to 5.9. Results of analysis for isolated walls (zero slip load) and monolithic walls are also shown in these tables. The effects of slip load on each

of the four walls are discussed below with the aid of diagrams.

While these studies are carried out to optimize seismic response, it should be further ensured that the value of the slip load is not low enough to slip during service loads or high enough to cause damage to its anchors or to the concrete around it.

5.5.1 5 Story Building

From the study of Table 5.6, it is seen that for seismic intensities of 0.15 g and 0.25 g, all the joints remain within the elastic stage, i.e. joint deformation is less than 0.25 mm. As expected, monolithic walls being of lower fundamental period experience minimum forces. Jointed walls have slightly higher stress levels. For seismic intensities of 0.33 g and 0.5 g, LSB 320 and LSB 640 start slipping resulting in some energy dissipation and consequent reduction in bending stresses and base shears. The reduction in stresses is not of much significance as the benefit of energy dissipation is almost overridden by the negative effects of the prolonged building period. Base shears for LSB jointed walls are however always lower than isolated or monolithic walls. Effects of varying slip loads on maximum bending stresses at the base of structure, due to lateral forces alone, for different seismic intensities are shown in Fig. 5.5. It is seen that LSB 320 offers the optimum value for minimum stresses which are nearly the same as for a monolithic wall. This can also be seen in Fig. 5.9a. The effect of the slip load on the building deflection can also be seen in Fig. 5.10a in which it is seen that LSB 320 is the slip load that gives minimum deflections. From these figures we also see that the structural response is insensitive to any increase in slip load beyond 320 kN.

5.5.2 10 Story Building

Like the 5 story building, this building also lies in a period range where prolongation of the fundamental period means an amplification of building motion. From Table 5.3 and Fig. 5.6, it is seen that LSB 320 provides minimum stresses in case of a seismic intensity of 0.15 g, but LSB 640 for all other higher seismic intensities. The effect of slip load on total overturning moments is shown in Fig. 5.25. It is seen that LSB 640 provides minimum overturning moment for a seismic intensity of 0.33 g. Similar effects in stresses and deflections are seen in Figs. 5.9 and 5.10 respectively. Any increase in slip load beyond these values does not change the response significantly. Base shears for LSB jointed walls are always less than monolithic or isolated walls.

5.5.3 15 Story Building

Unlike 5 and 10 story walls, this wall lies in a period range where any softening of structure means a downward trend in the acceleration spectrum. This trend is clearly apparent from Tables 5.4 and 5.8 wherein the bending stresses and story shears for isolated walls are always less than monolithic walls. From these tables and Figs. 5.7, 5.9 and 5.10, it is seen that the response of the wall in respect to both stresses and deflections is the lowest for LSB 160 for seismic intensities up to 0.33 g. Total overturning moments for 0.33 g as shown in Fig. 5.25 are also lowest for LSB 160. For a seismic intensity of 0.5 g, LSB 640 gives the minimum forces and deflections. In this building, the two effects attributed to a slipping joint, i.e. softening of the building and energy dissipation, are beneficial. This results in a significant reduction in stresses and deflections when compared to monolithic or isolated walls

(Figs. 5.7, 5.9, 5.10, 5.23 and 5.24)

5.5.4 20 Story Building

The effect of different slip loads on stresses and deflections are shown in Tables 5.5 and 5.9 and Figs. 5.8, 5.9 and 5.10. The response of the wall is very similar to the 15 story wall. In this case also LSB 160 gives the optimum results for seismic intensities up to 0.33 g. Fig. 5.25 shows that LSB 160 provides minimum overturning moment for seismic intensity of 0.33g. LSB 320 is optimum for a seismic level of 0.5 g.

5.6 COMPARISON OF LSB JOINTED WALLS WITH ISOLATED AND MONOLITHIC WALLS

In this study, the results of optimum LSB jointed walls are compared with isolated and monolithic walls.

5.6.1 Story Shears

Figs. 5.11 to 5.14 show the plots in respect to story shears for all the four heights of wall. It is seen that in the case of 5 and 10 story walls, not much benefit is derived in story shears when compared to monolithic walls for seismic intensities up to 0.33 g. In the case of a seismic intensity of 0.5 g, the reduction in base shear is 15-20%. Compared to isolated walls, the reduction in story shears is about 30-35% for all seismic intensities. For 15 and 20 story walls, the reduction in story shear is 35% and 65% compared to isolated walls and monolithic walls respectively. The reductions in story shear are advantageous in protecting the horizontal joints from distress.

5.6.2 Bending Stresses in Panels

Bending stresses for different seismic levels and story heights are shown in Figs. 5.15 to 5.18. In the case of 5 and 10 story walls, the stresses in LSB jointed walls have almost the same stresses as that of monolithic walls but compared to isolated walls, the stresses are only 35 to 50%. In the case of 15 and 20 story walls, the stresses in LSB jointed walls are about 40% and 65% of those for monolithic walls and isolated walls respectively.

It is seen that even for a 10 story wall for a seismic intensity of 0.25 g, the stresses in isolated walls have exceeded the strength capacity of the concrete ($f_c = 35$ MPa) and for a seismic level of 0.5 g, the stresses due to bending alone are 67.5 MPa. For 15 and 20 story walls the stresses in the case of isolated walls as well as monolithic walls have exceeded the strength of concrete. Using LSB joints, the stresses for all the four walls do not exceed 30 MPa even for a seismic intensity of 0.5 g. The effectiveness of LSB joints in reducing stresses compared to isolated walls and monolithic walls is shown in Fig. 5.23. Net stresses at the base, i.e. including the effect of gravity stresses, for all four types of walls for a seismic intensity of 0.33 g, are shown in Fig. 5.26. It is seen that both compressive and tensile stresses are considerably less in the case of LSB jointed walls compared to isolated and monolithic walls. To avoid any cracking of horizontal joints, there appears to be a necessity of post-tensioning which of course will be much less than that needed for isolated walls.

5.6.3 Building Deflections

Maximum building deflection envelopes are shown in Figs. 5.19

to 5.22. It is seen that in the case of the 5 and 10 story walls, the deflections of LSB jointed walls are similar to those for the monolithic wall but are about 30% of the isolated walls. For 15 and 20 story walls, the deflections are approximately 50% and 70% of the isolated walls and monolithic walls respectively. This is shown in Fig. 5.24 which shows the ratios of deflections for a seismic intensity of 0.33 g.

5.6.4 Time Histories

Time histories for the top most stories of 10, 15 and 20 story walls for seismic intensities of 0.25 g, 0.33 g and 0.5 g are shown in Figs. 5.27 to 5.35. Time histories for isolated and monolithic walls have also been plotted on the same diagram for better comparison. The plots are made up to 9 seconds only. It is observed that the effective period of vibration for LSB jointed walls changes with the amplitude of vibration and, therefore, resonance of the structure is more difficult to establish and this will help to reduce structural excitations. After the earthquake, 10 and 15 story buildings return to their original alignment. A longer period of time is required for 20 story building to come to rest.

For the 10 story wall, the peak amplitudes of both the LSB jointed wall and the monolithic wall are the same. However, since the effective period of vibration of the LSB jointed wall is longer, the accelerations experienced by this wall are less, giving an advantage in reducing secondary damage to non structural items like ceilings, finishings and equipment.

The effectiveness of the hysteretic damping of the LSB jointed wall is more clearly visualized in the case of 15 and 20 story buildings. The amplitudes of vibration and acceleration are considerably less than

for both monolithic and isolated walls.

Time histories of forces and displacement in the top story limited slip joints are shown in Figs. 5.36 to 5.38. It is seen that under the elastic action of cantilever walls, all the connections return almost to their original position and are ready to face future earthquakes with the same efficiency. There are some residual forces left in the connections at the end of the earthquake, but they do not affect the future performance. It is felt that if a longer period of earthquake record, i.e. gradually fading, was used and more time was allowed to lapse after termination of the earthquake, the deformations and residual forces in the connection would be further reduced.

5.7 SUMMARY

The parametric studies have demonstrated that slip load of the joint is the primary variable, the selection of which makes it possible to "tune" the structure for optimum response. This is another advantage of LSB joints which is not readily available in any other jointing system. Using these joints, the necessity of other energy dissipating or tuning devices like added masses or expensive hydraulic systems is reduced. LSB joints are designed to give an overall improved seismic response for panelized buildings. The principle may also be used for cast in place walls. During an earthquake, no damage is caused to the joints and they remain without adjustment ready to absorb future earthquakes with nearly the same efficiency.

Slip Length, mm. Stiffness ko, kN/m Slip Load, kN	10 Story Building				20 Story Building			
	Unre- stricted 64x10 ⁴ 320	6.0	5.5	Unre- stricted 128x10 ⁴ 320	Unre- stricted 64x10 ⁴ 320	9	8.8	Unre- stricted 128x10 ⁴ 320
a	b	c	d	e	f	g	h	i
1. Maximum building deflection at top, mm.	25	25	66	24	84	99	544	98
Percentage variation	0	0	164	-4	0	18	547	17
2. Maximum connection deformation, mm.	6.74	6.35	7	5.93	10.16	9.66	103	9.88
Percentage variation	0	-6	4	-12	0	-5	875	-3
3. Maximum base shear, kN	2121	2120	2780	1828	1743	1743	3634	1721
Percentage variation	0	0	21	-14	0	0	108	-1
4. Maximum moment at base, kN.m	23324	22443	44702	22567	27418	27417	107905	27042
Percentage variation	0	-4	92	-3	0	0	294	-1
5. Maximum axial coupling force, kN	3598	3705	9898	3860	6598	6554	25390	6590
Percentage variation	0	+3	175	7	0	-1	284	0
Number of connections in Stage 1 or 2	10	5	1	30	20	6	-	20
Number of connections in Stage 3	-	5	1	-	-	14	-	-
Number of failed connections	-	-	8	-	-	-	20	-

TABLE 5.1 - EFFECT OF RESTRICTED SLIP LENGTH AND INITIAL JOINT STIFFNESS
ON BUILDING RESPONSE, 0.25 g

Story	B.M, kN.m F, kN p, kPa	0.15 g								0.25 g							
		Slip Loads, kN								Slip Loads, kN							
		0	160	320	640	2560	Mono	0	160	320	640	2560	Mono	0	160	320	640
4	B.M F p	800 0 451	-- -- --	101 95 122	101 95 122	101 95 122	866 0 122	1333 0 751	-- -- --	169 159 204	169 159 204	169 159 204	2691 0 379				
3	B.M F p	2219 0 1250	-- -- --	469 223 417	469 223 417	369 223 417	3998 0 563	3701 0 2085	-- -- --	783 371 695	783 371 695	783 371 695	6661 0 938				
1	B.M F p	6242 1 3517	-- -- --	1791 557 1391	1791 557 1391	1791 557 1391	10240 0 1442	10408 1 5864	-- -- --	2986 928 2318	2986 928 2318	2986 928 2318	17080 0 2405				
G.F.	B.M F p	8575 1 4831	-- -- --	2969 694 2147	2969 694 2147	2969 694 2147	13918 0 1960	14298 1 8055	-- -- --	4950 1157 3580	4950 1157 3580	4950 1157 3580	23204 0 3269				

TABLE 5.2 - BENDING MOMENT (B.M), AXIAL COUPLING FORCE (F), MAXIMUM STRESS \pm (p) -
5 STORY BUILDING

Story	B.M, kN.m F, kN P, kPa	0.33 g							0.50 g						
		Slip Loads, kN							Slip Loads, kN						
		0	160	320	640	2560	Mono		0	160	320	640	2560	Mono	
	B.M	1761	--	256	223	223	3665		2641	--	734	334	334	5347	
	F	0	--	257	210	210	0		0	--	412	315	315	0	
	P	992	--	320	270	270	502		1488	--	695	404	404	753	
3	B.M	4888	--	968	1034	1034	8806		7332	--	1679	1551	1551	13201	
	F	0	--	602	490	490	0		0	--	898	735	735	0	
	P	2753	--	957	918	918	1240		4130	--	1561	1377	1377	1859	
1	B.M	13746	--	4112	3944	3944	22554		20619	--	6460	5917	5917	33831	
	F	1	--	1200	1226	1226	0		0	--	1683	1838	1838	2317	
	P	7744	--	3138	3062	3062	3176		11614	--	4792	4592	4592	4764	
G.F.	B.M	18884	--	6688	6538	6538	30657		28326	--	10338	8728	8728	45981	
	F	1	--	1507	1528	1528	0		0	--	2084	2555	2555	0	
	P	10638	--	4799	4730	4730	4317		15955	--	7250	6666	6666	6475	

TABLE 5.2 - BENDING MOMENT (B.M), AXIAL COUPLING FORCE (F), MAXIMUM STRESS \pm (p) -
5 STORY BUILDING (CONT'D)

Story	B.M, kN.m F, kN p, kPa	0.15 g							0.25 g						
		Slip Loads, kN							Slip Loads, kN						
		0	160	320	640	2560	Mono		0	160	320	640	2560	Mono	
8	B.M	3733	1769	1305	111	112	4624		6224	3281	2446	1736	234	7710	
	F	0	567	676	567	680	--		0.58	524	800	1179	968	--	
	p	2103	1384	1198	451	536	651		3506	2207	1925	1786	795	1086	
6	B.M	10767	4222	1966	2695	2702	14094		17953	10765	5756	3640	4505	23501	
	F	1	906	1029	1066	1066	--		0.85	854	1391	1830	1777	--	
	p	6066	2998	1812	2248	2252	1985		10113	6648	4195	3303	3755	3309	
4	B.M	19272	7668	3475	4711	4663	26803		32135	18739	10604	5875	7775	44692	
	F	1	1430	1673	2105	2105	--		1.35	1329	2125	3179	3510	--	
	p	10856	5298	3103	4097	4069	3774		18102	11465	7428	5486	6783	6293	
2	B.M	27959	11269	6738	7312	7231	41284		46619	26276	16499	10858	12057	68838	
	F	1	1947	2328	3236	3236	--		1.73	1849	2824	4509	5396	--	
	p	15750	7680	5390	6335	6289	5814		26260	16066	11228	9204	10487	9694	
G.F.	* B.M	36232	15369	11531	11516	11534	56446		60398	33002	23324	18723	19231	94118	
	F	1	2393	2975	4231	4231	--		1.91	2236	3598	5728	7055	--	
	p	20404	10296	8533	9384	9395	7949		34021	20120	15602	14469	15664	13253	

TABLE 5.3 - BENDING MOMENT (B.M), AXIAL COUPLING FORCE (F), MAXIMUM STRESS \pm (p) - 10 STORY BUILDING

Story	B.M, kN.m F, kN p, kPa	0.33 g										0.50 g									
		Slip Loads, kN										Slip Loads, kN									
		0	160	320	640	2560	Mono	0	160	320	640	2560	Mono								
8	B.M	8220	5051	3868	2957	309	10184	12331	--	7500	5269	368	15275								
	F	0.76	738	1015	1391	1279	--	1	--	1837	1856	2279	--								
	p	4631	3350	1922	2619	1050	1434	6947	--	5483	4239	1768	2151								
6	B.M	23711	15857	10884	3943	5950	31038	35567	--	20999	10757	7363	46558								
	F	1.13	971	1590	2053	2348	--	2	--	2369	2919	4300	--								
	p	13357	9597	7219	3627	4959	4371	20035	--	13451	8059	7092	6556								
4	B.M	42441	27894	18997	8764	10269	59027	63663	--	36394	20245	15403	88540								
	F	2.06	1445	2436	3377	4636	--	3	--	3391	4383	6954	--								
	p	23907	16702	12368	7250	8959	8312	35862	--	22823	14405	13439	12468								
2	B.M	61572	39329	27477	15676	15924	90918	92358	--	50473	31451	23886	136377								
	F	2.28	2035	3257	4684	7127	--	3	--	4955	5791	12598	--								
	p	34684	23547	17708	12038	8896	12803	52025	--	31824	21681	22083	19204								
G.F.	B.M	79771	49197	36709	25608	25400	124307	119657	--	63721	44408	38100	186461								
	F	2.53	2476	4132	5976	9318	--	4	--	5749	7756	13976	--								
	p	44935	29407	23507	18517	20689	17505	67402	--	40467	30326	31034	26257								

TABLE 5.3 - BENDING MOMENT (B.M), AXIAL COUPLING FORCE (F), MAXIMUM STRESS \pm (p) -
10 STORY BUILDING (CONT'D)

Story	B.M, kN.m F, kN P, kPa	0.15 g							0.25 g						
		Slip Loads, kN							Slip Loads, kN						
		0	160	320	640	2560	Mono		0	160	320	640	2560	Mono	
13	B.M	1670	1943	2224	1909	736	6236		2785	3000	3634	3391	1228	10397	
	F	0	588	742	816	616	--		1	930	1178	1490	1028	--	
	P	941	1496	1761	1634	837	878		1570	2327	2864	2931	1396	1484	
11	B.M	4727	2753	3514	5053	2806	19026		7882	4281	5009	6150	4468	31724	
	F	1	1034	1415	2132	1571	--		2	1341	1837	2694	2854	--	
	P	2664	2259	2946	4506	2656	2679		4441	3329	4079	5309	4477	4467	
9	B.M	8656	4805	4582	6430	5512	36280		14434	7863	7873	7624	9190	60494	
	F	1	1385	2060	3407	2955	--		2	1728	2488	4009	4926	--	
	P	4877	3654	3992	5955	5129	5109		8131	5612	6151	7034	8550	8519	
7	B.M	13174	7224	7042	6243	8526	7981		21966	11701	11781	11078	14216	94508	
	F	1	1717	2711	4612	4625	--		2	2093	3146	5318	7712	--	
	P	7422	5245	5823	6676	7970	7981		12374	8023	8791	9881	11625	13308	
5	B.M	17760	9180	9000	9957	11686	79850		29614	15103	15055	16147	19486	133143	
	F	2	2033	3362	5073	6616	--		3	2437	3781	6515	11032	--	
	P	10004	6563	7372	9083	8380	11244		16683	10176	11070	13558	18532	18749	
3	B.M	22211	10845	11617	15760	15021	104312		37034	17610	18491	23110	23767	173932	
	F	2	2345	4009	6358	8963	--		3	2769	4417	7793	16113	--	
	P	12511	7715	9290	13232	11600	14689		20862	11815	13440	18355	24423	24493	
G.F.	B.M	29670	15255	19308	24574	23977	145856		49472	21507	28576	36327	39980	243203	
	F	2	2930	4995	8091	12279	--		3	3523	5419	9763	20475	--	
	P	16713	10600	14297	19364	21916	20539		27869	14527	19807	27149	36544	--	

TABLE 5.4 - BENDING MOMENT (B.M), AXIAL COUPLING FORCE (F), MAXIMUM STRESS \pm (p) - 15 STORY BUILDING

Story	B.M, kN.m F, kN p, kPa	0.33 g								0.50 g							
		Slip Loads, kN								Slip Loads, kN							
		0	160	320	640	2560	Mono			0	160	320	640	2560	Mono		
13	B.M	3678	3380	4247	4857	1622	12902			5517	4426	7383	--	8486	20598		
	F	1	948	1251	1478	1358	--			0	1052	2261	--	3909	--		
	p	2073	2557	3249	12859	1844	1817			3108	3214	5707	--	7457	2901		
11	B.M	10410	5644	5960	6598	5901	41899			15615	9711	11580	--	19327	62849		
	F	2	1372	2179	2918	3770	--			0	1737	3056	--	9193	--		
	p	5865	4119	4849	5715	2906	5900			8795	6660	8616	--	17183	8850		
9	B.M	19064	10696	10376	10177	12128	79898			28596	17661	19417	--	24303	119846		
	F	3	1775	2884	4245	6507	--			0	2209	3807	--	14352	--		
	p	10739	7241	60420	8640	11294	11251			16107	11461	13544	--	23519	16876		
7	B.M	29012	15709	15638	15380	18776	124821			43518	25240	26725	--	28464	187232		
	F	3	2157	3549	5560	10186	--			0	2692	4513	--	19550	--		
	p	16344	10325	11239	12471	17553	17577			24512	16061	18144	--	29423	26366		
5	B.M	39112	19972	19981	19227	23024	175850			58669	31407	32855	--	44667	263774		
	F	4	2521	4184	6865	16351	--			0	3146	5185	--	24740	--		
	p	22034	12977	14120	25532	24168	24763			33047	19846	22058	--	42105	37144		
3	B.M	48913	23250	23479	24659	33080	229722			73370	37482	36626	--	61451	344583		
	F	5	2871	4805	7879	19708	--			0	3566	5876	--	29912	--		
	p	27554	15062	16516	19287	32132	32349			41327	23555	24655	--	55101	48523		
G.F	B.M	65340	30558	31008	42120	52767	321213			98010	56988	42326	--	77610	481817		
	F	5	3435	5929	9810	27042	--			0	4115	7033	--	35171	--		
	p	36807	19565	21527	30444	48244	45232			55206	34918	28658	--	67805	67848		

TABLE 5.4 - BENDING MOMENT (B.M), AXIAL COUPLING FORCE (F), MAXIMUM STRESS \pm (p) -
15 STORY BUILDING (CONT'D)

Story	B.M, kN.m F, kN p, kPa	0.15 g										0.25 g									
		Slip Loads, kN										Slip Loads, kN									
		0	160	320	640	2560	Mono	0	160	320	640	2560	Mono								
18	B.M	1462	1302	1768	552	543	440	2438	2244	2453	2305	906	7347								
	F	0	448	701	344	495	--	1	594	771	917	595	--								
	p	824	1009	1476	546	645	621	1374	1670	1910	1926	918	1035								
15	B.M	5381	2676	3728	3182	2879	19157	8972	5045	4779	6711	4801	31943								
	F	0	897	1681	1448	1430	--	2	1253	1776	2874	2385	--								
	p	3031	2122	3250	2784	2607	2698	5055	3700	3908	5748	4338	4498								
12	B.M	8713	4205	4172	7057	5608	39258	14528	9267	5658	8066	9350	65459								
	F	0	1392	2658	3344	3120	--	3	1787	2767	4816	5203	--								
	p	4908	3325	4170	6265	5299	5528	8185	6444	5082	7841	8831	9218								
9	B.M	9723	5497	5041	8672	8301	60920	16211	11103	8955	9285	13462	101580								
	F	0	1885	3631	5130	5257	--	4	2390	3750	6705	9083	--								
	p	5477	4387	5326	8399	8277	8579	9134	7891	7612	9822	13804	14304								
6	B.M	11463	8218	8028	10035	11789	83779	19114	12216	13571	13818	19657	139695								
	F	0	2451	4477	6865	7722	--	4	2918	4730	8340	12876	--								
	p	6457	6308	7588	10354	11930	11798	10769	8879	10884	13495	19891	19672								
3	B.M	15413	11918	12410	16378	15291	114931	25700	17259	19788	22268	26699	191637								
	F	0	2873	5405	8776	10775	--	4	2950	5711	10314	17330	--								
	p	8682	8680	10692	15237	15993	16184	14479	11742	15058	19607	26909	26986								
G.F.	B.M	21748	16263	17454	23099	22091	147145	36263	22790	27418	31566	36834	245352								
	F	0	3339	6214	10527	13017	--	5	3435	6598	12027	21705	--								
	p	12250	11432	14087	20221	21359	20720	20429	15190	19962	26018	35614	34550								

TABLE 5.5 - BENDING MOMENT (B.M), AXIAL COUPLING FORCE (F), MAXIMUM STRESS \pm (p), 20 STORY BUILDING

Story	B.M, kN.m F, kN p, kPa	0.33 g										0.50 g				
		Slip Loads, kN										Slip Loads, kN				
		0	160	320	640	2560	Mono	0	160	320	2560	Mono	0	160	320	2560
18	B.M	3220	2856	2511	3345	1197	9704	4830	4287	4394	3914	14556	4830	4287	4394	3914
	F	1	813	810	1549	786	--	1	947	1151	2456	--	1	947	1151	2456
	p	1815	2166	1969	2905	21212	1366	2722	3063	3263	3887	2050	2722	3063	3263	3887
15	B.M	11850	7109	5639	7055	6341	42189	17774	11131	9956	12348	63283	17774	11131	9956	12348
	F	2	1484	1849	3498	3150	--	3	1467	2481	7059	--	3	1467	2481	7059
	p	6676	5020	7618	6370	5728	5941	10014	7275	7307	11790	8911	10014	7275	7307	11790
12	B.M	19189	12759	10056	7961	12350	86455	28783	19598	18324	23414	129683	28783	19598	18324	23414
	F	3	2014	2867	5485	6872	--	5	2072	3571	12531	--	5	2072	3571	12531
	p	10810	8566	7628	8241	11663	12174	16216	12728	12766	21771	18262	16216	12728	12766	21771
9	B.M	21411	15102	12462	10605	17780	134162	32117	22999	21977	32735	201243	32117	22999	21977	32735
	F	5	2622	3927	7455	11996	--	7	2384	4780	20095	--	7	2384	4780	20095
	p	12063	10603	9709	11079	18231	18892	18096	14588	15653	32202	28339	18096	14588	15653	32202
6	B.M	25245	16482	17722	17279	25961	184502	37867	30255	24245	42091	276753	37867	30255	24245	42091
	F	5	2720	5079	9359	17006	--	8	2897	5780	27874	--	8	2897	5780	27874
	p	14223	11147	13461	15743	26271	25981	21334	19026	17616	42800	38972	21334	19026	17616	42800
3	B.M	33944	23143	25589	26037	35262	253105	50916	44593	34244	59214	379658	50916	44593	34244	59214
	F	6	3104	5809	10962	22889	--	9	3559	5889	35898	--	9	3559	5889	35898
	p	19124	15162	18393	22174	35539	35642	28686	27556	23323	57941	53463	28686	27556	23323	57941
G.F.	B.M	47895	29475	34536	37263	48649	324050	71842	52256	45233	73700	486076	71842	52256	45233	73700
	F	7	3585	6741	12547	28667	--	10	3882	6862	39928	--	10	3882	6862	39928
	p	26983	19057	24070	29582	47038	45632	40474	32093	30178	68861	68448	40474	32093	30178	68861

TABLE 5.5 - BENDING MOMENT (B.M), AXIAL COUPLING FORCE (F), MAXIMUM STRESS $\pm(p)$ - 20 STORY BUILDING (CONT'D)

Story	Δ , mm V , kN	0.15 g								0.25 g							
		Slip Load, kN								Slip Load, kN							
		0	160	320	640	2560	Mono	0	160	320	640	2560	Mono	0	160	320	640
5	Δ Bldg Δ Conn. V	3 1.80 302	-- -- --	1 0.08 177	1 0.08 177	1 0.08 177	1 -- 199	5 3.01 503	-- -- --	2 0.13 295	2 0.13 295	2 0.13 295	1 -- 332	1 -- 332	2 0.13 295	2 0.13 295	2 0.13 295
4	Δ Bldg Δ Conn. V	2 1.76 536	-- -- --	1 0.11 326	1 0.11 326	1 0.11 326	1 -- 364	4 2.94 893	-- -- --	1 0.18 543	1 0.18 543	1 0.18 543	1 -- 607	1 -- 607	1 0.18 543	1 0.18 543	1 0.18 543
2	Δ Bldg Δ Conn. V	1 1.27 814	-- -- --	0 0.15 563	0 0.15 563	0 0.15 563	0 -- 593	1 2.14 1357	-- -- --	1 0.25 939	1 0.25 939	1 0.25 939	1 -- 990	1 -- 990	1 0.25 939	1 0.25 939	1 0.25 939
1	Δ Bldg Δ Conn. V	0 0.76 880	-- -- --	0 0.12 654	0 0.12 654	0 0.12 654	0 -- 677	0 1.26 1468	-- -- --	0 0.20 1090	0 0.20 1090	0 0.20 1090	0 -- 1129	0 -- 1129	0 0.20 1090	0 0.20 1090	0 0.20 1090

TABLE 5.6 - BUILDING DEFLECTION (Δ Bldg), CONNECTION SLIPPAGE (Δ Conn.), AND STORY SHEARS (V) - 5 STORY BUILDING

Story	Δ , mm V, kN	0.33 g										0.50 g									
		Slip Loads, kN										Slip Loads, kN									
		0	160	320	640	2560	Mono	0	160	320	640	2560	Mono	0	160	320	640	2560	Mono		
5	Δ Bldg	6	--	2	2	--	2	9	--	3	3	--	3	3	--	3	3	--	3		
	Δ Conn.	3.97	--	0.19	0.17	--	--	5.95	--	0.88	0.26	--	--	5.95	--	0.88	0.26	--	--		
	V	665	--	384	390	--	438	997	--	572	584	--	658	997	--	572	584	--	658		
4	Δ Bldg	5	--	2	2	--	1	7	--	3	2	--	2	7	--	3	2	--	2		
	Δ Conn.	3.88	--	0.26	0.23	--	--	5.82	--	0.95	0.35	--	--	5.82	--	0.95	0.35	--	--		
	V	1180	--	700	718	--	802	1770	--	942	1076	--	1203	1770	--	942	1076	--	1203		
2	Δ Bldg	2	--	1	1	--	1	3	--	1	1	--	1	3	--	1	1	--	1		
	Δ Conn.	2.83	--	0.39	.33	--	--	4.25	--	0.88	0.49	--	--	4.25	--	0.88	0.49	--	--		
	V	1793	--	1215	1240	--	1307	2689	--	1440	1860	--	1960	2689	--	1440	1860	--	1960		
1	Δ Bldg	1	--	0	0	--	0	1	--	1	1	--	0	1	--	1	1	--	0		
	Δ Conn.	1.67	--	0.29	0.26	--	--	2.50	--	0.59	0.39	--	--	2.50	--	0.59	0.39	--	--		
	V	1939	--	1416	1440	--	1491	2908	--	1989	2160	--	2236	2908	--	1989	2160	--	2236		

TABLE 5.6 - BUILDING DEFLECTION (Δ Bldg), CONNECTION SLIPPAGE (Δ Conn.), AND STORY SHEARS (V) - 5 STORY BUILDING (CONT'D)

Story-	Δ , mm V, kN	0.15 g										0.25 g									
		Slip Load, kN										Slip Load, kN									
		0	160	320	640	2560	Mono	0	160	320	640	2560	Mono	0	160	320	640	2560	Mono		
10	Δ Bldg Δ Conn. V	44 16.24 502	17 5.13 299	10 0.86 239	11 0.21 308	11 0.21 308	9 -- 303	73 27.08 836	41 14.11 604	25 6.64 450	16 0.42 422	18 0.35 513	16 -- 505	16 0.42 422	18 0.35 513	25 6.64 450	16 0.42 422	18 0.35 513	16 -- 505		
8	Δ Bldg Δ Conn. V	32 0.10 1218	13 0.08 676	8 0.11 565	9 0.13 818	9 0.13 818	7 -- 798	53 0.16 2031	30 0.14 1415	19 0.14 1045	12 0.19 1037	14 0.22 1364	12 -- 1331	12 0.19 1037	14 0.22 1364	19 0.14 1045	12 0.19 1037	14 0.22 1364	12 -- 1331		
6	Δ Bldg Δ Conn. V	20 14.46 1576	8 4.78 865	5 1.37 841	6 0.48 1175	6 0.48 1177	5 -- 1141	34 24.11 2628	19 12.68 1738	12 6.43 1387	9 1.44 1523	10 0.80 1963	8 -- 1902	9 1.44 1523	10 0.80 1963	12 6.43 1387	9 1.44 1523	10 0.80 1963	8 -- 1902		
4	Δ Bldg Δ Conn. V	10 11.40 1667	4 3.87 1017	3 1.40 1088	3 0.57 1395	3 0.53 1406	3 -- 1340	17 19.01 2780	9 9.92 1817	7 5.32 1666	5 1.76 1906	6 0.89 2344	4 -- 2233	5 1.76 1906	6 0.89 2344	7 5.32 1666	5 1.76 1906	6 0.89 2344	4 -- 2233		
2	Δ Bldg Δ Conn. V	3 6.57 1720	1 2.31 1098	1 1.05 1322	1 0.50 1523	1 0.49 1523	1 -- 1423	5 10.95 2868	3 5.64 1921	2 3.25 1852	2 1.43 2304	2 0.81 2556	2 -- 2373	2 1.43 2304	2 0.81 2556	2 3.25 1852	2 1.43 2304	2 0.81 2556	2 -- 2373		
1	Δ Bldg Δ Conn. V	1 3.50 1714	0 1.25 1196	0 0.63 1425	0 0.35 1554	0 0.34 1562	0 -- 1438	2 5.83 2857	1 2.99 1988	1 1.78 2021	1 0.88 2461	1 0.57 2605	1 -- 2397	1 0.88 2461	1 0.57 2605	1 1.78 2021	1 0.88 2461	1 0.57 2605	1 -- 2397		

TABLE 5.7 - BUILDING DEFLECTION (Δ Bldg), CONNECTION SLIPPAGE (Δ Conn.), AND STORY SHEARS (V) - 10 STORY BUILDING

Story	Δ , mm V, kN	0.33 g								0.5 g							
		Slip Load, kN								Slip Load, kN							
		0	160	320	640	2560	Mono	0	160	320	640	2560	Mono	0	160	320	640
10	Δ Bldg	96	61	42	23	24	21	145	--	79	47	37	31	145	--	79	47
	Δ Conn.	35.77	21.77	13.33	3.21	0.46	--	53.65	--	27.15	12.22	0.69	--	53.65	--	27.15	12.22
	V	1105	841	706	507	678	667	1657	--	1190	849	1017	1001	1657	--	1190	849
8	Δ Bldg	70	45	31	18	19	16	105	--	57	35	28	24	105	--	57	35
	Δ Conn.	0.21	0.19	0.19	0.22	0.28	--	0.32	--	0.28	0.28	0.43	--	0.32	--	0.28	0.43
	V	2682	1992	1628	1238	1802	1758	4024	--	2770	2012	2702	2637	4024	--	2770	2012
6	Δ Bldg	45	28	20	12	13	11	67	--	36	23	19	16	67	--	36	23
	Δ Conn.	31.85	19.47	12.25	3.99	1.05	--	47.77	--	24.32	11.96	1.58	--	47.77	--	24.32	11.96
	V	3472	2475	2027	1743	2593	2513	5207	--	3352	2678	3889	3769	5207	--	3352	2678
4	Δ Bldg	22	14	10	7	7	6	84	--	18	13	11	9	84	--	18	13
	Δ Conn.	25.11	15.24	9.75	3.72	1.18	--	37.66	--	19.06	9.96	1.77	--	37.66	--	19.06	9.96
	V	3672	2516	2318	2282	3096	2950	5508	--	3571	3223	4644	4425	5508	--	3571	3223
2	Δ Bldg	7	4	3	3	3	2	10	--	5	4	4	3	10	--	5	4
	Δ Conn.	14.47	8.67	5.73	2.58	1.08	--	21.70	--	10.86	6.08	1.61	--	21.70	--	10.86	6.08
	V	3787	2564	2542	2839	3375	3134	5681	--	3807	3770	5063	4701	5681	--	3807	3770
1	Δ Bldg	2	1	1	1	1	1	3	--	2	1	2	1	3	--	2	1
	Δ Conn.	7.70	4.59	3.09	1.51	0.76	--	11.55	--	5.77	3.34	1.14	--	11.55	--	5.77	3.34
	V	3774	2666	2614	3063	3441	3166	5661	--	3964	4117	5161	4749	5661	--	3964	4117

TABLE 5.7 - BUILDING DEFLECTION (Δ Bldg); CONNECTION SLIPPAGE (Δ Conn.), AND STORY SHEARS - 10 STORY BUILDING (CONT'D)

Story	Δ , mm V, kN	0.15 g										0.25 g									
		Slip Load, kN										Slip Load, kN									
		0	160	320	640	2560	Mono	0	160	320	640	2560	Mono	0	160	320	640	2560	Mono		
15	Δ Bldg	76	36	37	46	49	48	127	59	62	71	81	79								
	Δ Conn.	19.36	6.83	4.40	0.25	0.19	--	32.29	12.64	10.82	6.56	0.32	--								
	V	226	219	320	324	367	408	377	326	405	549	612	681								
12	Δ Bldg	55	26	28	36	36	35	91	42	45	54	61	59								
	Δ Conn.	19.00	6.94	4.82	1.00	0.47	--	31.69	12.61	11.10	7.57	0.78	--								
	V	640	624	868	980	1257	1336	1067	850	1119	1534	2096	2228								
9	Δ Bldg	35	17	18	25	24	23	58	26	29	37	40	39								
	Δ Conn.	17.27	6.44	4.80	2.50	0.72	--	28.80	11.52	10.41	8.18	1.20	--								
	V	843	706	992	1540	1830	1912	1405	999	1267	1897	3052	3189								
6	Δ Bldg	17	8	10	14	13	12	29	13	15	20	21	21								
	Δ Conn.	13.60	5.02	4.02	3.38	0.87	--	22.67	8.83	8.29	7.60	1.45	--								
	V	967	785	1254	1902	2177	2347	1613	991	1507	2421	3629	3914								
3	Δ Bldg	5	3	3	4	4	4	8	4	5	6	7	7								
	Δ Conn.	7.91	2.90	2.76	2.68	0.94	--	13.19	4.81	5.15	5.22	1.56	--								
	V	1240	1056	1486	2068	2549	2629	2067	1351	1959	2730	4250	4383								
1	Δ Bldg	1	0	1	1	1	1	1	1	1	1	1	1								
	Δ Conn.	2.90	1.12	1.16	1.11	0.60	--	4.84	1.79	2.07	2.11	0.99	--								
	V	1349	1185	1548	2267	2705	2727	2249	1545	2154	2727	4511	4548								

TABLE 5.8 - BUILDING DEFLECTION (Δ Bldg), CONNECTION SLIPPAGE (Δ Conn.), AND STORY SHEARS (V) - 15 STORY BUILDING

Story	Δ , mm V, kN	0.33 g								0.5 g							
		Slip Load, kN								Slip Load, kN							
		0	160	320	640	2560	Mono	0	160	320	640	2560	Mono	0	160	320	640
15	Δ Bldg Δ Conn. V	167 42.64 498	78 17.86 384	78 15.09 450	77 9.58 666	107 0.42 808	105 -- 900	251 63.97 747	125 30.20 569	116 24.89 649	-- -- --	-- -- --	157 -- 1350	-- -- --	-- -- --	-- -- --	-- -- --
12	Δ Bldg Δ Conn. V	121 41.85 1410	56 17.71 1065	57 15.28 1303	58 10.36 1814	80 1.03 2769	78 -- 2943	181 62.78 2115	92 29.74 1592	83 24.85 1685	-- -- --	-- -- --	117 -- 4414	-- -- --	-- -- --	-- -- --	-- -- --
9	Δ Bldg Δ Conn. V	76 38.04 1856	35 16.02 1225	36 14.16 1496	40 10.08 2021	53 1.59 4031	51 -- 4171	114 57.06 2784	60 26.62 1755	52 22.72 1982	-- -- --	-- -- --	77 -- 6317	-- -- --	-- -- --	-- -- --	-- -- --
6	Δ Bldg Δ Conn. V	38 29.94 2131	17 12.24 1304	18 10.99 1583	22 8.75 2553	28 1.93 4789	27 -- 5169	57 44.91 3196	32 22.20 2128	25 17.40 1959	-- -- --	-- -- --	41 -- 7754	-- -- --	-- -- --	-- -- --	-- -- --
3	Δ Bldg Δ Conn. V	11 17.42 2730	5 7.11 1676	5 6.22 2148	7 6.41 3133	10 2.11 5592	9 -- 5789	17 26.12 4095	10 13.82 2624	7 9.50 2685	-- -- --	-- -- --	14 -- 8684	-- -- --	-- -- --	-- -- --	-- -- --
1	Δ Bldg Δ Conn. V	2 16.39 2971	1 2.73 1927	1 2.31 2425	1 2.67 3339	2 1.32 5941	2 -- 6006	2 9.58 4456	1 5.27 2835	1 3.52 3070	-- -- --	-- -- --	3 -- 9009	-- -- --	-- -- --	-- -- --	-- -- --

TABLE 5.8 - BUILDING DEFLECTION (Δ Bldg), CONNECTION SLIPPAGE (Δ Conn.), AND STORY SHEARS (V) - 15 STORY BUILDING (CONT'D)

Story	Δ , mm V, kN	0.15 g										0.25 g									
		Slip Load, kN										Slip Load, kN									
		0	160	320	640	2560	Mono	0	160	320	640	2560	Mono								
20	Δ Bldg	83	50	56	75	80	80	139	81	84	99	130	133								
	Δ Conn.	15.76	5.36	0.42	0.12	0.13	--	26.27	12.23	7.23	0.28	0.18	--								
	V	200	163	173	246	264	288	334	281	270	316	441	482								
16	Δ Bldg	60	37	43	57	60	59	101	58	63	77	97	99								
	Δ Conn.	15.50	5.66	1.42	0.36	0.37	--	25.85	12.29	7.94	1.7	0.56	--								
	V	518	513	615	918	981	1084	864	811	857	1112	1636	1808								
12	Δ Bldg	39	25	30	39	39	39	65	38	43	53	64	65								
	Δ Conn.	14.21	5.49	2.72	1.23	0.54	--	23.7	11.15	8.11	3.96	0.88	--								
	V	390	564	818	1177	1349	1391	651	695	1030	1491	2249	2321								
8	Δ Bldg	20	13	16	21	20	20	33	20	23	29	34	34								
	Δ Conn.	11.51	4.67	3.4	2.42	0.72	--	19.19	8.78	7.24	5.39	1.11	--								
	V	693	716	999	1460	1766	1856	1156	917	1299	1867	2945	3094								
4	Δ Bldg	6	4	5	1	7	6	9	6	7	9	11	11								
	Δ Conn.	6.86	3.09	2.71	2.29	0.75	--	11.44	5.52	4.93	4.49	1.22	--								
	V	1047	877	1144	1705	1879	2051	1746	1162	1580	2093	3133	3419								
1	Δ Bldg	0	0	1	1	1	1	1	1	1	1	1	1								
	Δ Conn.	1.93	0.96	0.89	0.80	0.44	--	3.21	1.64	1.57	1.5	0.74	--								
	V	1217	965	1255	1809	1767	2071	2030	1361	1743	2228	3318	3452								

TABLE 5.9 - BUILDING DEFLECTION (Δ Bldg), CONNECTION SLIPPAGE (Δ Conn.), AND STORY SHEARS (V) - 20 STORY BUILDING

Story	Δ , mm V, kN	0.33 g										0.5 g					
		Slip Load, kN										Slip Load, kN					
		0	160	320	640	2560	Mono	0	160	320	640	2560	Mono	0	160	320	640
20	Δ Bldg Δ Conn. V	183 34.70 441	117 17.79 352	130 14.91 367	124 2.78 376	176 0.29 582	176 -- 637	275 52.05 662	216 37.50 498	174 24.49 556	-- -- --	-- -- --	264 -- 955				
16	Δ Bldg Δ Conn. V	133 34.14 1141	86 17.91 1016	96 15.56 1127	94 4.74 1305	131 0.82 2161	130 -- 2388	200 51.21 1711	158 37.20 1419	128 24.28 1609	-- -- --	-- -- --	195 -- 3582				
12	Δ Bldg Δ Conn. V	85 31.30 826	57 16.87 882	63 15.42 1161	63 7.10 1716	87 1.19 2970	85 -- 3065	128 46.96 1289	102 34.19 1375	84 23.35 1382	-- -- --	-- -- --	128 -- 4597				
8	Δ Bldg Δ Conn. V	45 25.34 1527	29 14.23 1139	33 13.72 1489	34 8.16 2077	46 1.58 3889	45 -- 4086	67 38.01 2290	52 27.63 1370	44 20.38 1824	-- -- --	-- -- --	67 -- 6129				
4	Δ Bldg Δ Conn. V	14 15.74 2306	9 8.87 1423	10 8.82 1840	11 6.30 2449	14 1.66 4138	14 -- 4516	20 23.62 3459	15 16.60 2049	13 12.91 2305	-- -- --	-- -- --	21 -- 6774				
1	Δ Bldg Δ Conn. V	1 4.65 2681	1 2.54 1680	1 2.57 2029	0 2.03 2676	0 0.97 4382	1 -- 4560	2 6.97 4021	1 4.70 2886	1 3.73 2703	-- -- --	-- -- --	2 -- 6839				

TABLE 5.9 - BUILDING DEFLECTION (Δ Bldg), CONNECTION SLIPPAGE (Δ Conn.), AND STORY SHEARS (V) - 20 STORY BUILDING (CONT'D)

Type of Wall	Type of Stress (kPa)		Building Height (stories)			
			20	15	10	5
Individual Walls	1	Bending Stress	26978	36804	44233	10637
	2	Gravity Stress	3356	2512	1678	839
	3	Maximum Tension (1-2)	23622	34292	43255	9798
	4	Maximum Compression (1+2)	30334	39316	46611	11467
Monolithic Wall	5	Bending Stress	45632	45232	17505	2785
	6	Gravity Stress	3356	2512	1678	839
	7	Maximum Tension (5-6)	42276	42720	15827	1946
	8	Maximum Compression (5+6)	48988	47744	19183	3624
Walls with LSB Joints	9	Bending Stress	16602	17212	14424	3683
	10	Axial Couple Stress	2455	2353	4093	1047
	11	Gravity Stress	3356	2565	1678	839
	12	Maximum Tension (9+10-11)	15701	17000	16839	3891
	13	Maximum Compression (9+10+11)	22413	22130	20195	5569
	14	Minimum Tension (9-10-11)	10791	12294	3683	1797
	15	Minimum Compression (9-10+11)	17503	17424	12009	3475

TABLE 5.10 - NET STRESSES AT BASE, kPa (accln = 0.33g)

Type of Wall	Fundamental Period, Seconds		
	Isolated Walls	Monolithic Walls	Coupled Walls with LSB Joints (initial period)
5 Story Wall	0.11	0.05	0.08
10 Story Wall	0.43	0.21	0.3
15 Story Wall	0.97	0.48	0.6
20 Story Wall	1.72	0.86	0.97

TABLE 5.11 - FUNDAMENTAL PERIODS OF VIBRATION

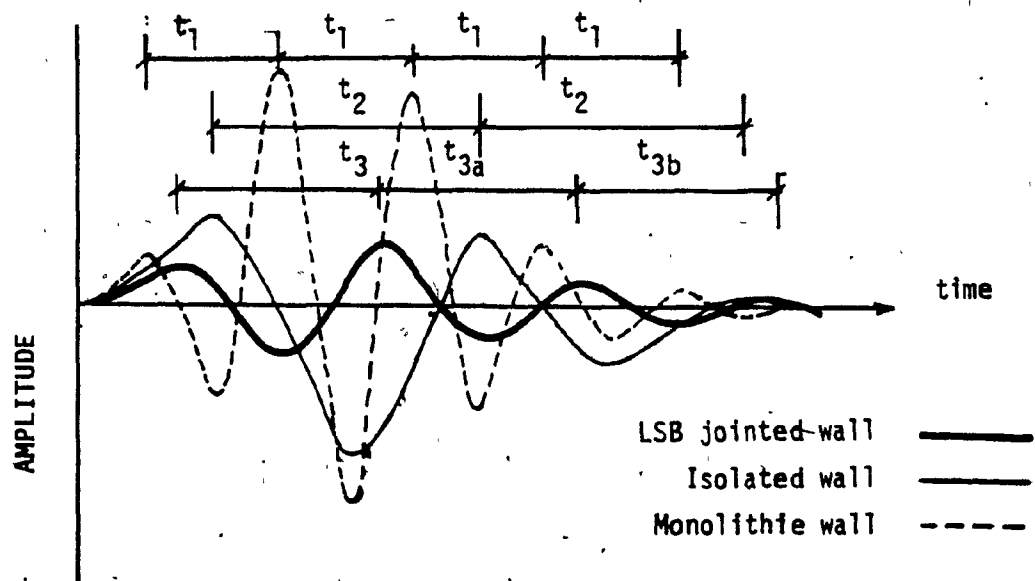


FIG. 5.1 NATURAL FREQUENCY OF LSB JOINTED WALL

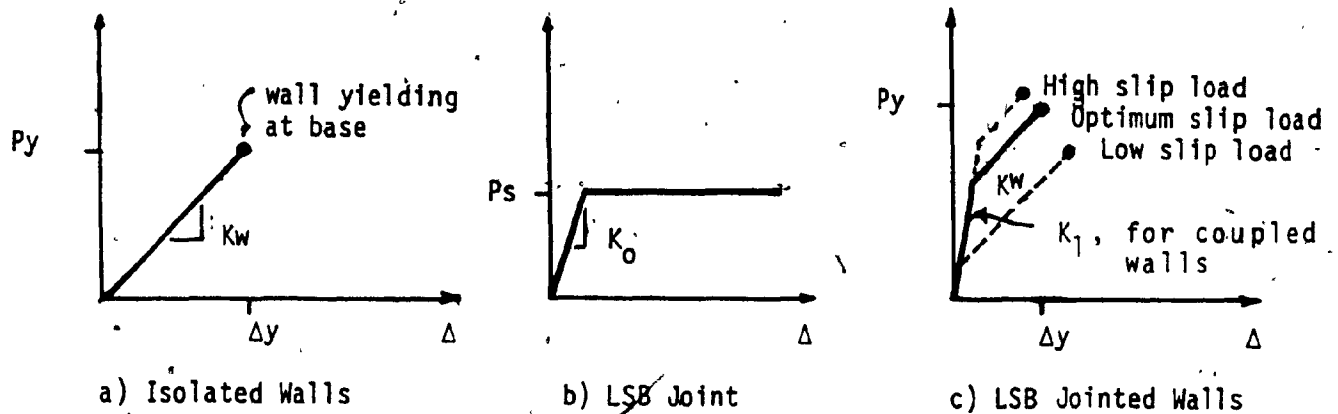


FIG. 5.2 EFFECT OF SLIP LOAD ON LOAD-DEFORMATION CHARACTERISTICS OF COUPLED WALLS

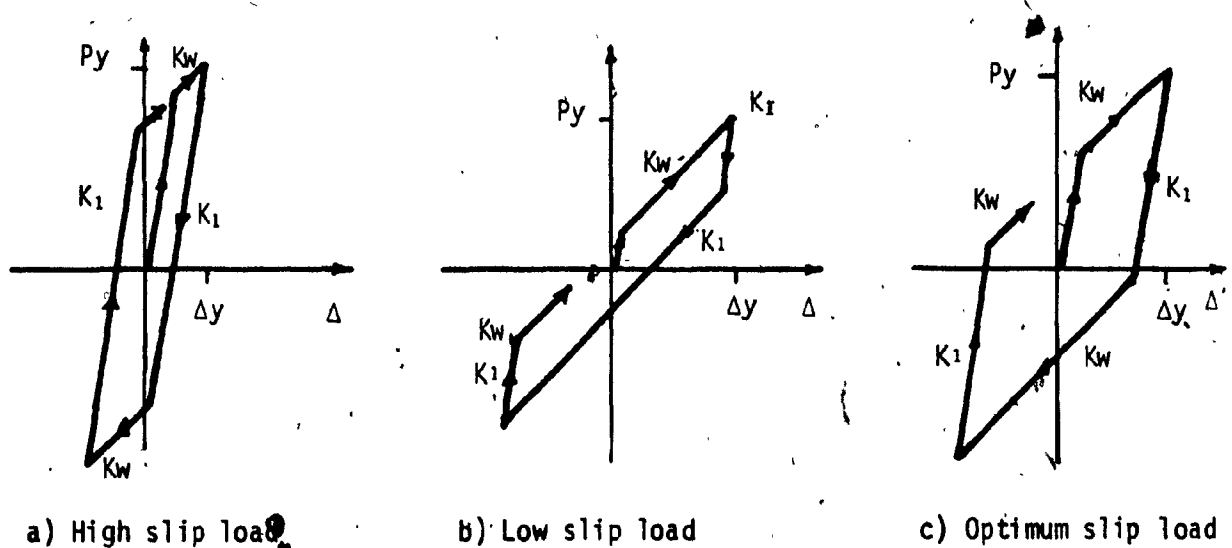


FIG. 5.3 EFFECT OF SLIP LOAD ON HYSTERETIC BEHAVIOUR OF COUPLED WALLS

IMPERIAL VALLEY EARTHQUAKE MAY 18, 1940 - 2037 PST

111A001 40.001.0 EL CENTRO SITE IMPERIAL VALLEY IRRIGATION DISTRICT COMP 500E

DAMPING VALUES ARE 0, 2, 5, 10 AND 20 PERCENT OF CRITICAL

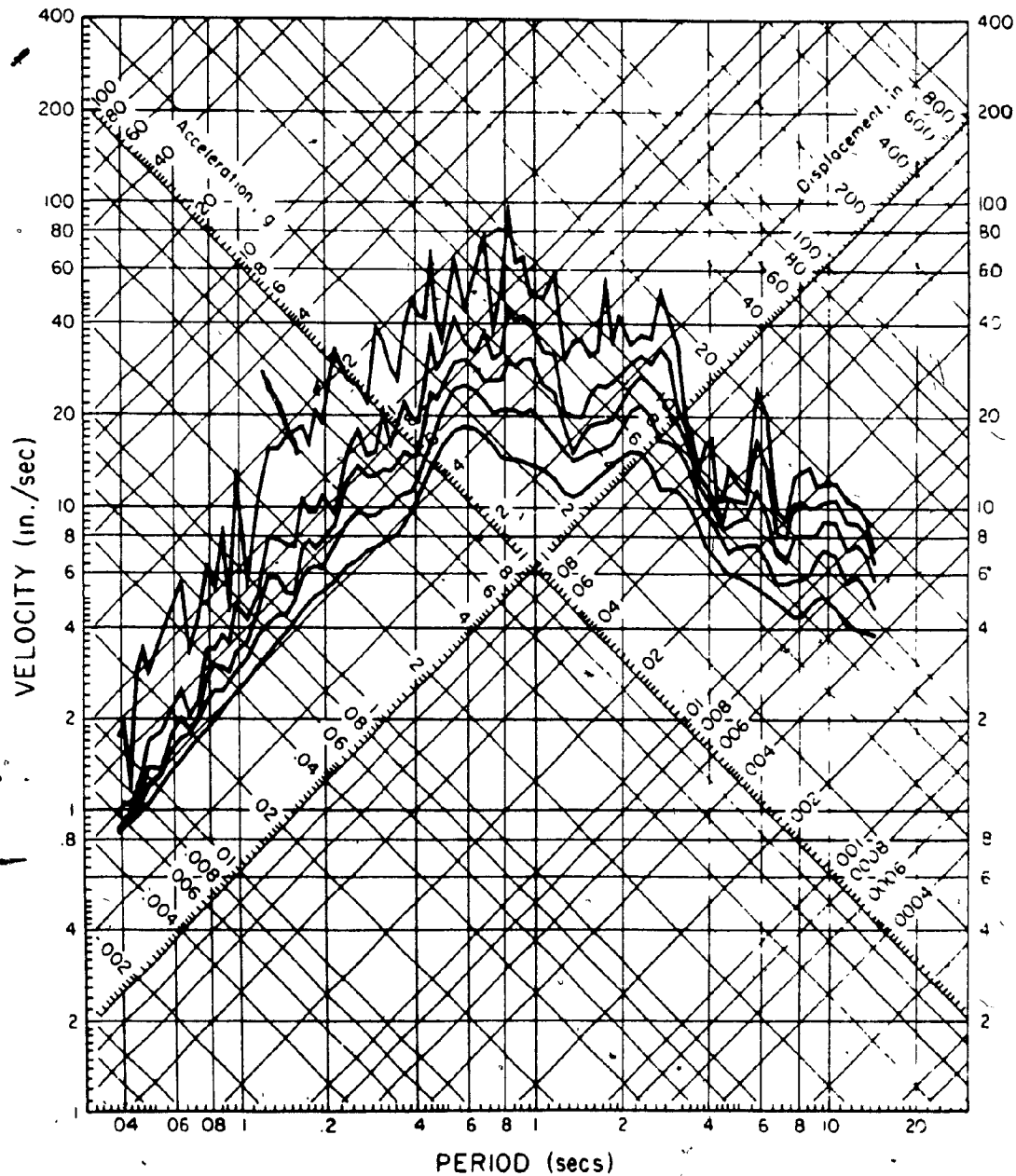


FIG. 5.4- EL CENTRO RESPONSE SPECTRUM, N.S COMPONENT

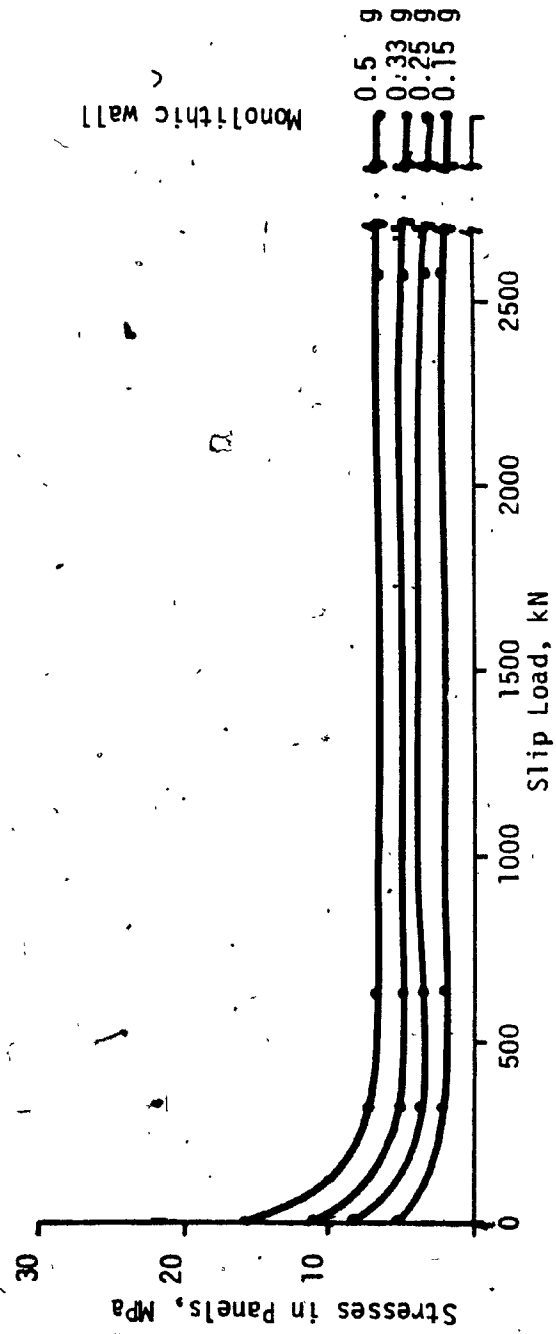


FIG. 5.5 - SLIP LOAD - STRESS RELATION, 5 STORY BUILDING

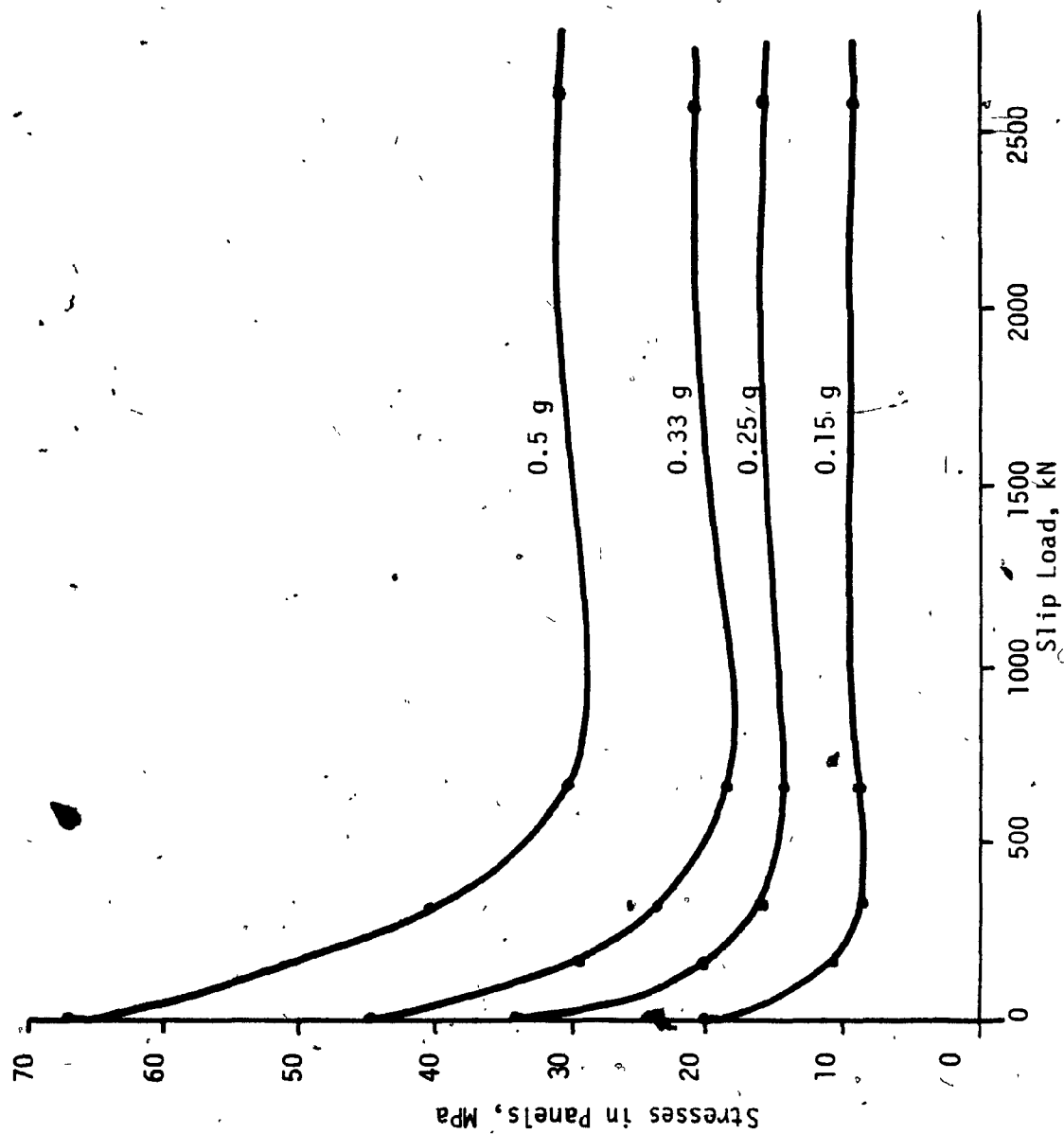


FIG. 5.6 - SLIP LOAD - STRESS RELATION, 10 STORY BUILDING

Monolithic wall

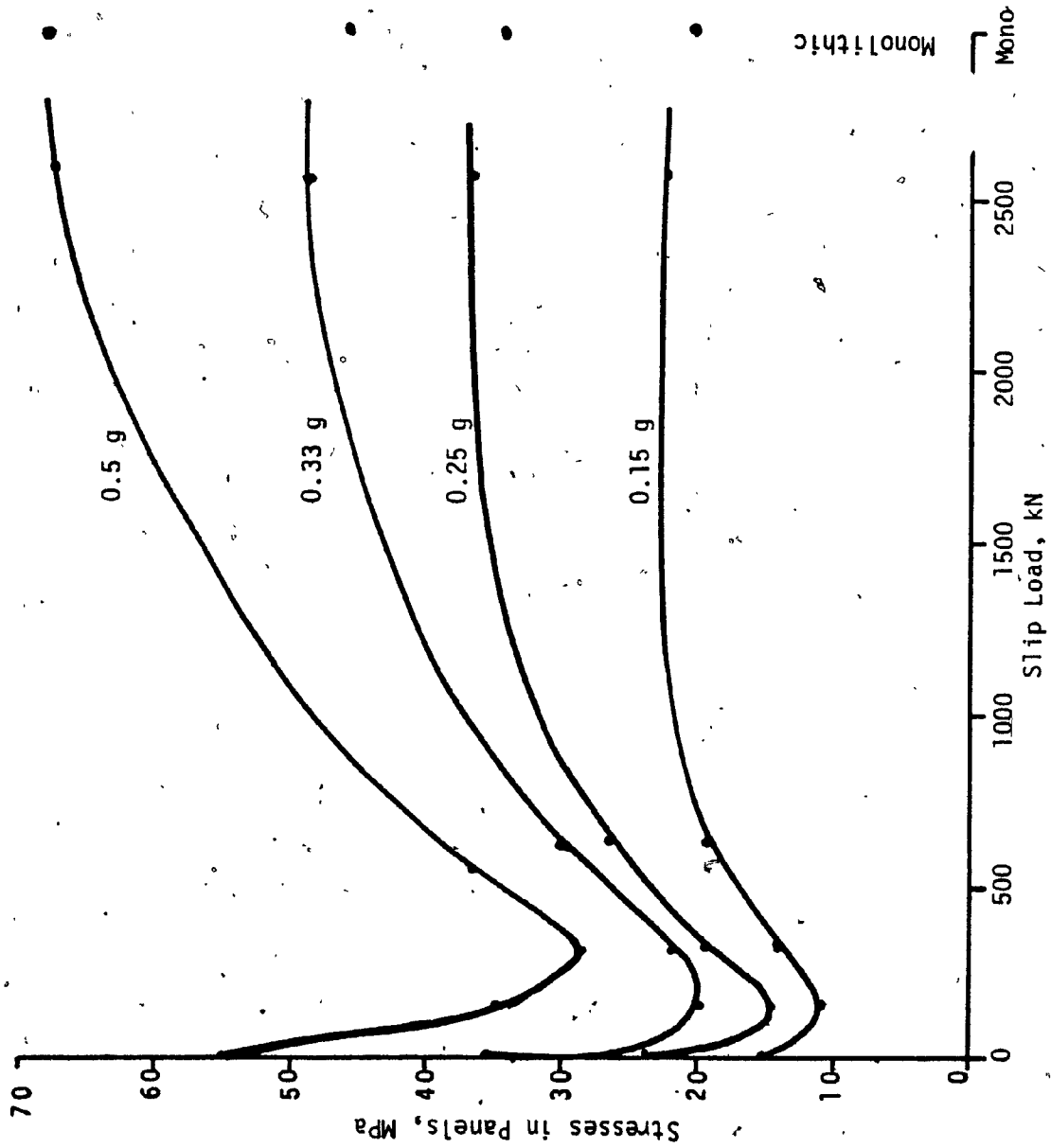


FIG. 5.7 - SLIP LOAD - STRESS RELATION, 15 STORY BUILDING

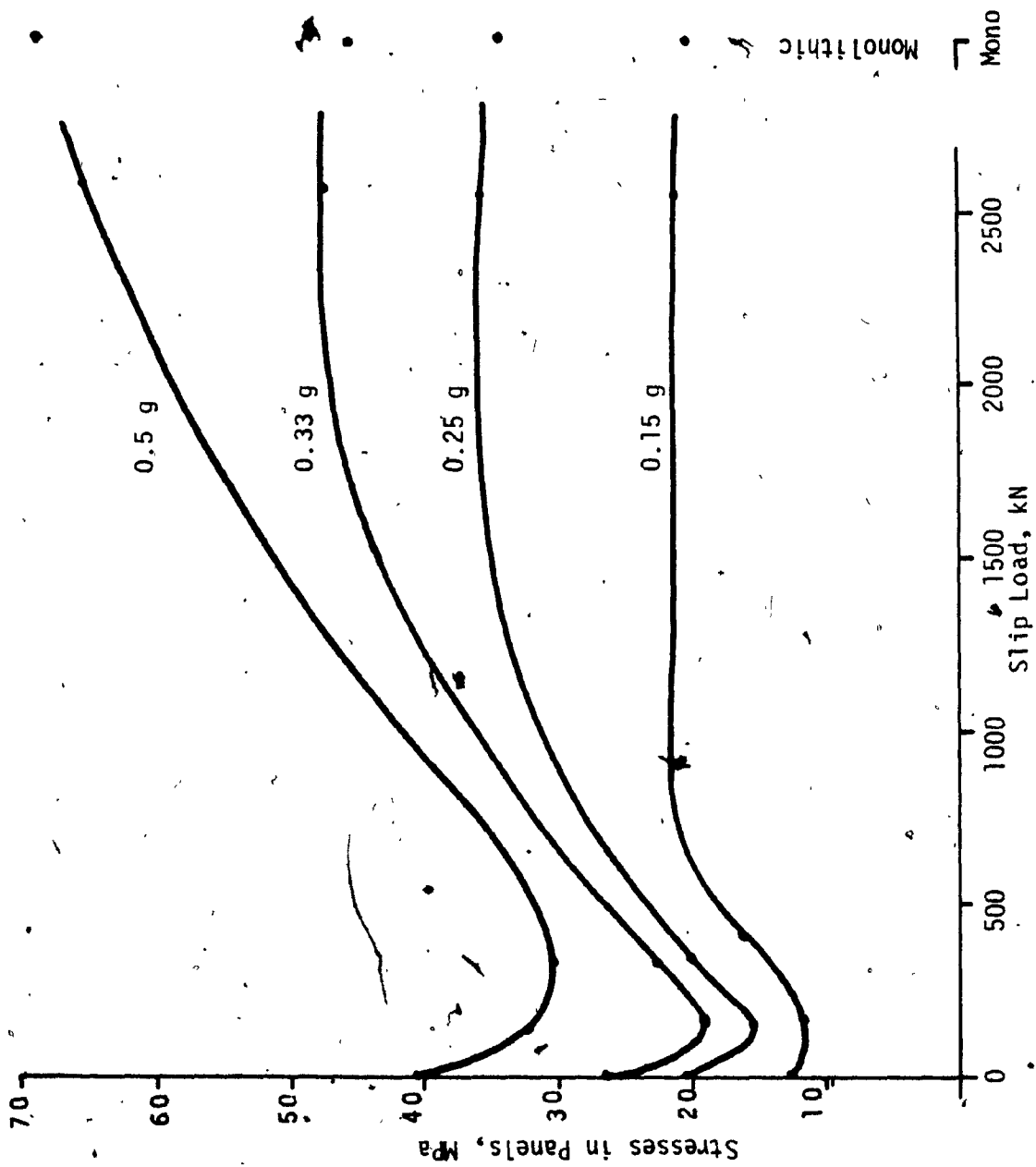
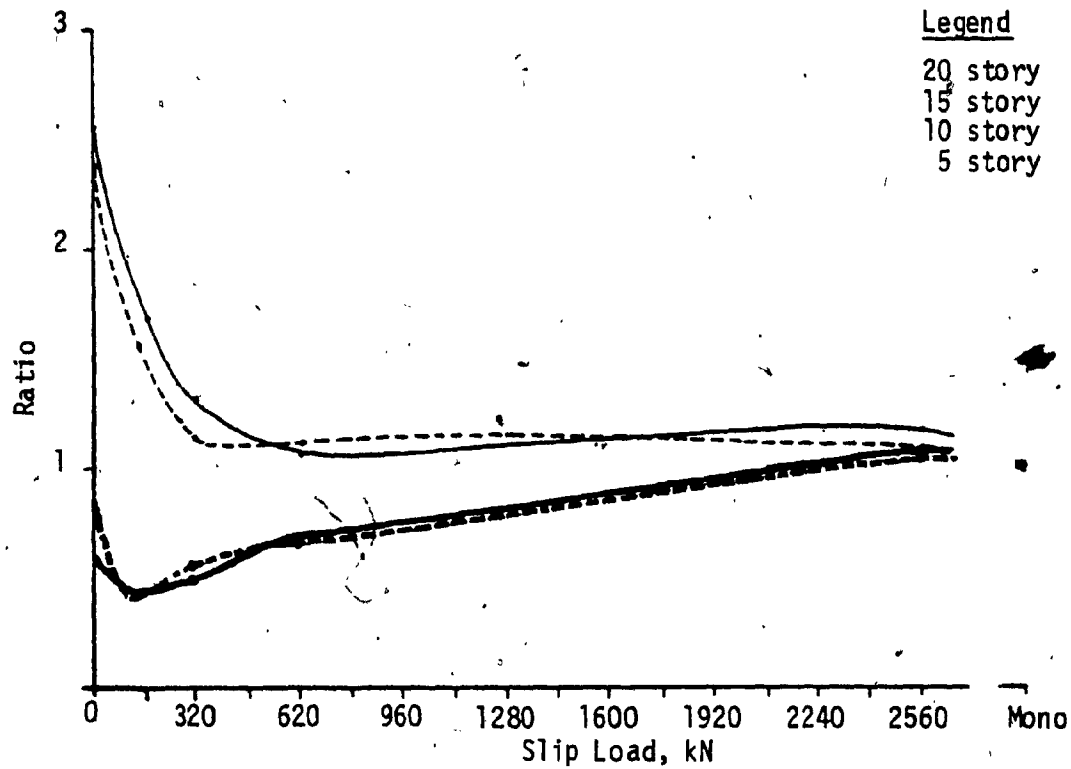
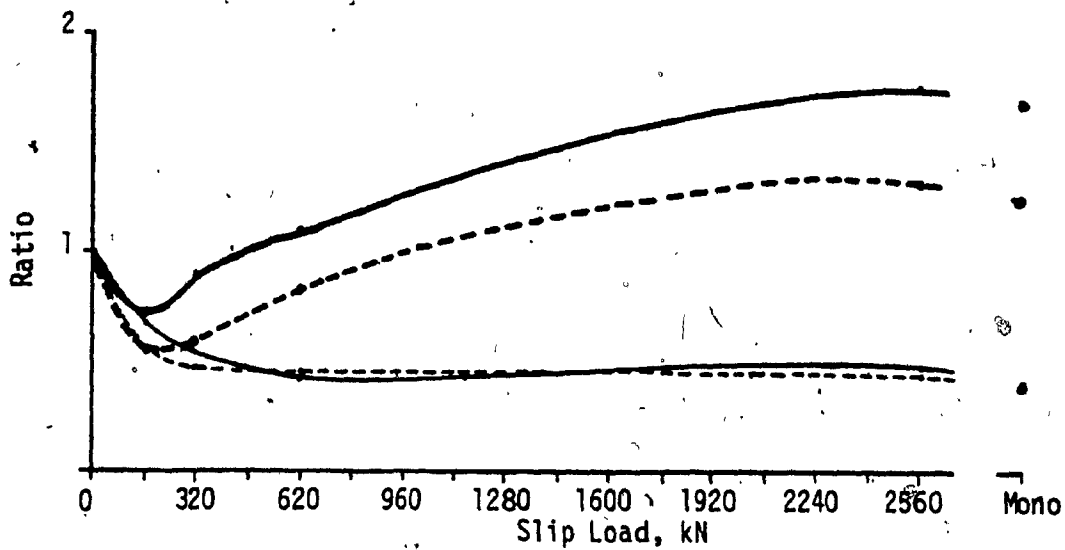


FIG. 5.8 - SLIP LOAD - STRESS RELATION, 20 STORY BUILDING

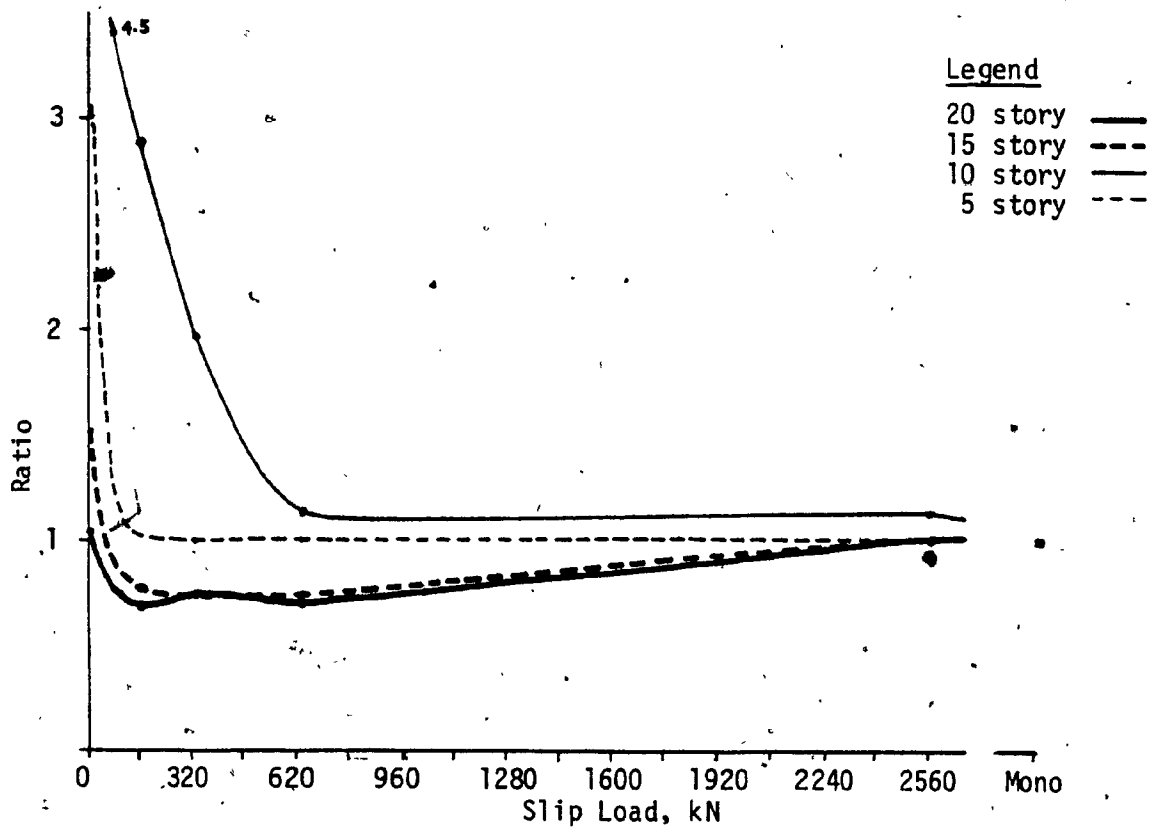


a) Ratio of stress of jointed wall to monolithic wall

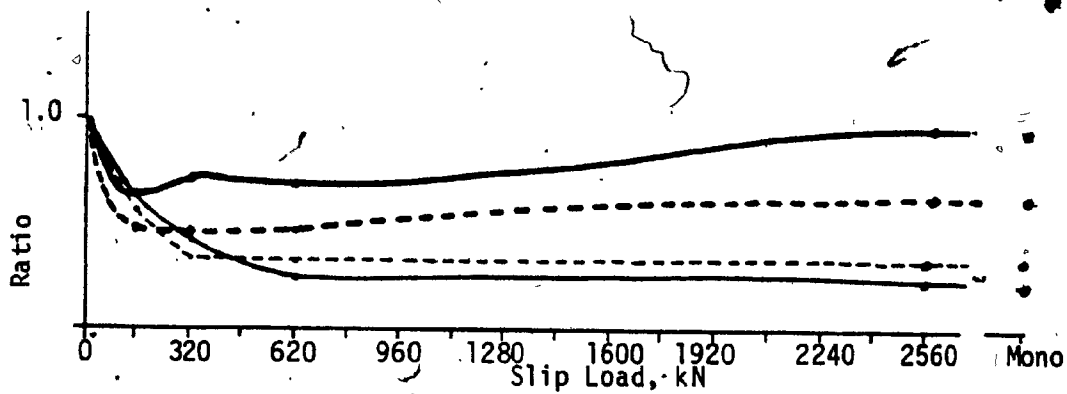


b) Ratio of stress in jointed wall to isolated wall

FIG. 5.9 - EFFECT OF SLIP LOAD ON STRESSES, 0.33 g



a) Ratio of top deflection of jointed wall to monolithic wall



b) Ratio of top deflection of jointed wall to isolated wall

5.10 - EFFECT OF SLIP LOAD ON BUILDING DEFLECTION, 0.33 g

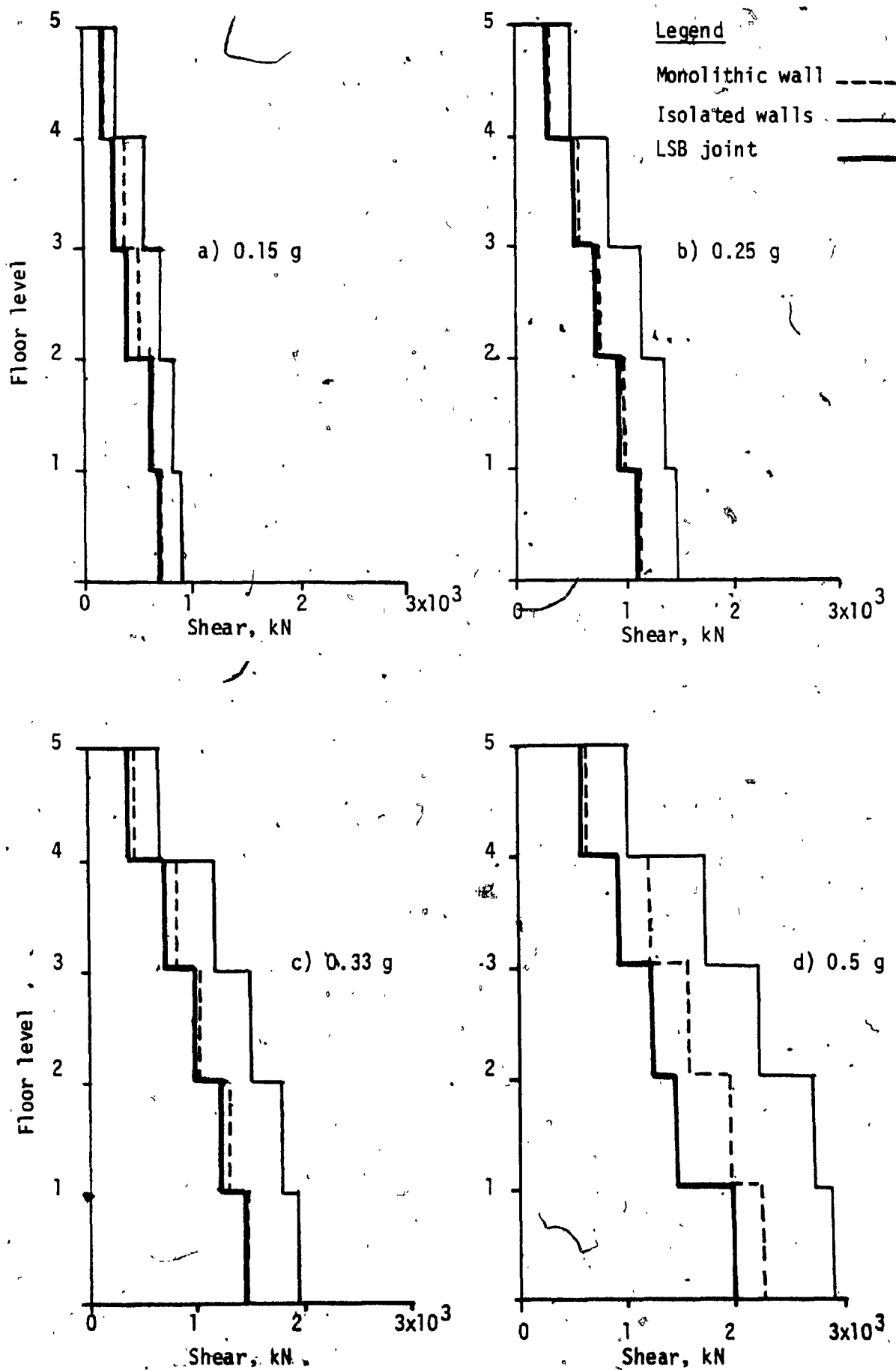


FIG. 5.11 - STORY SHEAR ENVELOPE, 5 STORY BUILDING

Legend

Monolithic wall ---
Isolated walls —
LSB joint —

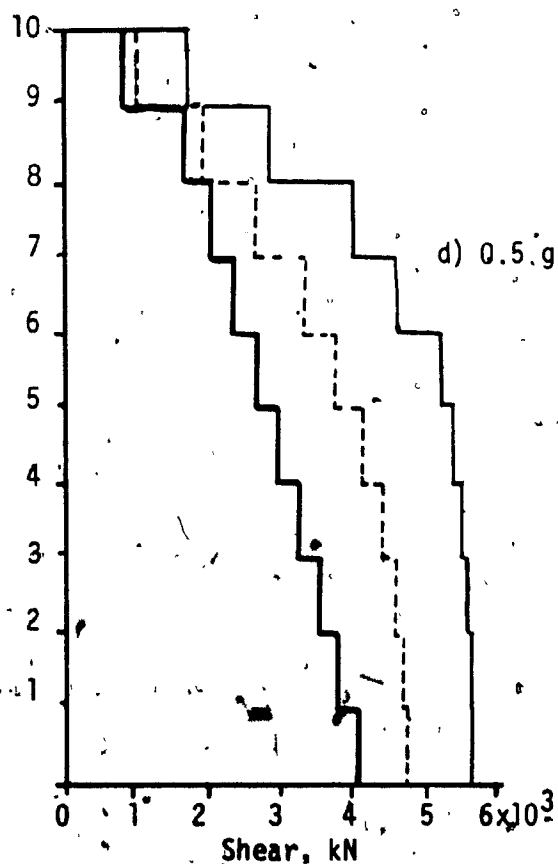
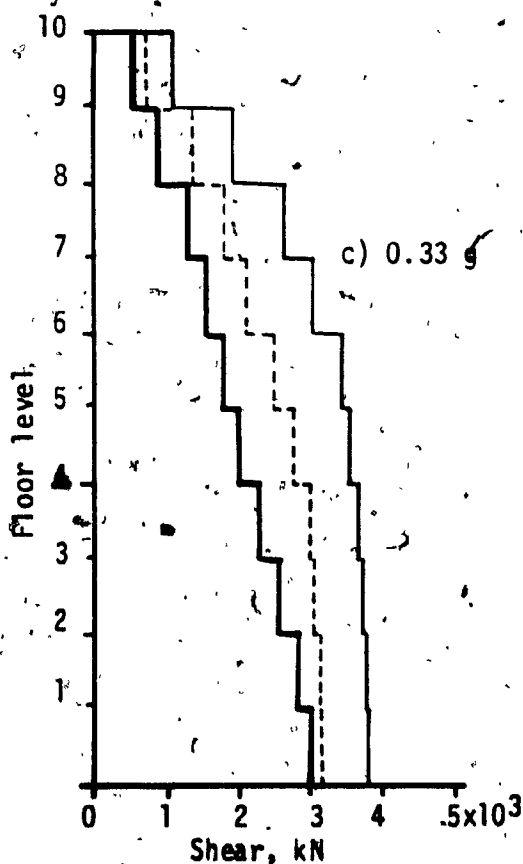
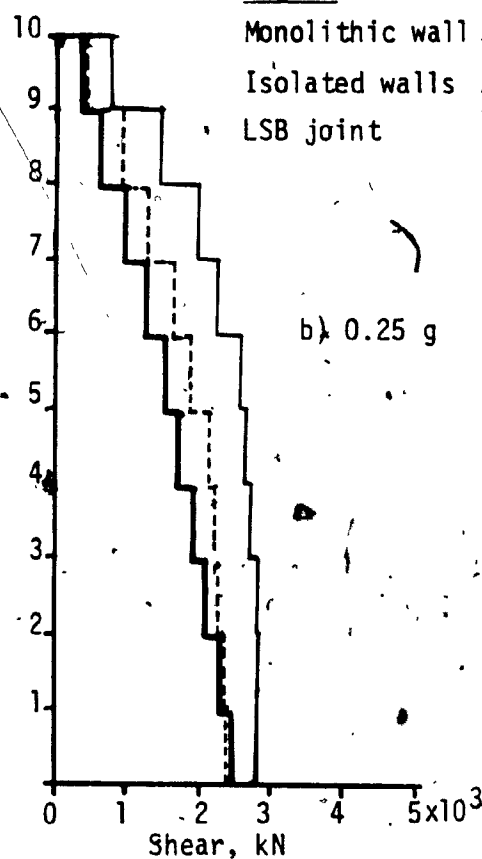
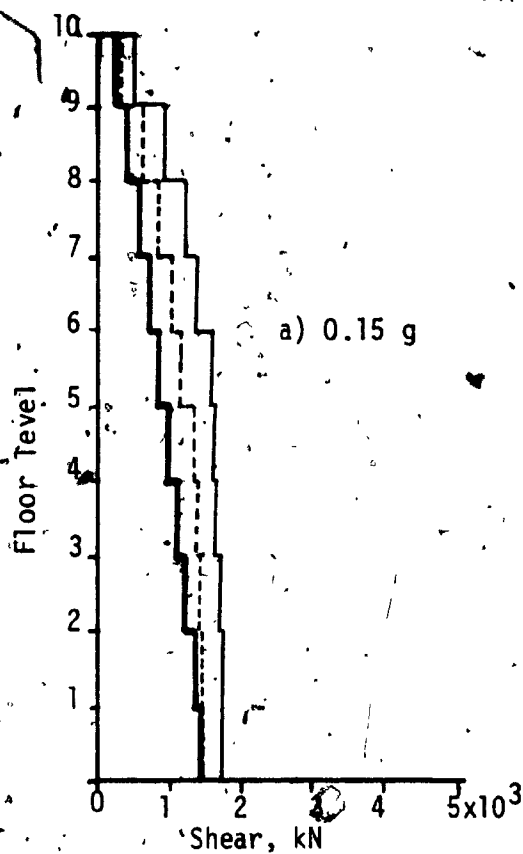


FIG. 5.12 - STORY SHEAR ENVELOPE, 10 STORY BUILDING

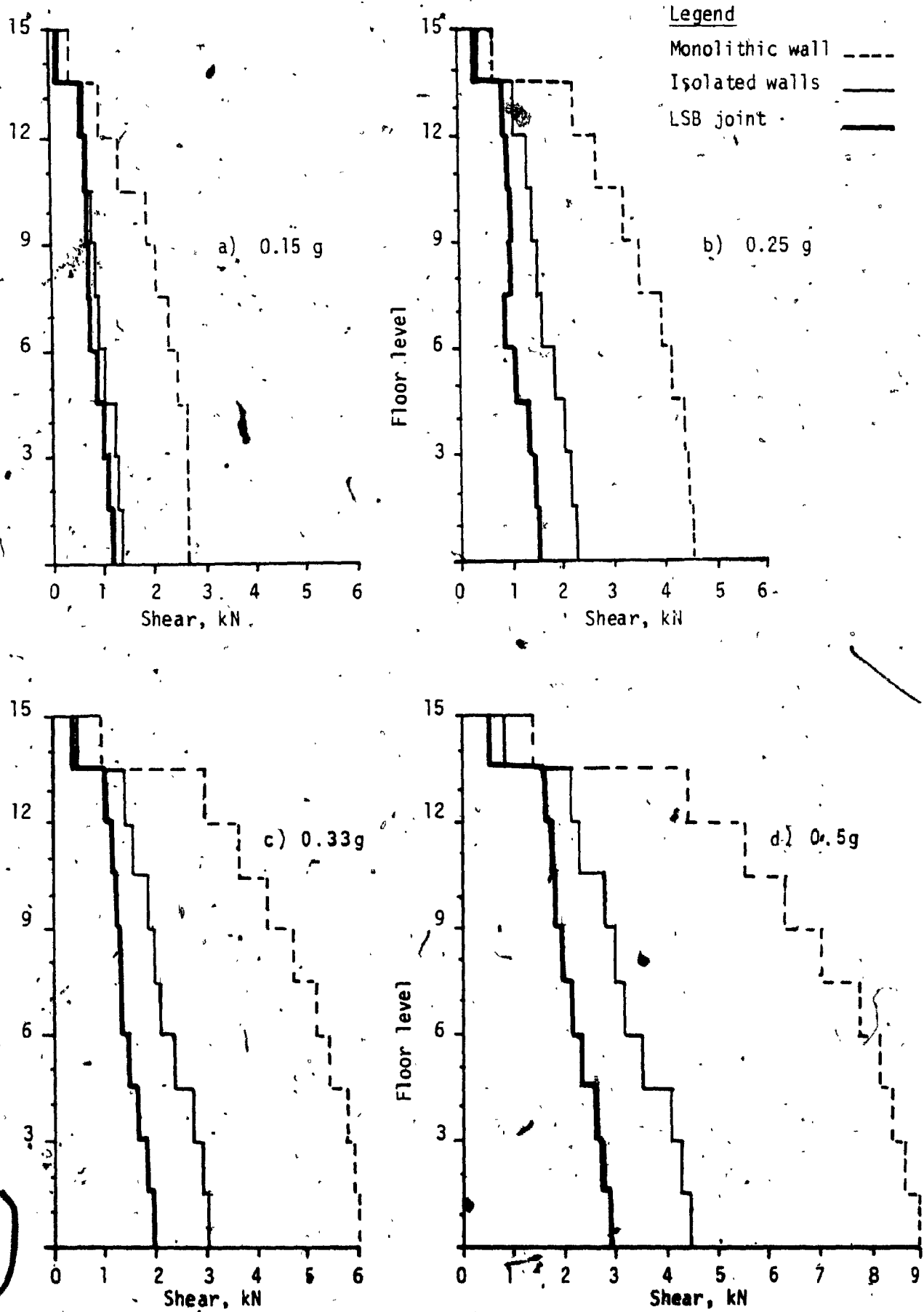


FIG. 5.13 - STORY SHEAR ENVELOPE, 15 STORY BUILDING

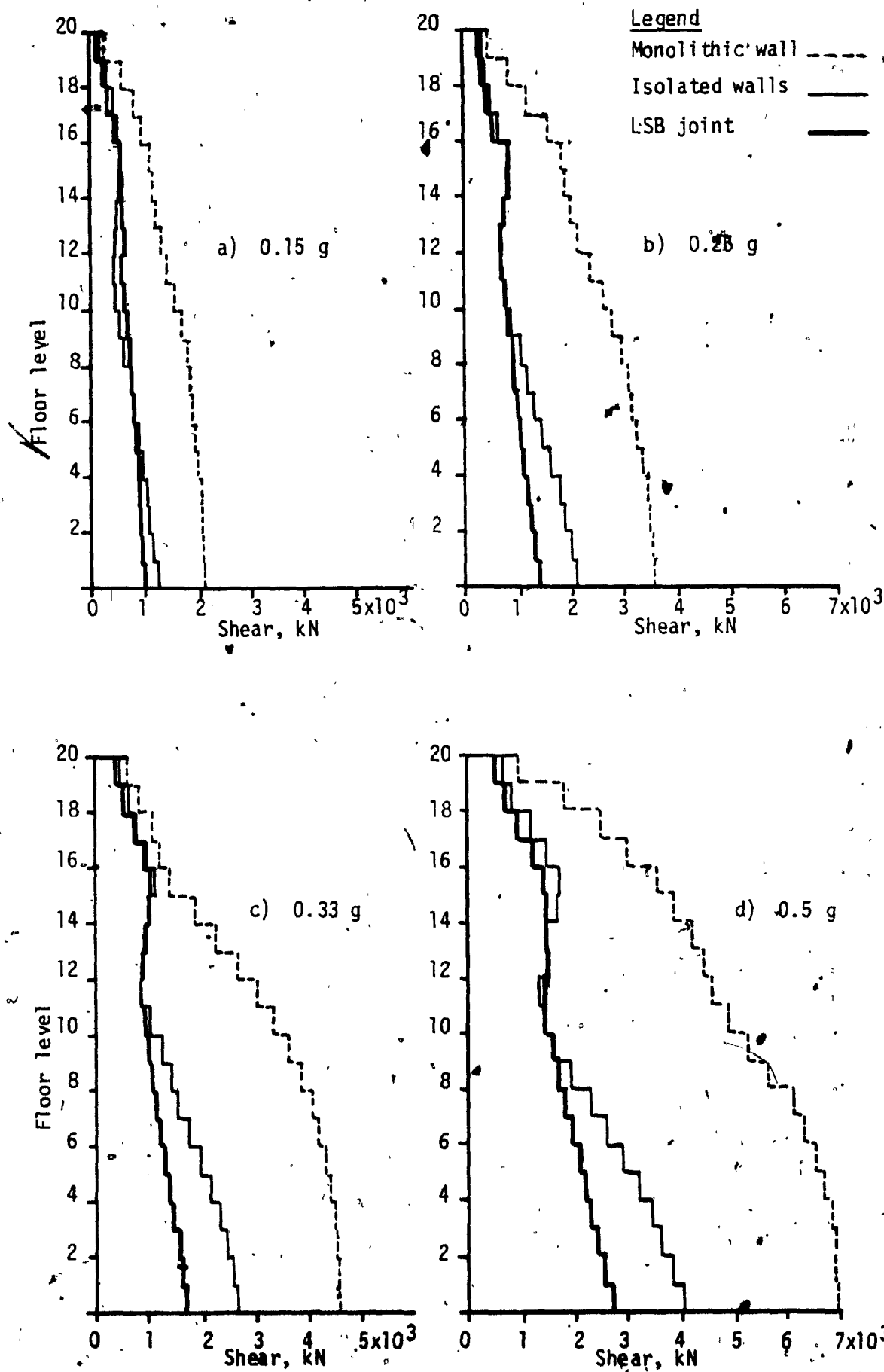


FIG. 5.14 - STORY SHEAR ENVELOPE, 20 STORY BUILDING

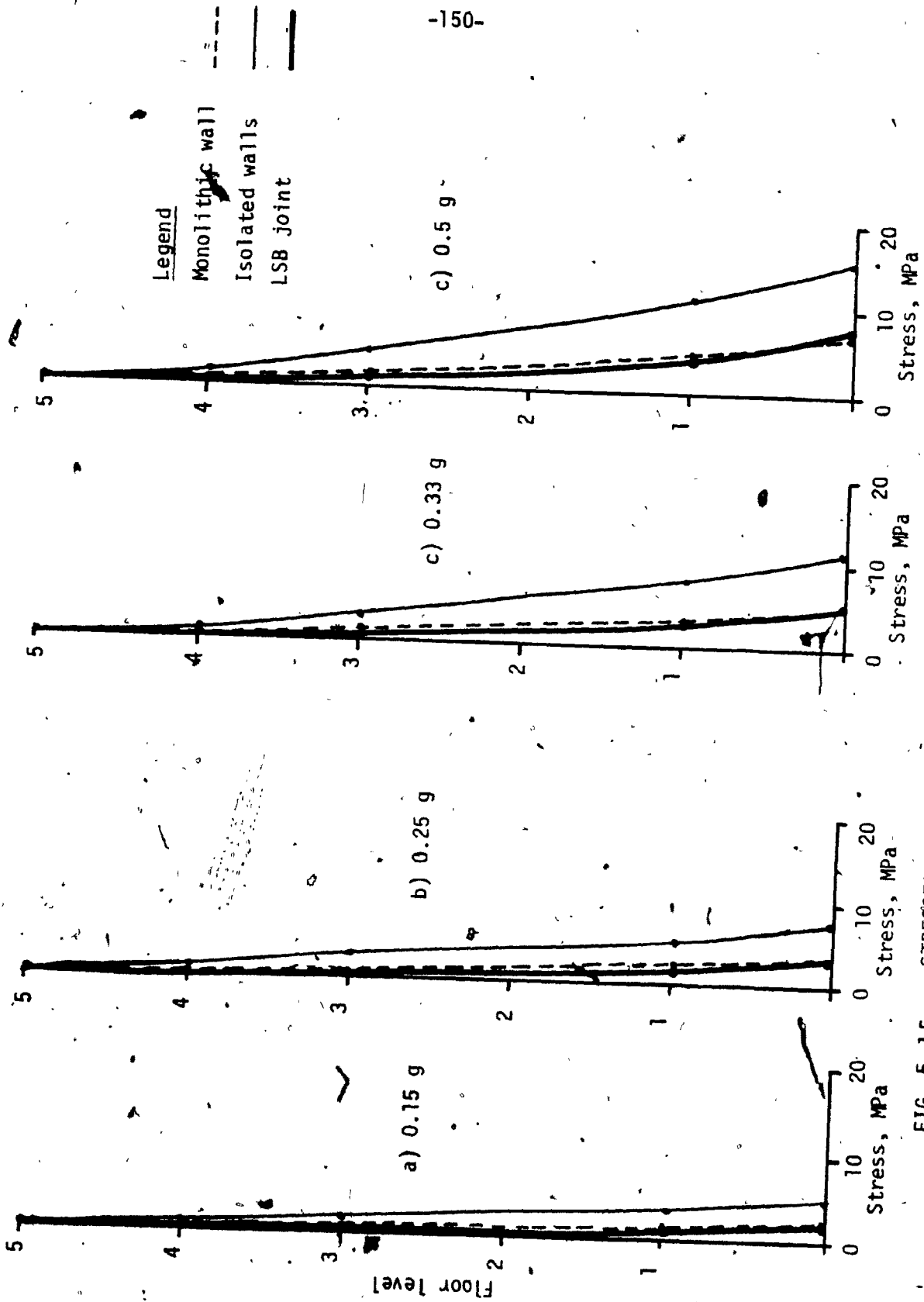


FIG. 5.15 - STRESSES IN PANELS, 5 STORY BUILDING

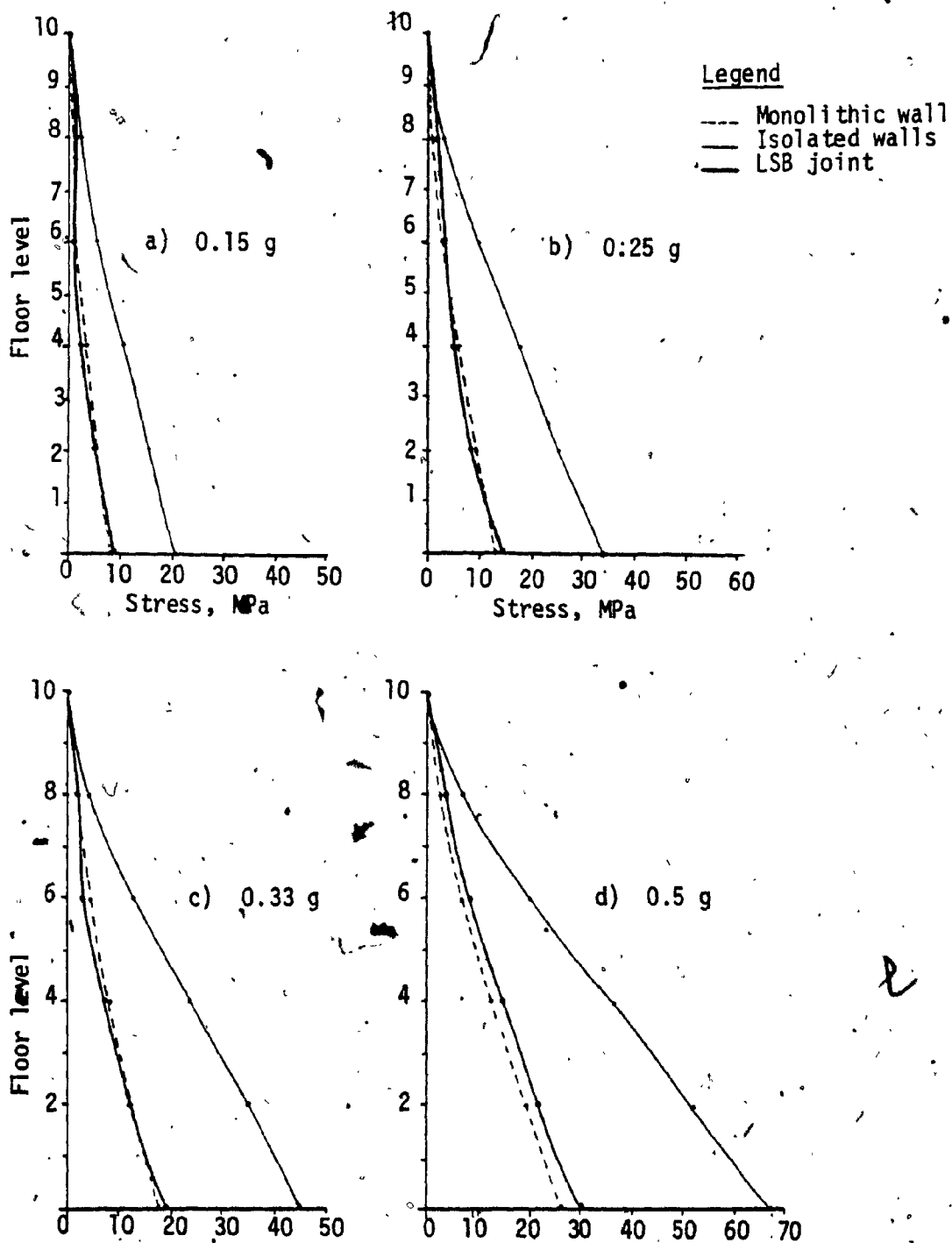


FIG. 5. 16 - STRESSES IN PANELS, 10 STORY BUILDING

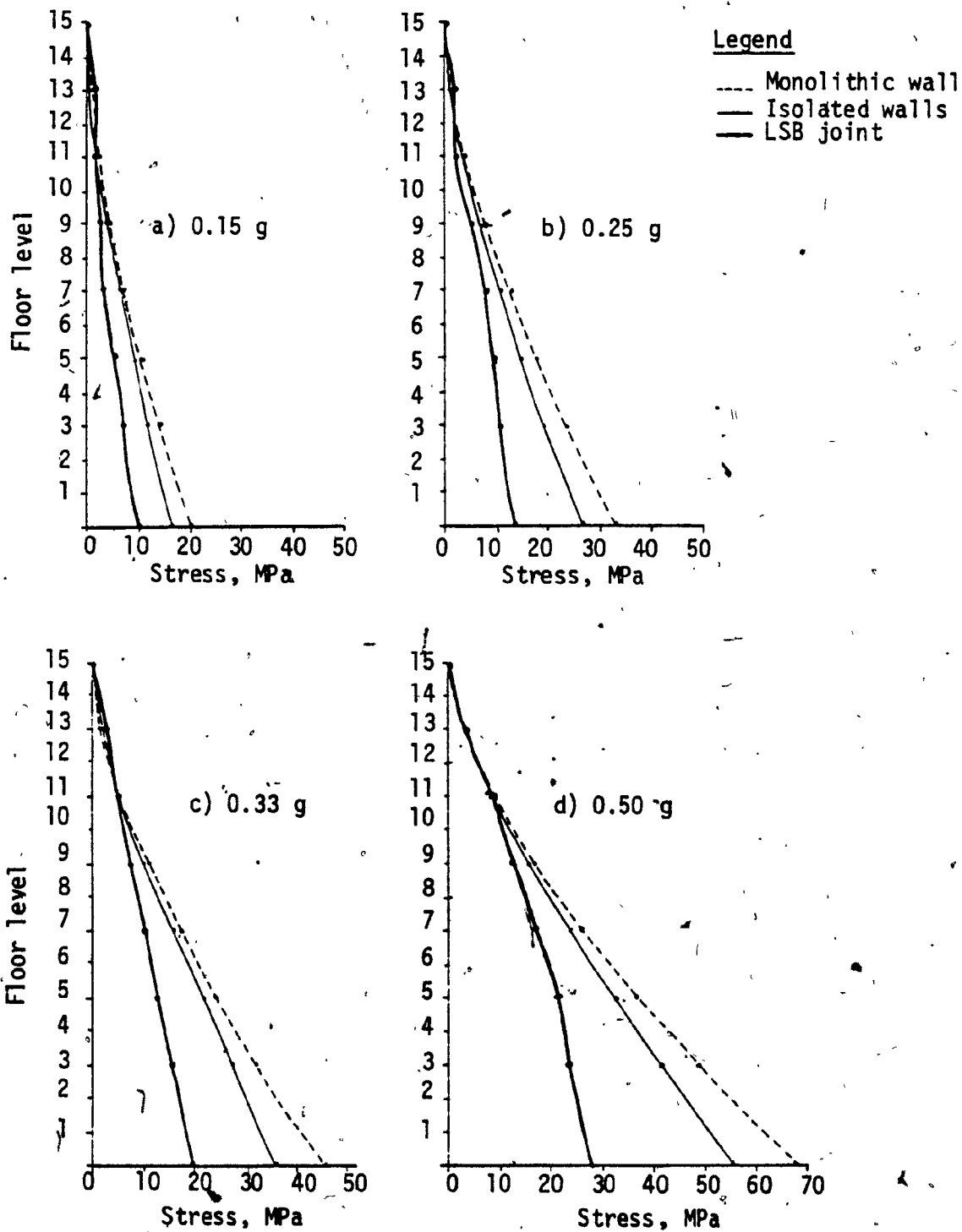
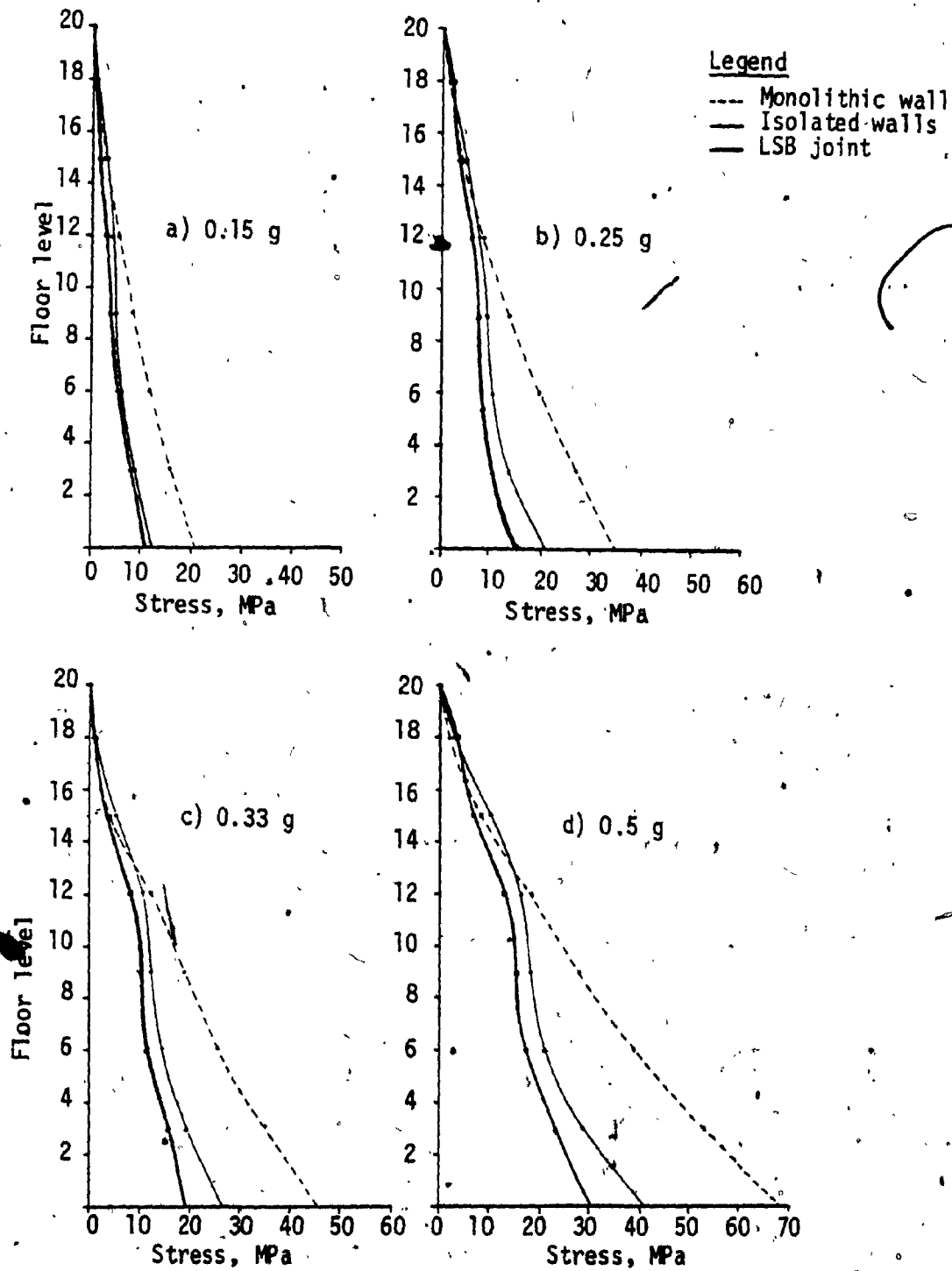


FIG. 5. 17- STRESS IN PANELS, 15 STORY BUILDING



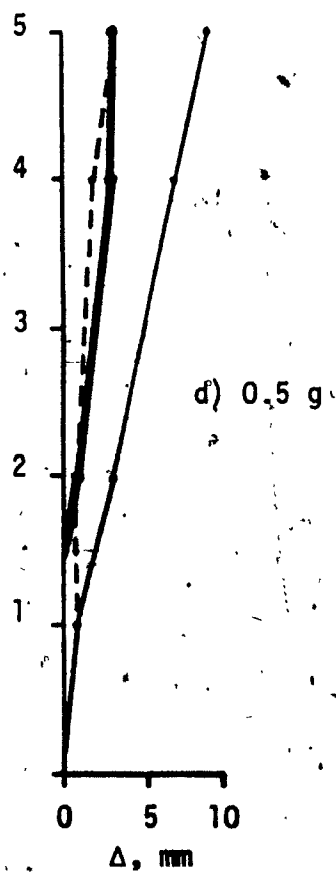
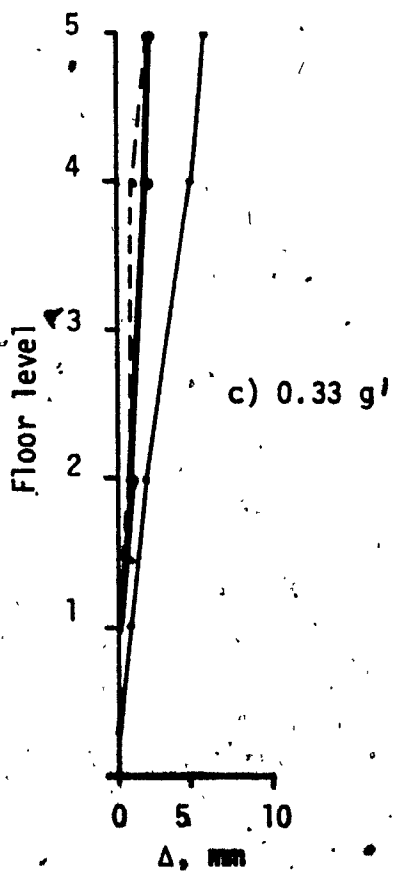
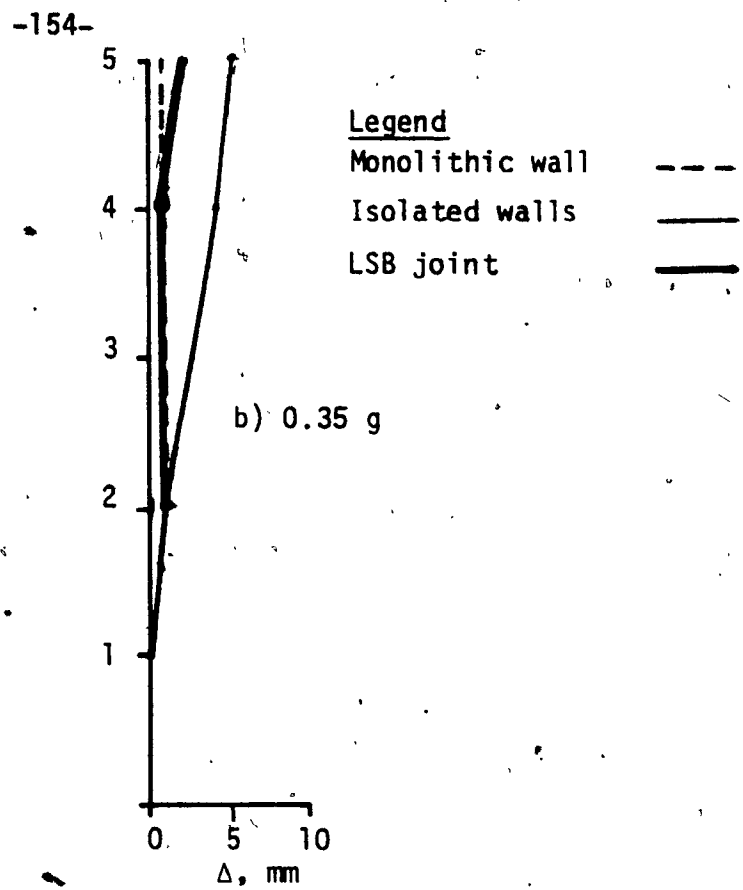
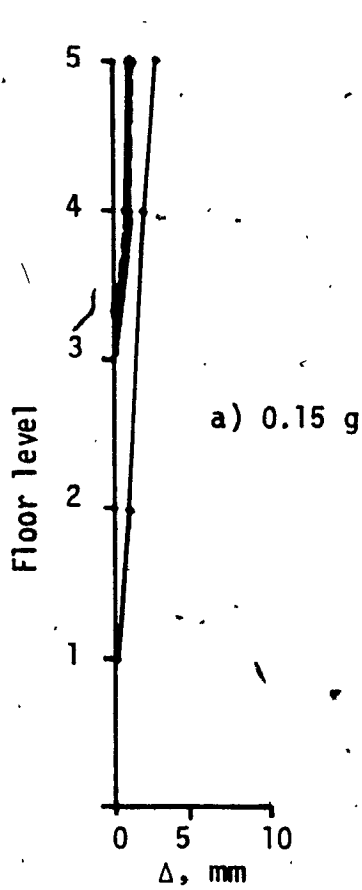


FIG. 5.19-- DEFLECTION ENVELOPE, 5 STORY BUILDING

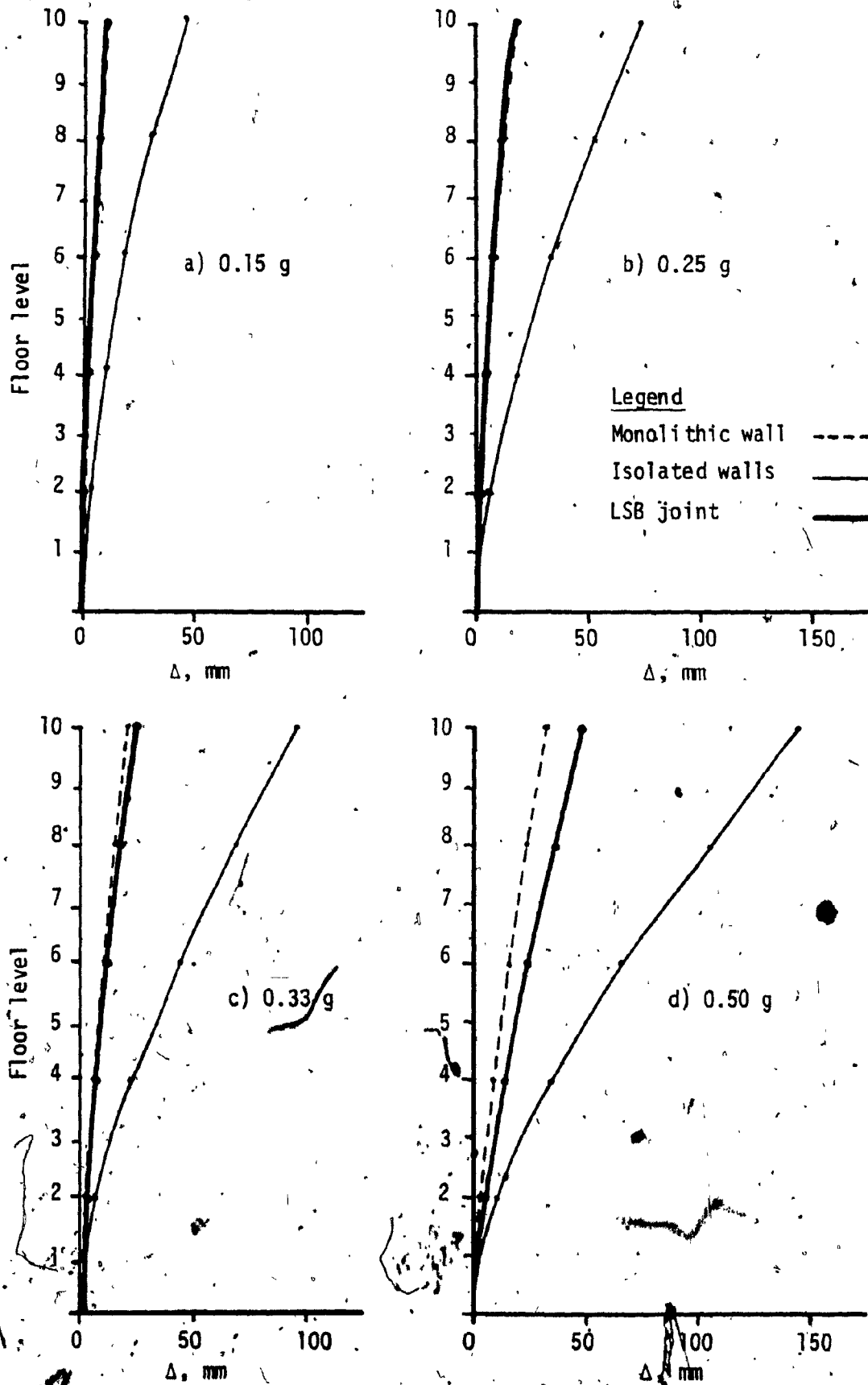


FIG. 5.20 - DEFLECTION ENVELOPE, 10 STORY BUILDING

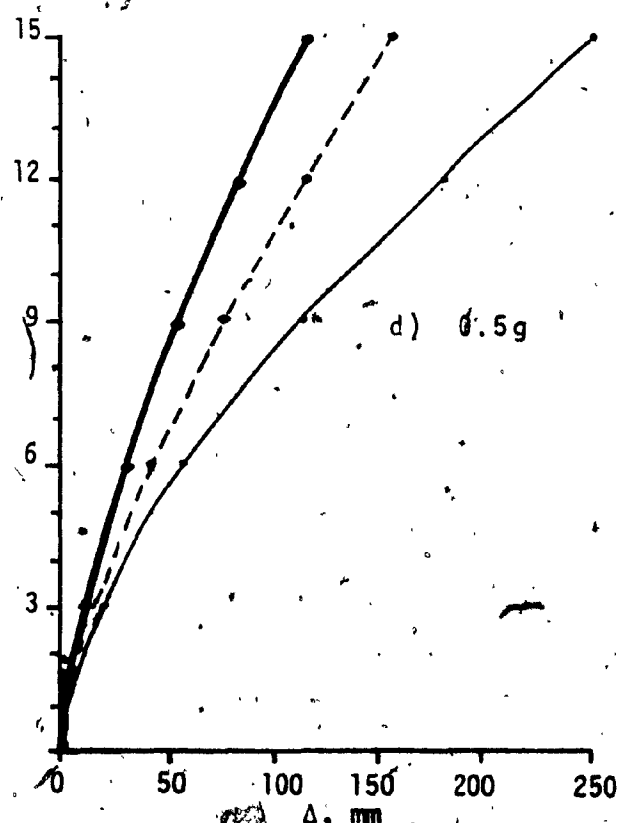
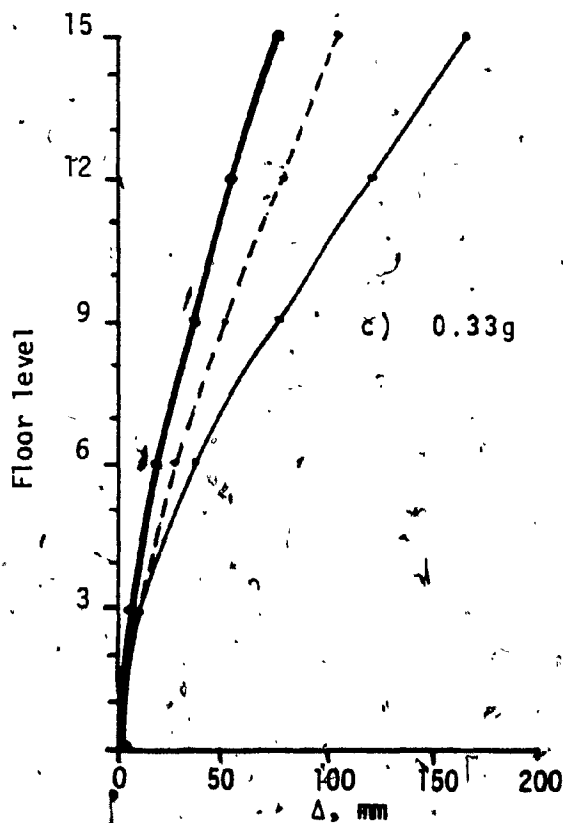
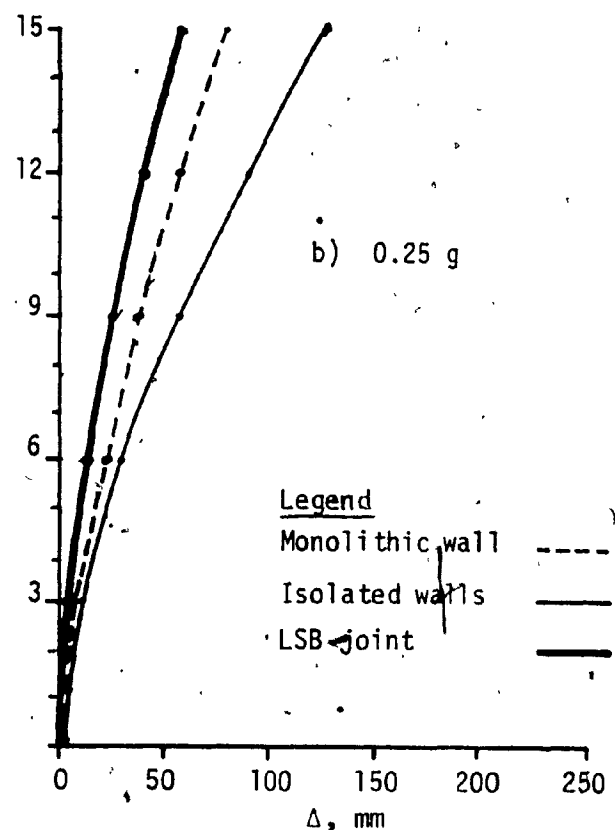
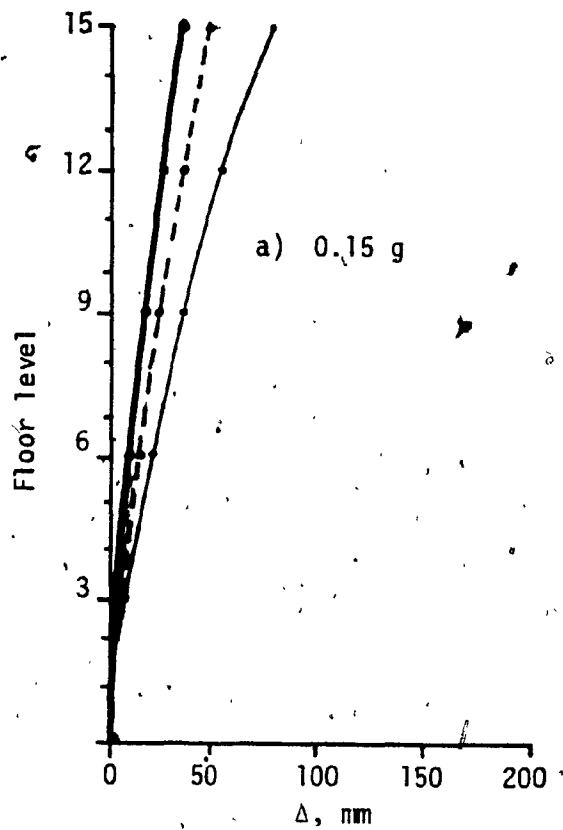


FIG. 5.21 - DEFLECTION ENVELOPE, 15 STORY BUILDING

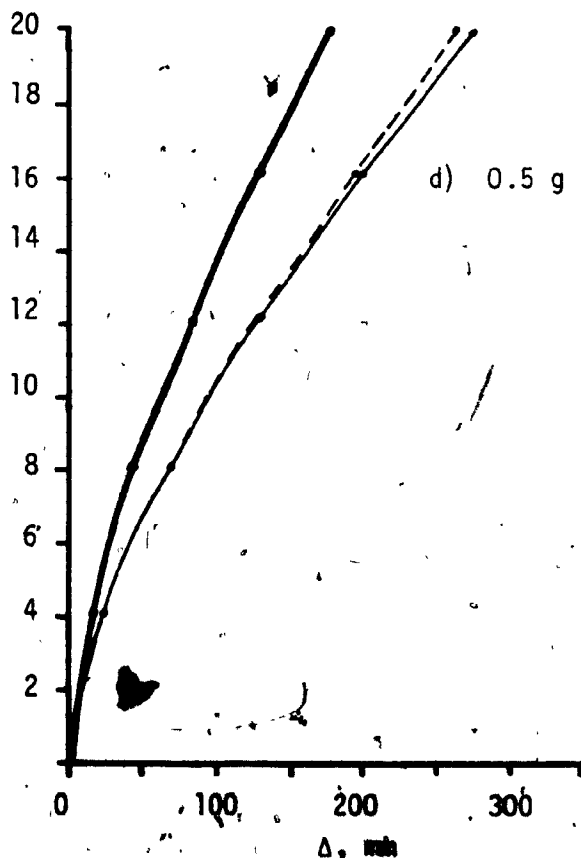
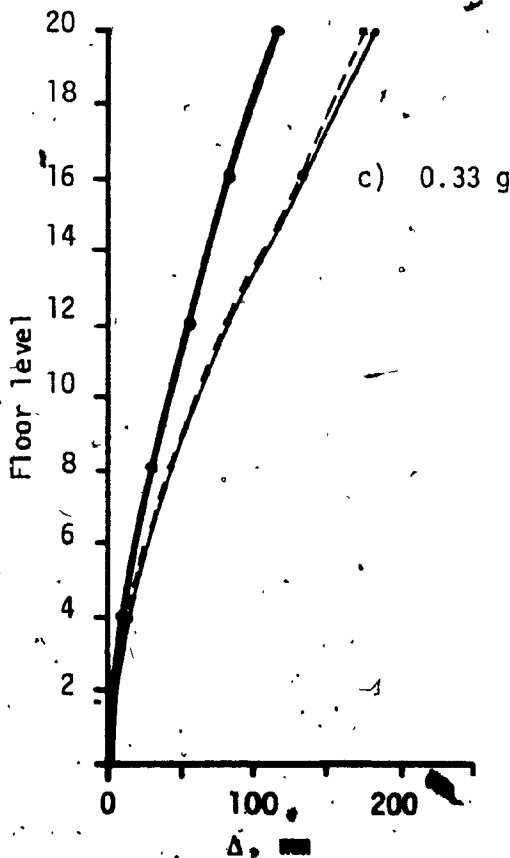
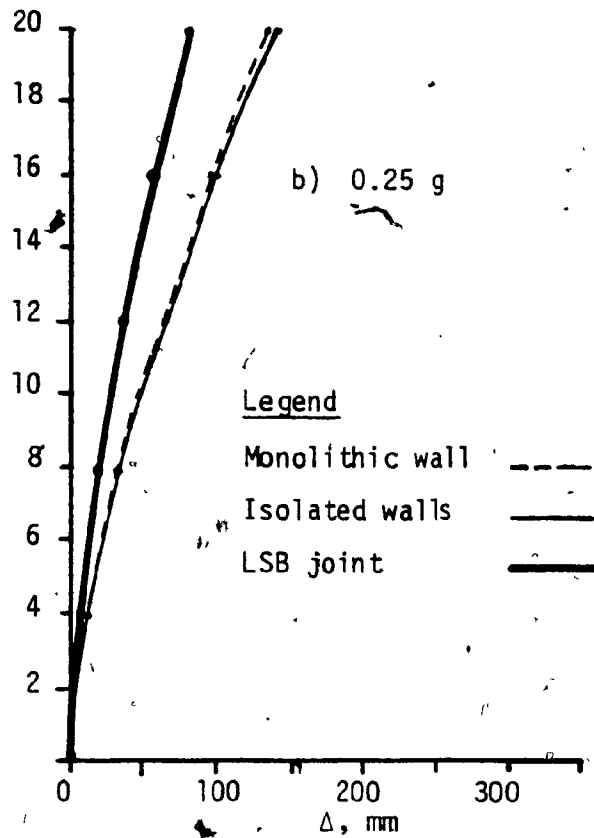
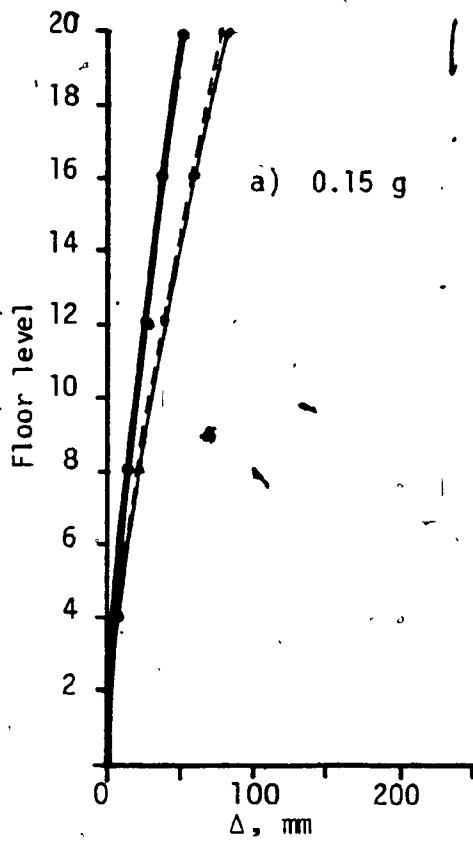


FIG. 5.22 - DEFLECTION ENVELOPE, 20 STORY BUILDING

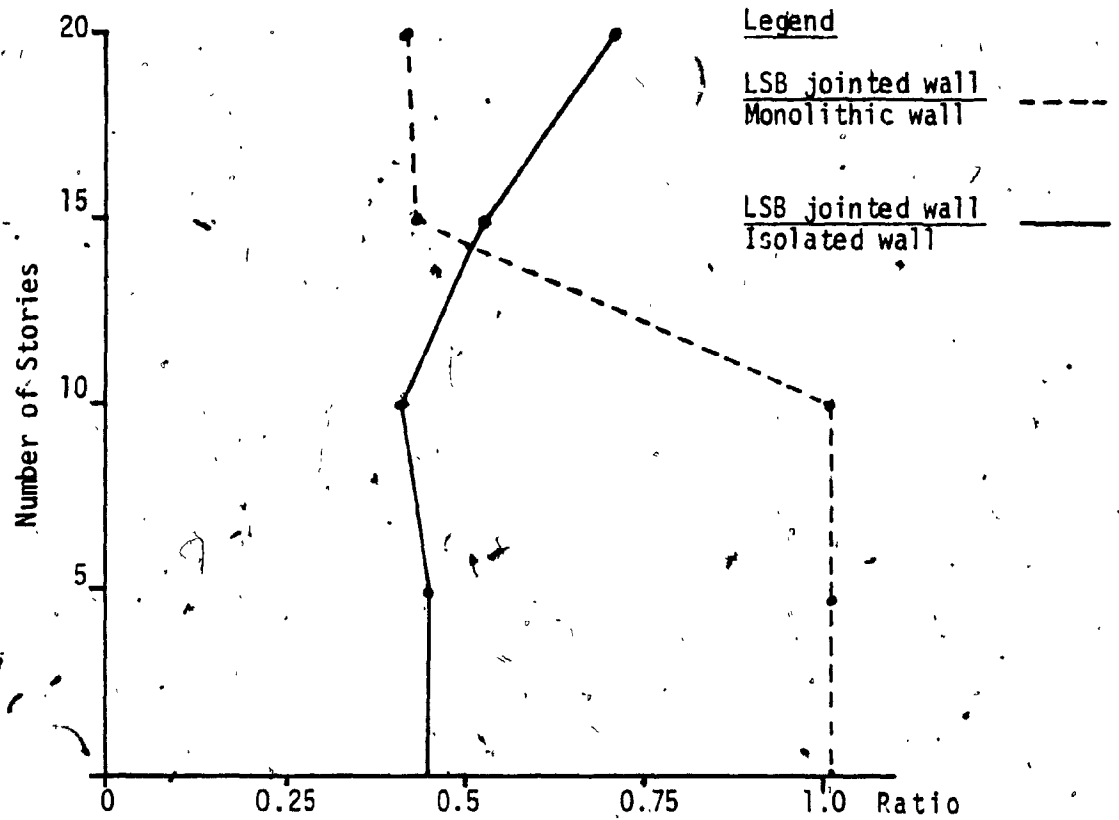


FIG. 5.23 - EFFECT OF LSB JOINT ON BENDING STRESSES

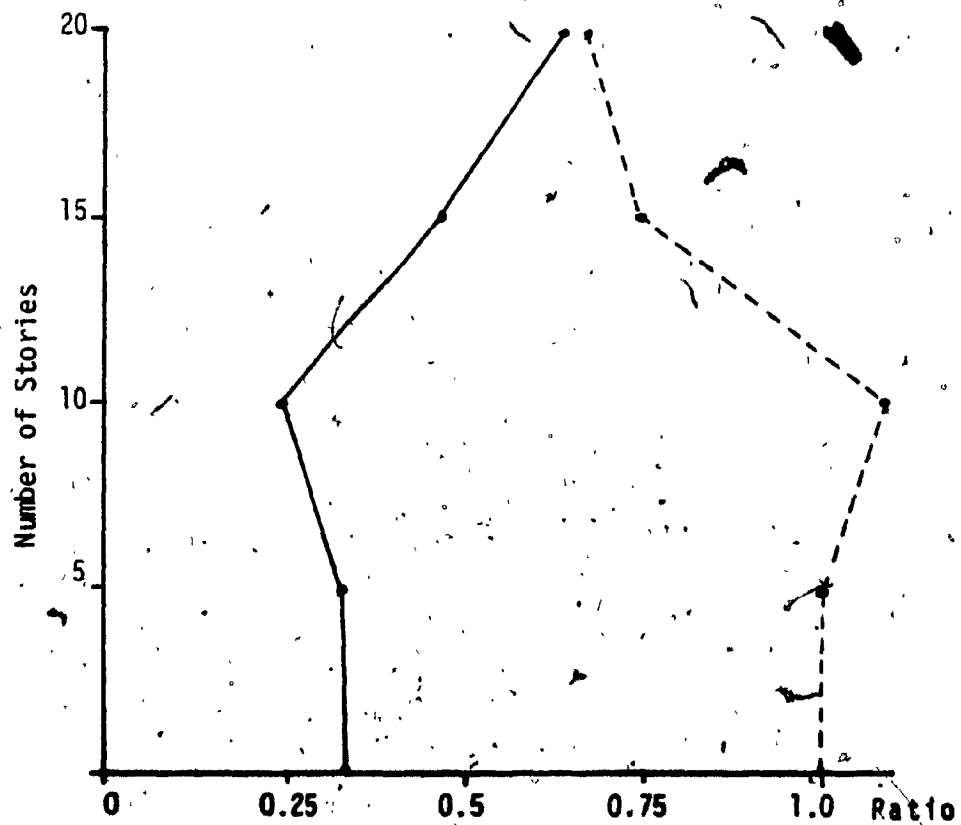
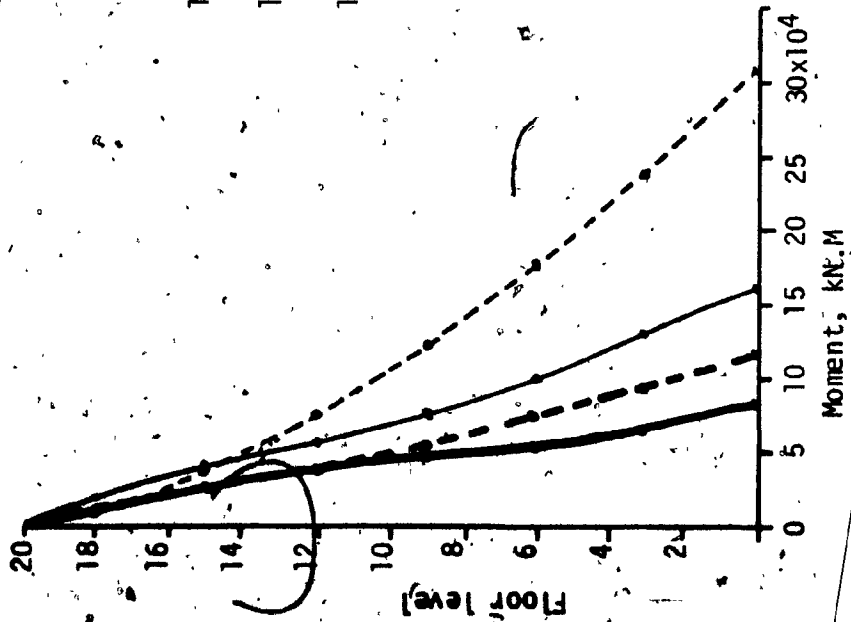
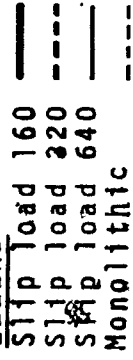
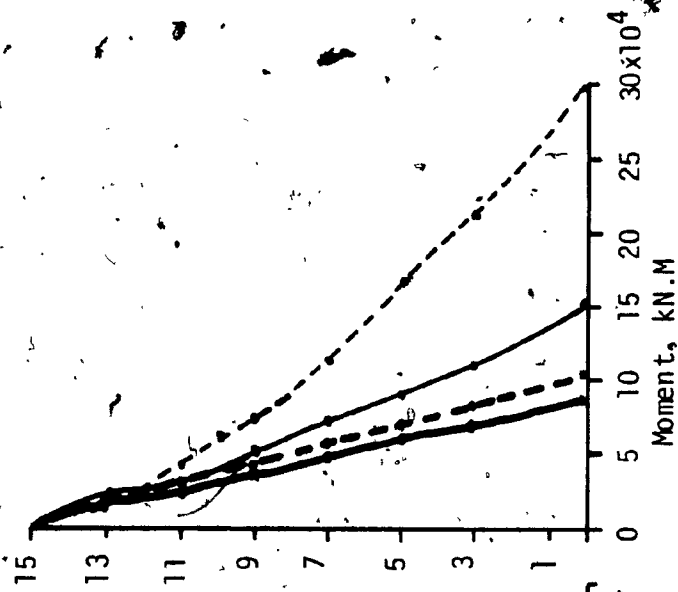


FIG. 5.24 - EFFECT OF LSB JOINT ON BUILDING DEFLECTION, 0.33 g

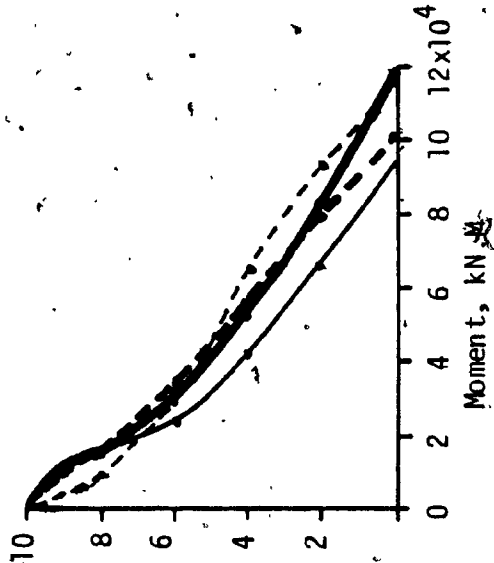
LEGEND



a) 20 story building



b) 15 story building



c) 10 story building

FIG. 5.25 - EFFECT OF SLIP LOAD ON OVERTURNING MOMENTS, 0.33g

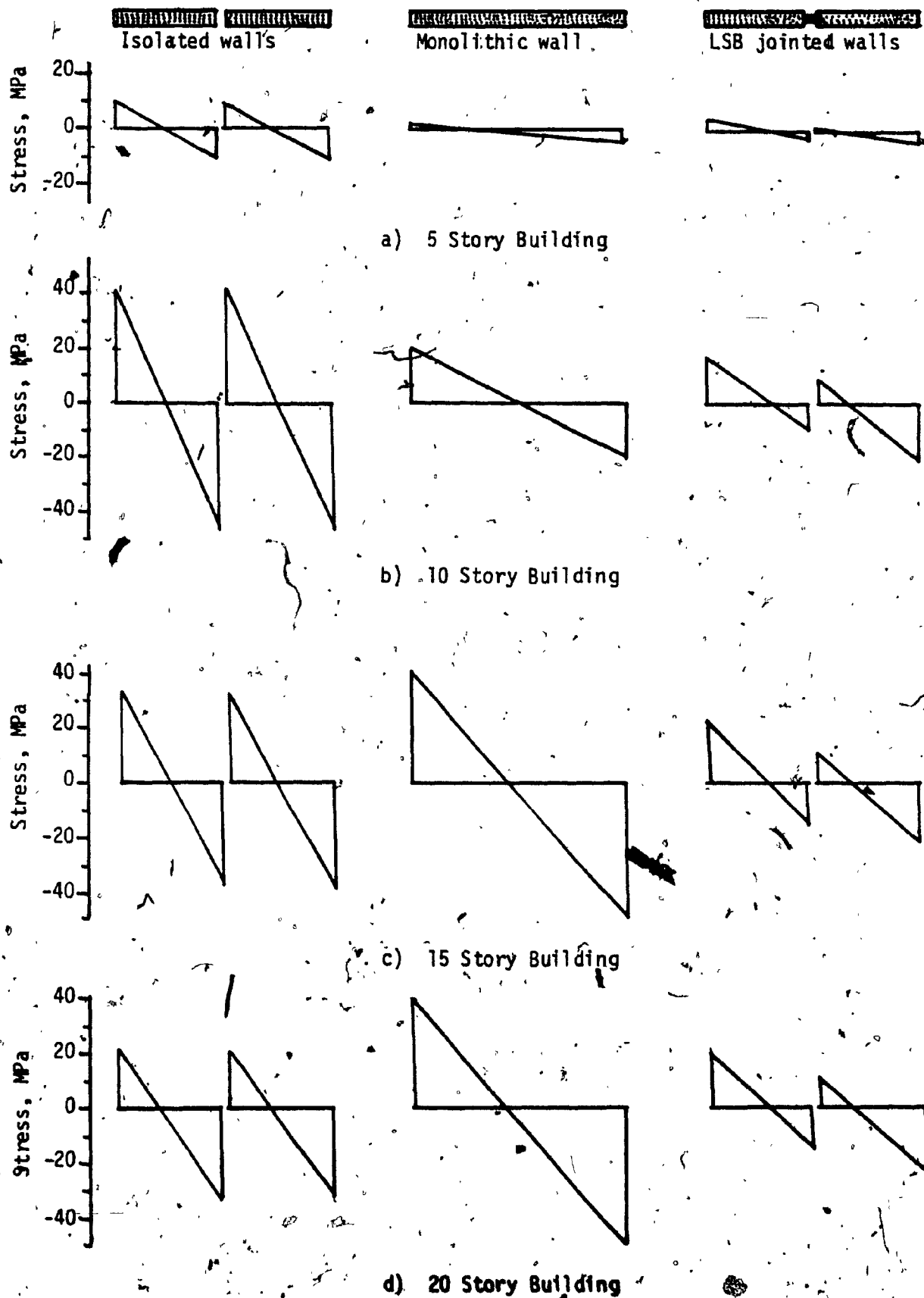


FIG. 5.26-NET STRESSES AT BASE, 0.33 g

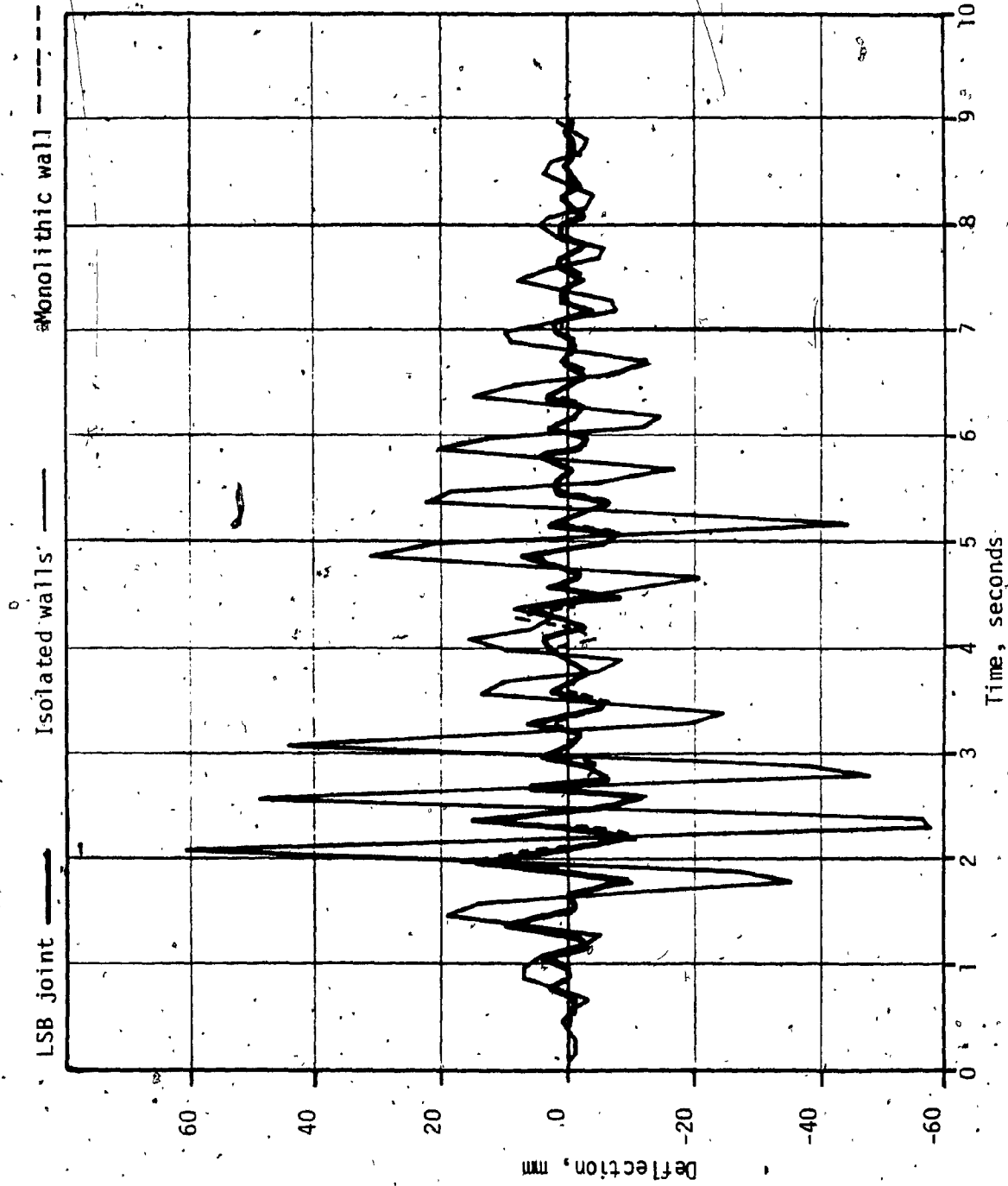


FIG. 5. 27 - TIME HISTORY, 10 STORY BUILDING, TOP DEFLECTION, 0.25 g

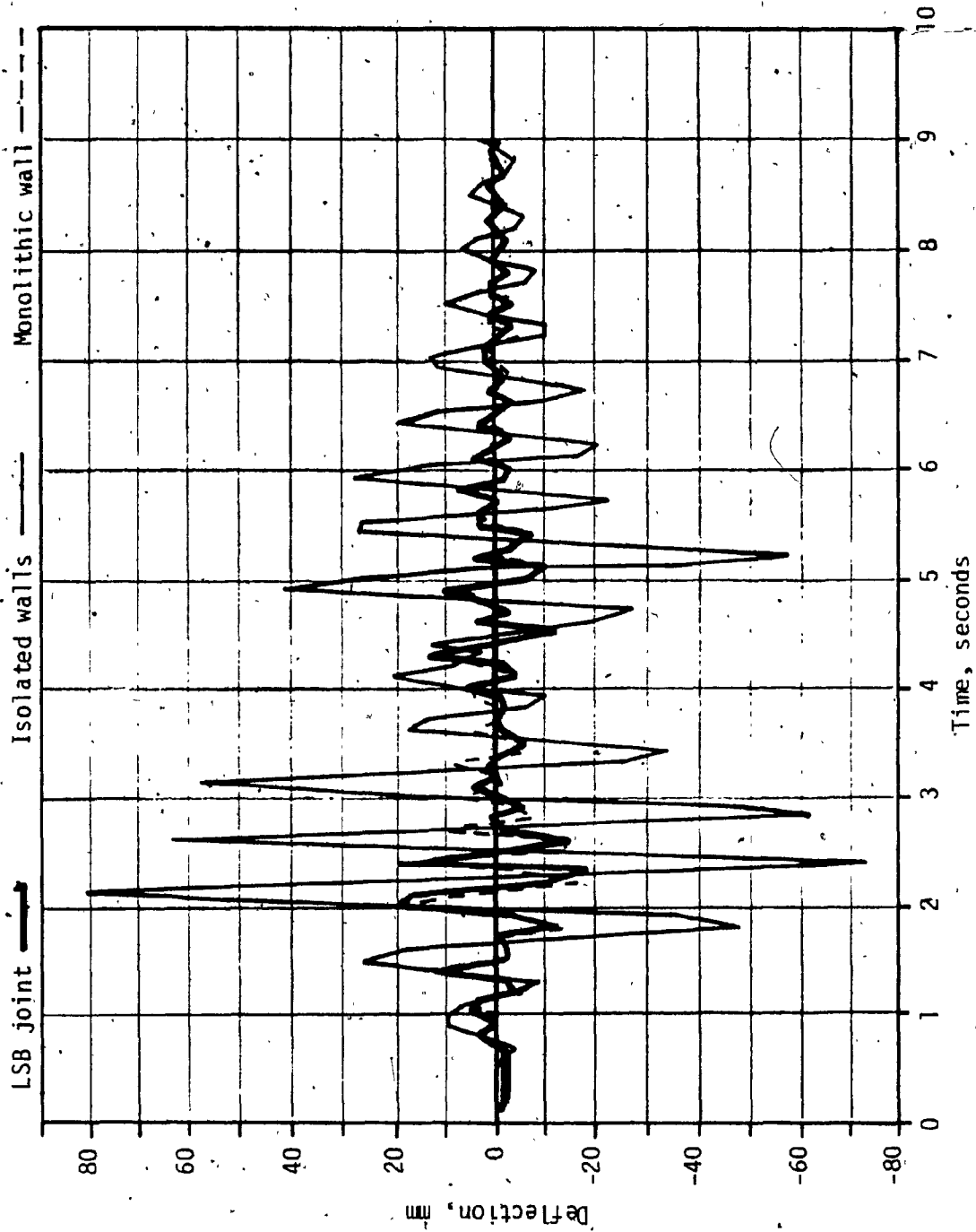


FIG. 5.28 - TIME HISTORY, 10 STORY BUILDING TOP DEFLECTION, 0.33 g

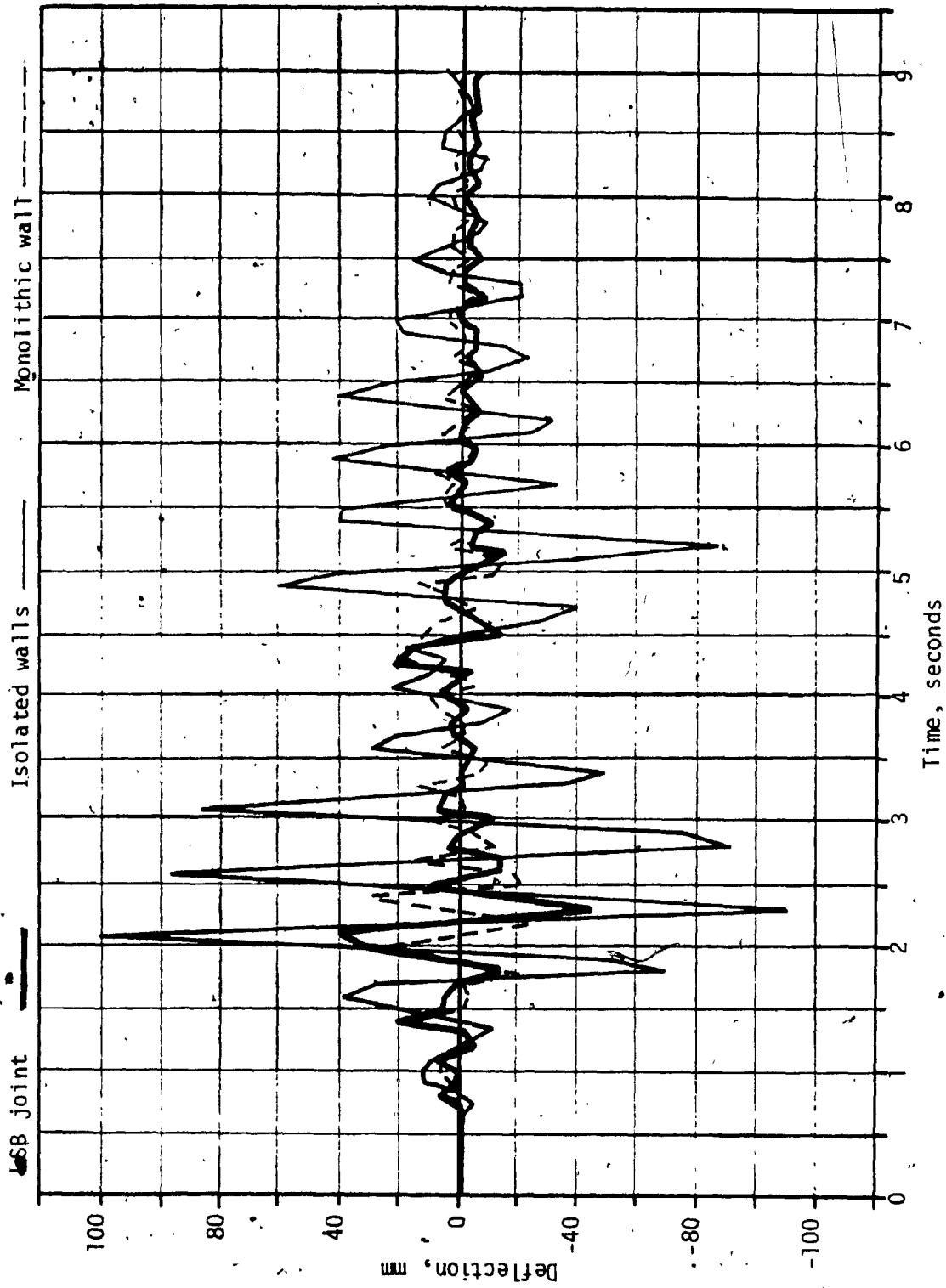


FIG. 5.29 - TIME HISTORY, 10 STORY BUILDING TOP DEFLECTION, 0.5 g

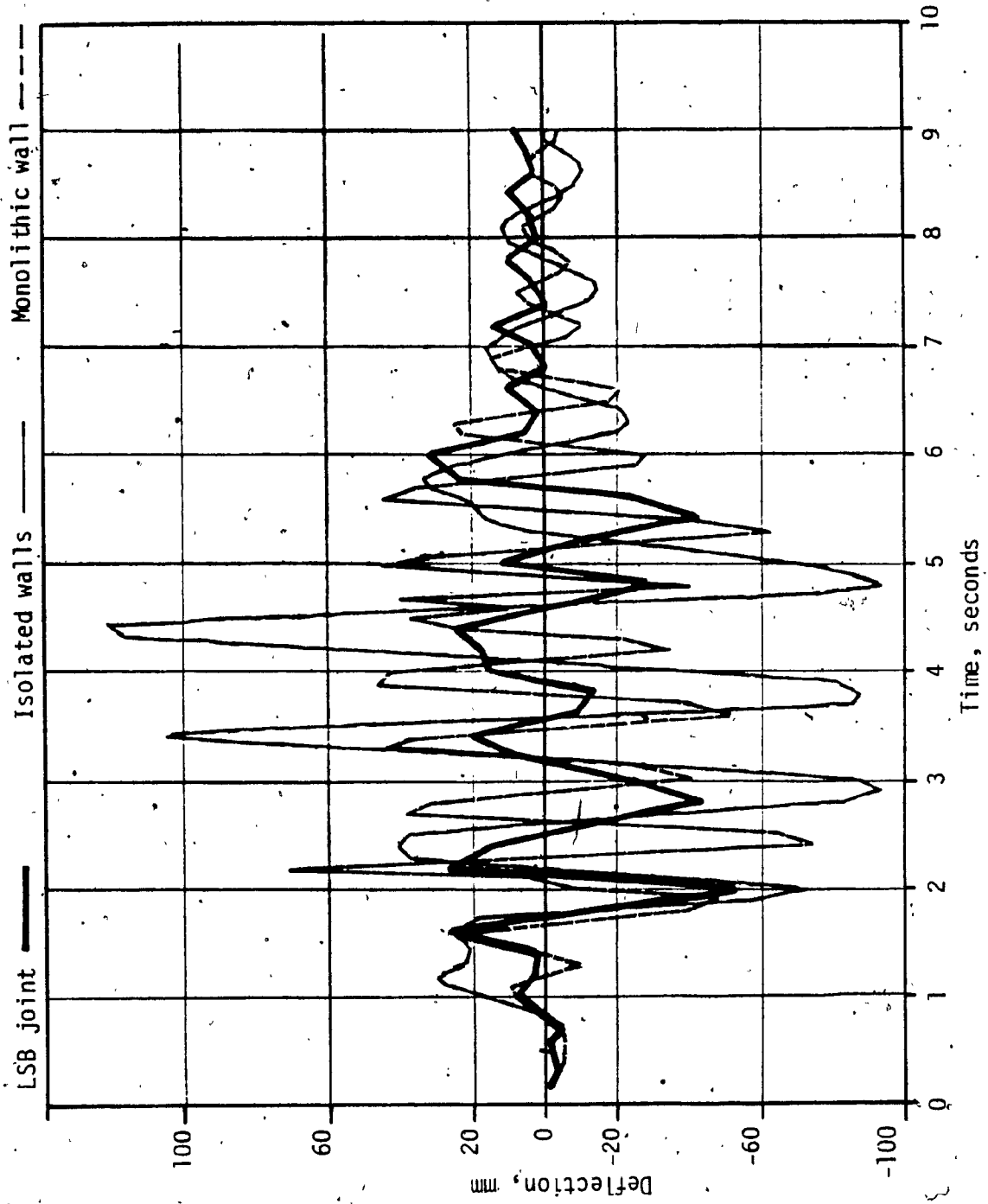


FIG. 5.30. - TIME HISTORY, 15 STORY BUILDING TOP DEFLECTION, 0.25 g

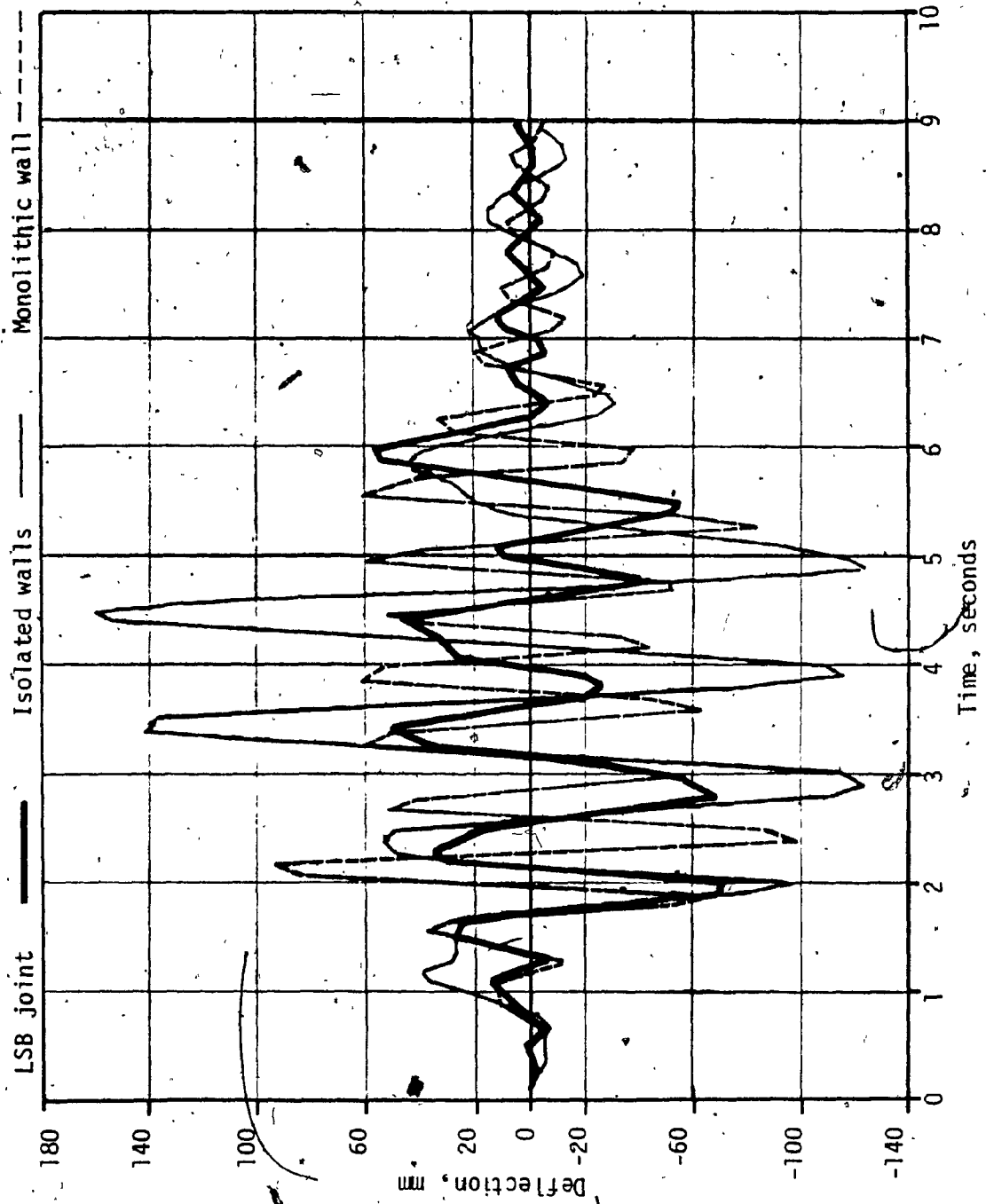


FIG. 5. 31 - TIME HISTORY, 15 STORY BUILDING TOP DEFLECTION, 0.33 g

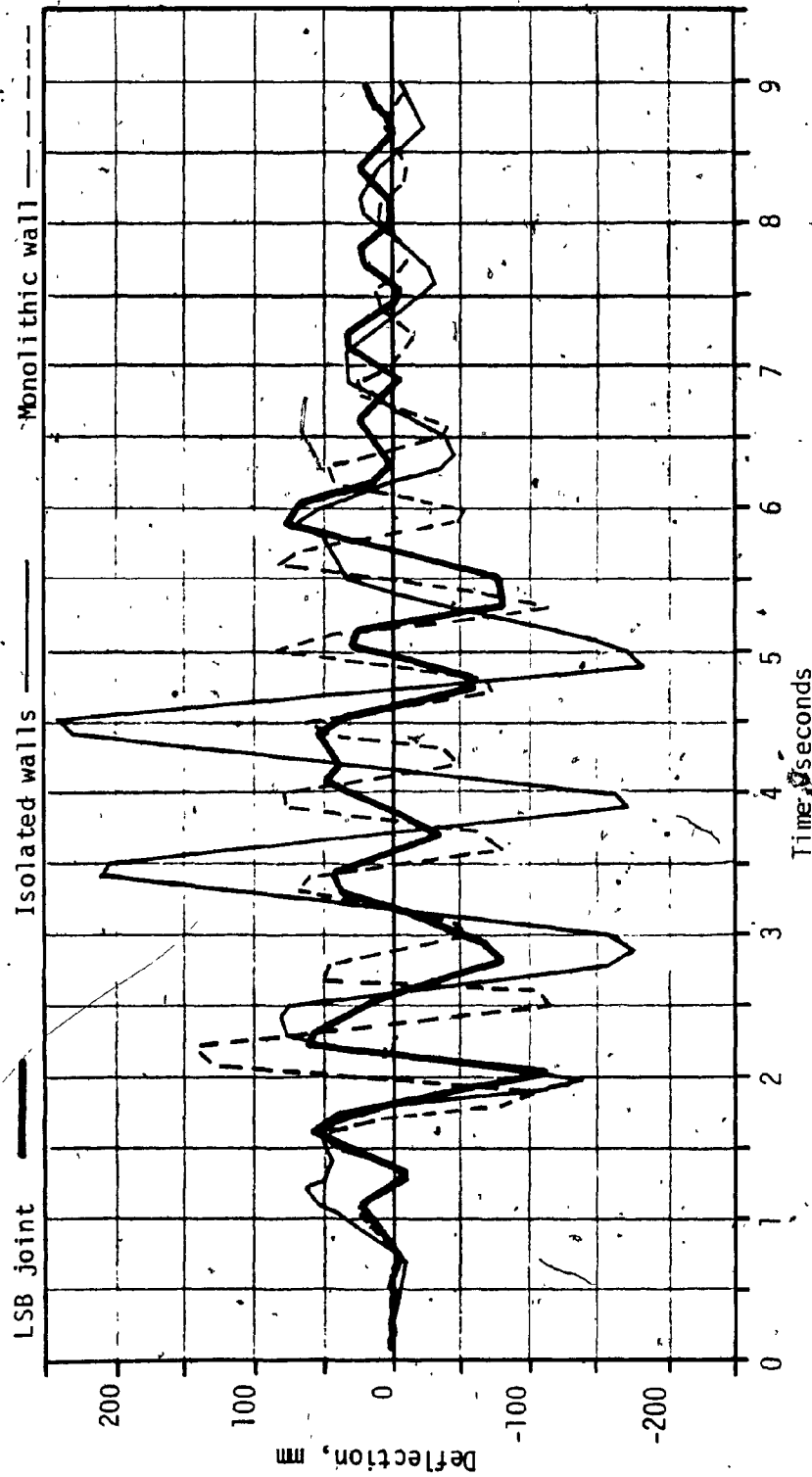


FIG. 5.32 - TIME HISTORY, 15 STORY BUILDING TOP DEFLECTION, 0.5 g

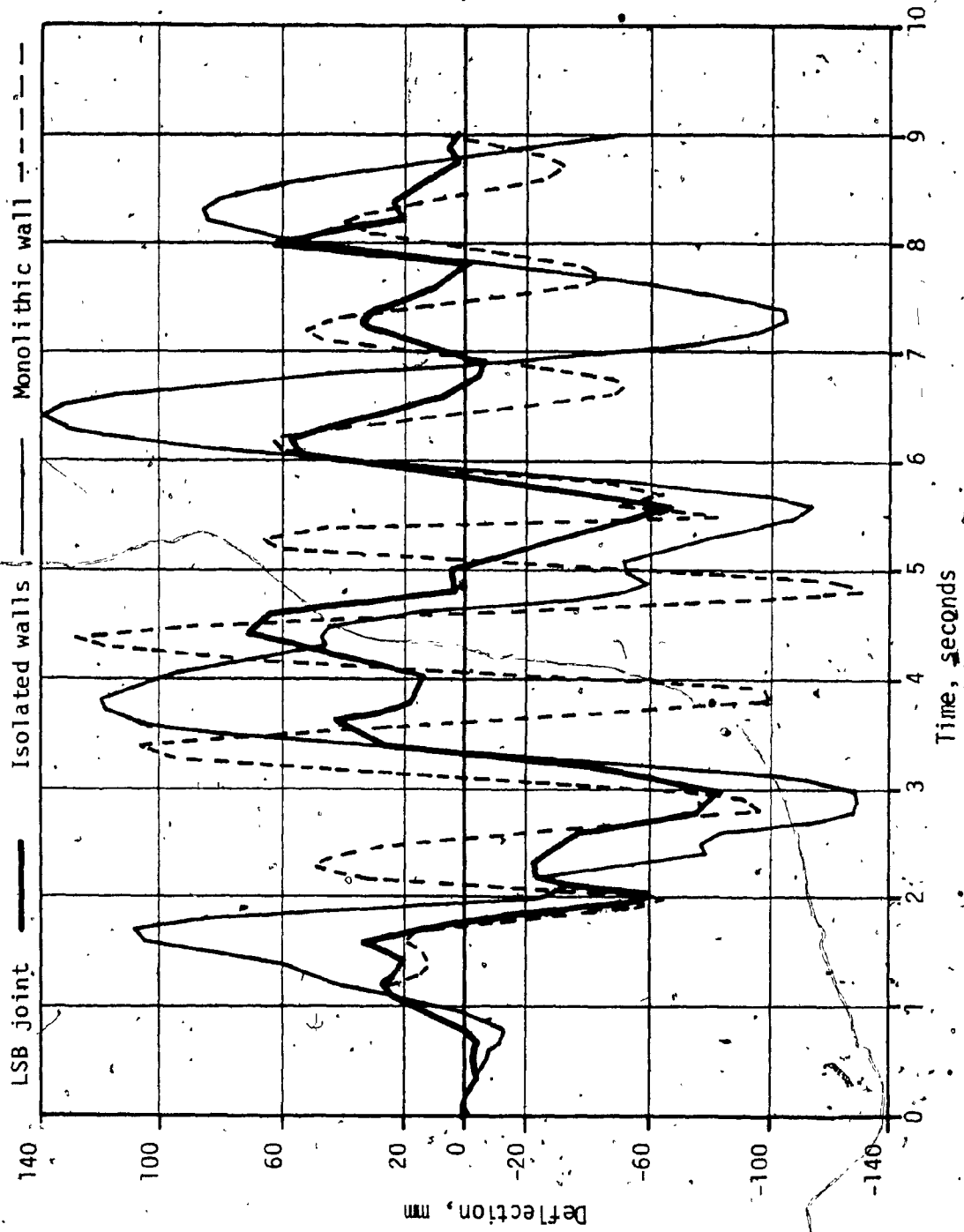


FIG. 5.33 - TIME HISTORY, 20 STORY BUILDING TOP DEFLECTION, 0.25 g

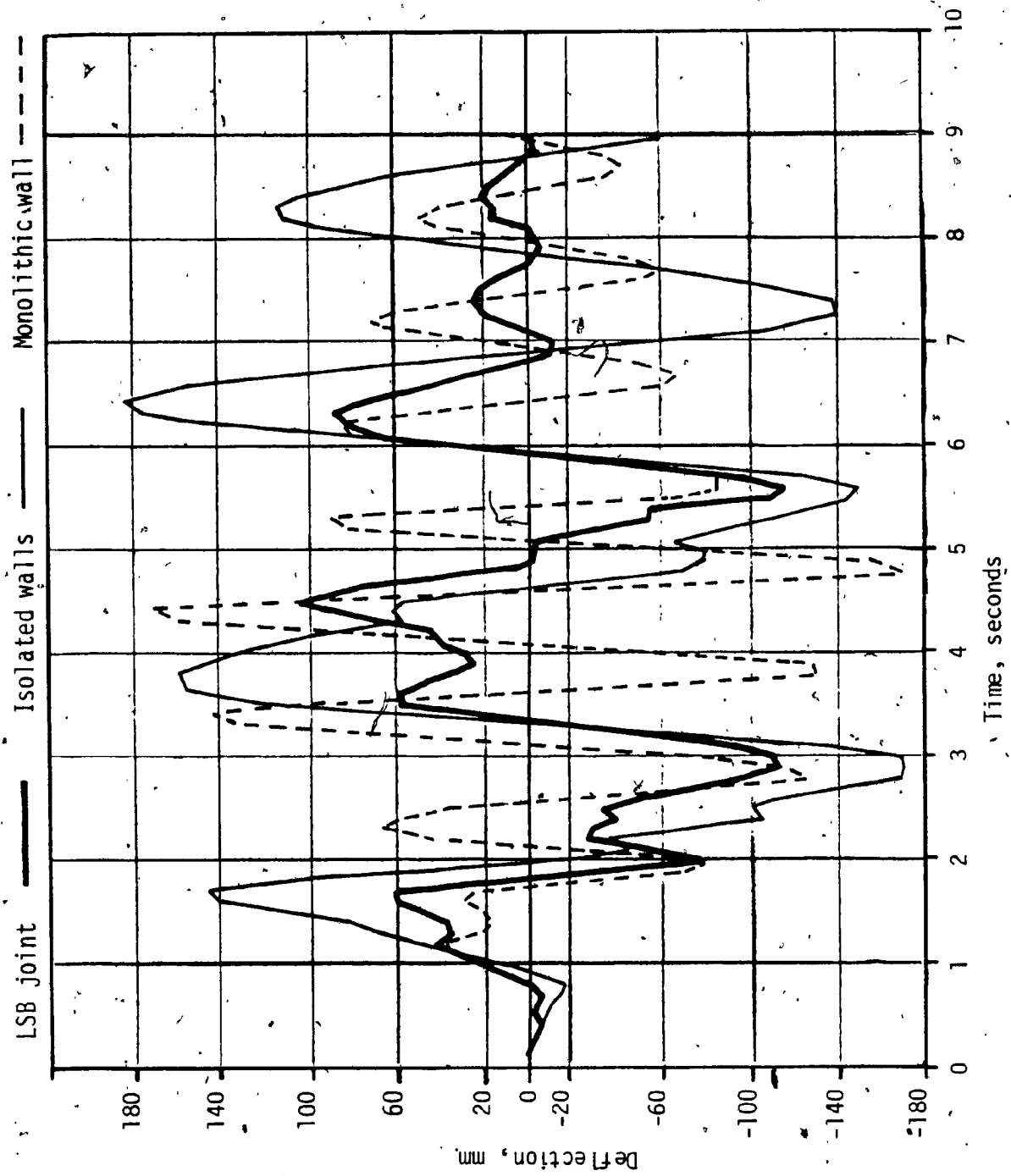


FIG. 5.34 - TIME HISTORY, 20 STORY BUILDING TOP DEFLECTION, 0.33 g

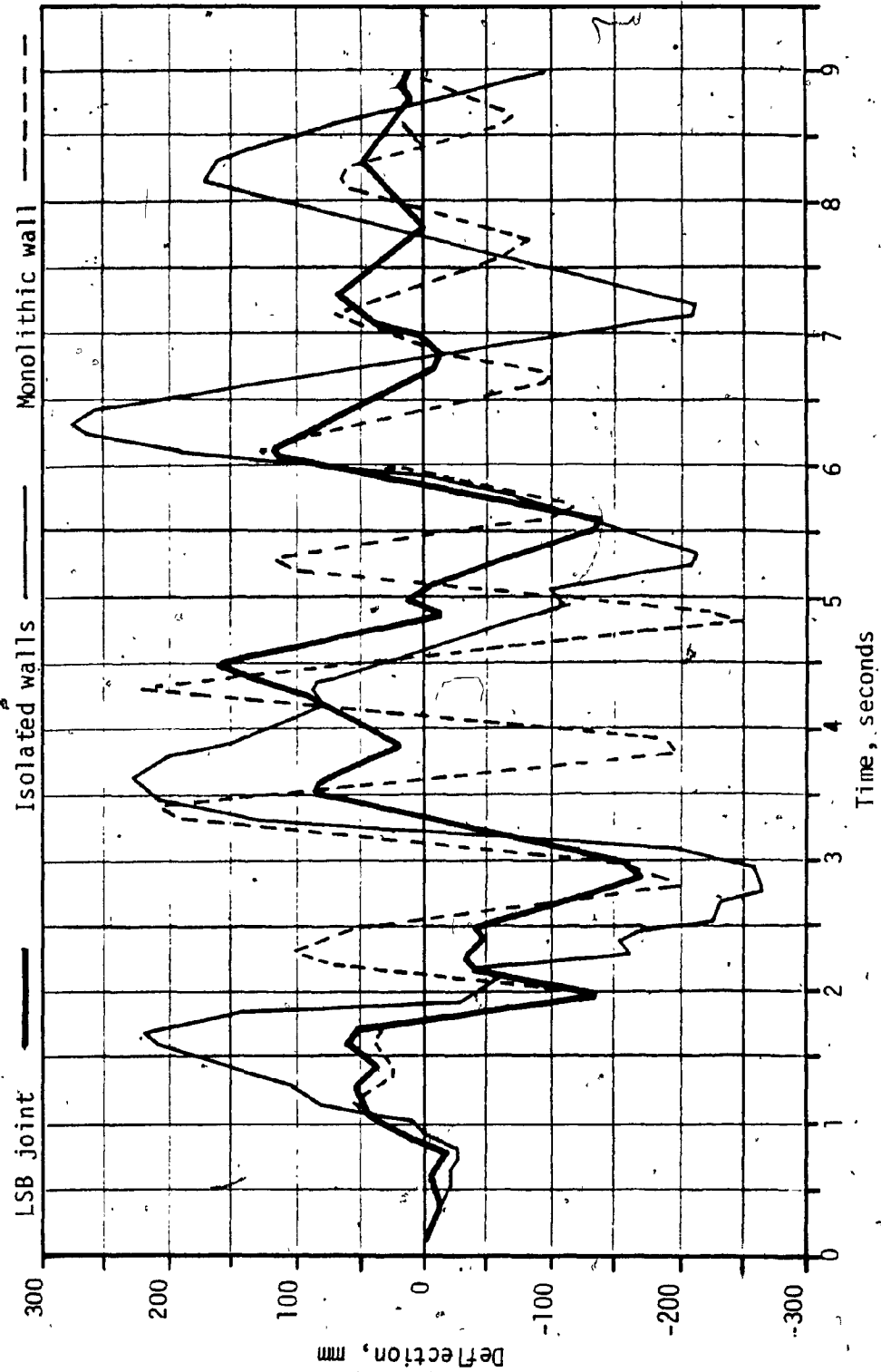
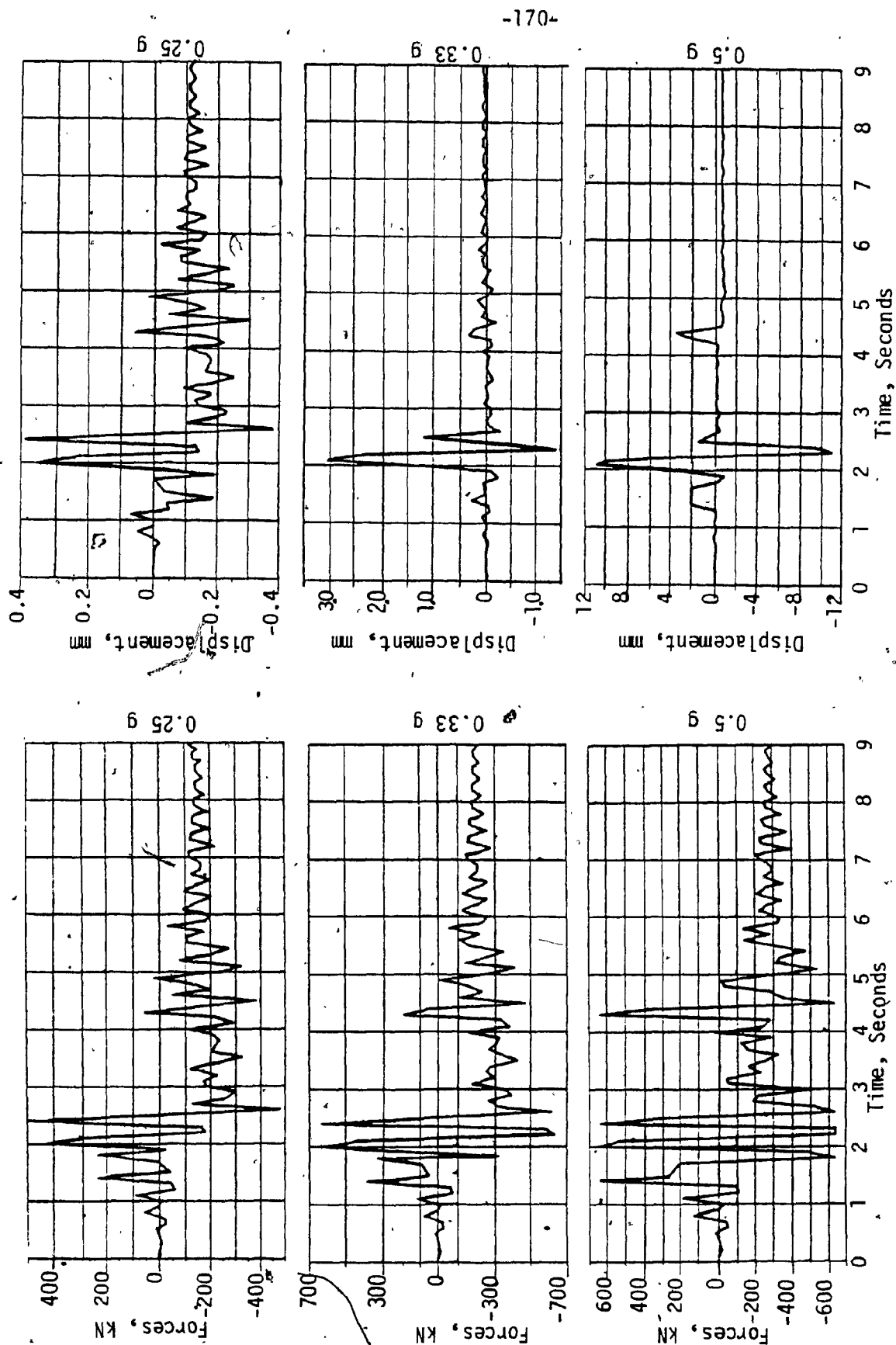


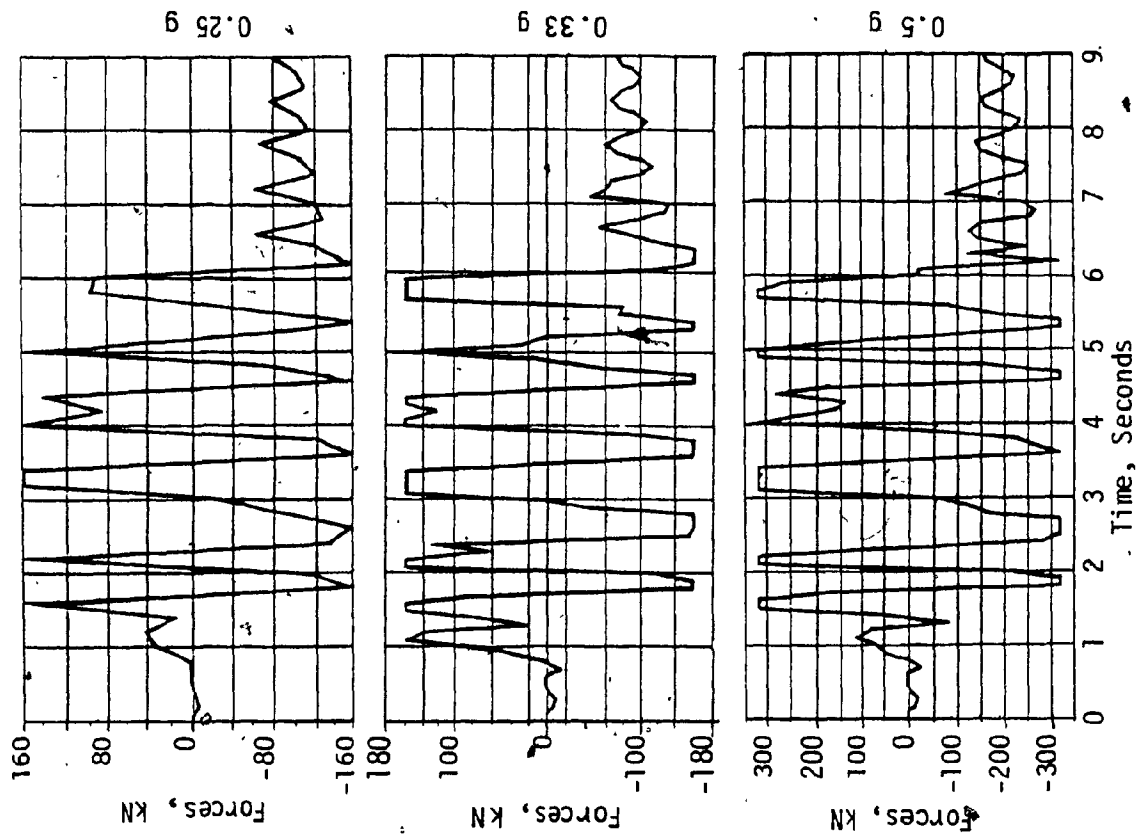
FIG. 5.35 - TIME HISTORY, 20 STORY BUILDING TOP DEFLECTION, 0.5 g



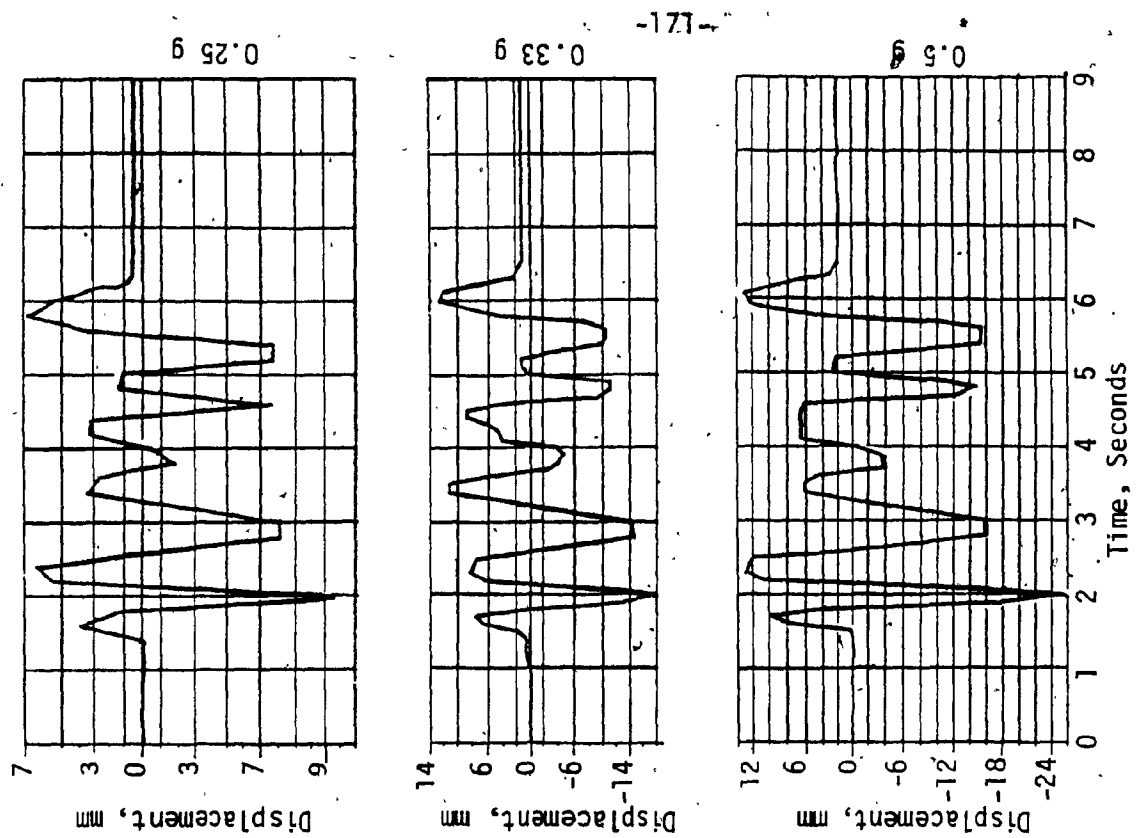
a) Time histories for forces in connection

b) Time histories for displacement in connection

FIG. 5.36 - TIME HISTORIES, TOP CONNECTION, 10 STORY BUILDING

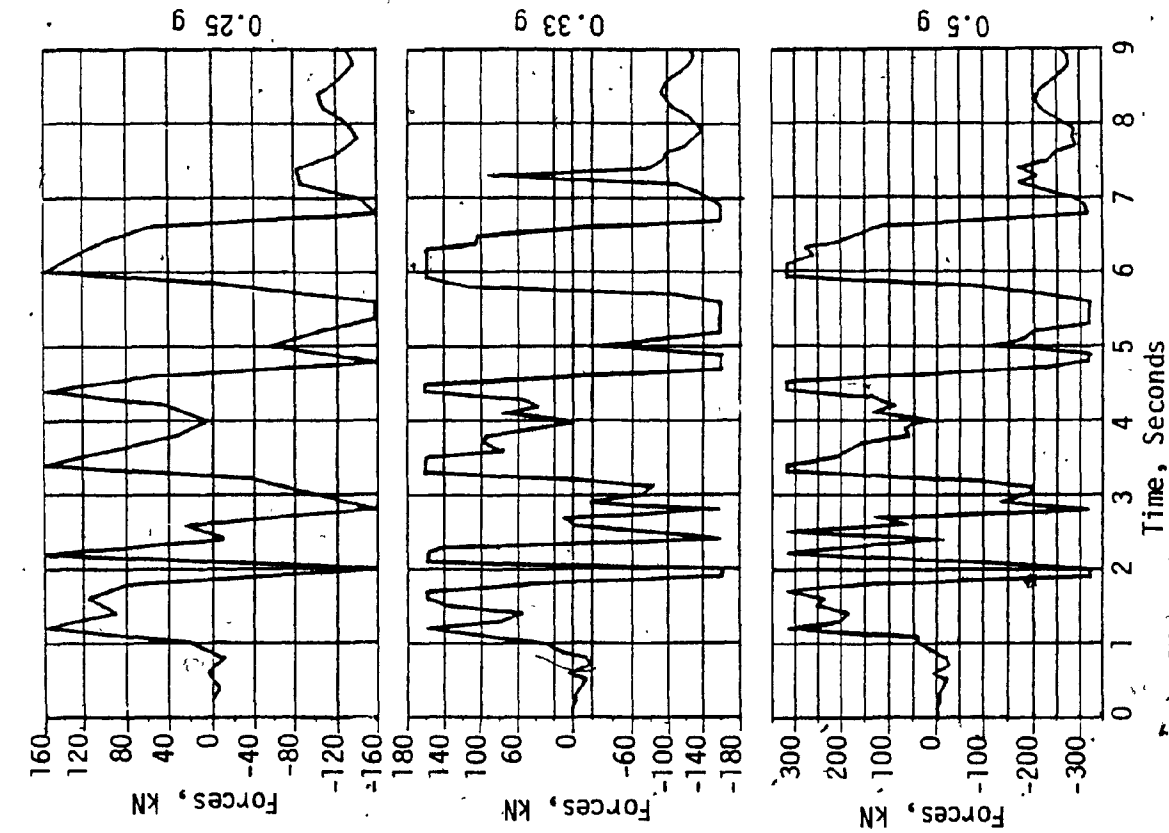


a) Time histories for forces in connection

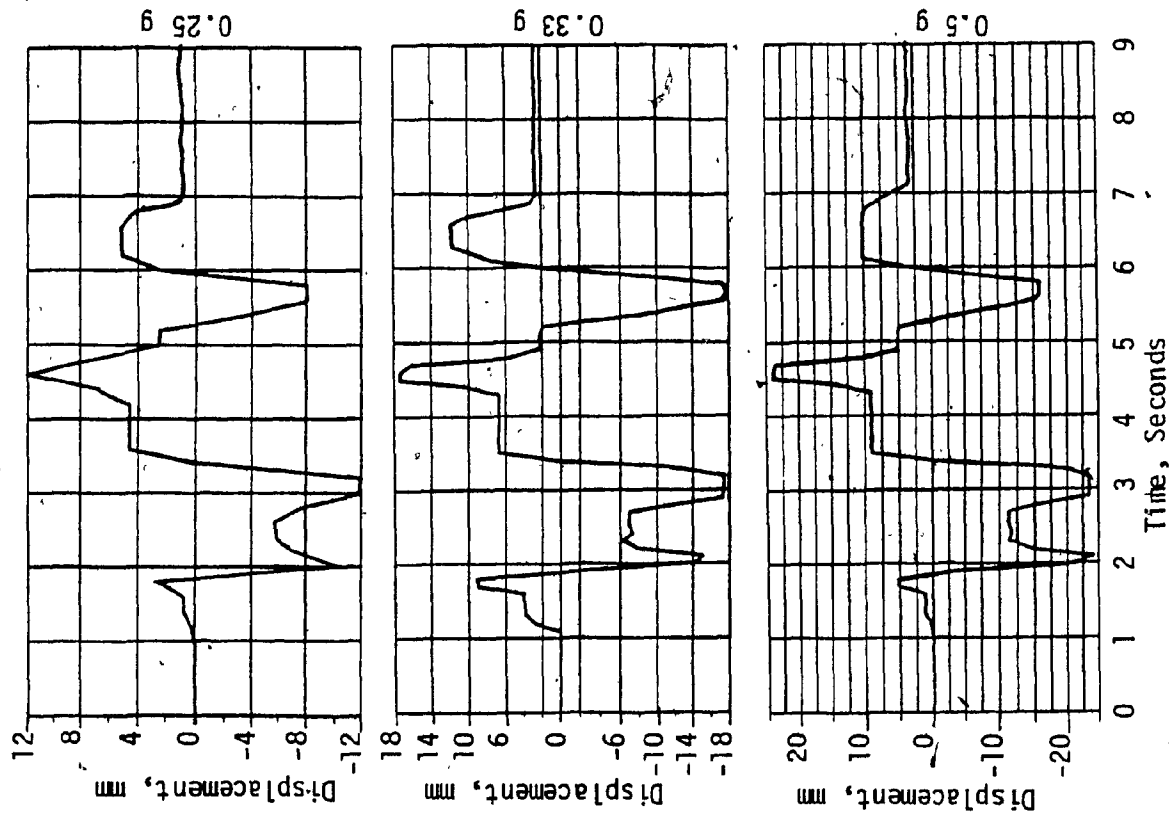


b) Time histories for displacement in connection

FIG. 5.37 - TIME HISTORIES, TOP CONNECTION, 15 STORY BUILDING



a) Time histories for forces in connection



b) Time histories for displacement in connection

FIG. 5.38 - TIME HISTORIES, TOP CONNECTION, 20 STORY BUILDING

CHAPTER VI

APPROXIMATE APPROACH TO NONLINEAR ANALYSIS

CHAPTER VI

APPROXIMATE APPROACH TO NONLINEAR ANALYSIS

The time history nonlinear dynamic analysis, as explained and used in previous chapters, is not difficult in concept but it leads to high computing costs even for simple wall configurations. To obtain a reasonable measure of the nonlinear seismic response, without recourse to true nonlinear analysis, the ductility-factor method, as contained in most codes, is widely used for conventional structures. In this approach the inelastic or nonlinear response can be interpreted directly from the linear elastic response spectrum analysis. In the absence of the availability of a ductility factor in panelized buildings, this simple approach cannot be utilized.

In this chapter, the reserve energy technique, originally developed by Blume [85] is briefly reviewed and modified to suit panelized buildings [86]. Walls of 10 and 15 story height, as already analyzed in Chapter 4, have been analyzed using this technique and the results of two approaches are compared. An approximate means of determining the optimum slip load of the joint is also derived using the energy method. There being so many paradoxes and anomalies in the subject of earthquake resistance, it is advisable to carry out at least one complete nonlinear analysis as a final check on the adequacy of the completed design.

6.1 RESERVE ENERGY TECHNIQUE

A nonlinear time history dynamic analysis is valid for only one particular ground motion history. Any other ground motion requires an additional computer run. Such analysis may be justified for research or

for large projects but it would be difficult to justify its use by the average practicing engineer. The nonlinear behaviour of panelized structures under severe seismic excitations can however be approximated by a simple and practical method based on the reserve energy technique [85] which is briefly explained below.

At peak seismic demands, fed-in kinetic energy less feedback from the structure into the soil layer, must balance the elastic strain energy plus the energy lost in friction and the work done in nonlinear deformations. It is convenient to calculate the kinetic energy fed into the building by using the elastic response spectrum. The force-deflection diagram of a structure is used as a measure of its total work capacity. The diagram is plotted for some trial deflections until the energy demand and energy capacity of the structure are reconciled. This can be mathematically expressed as under :

$$\text{Kinetic energy demand, } E_d = \frac{\sum W_i v_i^2}{2g} = \frac{g \sum W_i \alpha_i^2 T_i^2}{8\pi^2} \quad (6.1)$$

$$\text{Energy capacity of structure, } E_s = \sum [(U_i - \gamma H_i) + U_{ci}] \Omega \quad (6.2)$$

$$\begin{aligned} \text{So, Factor of Safety, F.S} &= \sqrt{\frac{\text{Energy capacity}}{\text{Energy demand}}} \\ &= \sqrt{\frac{8.057 \sum [(U_i - \gamma H_i) + U_{ci}] \Omega}{W_i \alpha_i^2 T_i^2}} \quad (6.3) \end{aligned}$$

$$\begin{aligned} \text{Earthquake force [83], } V &= ASKIFW \\ &= \bar{C}W \quad (6.4) \end{aligned}$$

Let $R_{iz} \alpha_i$ be the equivalent static coefficient

$$\therefore F.S = \frac{\bar{C}}{R_{iz} \alpha_i} \quad (6.5)$$

From Eqn. 6.3 and Eqn. 6.5

$$R_{iz} = T_i \bar{C} \sqrt{\frac{\Sigma W_i}{8.057 \Sigma [(U_i - \gamma H_i) + U_{ci}] \Omega}}$$

Considering 10% energy feedback into soil,

$$R_{iz} = T_i \bar{C} \sqrt{\frac{0.9 \Sigma W_i}{8.057 \Sigma [(U_i - \gamma H_i) + U_{ci}] \Omega}} \quad (6.6)$$

where W_i and W are the story weight and total weight respectively. α_i , in the case of a multidegree freedom structure, can be determined at different story heights by dividing the story shear, evaluated using the response spectrum analysis, by the weight of structure above that particular story. U_i and H_i are the areas of the load deformation curves as shown in Fig. 6.2. U_{ci} is the area of the load deformation curve of the connection. γ is the deterioration factor to account for the reduction in the work capacity after several excursions. Ω is the participation of other stories in draining energy.

A conceptual model of the reserve energy technique is shown in Fig. 6.1, and the general construction of the load deformation diagram is shown in Fig. 6.2. The reserve energy technique was originally developed for framed buildings. The following modifications have been carried out to suit panelized structures :

- a). The energy dissipated in friction is added to the elastic energy of the walls.

- b). Since the structure is of uniform section throughout, the possibility of failure is most likely at the base of the wall, so it is sufficient to reconcile the energy demand at the lowermost story.
- c) Since the degradation is already accounted for in the slip load capacity of the LSB joints, while the concrete panels basically remain in the elastic range, the deterioration factor (γ) is zero.
- d) Since the structural rigidity is constant over the height and fewer modes are excited than in framed buildings, the participation of other stories in draining energy (Ω) is assumed as 75% instead of 50% for framed buildings.
- e) Since panelized walls essentially deform in the bending mode, the work done is predominantly due to the primary moments with a small contribution from shear forces. In order to keep the original character for the construction of story shear deformation diagrams, the work capacity determined from such diagrams is multiplied by a magnification factor to include the effect of additional work done in flexural deformations. The derivation of this magnification factor is given in Appendix B.1.

6.2 ENERGY APPROACH FOR OPTIMUM SLIP LOAD OF JOINT

Before starting analysis it is necessary to determine the slip load of the joint which will give the minimum stresses at the base. This can be approximately determined by adopting the energy approach, i.e. maximizing the energy capacity of the structure for a given maximum stress level. For simple coupled walls, typical of our case, the method is explained below (refer to Fig. 6.3).

Total energy in the system, $U = U_1 + U_2 + U_3$

where U_1 = Strain energy due to bending

U_2 = Strain energy due to the axial force from
the coupling action by the joint

U_3 = Energy dissipated in the joint.

(Strain energy due to shear is neglected).

a) Strain energy due to bending moment in two walls is

$$U_1 = 2 \int_0^h \frac{M_x^2}{2EI} dx \quad (6.7)$$

For a triangular load distribution representing seismic loads

$$M_x = \frac{3M_o \cdot x^2}{4h^2} \left(1 - \frac{x}{3h}\right) - \frac{Q \cdot b \cdot x}{2h} \quad (6.8)$$

where M_o and Q are the maximum total overturning moment and
axial coupling force at base.

$$\begin{aligned} U_1 &= \frac{1}{EI} \int_0^h \left[\frac{3M_o \cdot x^2}{4h^2} \left(1 - \frac{x}{3h}\right) - \frac{Q \cdot b \cdot x}{2h} \right]^2 dx \\ &= \frac{12}{Etb^3} \int_0^h \left[\frac{\sigma \cdot tb^2 x^2}{4h^2} \left(1 - \frac{x}{3h}\right) - \frac{\sigma_t \cdot tb^2 x}{2h} \right]^2 dx \\ &= \frac{V}{E} (0.0786\sigma^2 + \sigma_t^2 - 0.55\sigma\sigma_t) \end{aligned} \quad (6.9)$$

where σ is max. bending stress in uncoupled walls. b, h, t and V are the width,
height, thickness and volume respectively of each wall. E is the modulus
of elasticity and σ_t is the stress at base due to axial force.

b) Strain energy due to axial force from the coupling action, U_2

$$\delta U_2 = \frac{2\sigma^2 t(x,y) \delta v}{2E} \quad (6.10)$$

where $\sigma_t(x,y) = \sigma_t \left(\frac{x}{h}\right)$, σ_t = stress at base due to axial force. (6.11)

$$U_2 = \frac{\sigma_t^2}{h^2 E} \int_0^h \int_{-b/2}^{b/2} x^2 dx dy$$

$$= \frac{0.333 V \sigma_t^2}{E} \quad (6.12)$$

c) Energy dissipated in the joint, U_3

$$dU_3 = q \cdot d\Delta dx \quad (6.13)$$

where $d\Delta = \frac{2}{E} \int_x^h [\sigma_b(x) - \sigma_t(x)] \cdot dx \quad (6.14)$

in which $\sigma_b(x) = \frac{6 M_x}{tb^2} = \left[\frac{3q x^2}{2h^2} \left(1 - \frac{x}{3h}\right) - \frac{3\sigma_t \cdot x}{h} \right]$ and $\sigma_t(x) = \frac{\sigma_t \cdot x}{h}$

$$d\Delta = \frac{2}{E} \left[\frac{\sigma (h^3 - x^3)}{2h^2} - \frac{\sigma (h^4 - x^4)}{8h^3} - \frac{2\sigma_t (h^2 - x^2)}{h} \right] \quad (6.15)$$

and $U_3 = \frac{2q}{E} \int_0^h \left[\frac{\sigma (h^3 - x^3)}{2h^2} - \frac{\sigma (h^4 - x^4)}{8h^3} - \frac{2\sigma_t (h^2 - x^2)}{h} \right] dx$

$$= \frac{qh^2}{E} (0.55\sigma - 2.66\sigma_t) \quad (6.16)$$

Since $q = \sigma_t bt/h$ then,

$$U_3 = \frac{V\sigma_t}{E} (0.55\sigma - 2.66\sigma_t) \quad (6.17)$$

$$U = U_1 + U_2 + U_3$$

$$U_3 = \frac{V}{E} (0.0786\sigma^2 - 1.333\sigma_t^2) \quad (6.18)$$

knowing $\sigma_b(x) = \left[\frac{3\sigma}{2h^2} \left(1 - \frac{x}{3h}\right) - \frac{3\sigma_t \cdot x}{h} \right] \therefore \sigma_b = \sigma - 3\sigma_t$

and since $\sigma_o = \sigma_b + \sigma_t$, therefore $\sigma = \sigma_o + 2\sigma_t$

Substituting the value of σ in Eqn. 6.17, we get

$$U = \frac{V}{E} (0.0786\sigma_o^2 + 0.3144\sigma_o\sigma_t - 1.0186\sigma_t^2)$$

For maximum energy :

$$\frac{dU}{d\sigma_t} = -2.0372\sigma_t + 0.3144\sigma_o = 0$$

$$\therefore \sigma_t = 0.15\sigma_o \text{ and } \sigma = 1.3\sigma_o \quad (6.19)$$

Distribution of energy :

$$\left. \begin{aligned} U_1 &= 0.0480 \sigma_o^2 \frac{V}{E} = 47\% \\ U_2 &= 0.0075 \sigma_o^2 \frac{V}{E} = 7\% \\ U_3 &= 0.0473 \sigma_o^2 \frac{V}{E} = 46\% \end{aligned} \right\} \quad (6.20)$$

Now $qh = \sigma_t bt$
 $= 0.15 \sigma_o bt$

$$\therefore \text{Optimum slip load per story, } P_s = qh/n = 0.15\sigma_0 bt/n \quad (6.21)$$

where n is the number of stories.

In order to compare the results with the computer studies made in Chapter V, choosing the lowest stress values σ_0 from Figs. 5.6 to 5.8 for a seismic intensity of 0.25 g, the optimum slip load P_s becomes 300, 190 and 160 kN for 10, 15 and 20 stories respectively. This is in reasonably close agreement with the curves established for optimum slip loads (Figs. 5.6 to 5.8). Variations are attributed to the facts that 1) constant energy input is assumed in coupled and uncoupled walls whereas, when using the record of the El Centro earthquake, the energy changes during the uncoupling process (Fig. 5.4); and 2) the change in viscous damping caused by uncoupling. Clearly the approximate approach indicates only the trend and final values must be established by computer studies.

6.3 ANALYSIS USING THE RESERVE ENERGY TECHNIQUE

In this study to walls of 10 and 15 story height were analyzed using the modified reserve energy technique. The properties of the wall and the LSB joint were kept the same as in Chapter IV so that a comparative study of the two approaches could be made. In addition to the general modeling assumptions already made in Chapter IV, a 10% energy feedback from the structure to the soil was allowed in the present analysis. This was done so as to partly compensate for the effect of the difference between the response spectrum followed in this study and the El Centro spectrum.

Response spectrum analysis using the elastic response spectrum of NBC [83] was carried out using the computer program TABS [87], for

peak ground accelerations of 0.08 g, 0.10 g, 0.15 g, 0.20 g and 0.25 g. The root mean square combination was employed for the first three modes only. Probable elastic shears and quasi-static design shears for the 15 story building are shown in Fig. 6.4.

Analysis of the wall for static lateral loads was carried out by the displacement method using the plane frame computer program MAP [88]. Bending, axial and shear deformations were taken into account. Member stiffness matrices are given in Appendix B.2. Due to slipping of the connections in the vertical joints, the analysis involved a step-by-step integration of short load increments, assuming the stiffness properties of the connection remain constant during each increment but changing in accordance with the load deformation state existing at the end of an increment.

Force displacement diagrams for some stories were prepared for panel walls as well as for joints for different trial deflections, an example of which is shown in Fig. 6.5. The areas of each of these diagrams represent the total work capacity and the energy dissipation of the story. For intermediate stories, the values were interpolated.

Curves were plotted for reconciliation of energy demand at the lowest story, Fig. 6.6. Intersection of these curves with the code design coefficient \bar{C} (Eqn. 6.4) is the point up to which the building must deform to balance the energy demand.

6.4 DISCUSSION OF RESULTS

The results obtained from the approximate analysis show reasonable agreement with the rigorous nonlinear time history analysis. The

deflection envelopes of 10 and 15 story buildings are shown in Fig. 6.7:

The slight variation in response is attributed to the following:

- a) The response spectrum of NBC [83] is the average derived from a large number of recorded earthquakes and is slightly higher than the response spectrum of El Centro, N.S. Component, the earthquake record of which was used in the time history analysis. (The 10% energy feedback to the soil, assumed in the reserve energy technique narrowed this gap).
- b) The various assumptions of the reserve energy technique are based on judgement and hence are approximate only.

The results using the reserve energy method, however, are reasonable enough for all practical purposes.

The energy dissipation capacity of the LSB joints used in this analysis is shown in Figs. 6.8 and 6.9. It is seen that nearly 25% of the total energy is dissipated by friction alone. It may be mentioned here that the slip load value of 320 kN assumed for both walls was an arbitrary choice and is not the optimum value. With optimum slip load values, the percentage of energy dissipation will be higher.

6.5 EQUIVALENT DUCTILITY

The need for the building to deform into the nonlinear range to reconcile energy places high deformation demands on the joint as shown in Fig. 6.10. As there is no yielding of the materials involved, the equivalent ductility needs clarification.

System ductility has been defined in many ways but applied to panelized buildings it can be stated to be the ratio of the maximum displacement at the top for a limiting stress at the base to the

displacement when about half joints have slipped. For the optimum slip load in simple coupled shear walls, this value is 4.0 (Appendix B-3). This compares with 2 to 3 for well detailed cast-in-place concrete walls.

The equivalent viscous damping of the equivalent linear elastic system for this case works out to be 19%. Following the approach recently proposed by Mueller and Becker [22], this value is 19% and 20% for 10 and 15 story walls respectively. The damping in LSB jointed walls is therefore very high when compared to the 3-5% available in conventional buildings.

6.6 SUMMARY

The modified reserve energy technique provides a reasonable approximation of the nonlinear response of panelized buildings and can be adopted for preliminary analysis. The magnitude of the error is within the range of acceptability for most seismic analyses. However, it is advisable to carry out at least one complete nonlinear analysis as a final check of the adequacy of the completed design.

LSB joints dissipate large amounts of seismic energy and act as structural dampers, and could be the key factor in the survival of a structure during catastrophic earthquake.

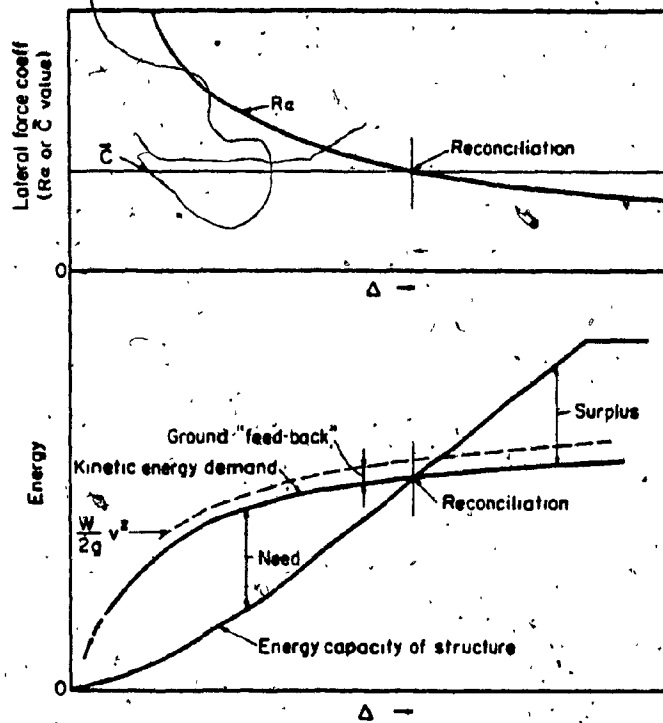


FIG. 6.1 - CONCEPTUAL MODEL, RESERVE ENERGY TECHNIQUE [85]

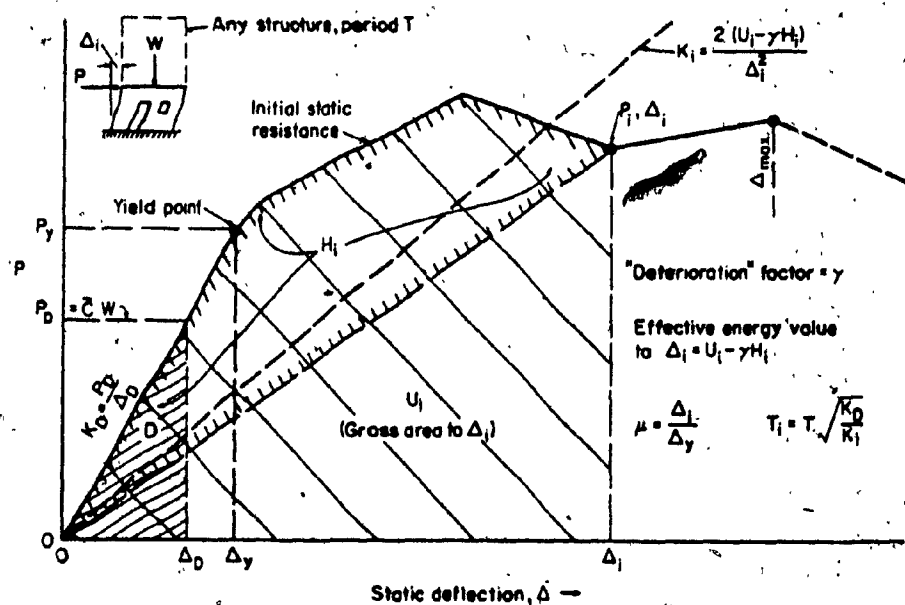


FIG. 6.2 - GENERAL CONSTRUCTION OF FORCE-DEFORMATION DIAGRAM OF A STORY. [85]

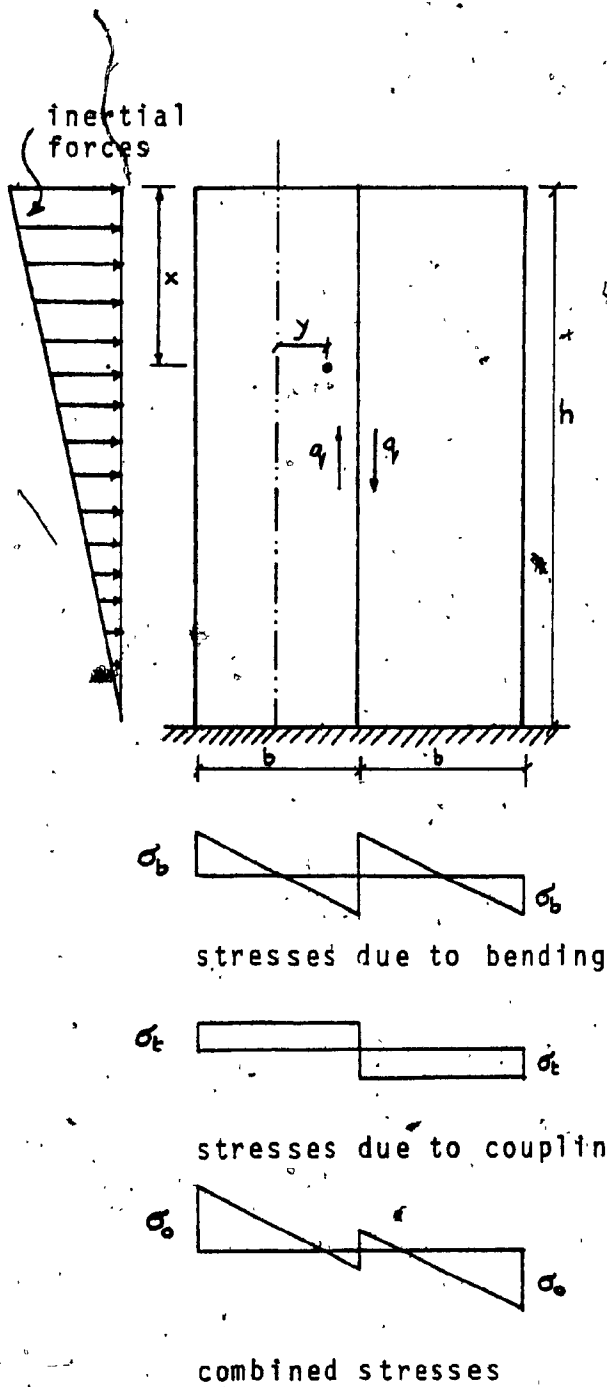


FIG. 6.3- OPTIMIZATION OF SLIP LOAD, SIMPLE WALLS.

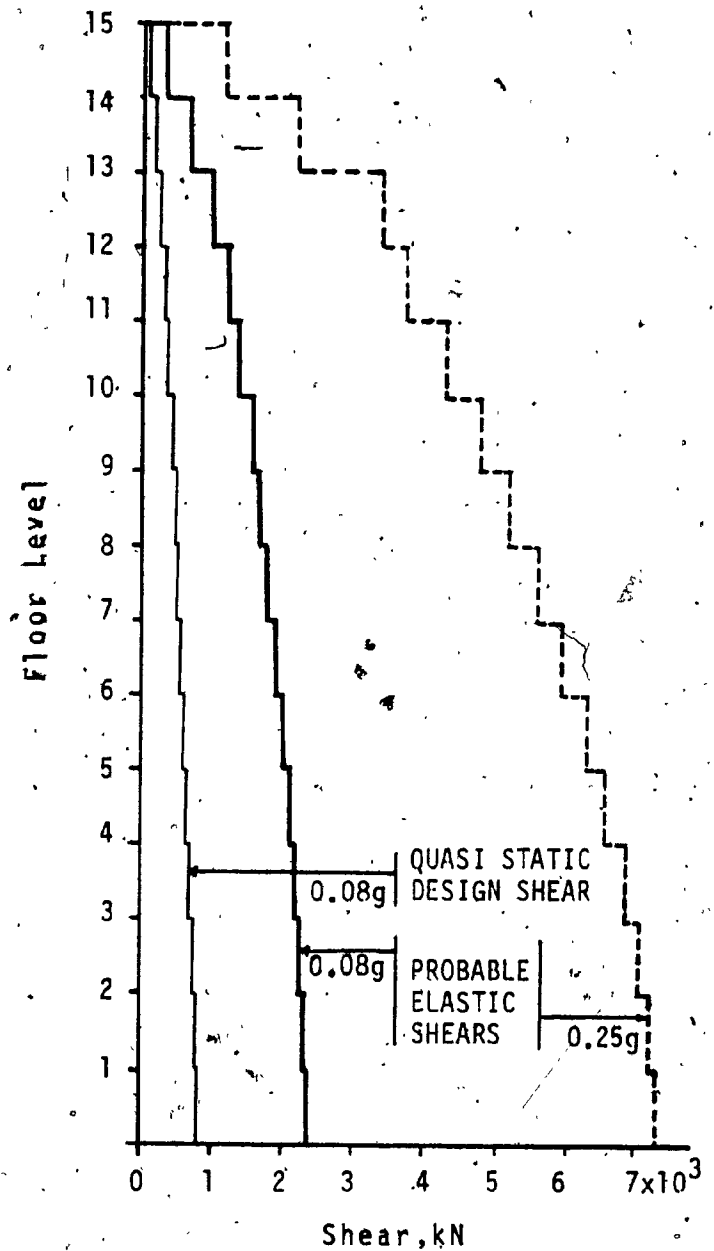


FIG. 6.4- STORY SHEAR ENVELOPE 15 STORY WALL

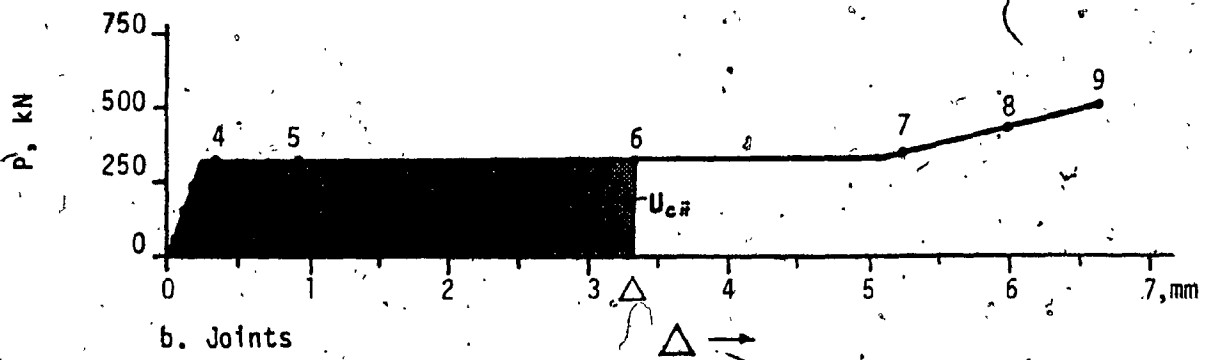
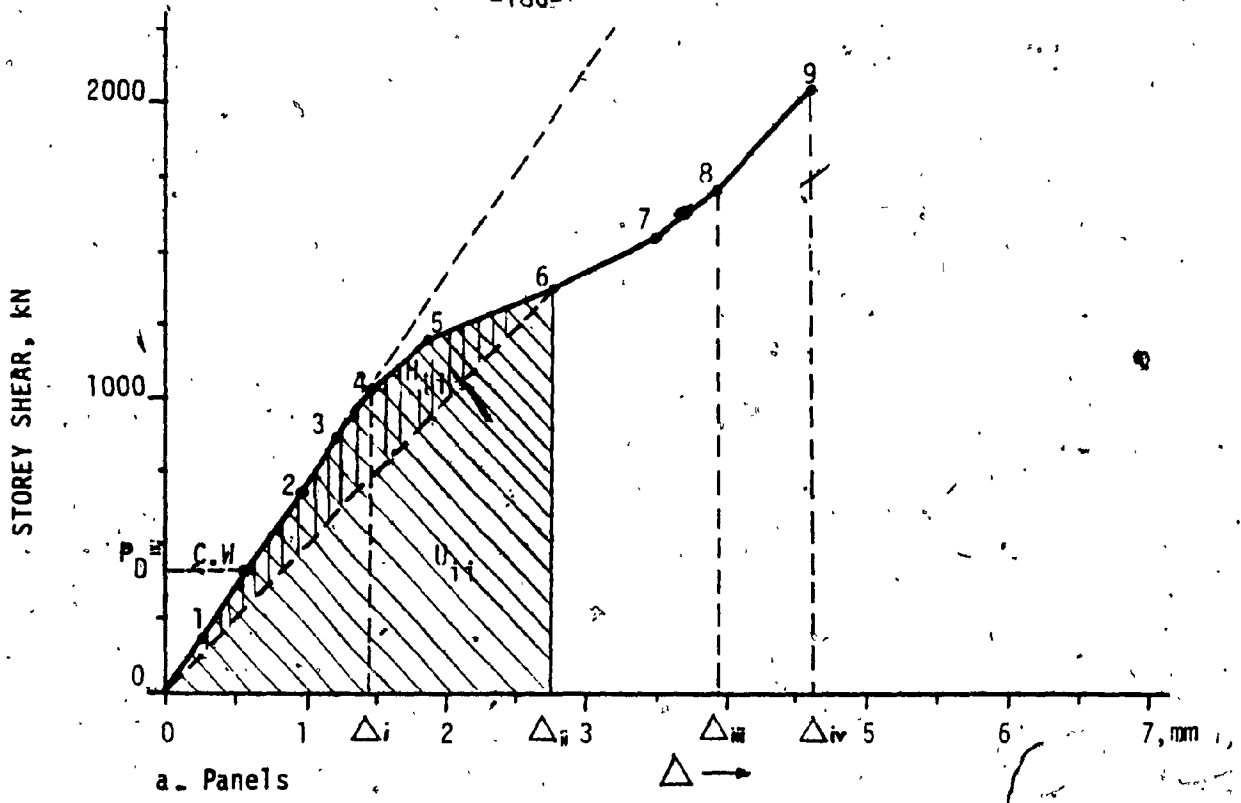


FIG.6.5 TYPICAL LOAD DISPLACEMENT DIAGRAM, 15 STOREY BUILDING (11th:STOREY)

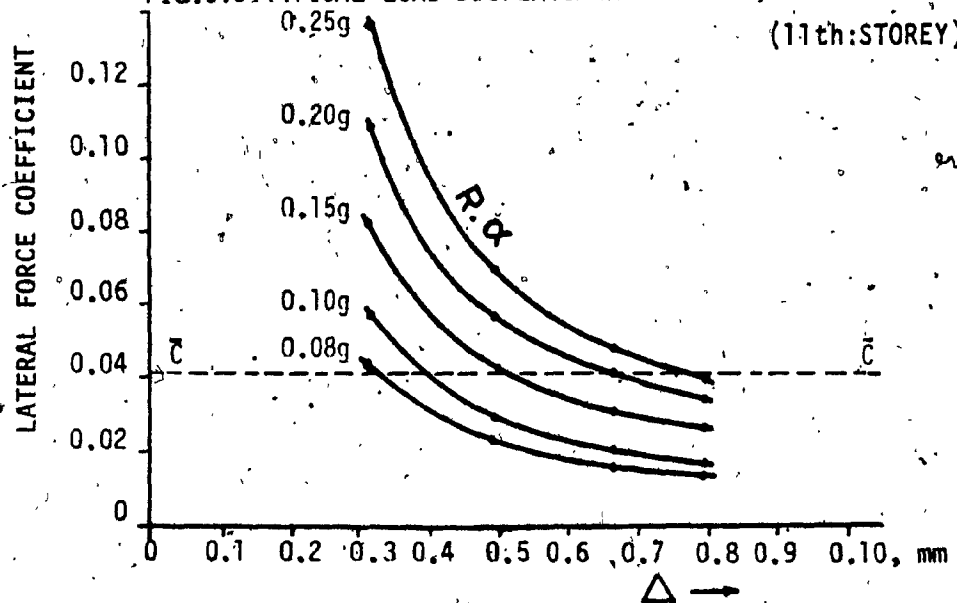
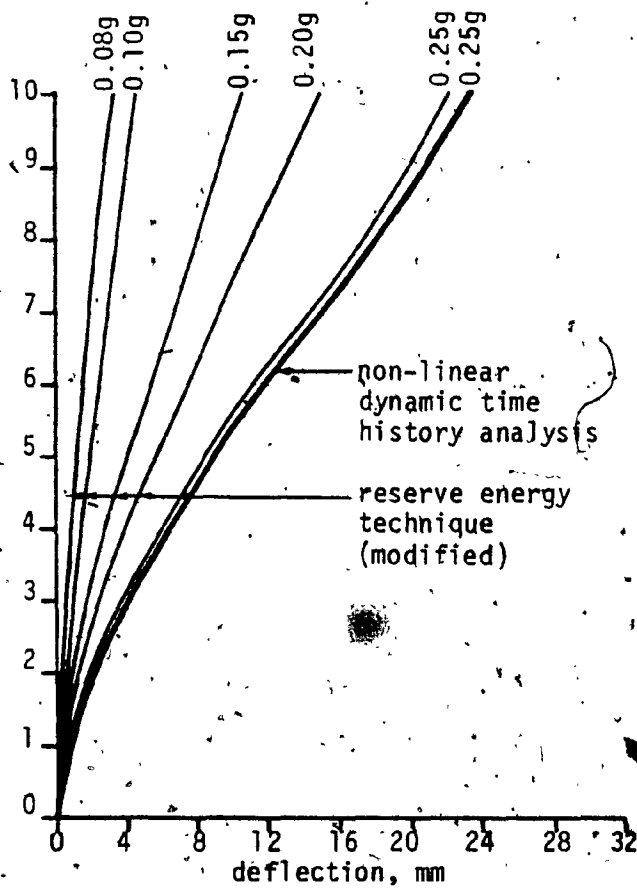
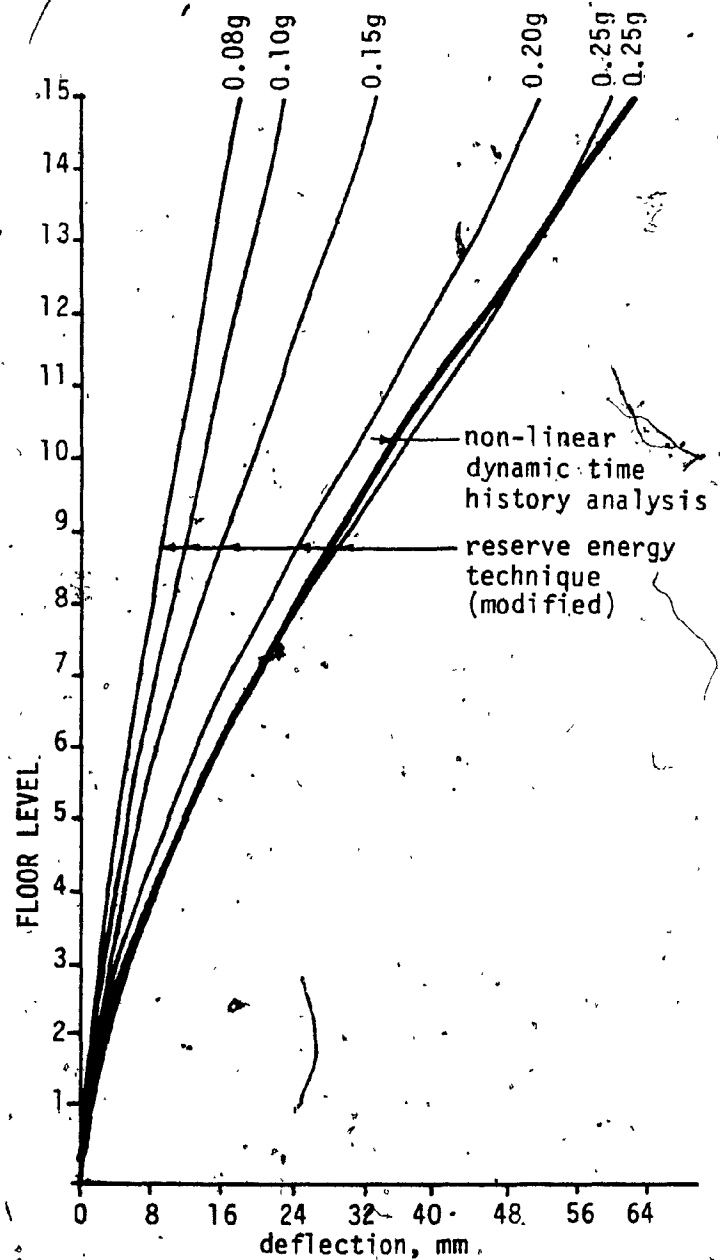


FIG.6.6 ENERGY RECONCILIATION AT 1ST:STOREY, 15 STOREY BUILDING



a. 10 storey building



b. 15 storey building

FIG. 6.7 DEFLECTION ENVELOPES

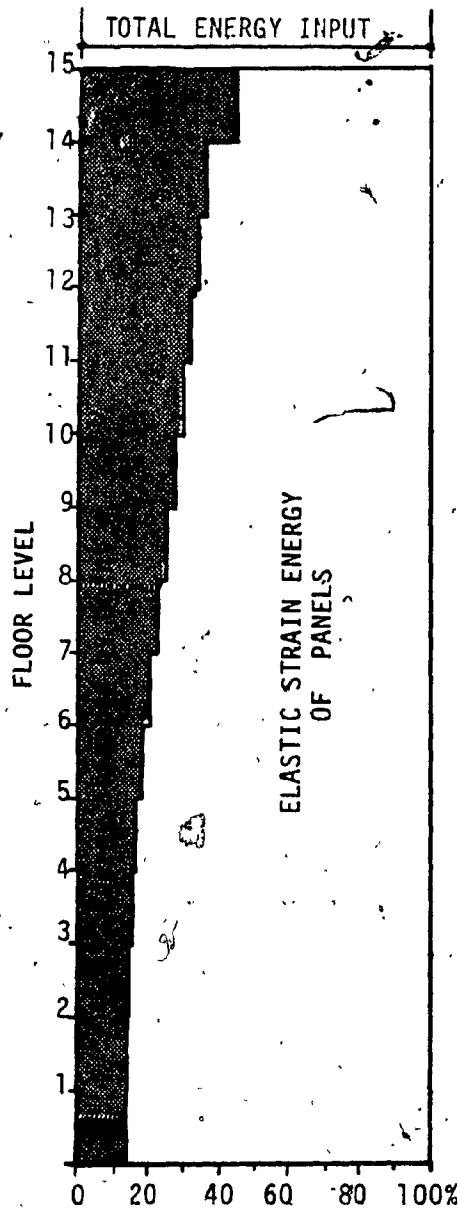
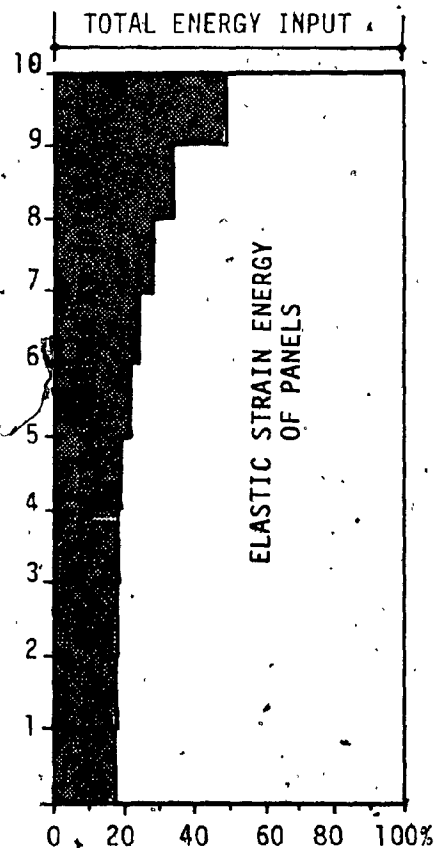


FIG. 6.8 ENERGY DISSIPATED BY JOINTS AT DIFFERENT STOREY LEVELS (0.25g)



a. 15 STOREY BUILDING

b. 10 STOREY BUILDING

FIG. 6.9 TOTAL ENERGY DISSIPATED BY JOINTS

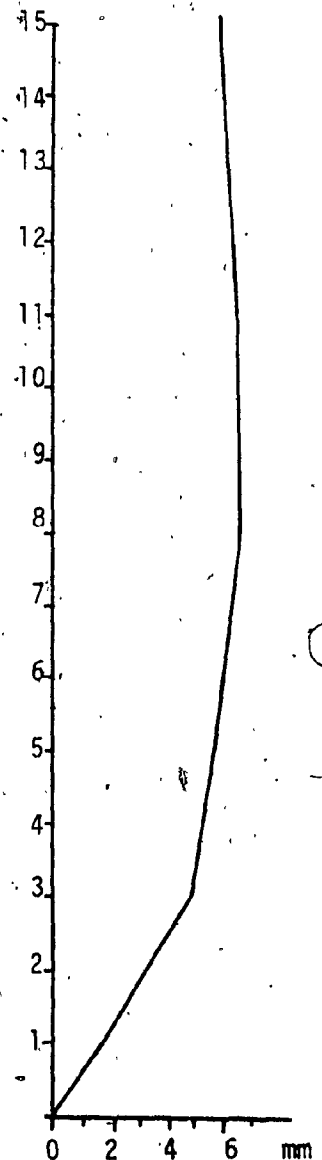
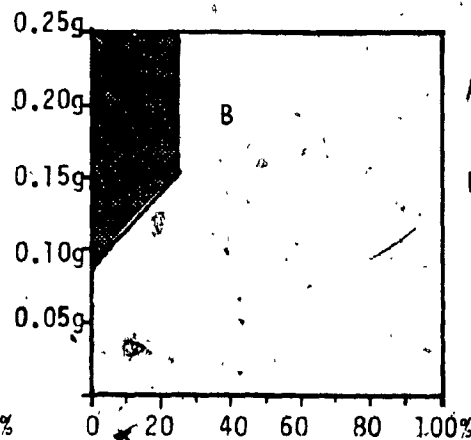
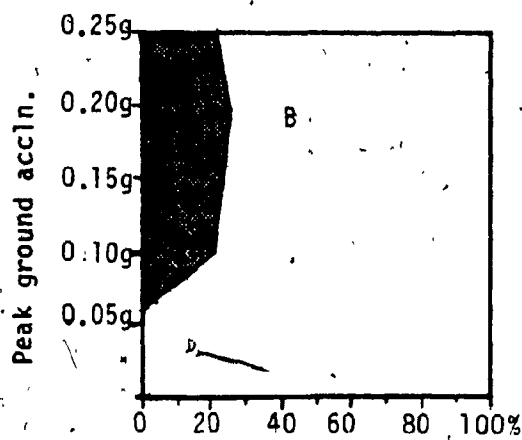


FIG. 6.10 DEFORMATIONS IN JOINTS (0.25g)



A = energy dissipated by joint
B = elastic strain energy of panels

CHAPTER VII
CONCLUSIONS AND RECOMMENDATIONS

CHAPTER VII

CONCLUSIONS AND RECOMMENDATIONS

7.1 CONCLUSIONS

The seismic response of a large panel structure is mainly dependent upon the behaviour of its joints. In this study, the role of joints has been reviewed and it was concluded that, in a panelized building they can be the prime source of energy dissipation and that the vertical lines of connection are the most logical choice for their location. The aim therefore lies in maximizing the energy dissipation in the vertical joints. For the joints to function as an efficient source of energy dissipation, they must possess nearly "elasto-plastic" behaviour with reasonably stable hysteretic characteristics under several cycles of reversals. They should also be able to accommodate large deformations to dissipate sufficient energy to relieve the structure from distress, without themselves undergoing any damage. Survey of the existing jointing systems indicates that none of them can meet all these requirements. It is towards the development of such a jointing system that the present project was directed.

Slipping joints, made out of steel plates or sections having slotted holes, are conceived to simulate the "elasto-plastic" behaviour. Provision of suitable surface finishes can ensure stable hysteretic characteristics necessary for predictable seismic response. One of the main variables in the tests was therefore the use of different surface finishes. Several specimens were subjected to static and dynamic cyclic loading and it was concluded that the commonly known externally applied surface finishes, although they may possess high static slip coefficients, are not suitable

for cyclic loading as they undergo wide variations in behaviour. Insertion of brake lining pads between the moving plates results in a high frictional force which does not deteriorate during several cycles of reversals. This meets the criteria of an efficient energy dissipating joint.

Nonlinear time history dynamic analysis was carried out for a typical crosswall panelized building using the existing program "Drain-2-D" in which the subroutines for truss element were modified to incorporate the behaviour of LSB joints. The earthquake record of North South component of El Centro 1940, was used as input motion.

For a given earthquake the response of the panelized structure is determined by the two factors - energy fed-in and the energy dissipation. The energy input is basically dependent upon the natural frequency of the structure which is influenced by the strength and stiffness of its coupling system. By selecting appropriate slip loads of the joints, minimum energy input can be obtained by avoiding the phenomenon of resonance and quasi-resonance. Similarly, the energy dissipation is again dependent on the slip load of the joint. By selecting appropriate slip load of the joint, energy dissipation could be maximized. Softening of the structure due to slipping of the joints may mean an invitation to either higher or lower seismic forces depending upon the relationship of the frequency of the structure to the ground motion. The beneficial effects of energy dissipation may then combine with the negative or positive effects of prolonged period of vibration.

Parametric studies were carried out by varying 1) the stiffness of the joint assembly, 2) slip load of the joint, 3) the wall heights, 4) the slot length, and 5) the seismic intensity.

It was concluded that:

- 1) the variation in the initial stiffness of the joint assembly, within the practical range for such joints, does not cause appreciable change in response.
- 2) the slip load is the main variable which influences the input energy and energy dissipation and thus the seismic response. By varying the slip load of the LSB joint, it is therefore possible to "tune" the response of the structure to an optimum value. This is one of the advantages available in LSB joints which is possible in few other jointing systems. It may however be mentioned here that the optimum slip load of the joint should not be low enough to cause slipping during service load conditions, like wind loading etc., or high enough to cause damage to the anchors or concrete.
- 3) the response of 5 and 10 story walls, having natural period of 0.11 and 0.3 seconds respectively, is distinctly different from the 15 and 20 story walls having period of 0.6 and 0.97 seconds respectively. Whereas in 5 and 10 story walls, the lower the natural frequency - the higher the seismic forces, while for 15 and 20 story walls, the lower the natural frequency - the lower the seismic forces. This is also evident from response spectrum in Fig. 5.4, in which the shift in response takes place at about 0.5 seconds for 5% damping.
- 4) the restriction of slot length in the connecting plate does not improve the response of the structure but on the contrary this could result in permanent damage to the joint and panels due to the sudden increase in force level caused due to shock loading by the shear failure of some joints. If the slip

length of the joint requires to be limited to avoid excessive deformations it could best be done by increasing the slip load of the joint rather than shortening its slot length. It is therefore desirable to leave some additional margin of clearance when deciding the slot length, as the nature of future earthquakes could be completely different from that assumed in the analysis.

5) the intensity of earthquake alters the effective period of vibration of the structure.

Comparison of response with cast-in-place monolithic walls and isolated walls (panelized walls without vertical joint) is shown in Table 7.1. For less than 10 story height, the response of two isolated walls is basically improved due to the increased rigidity provided by the joints. For higher stories the improvement in response is due to the energy dissipation mechanism of the LSB joint. LSB joints are thus effective in improving the seismic response and reducing the stresses for all heights of panelized buildings.

LSB joints may also be used in cast-in-place shear walls higher than 10 stories to increase the flexibility of the otherwise rigid walls and to dissipate energy, resulting in overall improved seismic response. In this case it will provide the required level of "ductility" without the need for special detailing demanded by codes.

The nonlinear response of the structure can be approximated by using the reserve energy technique which has been modified to suit panelized buildings. An energy method to approximate the optimum slip load of the joint is also presented. The results of the approximate methods show reasonable agreement with rigorous time history analysis.

The equivalent viscous damping of an equivalent linear elastic system for LSB jointed walls is very high (16-20%) compared to 3-5% available in conventional buildings. It is therefore possible to dissipate large amounts of seismic energy without damage caused by inelastic yielding of the structure or its components. Using this system, the necessity of other energy dissipating or tuning devices, such as expensive hydraulic systems or added masses is avoided. The basic philosophy of building earthquake resistant structures can be raised from the present level of protecting human life by preventing collapse, to that of controlling secondary damage.

In summary: 1) Limited slip bolted joints can meet the requirements of an efficient energy dissipating joint i.e. one simulating near "elasto-plastic" behaviour with reasonably stable hysteretic characteristics. 2) Data from the experiments provide basic design information. 3) That it be the vertical lines of connections in which these LSB joints are incorporated is of particular importance as a) the level of energy dissipation is higher than with horizontal joints; b) the joint strength can be uniform and all joints can contribute; c) the building remains elastic and recovers with little or no permanent set; d) by slipping, these joints act as structural dampers and safety valves, limiting the load level exerted at the horizontal joints which are intended to remain intact; e) the building is softened without losing its elasticity and resilience; f) the building can be "tuned" for optimum response; g) since there is no yielding of the materials involved in the process of energy dissipation, damage and repairs are considerably reduced; h) the LSB joints loose little or no tension and remain without adjustment ready to face the next earthquake with nearly the same efficiency. 4) The concept

of energy dissipating slipping joints can be usefully employed in highrise cast-in-place shear walls and framed buildings clad with architectural curtain walls. 5) Also of significant interest is the fact that joints can provide a means of recording the severity of an earthquake and the response of the building.

7.2 RECOMMENDATIONS FOR FUTURE STUDIES

1) In the present study the optimization of joint slip load has been done assuming a constant value throughout the height which is desirable from the point of view of standardization. Varying the joint slip load for a group of stories might show improved response.

2) Three dimensional analysis although a formidable task might be performed to study the effect of oblique ground motion and torsional oscillations.

3) How soil structure interaction alters the vibrational characteristics and hence change the heights of building for which LSB joints become of interest.

4) Model testing on shaking table simulating seismic loading, or, if possible, testing full scale structures by associating with organizations, like "U.S.-Japan Cooperation Research program utilizing large scale testing facilities" in Japan. This should demonstrate the actual value of LSB joints in quantitative terms leading to improvement in mathematical modeling, and, furthermore, give a better estimate of the structural damping from sources other than the LSB joints.

With the development of the concept, it should be possible to provide economical and seismically safe tall panelized structures.

HEIGHT OF BUILDING	RESPONSE	REDUCTION COMPARED TO ISOLATED WALLS	REDUCTION COMPARED TO MONOLITHIC WALLS	REMARKS
5 Story	Shear Bending Deflection	30% 60% 65%	0% 0% 0%	suitable for panelized structure
10 Story	Shear Bending Deflection	35% 65% 78%	0% 0% - 5%	
15 Story	Shear Bending Deflection	35% 50% 55%	65% 60% 25%	suitable for both panelized structures and cast-in-place shear walled structures.
20 Story	Shear Bending Deflection	35% 30% 40%	65% 65% 35%	

TABLE 7.1 REDUCTION IN RESPONSE BY USING LIMITED SLIP JOINTS (0.33 g)

REFERENCES

7 REFERENCES

- [1] Division of International Affairs Special Report "Industrialized Buildings - A Comparative Analysis of European Experience", Department of Housing and Urban Development, Washington, D.C., April 1968.
- [2] Division of International Affairs, "Building Prefabrication - The State of Art in World Perspective", HUD, International Brief No. 14, U.S. Department of Housing and Urban Development Washington, D.C., June 1972.
- [3] Lewicki, B., "Building with Large Prefabricates", 1st Ed., Elsevier Publications Co., London, 1966.
- [4] Despeyroux, J., "Structural Connexion Problems and the Use of Special Materials in Precast Concrete Construction - Design Philosophy and its Application to Precast Concrete Structures", Cement and Concrete Association, London, 1968.
- [5] ACI-ASCE Committee 512, 1963, "Suggested Design of Joints and Connections in Precast Structural Concrete", ACI Manual of Concrete Practice Part 3, Products and Processes, 1974.
- [6] Diaconu, D., et al., "Seismic Response of Great Panel Structures with 10 Stories", 5WCEE, Rome, 1973.
- [7] Becker, J.M., Llorente, C., "Seismic Design of Precast Concrete Panel Buildings", Proc. Workshop on Earthquake - Resistant Reinforced Concrete Building Construction, University of California, Berkeley, July 1977.
- [8] Polyakov, S., "Design of Earthquake Resistant Structures", 1st Ed., MIR Publishers, Moscow, 1974.
- [9] Fintel, M., Schultz, D.M., "A Philosophy for Structural Integrity of Large Panel Buildings", Journal of PCI, Vol. 21, No. 3, May/June 1976.
- [10] Djabua, S.A., Chachava, T.N., Abashidze, G.G., Djishkariani, N.M., and Kemoklidze, G.S., "Research on Seismic Resistance of Large Panel Apartment Buildings", 6WCEE, New Delhi, 1977, pp.5-299 to 303.
- [11] Ikeda, A., Yamada, T., Kwamuici, S., and Fujii, S., "State of Art of Precast Concrete Techniques in Japan", Proc. Workshop on Earthquake Resistant Reinforced Concrete Building Construction, University of California, Berkeley, 1977.
- [12] Hawkins, N.M., "State of Art Report on Seismic Resistance of Prestressed and Precast Concrete Structures - Part 2", Journal of PCI, Vol. 23, No. 1, January/February 1978.

- [13] Polyakov, S.V., et al., "Investigations into Earthquake Resistance of Large Panel Buildings", 4WCEE, Santiago, Chile, 1969, pp. B-1, 165 to 180.
- [14] Barkov, Y.V., Glina, Y.V., "Theoretical and Experimental Investigations of Precast and Monolithic Frameless Buildings on Large Scale Reinforced Concrete Models", 5WCEE, Rome, 1973.
- [15] Velkov, M.P., "Earthquake Resistant Design of Twenty One Storey Prefabricated Large Panel Building", 6WCEE, New Delhi, 1977.
- [16] Fintel, M., "Performance of Precast Concrete Structures during Rumanian Earthquakes of March 4, 1977", Journal PCI, Vol. 22, No. 2, March/April 1977.
- [17] Llorente, C., Becker, J.M., Roesset, J.M., "The Effect of Nonlinear-Inelastic Connection Behaviour on Precast Panelized Shear Walls", paper prepared for the Symposium on Mathematical Modeling of Reinforced Concrete Structures, Committee 422, ACI, 1978.
- [18] Becker, J.M., Llorente, C., "The Seismic Response of Simple Precast Concrete Panel Walls", paper prepared for the U.S. National Conference on Earthquake Engineering, Stanford, California, August 22-24, 1979.
- [19] Pall, A.S., Marsh, C., "Seismic Response of Large Panel Structures Using Limited-Slip Bolted Joints", Proc. of the Third Canadian Conference on Earthquake Engineering, Montreal, 1979, pp. 899-916.
- [20] Muto, K., Ohmori, N., and Takahashi, T., "A Study on Reinforced Concrete Slitted Shear Walls for High Rise Buildings", 5WCEE, Rome, 1973, pp. 1135-1138.
- [21] Paulay, T., "Earthquake Resistant Structural Walls", Proc. of the Workshop on Earthquake-Resistant Reinforced Concrete Building Construction, University of California, Berkeley, 1977, pp. 1339-1365.
- [22] Mueller, P., Becker, J.M., "Seismic Characteristics of Composite Precast Walls", Proc. of the Third Canadian Conference on Earthquake Engineering, Montreal, 1979, pp. 1169-1199.
- [23] Lewicki, B., Pauw, A., "Joints in Precast Panel Buildings", Planning and Design of Tall Buildings, Vol. III, American Society of Civil Engineers, New York, 1973.
- [24] Cholewicki, A., "Load Bearing Capacity and Deformability of Vertical Joints in Structural Walls of Large Panel Buildings", Building Science, Vol. 6, Great Britain, 1971.
- [25] Backler, A.P., et al., "Local Behaviour of Shear Transfer and Compression Transfer Joints, Part 1", The Behaviour of Large

Panel Structures, CIRIA Report No. 45, London, 1973.

- [26] Polloner, E., and Gropner, M., "Behaviour of Large Panel Construction under Alternating Loads, Bulletin No. 214, Israel Institute of Technology, Israel, 1974.
- [27] Zeck, U.I., "Joints in Large Panel Precast Concrete Structures", Publication No. R76-16, Massachusetts Institute of Technology, Cambridge, Massachusetts, 1976.
- [28] Konzc, T., "Manual of Precast Concrete Construction", 1st Ed., Vol. 3, Bauverlag GMBH, Wiesbaden and Berlin, 1968.
- [29] Architectural Institute of Japan, "Design Essentials in Earth-Quake Resistant Buildings", Elsevier Publishing Company, New York, 1970.
- [30] Suenaga, Y., "On Box-Frame Type Precast Reinforced Concrete Construction of Five Storeyed Multiple Houses - Problems in the Present Jointing Methods and Stress Coveyance Methods in Earthquakes", Concrete Journal, Vol. 12, No. 7, Japan, 1974.
- [31] Spencer, R.A., and Neille, D., "Cyclic Tests of Welded Headed Stud Connections", Journal PCI, Vol. 21, No. 3, May/June 1976.
- [32] PCI Manual on "Design of Connections for Precast Prestressed Concrete", Prestressed Concrete Institute, Chicago, 1973.
- [33] Dawson, W.F., and Shemie, M., "Bolted Connections as a Substitute for on Site Welding and Wet Joints in Precast Concrete", Proc. of the Canadian Structural Concrete Conference, Ottawa, Canada, 1977.
- [34] Shemie, M., "Bolted Connections in Large Panel System Buildings", Journal PCI, Vol. 18, No. 1, January/February 1973.
- [35] Paulay, T., "Design Aspects of Shear Walls for Seismic Areas", Canadian Journal of Civil Engineers, Vol. 2, 1975.
- [36] Bibliography on Bolted and Riveted Joints, Manual No. 48, ASCE, 1967.
- [37] Specifications for Structural Joints using ASTM A325 or A490 Bolts, approved by the Research Council on Riveted and Bolted Structural Joints of the Engineering Foundation, February 4, 1976.
- [38] Fisher, J.W., and Struik, J.H.A., "Guide to Design Criteria for Bolted and Riveted Joints", John Wiley and Sons, New York, 1974.
- [39] Vitelleschi, S., and Schmidt, L.C., "Damping in Friction Grip Bolted Joints", Journal of Structural Division, ASCE, Vol. 103, No. ST7, July 1977, pp. 1447 to 1460.

- [40] Cattaneo, L.E., and Yokel, F.Y., "Structural Tests of Mechanical Connections for Concrete Panels", National Bureau of Standards, Prepared for the Office of Research and Technology, Department of Housing and Urban Development, Washington, D.C., November 1972.
- [41] Brookhart, G.C., Siddiqi, I.H., and Vasarhelyi, D.D., "Surface Treatment of High Strength Bolted Joints", Journal of Structural Division, ASCE, Vol. 94, ST3, March 1968.
- [42] Canadian Standards Association, "Steel Structures for Buildings - Limit States Design, CSA S16.1-1974", Rexdale, Ontario.
- [43] Allan, R.N., and Fisher, J.W., "Bolted Joints with Oversize or Slotted Holes", Journal of Structural Division, ASCE, Vol. 94, No. ST9, September 1968.
- [44] Bowden, F.P., Moore, A.J.W., Tabor, D., "The Ploughing and Adhesion of Sliding Metals", Journal of Applied Physics, London, Vol. 14, 1943, pp. 80-91.
- [45] Pauw, A., and Howard, L.L., "Tension Control for High-Strength Structural Bolts", Proc. of the American Institute of Steel Construction, April 1955.
- [46] Hyler, W.S., Humphrey, K.D., Croth, N.S., "An Evaluation of the High Tensile Huck-Bolt Fastener for Structural Application", Report No. 72, Huck Manufacturing Co., Detroit, Michigan, March 1961.
- [47] Struik, J.H.A., Oyelundun, A.O., Fisher, J.W., "Bolt Tension Control with a Direct Tension Indicator", Engineering Journal AISC, Vol. 10, No. 1, 1973.
- [48] High Strength Bolting for Structural Joints - Bethlehem Steel Corp., Bethlehem, PA.
- [49] Tajima, J., "Effect of Relaxation and Creep on the Slip Load of High Strength Bolted Joints", Structural Design Office, Japanese National Railways, Tokyo, June 1964.
- [50] Christopher, R.J., Kulak, G.L., Fisher, J.W., "Calibration of Alloy Steel Bolts", Journal of Structural Division, ASCE, Vol. 92, ST2, April 1966.
- [51] Chesson, E. Jr., and Munse, W.H., "Studies of the Behaviour of High Strength Bolts and Bolt Joints", University of Illinois Engineering Experimental Station Bulletin No. 469, 1964.
- [52] "TURN-OFF-NUT" Motion Movie (15 minutes duration) lent free by Bethlehem Steel Corporation, Bethlehem, USA.
- [53] Coull, A., and Stafford-Smith, B., "Analysis of Shear Wall Structures", Proc. of the Symposium on Tall Buildings held at the University of Southampton, April 1966.

- [54] McLeod, I.A., "Lateral Stiffness of Shear Walls with Openings", Proc. of the Symposium on Tall Buildings held at the University of Southampton, April 1966.
- [55] Chitty, L., "On the Cantilever Composed of a Number of Parallel Beams Interconnected by Crossbars", Philosophical Magazine (London), Vol. 38, Series 7, 1947.
- [56] Beck, H., "Contribution to the Analysis of Coupled Shear Walls", ACI Journal, Vol. 59, No. 8, August 1962.
- [57] Rosman, R., "Approximate Analysis of Shear Walls Subject to Lateral Loads", ACI Journal, Vol. 61, No. 6, June 1964.
- [58] Coull, A., Chaudhary, J.R., "Stresses and Deflections in Coupled Shear Walls", ACI Journal, February 1967.
- [59] Coull, A., Chaudhary, J.R., "Analysis of Coupled Shear Walls", ACI Journal, Vol. 64, September 1967.
- [60] Rosman, R., "Tables for the Internal Forces of Pierced Shear Walls Subject to Lateral Loads", Bauingenieur-Praxis, Heft 66, W. Ernest & Sohn, Berlin, 1966.
- [61] Sen, H.K., et al., "Analysis of Shear Walls Composed of Panels, Part 2", The Behaviour of Large Panel Structures, CIRIA Report No. 45, London, 1973.
- [62] Petersson, H., "Analysis of Building Structures", Department of Building Construction, Chalmers University of Technology, Göteborg, Sweden, 1973.
- [63] Hrennikoff, A.P., "Solution of Problems of Elasticity by the Framework Method", Journal of Applied Mechanics, Vol. 8, A146, 1941.
- [64] McHenry, D., "A Lattice Analogy for the Solution of Plane Stress Problems", Journal of the Institute of Civil Engineers, London, Vol. 21, No. 2, 1943-44.
- [65] McCormick, C.W., "Plane Stress Analysis", Journal of Structural Division, ASCE, Vol. 89, ST14, August 1963.
- [66] Grinter, L.E., "Statistical State of Stress by Grid Analysis", Numerical Methods of Analysis in Engineering, Macmillan Company, New York, 1949.
- [67] Pollner, E., Tso, W.K., and Heidebrecht, A.C., "Analysis of Shear Walls in Large Panel Construction", Canadian Journal of Civil Engineering, Vol. 2, 1975.
- [68] Brakov, G., and Sachanski, S., "Response of Large Panel Buildings for Earthquake Excitations in Nonlinear Stage", 6WCEE, New Delhi, 1977.

- [69] Frank, R., "Dynamic Modeling of Large Precast Panel Buildings Using Finite Elements with Substructuring", Report No. R76-36, Department of Civil Engineering, MIT, Cambridge, Mass., August 1976.
- [70] Pekau, O.A., Huttelmaier, H.P., "Seismic Integrity of Precast Panel Structures with Discrete Connections", Proc. of the Seventh Canadian Congress of Applied Mechanics, Sherbrooke, 1979.
- [71] Unemori, A., Roesset, J.M., Becker, J.M., "Effect of Inplane Floor Slab Flexibility on Response of Cross Wall Building System", paper prepared for the Symposium on Mathematical Modeling of Reinforced Concrete Structures, ACI Committee 442 - Response of Buildings to Lateral Forces, 1978.
- [72] Becker, J.M., Roesset, J.M., Llorente, C., Lanham, K., "The Seismic Response of Precast Concrete Panel Buildings Considering Connection Behaviour", Proc. of the Sixth European Conference on Earthquake Engineering, Detrovnik, Yugoslavia, September 1978.
- [73] Burnett, E.F.P., Rajendra, R.C.S., "Influence of Joints in Panelized Structural Systems", Journal of Structural Division, ASCE, ST9, September 1972.
- [74] Stafford-Smith, B., Rehman, K.M.K., "A Theoretical Study of the Sequence of Failure in Precast Panel Shear Walls", Proc. of the Institution of Civil Engineers, London, 1973, pp. 581-592.
- [75] Unemori, A.L., "Generalized Dynamic Behaviour of Cross Wall Building System", D.Sc. Thesis, MIT, Cambridge, Mass., March 1978.
- [76] Wilson, E.L., "A Method of Evaluation of Foundation Structure Interaction", 4WCEE, Santiago, Chile, 1969.
- [77] Newmark, N.M., "A Method of Computation for Structural Dynamics", Journal of Engineering Mechanics Division, ASCE, EM3, July 1959.
- [78] Clough, R.W., Penzien, J., "Dynamics of Structures", McGraw-Hill Book Co., 1975.
- [79] Bathe, K.J., and Wilson, E.L., "Numerical Methods in Finite Element Analysis", Prentice Hall Inc., Englewood Cliffs, New Jersey, 1976.
- [80] Borges, J.F., Ravara, A., Pereira, J., and Monteiro, V., "Methodology for Seismic Studies of Prefabricated Panel Buildings", 4th European Symposium on Earthquake Engineering, London, September 1972.
- [81] Derecho, A.T., Fugelso, L.E., Fintel, M., "Structural Walls in Earthquake Resistant Buildings, Dynamic Analysis of Isolated Structural Walls - Input Motions", Portland Cement Association, Skokie, December 1977.

- [82] Kannan, A.E., Powell, G.H., "Drain - 2D, A General Purpose Computer Program for Dynamic Analysis of Inelastic Plane Structures", College of Engineering, University of California, Berkeley, 1973.
- [83] National Building Code of Canada 1977, National Research Council of Canada, Ottawa.
- [84] Powell, G., Schrieker, V., "Ductility Demands on Joints in Large Panel Structures", Preprint No. 3022, ASCE Fall Convention, October 17-21, 1977, San Francisco.
- [85] Blume, J.A., Newmark, N.B., and Corning, L.H., "Design of Multi-Storey Reinforced Concrete Buildings for Earthquake Motions", P.C.A., Skokie, Ill., USA, 1961.
- [86] Pall, A.S., Marsh, C., "Energy Dissipation in Panelized Buildings Using Limited-Slip Bolted Joints", Proceedings AICAP-CEB Symposium, Vol. III, Rome, Italy, May 1979.
- [87] Wilson, E.L., and Dovey, H.H., "Three Dimensional Analysis of Building Systems, TABS", Report No. EERC 72-8, University of California, 1972.
- [88] Ha, H.K., "Matrix Algebra Package" - MAP", Centre for Building Studies, Concordia University, 1975.
- [89] Gjelsvick, A., "Interaction between Frames and Precast Panel Walls", Journal of Structural Division, ASCE, ST2, February, 1974.

APPENDICES

APPENDIX A.1

1. PROPERTIES OF END WALL (Composed of Two Panel Walls) (Fig. 4.5)

- a. Section area of each panel wall
 $(7.3 \text{ m} \times 0.2 \text{ m} = 1.46 \text{ m}^2)$ = 1.46 m^2
- b. Effective shear area
 $\frac{1.46}{1.2} = 1.22 \text{ m}^2$ = 1.22 m^2
- c. Moment of inertia of each panel wall
 $\frac{0.2 \times 7.3^3}{12} = 6.48^4$ = 6.48 m^4
- d. Gravity load for each panel wall for each story height i.e. load of wall + dead load and live load from tributary area of floor panels = 245 kN
- e. Mass for lateral forces for each panel wall for each story height
 $\frac{1}{2} \times \frac{1 \text{ end wall}}{\Sigma I} \times \text{Mass of building for each story}$
 $= \frac{1}{2} \times \frac{1}{4} \times 512 = 64 \text{ tons}$ = 64 tons
- f. Modulus of elasticity, E
 (using concrete of $f_c = 35 \text{ MPa}$, $E = 5000\sqrt{f_c}$) = $2.92 \times 10^7 \text{ kPa}$
- g. Poisson's ratio = 0.15

2. CONNECTION PROPERTIES (Fig. 4.6)

- a. Slip load for each LSB joint using brake lining pads for 2-24 mm dia bolts of ASTM A325M as per Table 3.7 = 160 kN
- b. Initial stiffness, $k_0 = \frac{160}{0.00025}$ = $64 \times 10^4 \text{ kN/m}$
- c. 2nd stage stiffness, k_1 = 0
- d. 3rd stage stiffness, $k_2 = \frac{480}{0.0015}$ = $32 \times 10^4 \text{ kN/m}$

NOTE : If two LSB joints are used at each story, the above values should simply be doubled to correspond to the lumped effect of the joints for each story .

LISTING OF MODIFIED SUBROUTINES FOR
LSB JOINTS

79/08/22. 17.44.35 PAGE 1

```

SUBROUTINE INEL1 73/172 OPT=1 FTM 4.7+470
C
1 SUBROUTINE INEL1 (KCONT,FCONT,NDOP,NIMFG,ID,X,Y,NN)
COMMON /INFEL/ IMEN,KST,LM(4),KGEOM,EALP,EALF,FL,COSA,SINA,
5 KODYX,KODY,SEP,SEL,VTOT,VPACP,VPACN,VBUCK,VENP,
TVENP,VENN,TVENN,SENP,TSENP,SENN,TSENN,SFO,NOOI,
3 NODJ,KOUTOT,KBUCK,PYP,PYN,SLPHX,SEPHX,EALPB,PPSL,
4 REST(161)
COMMON /WORK/ FTYP(40,6),KBUCC(40),FEF(40,4),KDFEF(40),DO(4),
10 GA(4,4),FFEF(4),SFF(4),SSFF(4),NMEN,NMST,NFEF,
GNEL,INEL,INODI,INODJ,INC,IINC,INBT,INBT,IRGH,
3 IKDI,KFOL,IKFOL,KFLL,IKFLL,FOL,FFOL,FL,FFLL,
4 FINIT,FFINIT,XL,YL,PSH,PPSH,AREA,W(1500)
COMMON/THIST/THOUT(10),THOUT(20),ITHP,ISAVE,NELTH,NSTH,NF7,ISE
C
15 DIMENSION KCONT(1),ID(MN,1),X(1),Y(1),COM(1)
DIMENSION AST(2),YESNO(2)
EQUIVALENCE (IMEN,COM(1))
DATA AST /2H ,2H */
DATA YESNO/4H YES,4H NO /
C
20 CONTROL VARIABLES
C
25 NDOF=4
NINFC=36
NMEN=KCONT(2)
NMST=KCONT(3)
NFEF=KCONT(4)
30 PRINT 10, (KCONT(I),I=2,4)
10 FORMAT(30H TRUSS ELEMENTS (TYPE 1) OR LSB JOINTS////
1 25H NO. OF ELEMENTS =14/
2 25H NO. OF STIFFNESS TYPES =14/
3 25H NO. OF F.E.F. PATTERNS =14)
C
35 INPUT STIFFNESS PROPERTIES
C
40 DO 30 IT=1,NMST
30 READ 40, I, (FTYP(II,J),J=1,6),KBUCC(II)
40 FORMAT (15,6F10.0,2F5.0,I5)
IF (KBUCC(1).EQ.2) GO TO 25
PRINT 20
20 FORMAT(////16H STIFFNESS TYPES//
1 5H TYPE,6X,7H YOUNGS,4X,9HHARDENING,6X,7HSECTION,3X,
2 10HPOS. YIELD,3X,10HNEG. YIELD,4X,8HBUCKLING/
3 5H NO.,6X,7HMODULUS,4X,9H RATIO ,6X,7H AREA ,3X
4 10H STRESS ,3X,10H STRESS 4X,6H CODE /)
DO 21 IT=1,NMST
21 PRINT 50, IT, (FTYP(II,J),J=1,5),KBUCC(II)
GO TO 55
25 PRINT 26
26 FORMAT(////15H LSB JOINT DATA//5H TYPE,6X,7HINITIAL,5X,9HSTIFFNESS
1,6X,9HSTIFFNESS,7X,4HSLIP,5X,4HSLIP,5X,7HFAILURE/
25H NO.,5X,9HSTIFFNESS,5X,7HTRATIO 1,6X,7HTRATIO 2,7X,6HLENGTH,4X,
34HLOAD,7X,4HLOAD/)
DO 27 IT=1,NMST
KBUCC(II)=0
55

```

```

      STIF=FTYP(IIT,1)*FTYP(IIT,3)*100
      SLLO=FTYP(IIT,4)*FTYP(IIT,3)
60  27 PRINT 51,IIT,STIF,FTYP(IIT,2),FTYP(IIT,6),FTYP(IIT,7),SLLO,FTYP(IIT,8)
      50 FORMAT (I4,E14.4,E13.4,3F13.2,2,110)
      51 FORMAT (I4,F15.2,F13.5,F15.7,F12.5,F9.2,F11.2)
      C
      C      FIXED END FORCE PATTERNS
65  55 IF (NFEF.EQ.0) GO TO 100
      PRINT 60
60  60 FORMAT (///25H FIXED END FORCE PATTERNS//
      1      8H PATTERN,3X,4HAXIS,2(7X,5HAXIAL,7X,5HSHARP)
      2      8H NO. ,3X,4HCODE,2(7X,5HAT 1),2(7X,5HAT 2))
      C
      DO 70 NF=1,NFEF
      READ 80, I,KOFEF(NF), (FEF(NF,J),J=1,4)
75  70 PRINT 90, NF,KOFEF(NF), (FEF(NF,J),J=1,4)
      80 FORMAT (2I5,4F10.0)
      90 FORMAT (I5,I8,1X,4F12.2)
      C
      C      ELEMENT DATA
80  100 PRINT 110
      110 FORMAT (///22H ELEMENT SPECIFICATION//
      1      3X,4HELEM,3X,4HNODE,2X,4HNODE,2X,4HNODE,2X,4HSTIF,2X,
      2      4HGEOM,2X,4HTIME,3X,12HFEF PATTERNS,3X,17HFEF SCALE FACTORS)
      3      5X,7HINITIAL/
      4      3X,4H NO.,3X,4H I ,2X,4H J ,2X,4HDIFF,2X,4HMTYPE,2X,
      5      4HSTIF,2X,4HMHIST,3X,12H DL LL ,3X,17H DL
      6      5X,7H FORCE /)
      C
      KODVX=0
      KODY=0
      KST=0
      DO 120 J=15,29
      120 CONT(J)=0.
      C
      IMEM=1
      130 READ 140, INEL,INODI,INODJ,IINC,IIMBT,IKGM,IKDT,IKFOL,IKFLL,FFOL,FINEL
      1FLL,FFINIT
      140 FORMAT (9I5,2F5.0,F10.0)
      IF (INEL.GT.IMEM) GO TO 170
      150 INODI=INODI
      INODJ=INODJ
      IINC=IINC
      IF (IINC.EQ.0) INC=1
      IMBT=IIMBT
      KGEOM=IKGM
      KOUTOT=IKDT
      YNG=YESNO(2)
      IF (KGEOM.NE.0) YNG=YESNO(1)
      YNT=YESNO(2)
      IF (KOUTOT.NE.0) YNT=YESNO(1)
      KFOL=IKFOL
      KFLL=IKFLL
      FOL=FFOL
      INEL1 49
      INEL1 50
      INEL1 51
      INEL1 52
      INEL1 53
      INEL1 54
      INEL1 55
      INEL1 56
      INEL1 57
      INEL1 58
      INEL1 59
      INEL1 60
      INEL1 61
      INEL1 62
      INEL1 63
      INEL1 64
      INEL1 65
      INEL1 66
      INEL1 67
      INEL1 68
      INEL1 69
      INEL1 70
      INEL1 71
      INEL1 72
      INEL1 73
      INEL1 74
      INEL1 75
      INEL1 76
      INEL1 77
      INEL1 78
      INEL1 79
      INEL1 80
      INEL1 81
      INEL1 82
      INEL1 83
      INEL1 84
      INEL1 85
      INEL1 86
      INEL1 87
      INEL1 88
      INEL1 89
      INEL1 90
      INEL1 91
      INEL1 92
      INEL1 93
      INEL1 94
      INEL1 95
      INEL1 96
      INEL1 97
      INEL1 98
      INEL1 99

```

```

115      FLL=FFLL
      FINIT=FFINIT
      ASTT=AST(1)
      IF (INEL.NE.NMEM) 130,170

120      C 160 NODI=NODI+INC
      NODJ=NODJ+INC
      ASTT=AST(2)

125      C 170 PRINT 180, ASTT, IMEM, NODI, NODJ, INC, IMBT, YNG, YNT, KFOL, KFL, FOL, FLL,
      IFINIT
      180 FORMAT (A2,I4,I7,3I6,3X,A4,2X,A4,I7,I6,F11.2,F10.2,F11.2)

      C COUNT NUMBER OF ELEMENT TIME HISTORIES
130      IF (KOUTDT.NE.0) NEMTH=NEMTH+1

      C LOCATION MATRIX
      C
      C DO 190 L=1,2
      LM(L)=ID(NODI,L)
135      190 LM(L*2)=ID(NODJ,L)
      CALL BAND

      C ELEMENT PROPERTIES
      C
      C XL=X(NODJ)-X(NODI)
      YL=Y(NODJ)-Y(NODI)
      FL=SQR(XL**2+YL**2)
      COSA=XL/FL
      SINA=YL/FL
      KBUCK=KBUC(IMBT)
      PSH=FTYP(IMBT,2)
      PPSH=1.-PSH
      PPSL=FTYP(IMBT,6)
      AREA=FTYP(IMBT,3)
      EALB=FTYP(IMBT,1)*FTYP(IMBT,3)*(PPSL-PSH)/FL
      SLPX=FTYP(IMBT,7)
      SEPHX=FTYP(IMBT,8)
      EALP=FTYP(IMBT,1)*PPSH*AREA/FL
      EALP=EALEP*PSH/PPSH
      PYP=AREA*FTYP(IMBT,4)*PPSH
      PYN=AREA*(-ABS(FTYP(IMBT,5)))*PPSH

      C LOADS DUE TO FIXED END FORCES
      C
      C SFEE=0.
      IF (KFOL+KFL.EQ.0) GO TO 310
      DO 200 I=1,NDOF
      DO 200 J=1,NDOF
165      200 GA(I,J)=0.
      GA(1,1)=COSA
      GA(1,2)=SINA
      GA(2,1)=-SINA
      GA(2,2)=COSA
      GA(3,3)=COSA
      GA(3,4)=SINA

170      INEL1100
      INEL1101
      INEL1102
      INEL1103
      INEL1104
      INEL1105
      INEL1106
      INEL1107
      INEL1108
      INEL1109
      INEL1110
      INEL1111
      INEL1112
      INEL1113
      INEL1114
      INEL1115
      INEL1116
      INEL1117
      INEL1118
      INEL1119
      INEL1120
      INEL1121
      INEL1122
      INEL1123
      INEL1124
      INEL1125
      INEL1126
      INEL1127
      INEL1128
      INEL1129
      INEL1130
      INEL1131
      INEL1132
      INEL1133
      INEL1134

      INEL1135
      INEL1136
      INEL1137
      INEL1138
      INEL1139
      INEL1140
      INEL1141
      INEL1142
      INEL1143
      INEL1144
      INEL1145
      INEL1146
      INEL1147
      INEL1148
      INEL1149
      INEL1150
      INEL1151
      INEL1152

```

```

175      GA(4,3)=-SINA
      GA(4,4)=COSA
      DO 210 I=1,4
      SFF(I)=0.
      210 SSFF(I)=0.
      IF (KPOL.EQ.0) GO TO 250
      DO 220 I=1,4
      220 FFEF(I)=FEF(KFLL,I)*FDL
      IF (KOFEF(KFLL).EQ.0) GO TO 230
      CALL MULT (GA,FEF,SSFF,4,4,1)
      GO TO 250
      230 DO 240 I=1,4
      240 SFF(I)=FFEF(I)
      C
      250 IF (KFLL.EQ.0) GO TO 298
      DO 260 I=1,4
      260 FFEF(I)=FEF(KFLL,I)*FLL
      IF (KOFEF(KFLL).EQ.0) GO TO 270
      CALL MULT (GA,FEF,SSFF,4,4,1)
      GO TO 290
      270 DO 280 I=1,4
      280 SSFF(I)=FFEF(I)
      C
      290 DO 300 I=1,4
      300 SSFF(I)=SSFF(I)+SFF(I)
      CALL MULT (GA,SSFF,DD,4,4,1)
      CALL SFORCE (DD)
      C
      C      INITIALIZE ELEMENT FORCE
      C
      SFEF=(SSFF(13)-SSFF(1))*0.5
      310 FF=FINIT+SFEF
      SEP=PPSH*FF
      SEL=PSH*FF
      IF (FINIT.LT.0.) GO TO 320
      SENP=FINIT
      SENN=0.
      GO TO 330
      320 SENN=FINIT
      SENP=0.
      C
      330 CALL FINISH
      C
      C      GENERATE MISSING ELEMENTS
      C
      IF (INEM.EQ.NNEM) RETURN
      INEM=INEM+1
      IF (INEM.EQ.INEL) GO TO 150
      GO TO 160
      C
      END

```

INEL1153
INEL1154
INEL1155
INEL1156
INEL1157
INEL1158
INEL1159
INEL1160
INEL1161
INEL1162
INEL1163
INEL1164
INEL1165
INEL1166
INEL1167
INEL1168
INEL1169
INEL1170
INEL1171
INEL1172
INEL1173
INEL1174
INEL1175
INEL1176
INEL1177
INEL1178
INEL1179
INEL1180
INEL1181
INEL1182
INEL1183
INEL1184
INEL1185
INEL1186
INEL1187
INEL1188
INEL1189
INEL1190
INEL1191
INEL1192
INEL1193
INEL1194
INEL1195
INEL1196
INEL1197
INEL1198
INEL1199
INEL1200
INEL1201
INEL1202
INEL1203
INEL1204

PAGE 1

79/08/22. 17.44.35

FTN 4.74470

SUBROUTINE STIF1 73/172 OPT=1

STIF1 2
STIF1 3
STIF1 4
STIF1 5
STIF1 6

SUBROUTINE STIF1 (MSTEP,NOOF,NINFC,CONS,FK,DFAC)
COMMON /INFEL/ IMEM,KST,LHIS,KGEOM,EALEP,EALE,FL,COSA,SINA,
1 KODYX,KODY,SEP,SEL,VTOT,VPACP,VPACN,VBUCK,VENP,
2 TVENP,VENN,TVENN,SEN,SENN,TSENN,SDFO,NODI,
3 NODJ,KOUTDT,KBUCK,PYP,PYN,SLPHX,SEPMX,EALEB,PPSL,
4 REST(161)

STIF1 8
STIF1 9
STIF1 10
STIF1 11
STIF1 12
STIF1 13
STIF1 14
STIF1 15
STIF1 16
STIF1 17
STIF1 18
STIF1 19
STIF1 20
STIF1 21
STIF1 22
STIF1 23
STIF1 24
STIF1 25
STIF1 26
STIF1 27
STIF1 28
STIF1 29
STIF1 30
STIF1 31
STIF1 32
STIF1 33
STIF1 34
STIF1 35
STIF1 36

COMMON/WORK/ SST(2,2),AA(2,4),AATK(4,2),FFK(4,4),W(1964)

STIF1 39
STIF1 40
STIF1 41
STIF1 42
STIF1 43
STIF1 44
STIF1 45
STIF1 46
STIF1 47
STIF1 48

DIMENSION COM(1),CONS(1),FK(4,4)
EQUIVALENCE (IMEM,COM(1))

TRUSS ELEMENT STIFFNESS FORMULATION

STIF1 39
STIF1 40
STIF1 41
STIF1 42
STIF1 43
STIF1 44
STIF1 45
STIF1 46
STIF1 47
STIF1 48

DO 10 J=3,14
10 COM(J)=CONS(J)

ELASTOPLASTIC COMPONENT, WITHOUT YIELD

STIF1 39
STIF1 40
STIF1 41
STIF1 42
STIF1 43
STIF1 44
STIF1 45
STIF1 46
STIF1 47
STIF1 48

FK(1,1)=EALP*GOSA**2
FK(1,2)=EALP*SINA*GOSA
FK(1,3)=-FK(1,1)
FK(1,4)=-FK(1,2)
FK(2,1)=EALP*SINA**2
FK(2,2)=FK(1,4)
FK(2,3)=-FK(2,2)
FK(2,4)=FK(1,1)
FK(3,1)=FK(1,1)
FK(3,4)=FK(1,2)
FK(4,1)=FK(2,2)
FK(4,4)=FK(2,2)
DO 20 I=2,4
JJ=I-1
DO 20 J=1,JJ
20 FK(I,J)=FK(J,I)

STIF1 39
STIF1 40
STIF1 41
STIF1 42
STIF1 43
STIF1 44
STIF1 45
STIF1 46
STIF1 47
STIF1 48

CHANGE SIGN IF YIELDS

STIF1 39
STIF1 40
STIF1 41
STIF1 42
STIF1 43
STIF1 44
STIF1 45
STIF1 46
STIF1 47
STIF1 48

KODZ=KODY+1
GO TO (40,25,21,23),KODZ
21 DO 22 I=1,16
22 FK(I,1)=FK(I,1)*(EALB/EALP)
GO TO 90
23 DO 24 I=1,16
24 FK(I,1)=-FK(I,1)*(EALB+EALP)/EALP
GO TO 90
25 DO 30 I=1,16
30 FK(I,1)=-FK(I,1)
GO TO 90

STIF1 39
STIF1 40
STIF1 41
STIF1 42
STIF1 43
STIF1 44
STIF1 45
STIF1 46
STIF1 47
STIF1 48

INITIAL STIFFNESS FOR STEP 0, RETA=0 ALLOWANCE FOR STEP 1

STIF1 39
STIF1 40
STIF1 41
STIF1 42
STIF1 43
STIF1 44
STIF1 45
STIF1 46
STIF1 47
STIF1 48

40 IF (MSTEP.GT.1) GO TO 90
CC=1.
IF (MSTEP.EQ.1) CC=DFAC
CC=(1.+EALP/EALP)*CC
DO 50 I=1,16

STIF1 39
STIF1 40
STIF1 41
STIF1 42
STIF1 43
STIF1 44
STIF1 45
STIF1 46
STIF1 47
STIF1 48

50

STIF1 39
STIF1 40
STIF1 41
STIF1 42
STIF1 43
STIF1 44
STIF1 45
STIF1 46
STIF1 47
STIF1 48

55


```

50 FK(I,1)=FK(I,1)*CG
C
60 C ADD GEOMETRIC STIFFNESS
C
IF (NSTEP.EQ.0.OR.KGEOM.EQ.0) GO TO 90
PFL=(CONS(15)+CONS(16))/FL
DO 60 I=1,4
60 SSI(I,1)=PFL
DO 70 I=1,8
70 AA(I,1)=0.
AA(I,1)=SINA
AA(1,2)=COSA
AA(2,3)=SINA
AA(2,4)=COSA
CALL MULT1 (AA,SSI,AAFK,FFK,4,2)
DO 80 I=1,16
80 FK(I,1)=FK(I,1)+FFK(I,1)
C
75 C 90 RETURN
END

```

CARD NR. SEVERITY DETAILS DIAGNOSIS OF PROBLEM

63 I COMS ARRAY REFERENCE OUTSIDE DIMENSION BOUNDS.
63 I COMS ARRAY REFERENCE OUTSIDE DIMENSION BOUNDS.

SYMBOLIC REFERENCE MAP (R=1)

ENTRY POINTS
3 STIF1

VARIABLES	SN	TYPE	RELOCATION	WORK
215 4 AA	REAL	ARRAY	WORK	WORK
215 0 COMS	REAL	ARRAY	F.P.	INFEL
0 0 OFAC	REAL	ARRAY	F.P.	INFEL
45 0 EALEB	REAL	INFEL	INFEL	INFEL
24 0 FFK	REAL	ARRAY	WORK	INFEL
11 0 FL	REAL	INFEL	INFEL	F.P.
0 0 IMEM	INTEGER	INFEL	INFEL	INFEL
213 6 JJ	INTEGER	INFEL	INFEL	INFEL
14 0 KGEOM	INTEGER	INFEL	INFEL	INFEL
14 0 KOBYX	INTEGER	INFEL	INFEL	INFEL
37 0 KOUTOT	INTEGER	INFEL	INFEL	INFEL
2 0 LM	INTEGER	INFEL	INFEL	INFEL
0 0 NOOF	INTEGER	INFEL	INFEL	INFEL
35 0 MODI	INTEGER	INFEL	INFEL	INFEL
216 0 PFL	REAL	INFEL	INFEL	INFEL
42 0 PYN	REAL	INFEL	INFEL	INFEL
47 0 REST	REAL	INFEL	INFEL	INFEL

```

1  SUBROUTINE RESP1 (NOOF,NINFC,KBAL,KPR,COMS,DDISM,DD,TIME,VELM,OFACRESPI
    1,DELTA)
    C
5  COMMON /INFEL/ IMEN,KST,LM(4),KGEON,EALP,EAL,FL,CBSA,SINA,
    KODYX,KODY,SEP,SEL,VTOT,VPACP,VPACK,BUCK,VENP,
    2  TVENP,VENN,TVENN,SENP,TSENP,SENN,TSENN,SFO,NODI,
    3  NODJ,KOUTOT,KBUCK,X,PYP,PYN,SLPHX,SEPHX,EALB,PPSL,
    4  REST(161)
    COMMON /WORK/ EAL,DSL,OSEP,DSML,FAC,FACTOR,DSUB,DSUB,POUT(1992)
    COMMON/THIST/ITHOUT(10),THOUT(20),ITHP,ISAVE,NELTH,NSTH,NF7,ISE
10  DIMENSION COM(1), COMS(1), DDISM(1), DD(1), VELM(1)
    EQUIVALENCE (IMEN,COM(1))
    C
15  STATE DETERMINATION FOR TRUSS ELEMENTS
    C
    DO 10 I=1,NINFC
    10 COM(I)=COMS(I)
    KODYX=KODY
    IF (IMEN.EQ.1) IMED=0
    C
20  EXTENSION INCREMENT
    C
    DV=COSA*(DDISM(3)-DDISM(1))+SINA*(DDISM(4)-DDISM(2))
    VTOT=VTOT+DV
    IFLAG=0
    IF (KODY.EQ.3) GO TO 190
    C
25  LINEAR FORCE INCREMENT
    IF ((ABS(VTOT)-LE.SLPHX).AND.(KODY.EQ.2)) GO TO 15
    IF ((ABS(VTOT)-GE.SLPHX).AND.(KODY.EQ.2)) GO TO 17
    IF ((ABS(VTOT)-LE.SLPHX) GO TO 17
    ENTERING STAGE 2.
    IFLAG=1
    IF (VTOT.LE.0.0) DV2=VTOT+SLPHX
    IF (VTOT.GE.0.0) DV2=VTOT-SLPHX
    KODY=2
    GO TO 17
    C
40  REVERSING FROM STAGE 2.
    15 IFLAG=2
    IF (VTOT.LE.0.0) DV2=VTOT+SLPHX
    IF (VTOT.GE.0.0) DV2=VTOT-SLPHX
    KODY=0
    SEP=SEP+(DV-DV2)*EALER
    17 EAL=EALP
    C
45  IF (KODY.NE.0) EAL=0.
    IF (KODY.EQ.2) EAL=EALB
    SLIN=SEP+EAL*DV
    IF (IFLAG.NE.0) SLIN=SEP+EAL*DV2
    C
50  INITIALIZE
    C
    FACAC=0.
    20 FACTOR=1.-FACAC
    C

```

RESPI 2
RESPI 3
RESPI 4
RESPI 5
RESPI 6
RESPI 7
RESPI 9
RESPI 10
RESPI 11
RESPI 12
RESPI 13
RESPI 14
RESPI 15
RESPI 16
RESPI 17
RESPI 18
RESPI 19
RESPI 20
RESPI 21
RESPI 22
RESPI 23
RESPI 24
RESPI 25
RESPI 26

RESPI 27
RESPI 28

RESPI 29
RESPI 31
RESPI 32
RESPI 33
RESPI 34
RESPI 35
RESPI 36
RESPI 37
RESPI 38

SUBROUTINE RESP1 73/172 OPT=1

C ELASTIC. GET FACTOR FOR STATUS CHANGE

IF (KODY.NE.0) GO TO 50
DSEP=EALEB*DV
IF (IFLAG.EQ.2) DSEP=EALEB*DV2

IF (IOP) 30,110,40
30 FAC=(PYN-SEP)/DSEP
IF (FAC.GE.FACTOR) GO TO 50

FACTOR=FAC
SEP=PYN

KODY=1

VBUCK=0.

GO TO 110

40 FAC=(PYP-SEP)/DSEP
IF (FAC.GE.FACTOR) GO TO 50

FACTOR=FAC
SEP=PYP

KODY=1

GO TO 110

50 SEP=SEP+FACTOR*DSEP
GO TO 110

C YIELDED OR BUCKLING, AND CONTINUING

60 IF (SEP.DV.LT.0.AND.KODY.NE.2) GO TO 80

IF (KODY.EQ.2) GO TO 75

IF (KBUCK.NE.0.AND.SEP.LT.0) GO TO 70

C UPDATE PLASTIC DEFORMATIONS

IF (KBUCK.NE.0.AND.SEP.LT.0) GO TO 70

DVP=FACTOR*DV

IF (DVP.GT.0.) VPACP=VPACP+DVP

IF (DVP.LT.0.) VPACN=VPACN+DVP

70 VBUCK=VBUCK-FACTOR*DV
GO TO 120

75 IF (IFLAG.NE.1) SEP=SEP+EALEB*DV

IF (IFLAG.EQ.1) SEP=SEP+EALEB*DV2

IF (ABS(SEP).GT.1.EPHX) GO TO 77

GO TO 120

77 KODY=3

VTOT=VTOT-DV

SLIN=SLIN-EALEB*DV

DV2=(SEP-SEPHX)/EALEB

IF (SEP.LT.0) DV2=(SEPHX/SEP)/EALEB

VTOT=VTOT+(DV-DV2)

SLIN=SLIN+EALEB*(DV-DV2)

SEP=SEP+SEPHX/ABS(SEP)

GO TO 120

C YIELDED BUT UNLOADING

80 IF (KBUCK.NE.0.AND.SEP.LT.0.) GO TO 90

KODY=0

GO TO 20

RESP1 39

RESP1 40

RESP1 41

RESP1 42

RESP1 43

RESP1 44

RESP1 45

RESP1 46

RESP1 47

RESP1 48

RESP1 49

RESP1 50

RESP1 51

RESP1 52

RESP1 53

RESP1 54

RESP1 55

RESP1 56

RESP1 57

RESP1 58

RESP1 59

RESP1 60

RESP1 61

RESP1 63

RESP1 64

RESP1 65

RESP1 66

RESP1 67

RESP1 68

RESP1 69

RESP1 70

RESP1 71

RESP1 72

RESP1 73

RESP1 74

RESP1 75

RESP1 76

RESP1 77

RESP1 78

Line	Code	Text	Response
1115	C	BUCKLING AND REVERSING	RESP1 79
	C		RESP1 80
		90 FAC=VBUCK/OV	RESP1 81
		IF (FAC.GE-FACTOR) GO TO 100	RESP1 82
		FACTOR=FAC	RESP1 83
		KODY=0	RESP1 84
120		100 VBUCK=VBUCK-FACTOR*OV	RESP1 85
	C		RESP1 86
	C	CHECK FOR COMPLETION OF CYCLE	RESP1 87
	C		RESP1 88
		110 FACAC=FACAC+FACTOR	RESP1 89
125		IF (FACAC.LT-0.9999999) GO TO 20	RESP1 90
	C		RESP1 91
	C	NEW FORCE, UNBALANCED FORCE DUE TO YIELD	RESP1 92
	C		RESP1 93
		120 SEL=SEL+EAL*OV	RESP1 94
130		SI=SEP+SEL	RESP1 95
		IF (KODY.EQ-3) SEP=0.0	
		DSUB=SLIN-SEP	
		IF (ABS(DSUB).GT-1.E-8) KRAL=1	
135	C	DEFORMATION RATE FOR DAMPING	RESP1 96
	C		RESP1 97
		IF (OFAC.EQ-0.0.AND.DELTA.EQ-0.0) GO TO 140	RESP1 98
		IF (TIME.EQ-0.) GO TO 150	RESP1 99
		KRAL=1	RESP100
		UV=COSA*(VELM(3)-VELM(1))+SINA*(VELM(4)-VELM(2))	RESP101
140	C	BETA=0 DAMPING FORCE	RESP102
	C		RESP103
		IF (OFAC.EQ-0.) GO TO 130	RESP104
		DSUB=DSUB+OFAC*(EAL+EALP)*OV	RESP105
145	C	STRUCTURAL DAMPING FORCE	RESP106
	C		RESP107
		130 IF (DELTA.EQ-0.) GO TO 140	RESP108
		DSL=DELTA*SIN(ABS(ST),OV)	RESP109
		DSUB=DSUB-DSL+SDF0	RESP110
		SDF0=DSL	RESP111
150	C	UNBALANCED LOAD VECTOR	RESP112
	C		RESP113
		140 IF (KRAL.EQ-0) GO TO 150	RESP114
		DD(3)=DSUB*COSA	RESP115
		DD(4)=DSUB*SINA	RESP116
		DD(1)=-DD(3)	RESP117
		DD(2)=-DD(4)	RESP118
155	C	ACCUMULATE ENVELOPES	RESP119
	C		RESP1120
		150 IF (SENP.GE-ST) GO TO 160	RESP1121
		SENP=ST	RESP1122
		ISENP=TIME	RESP1123
		GO TO 170	RESP1124
160		160 IF (SENN.LE-ST) GO TO 170	RESP1125
		SENN=ST	RESP1126
		ISENN=TIME	RESP1127
165	C		RESP1128
		150 IF (SENP.GE-ST) GO TO 160	RESP1129
		SENP=ST	RESP1130
		ISENP=TIME	RESP1131
		GO TO 170	RESP1132
170		160 IF (SENN.LE-ST) GO TO 170	RESP1133
		SENN=ST	RESP1134
		ISENN=TIME	RESP1135

PAGE

79/08/22. 17.44.35

FTN 4.7+470

73/172 OPT=1

SUBROUTINE RESP1

```

170 IF (VENP.GE.VTOT) GO TO 180
    VENP=VTOT
    TVENP=TIME
    GO TO 190
175
180 IF (VENN.LE.VTOT) GO TO 190
    VENN=VTOT
    TVENN=TIME
190 CONTINUE
    IF (KODY.EQ.3) ST=0.0
    PRINT TIME HISTORY
    ISAVE=0
    IF (KPR.LI.0) GO TO 200
    IF (KPR.EQ.0.OR.KOUTOT.EQ.0) GO TO 250
    IF (ITHP.GT.1) GO TO 240
    200 IF (IHED.NE.0) GO TO 220
        KKPR=IABS(KPR)
        PRINT 210, KKPR, TIME
    210 FORMAT('10H RESULTS FOR GROUP, I3, 37H, TRUSS ELEMENT OR L8B JOINTS
    1, TIME =, F4.3//5X, 5H ELE, 3X, 4H NODE, 3X, 5H YIELD, 8X, 5H AXIAL,
    2 4X, 9H TOTAL , 3X, 25H ACCUM. PLASTIC EXTENSIONS/5X,
    3 5H NO., 3X, 4H I, 3X, 4H J, 3X, 5H CODE, 8X, 5H FORCE, 4X,
    4 9H EXTENSION, 5X, 8H POSITIVE, 5X, 8H NEGATIVE//)
    IHED=1
    220 PRINT 230, IMEN, NOOI, NOOJ, KODY, ST, VTOT, VPACP, VPACH
    230 FORMAT (I9, 2I7, I8, F14.2, 3F13.5)
    C
    C
    240 IF (ITHP.LI.1.OR.KOUTOT.EQ.0) GO TO 250
        KKPR=IABS(KPR)
        ITHOUT(1)=KKPR
        ITHOUT(2)=1
        ITHOUT(3)=IMEN
        ITHOUT(4)=NOOI
        ITHOUT(5)=NOOJ
        ITHOUT(6)=KODY
        ITHOUT(11)=ST
        ITHOUT(12)=VTOT
        ITHOUT(13)=VPACP
        ITHOUT(14)=VPACH
        ITHOUT(15)=TIME
        ISAVE=1
    C
    C
    C
    SET INDICATOR FOR STIFFNESS CHANGE
    250 KST=0
    IF (KODYX.NE.KODY) KST=1
    C
    C
    C
    UPDATE INFORMATION IN COMS
    260 COMS(1)=COM(1)
    COMS(2)=COM(2)
    C
    C
    C
    RETURN
    END

```

RESP1135
RESP1136
RESP1137
RESP1138
RESP1139
RESP1140
RESP1141
RESP1142
RESP1143
RESP1144
RESP1145
RESP1146
RESP1147
RESP1148
RESP1149
RESP1150
RESP1151
RESP1152
RESP1155
RESP1156
RESP1157
RESP1158
RESP1159
RESP1160
RESP1161
RESP1162
RESP1163
RESP1164
RESP1165
RESP1166
RESP1167
RESP1168
RESP1169
RESP1170
RESP1171
RESP1172
RESP1173
RESP1174
RESP1175
RESP1176
RESP1177
RESP1178
RESP1179
RESP1180
RESP1181
RESP1182
RESP1183
RESP1184
RESP1185
RESP1186
RESP1187
RESP1188
RESP1189
RESP1190
RESP1191

PAGE 1

79/08/22. 17.44.35

FTN 4.7+470

SUBROUTINE OUT1 73/172 OPT=1

```

1      SUBROUTINE OUT1 (COMS,NINFC)
      COMMON /INFEL/ IMEM,KST,LH(4),KGEOM,EALBP,EALF,COSA,SINA,
      KODYX,KODY,SEP,SEL,VTOT,VPACP,VPACK,VBUCK,VENP,
      TVENP,VENN,TVENN,SENP,TSENP,SENN,SOF,NOODI,
      NODJ,KOUTDT,KBUCK,PYP,PYN,SLPMX,SEPMX,EALBP,PPSL,
      REST(161)
      C
      DIMENSION COM(1),COMS(1)
      EQUIVALENCE(IMEM,COM(1))
      C
      ENVELOPE OUTPUT, TRUSS ELEMENTS
      DO 10 J=1,NINFC
      10 COM(J)=COMS(J)
      C
      IF (IMEM.EQ.1) PRINT 20
      20 FORMAT(3M TRUSS ELEMENTS (TYPE 1) OR LSB JOINTS///
      5H ELEM,3X,4HNODE,3X,4HNODE,11X,20HMAXIMUM AXIAL FORCES,
      19X,18HMAXIMUM EXTENSIONS,12X,25HACCUH. PLASTIC EXTENSIONS/OUT1
      5H NO.,3X,4H I,3X,4H J,5X,7HTENSION,3X,4HTIME,
      6X,5HCOMP,3X,4HTIME,5X,8HPOSITIVE,3X,4HTIME,
      3X,8HNEGATIVE,3X,4HTIME,7X,6HPOSITIVE,5X,8HNEGATIVE/
      101X,20H(NOT FOR LSB JOINTS)/)
      C
      PRINT 30, IMEM,NOODI,SENP,TSENP,SENN,TSENN,VENP,TVENP,VENN,TVEOUT1
      1NM,VPACP,VPACK
      30 FORMAT(14,17,17,2X,2(F11.2,F7.2),2X,2(F11.5,F7.2),2X,2(F13.5)
      RETURN
      END
30      C

```

SYMBOLIC REFERENCE MAP (R=1)

ENTRY POINTS

3 OUT1

VARIABLES	SN	TYPE	RELOCATION	ARRAY	COMS	REAL	ARRAY	F.P.
8 COM	0	REAL	INFEL		0	REAL		INFEL
12 COSA	10	REAL	INFEL		10	REAL		INFEL
45 EALBP	7	REAL	INFEL		7	REAL		INFEL
11 FL	0	REAL	INFEL		0	INTEGER		INFEL
114 J	40	INTEGER	INFEL		40	INTEGER		INFEL
6 KGEOM	15	INTEGER	INFEL		15	INTEGER		INFEL
14 KODYX	37	INTEGER	INFEL		37	INTEGER		INFEL
1 KST	2	INTEGER	INFEL		2	INTEGER		INFEL
0 NINFC	35	INTEGER	F.P.		35	INTEGER		INFEL
36 NODJ	46	INTEGER	INFEL		46	REAL		INFEL
42 PYN	41	REAL	INFEL		41	REAL		INFEL
47 REST	34	REAL	INFEL	ARRAY	34	REAL		INFEL
17 SEL	32	REAL	INFEL		32	REAL		INFEL
30 SENP	16	REAL	INFEL		16	REAL		INFEL

PAGE 1

79/08/22, 17.44.35

FTN 4.7478

73/172 OPT=1

SUBROUTINE THPR1

```

1      SUBROUTINE THPR1 (NS)
      COMMON /THIST/ ITHOUT(10), THOUT(20), ITHP, ISAVE, MELTH, NSTH, NF7, ISE
      REORGANIZED TIME HISTORY OUTPUT, TRUSS ELEMENTS
      IF (NS.GT.1) GO TO 20
      PRINT 10, ITHOUT(1), ITHOUT(3)
      10 FORMAT(10I10, RESULTS FOR GROUP, I3, 29H, TRUSS ELE. DR LSB JOINT NO. I4, THPR1 11
      1 //5X, 5H TIME, 3X, 4H NODE, 3X, 4H YIELD, 8X, 5H AXIAL, 4X, THPR1 12
      2 9H TOTAL, 3X, 25H ACCUM. PLASTIC EXTENSIONS/5X, THPR1 13
      3 5H 93X, 4H I, 3X, 4H J, 3X, 5H CODE, 8X, 5H FORCE, 4X, THPR1 14
      4 9H EXTENSION, 5X, 4H POSITIVE, 5X, 8H NEGATIVE, THPR1 15
      5 63X, 28H (NOT FOR LSB JOINTS) //
      20 PRINT 30, THOUT(5), ITHOUT(1), I=4, 6), (THOUT(I), I=1, 4)
      30 FORMAT (10H, F8.3, 217, 18, F14.2, 3F13.5)
      IF (ISE.EQ.0) GO TO 40
      WRITE (NF7) THOUT(5), (ITHOUT(I), I=4, 6), (THOUT(I), I=1, 4)
      40 CONTINUE
      RETURN
      END

```

SYMBOLIC REFERENCE MAP (R=1)

ENTRY POINTS
3 THPR1

VARIABLES	SN	TYPE	RELOCATION
76 I		INTEGER	
43 ISE		INTEGER	
36 ITHP		INTEGER	
42 NF7		INTEGER	
41 NSTH		INTEGER	

FILE NAMES
- OUTPUT FMT

STATEMENT LABELS
24 10 FMT
16 48

COMMON BLOCKS
THIST

STATISTICS

PROGRAM LENGTH 778 63
CM LABELED COMMON LENGTH 448 36
520008 CM USED

37 ISAVE	INTEGER	THIST
0 ITHOUT	INTEGER <td>THIST </td>	THIST
40 MELTH	INTEGER <td>F.P. </td>	F.P.
0 NS	INTEGER <td>THIST </td>	THIST
12 THOUT	REAL <td>THIST </td>	THIST

65 30 FMT

11 20

PRINTOUT OF BEAM/COLUMN SPECIFICATIONS

ELEMENT SPECIFICATION, GROUP 2

BEAM COLUMN ELEMENTS (TYPE 2)

NO. OF ELEMENTS = 80
 NO. OF STIFFNESS TYPES = 3
 NO. OF ECCENTRICITY TYPES = 0
 NO. OF YIELD SURFACES = 3
 NO. OF FIXED END FORCE PATTERNS = 0
 NO. OF INITIAL FORCE PATTERNS = 0

STIFFNESS TYPES

TYPE NO.	YOUNG'S MODULUS	HARDENING RATIO	SECTION AREA	REFERENCE INERTIA	FLEXURAL STIFFNESS FACTORS JJ II	STIFFNESS FACTORS IJ	SHEAR AREA	POISSON RATIO
1	.2920E+08	.1000E-04	1.46	6.48	4.000	2.000	1.22	.150
2	.2920E+08	.1000E-04	10.00	10000.00	3.000	0.000	0.00	0.000
3	.2920E+08	.1000E-04	10.00	10000.00	0.000	0.000	0.00	0.000

YIELD SURFACE PROPERTIES

SURFACE NO.	SHAPE CODE	YIELD MOMENTS POSITIVE	YIELD MOMENTS NEGATIVE	YIELD FORCES COMPN	YIELD FORCES TENSION	COORDINATES OF A MOMENT	COORDINATES OF B MOMENT
1	1	1000000.00	1000000.00	0.00	0.00	0.000	0.000
2	1	1000000.00	1000000.00	0.00	0.00	0.000	0.000
3	1	1000000.00	1000000.00	0.00	0.00	0.000	0.000

ELEMENT SPECIFICATION

ELEM NO.	NODE I	NODE J	NODE DIFF	STIF TYPE	ECCY TYPE	YIELD SURFACES END I	YIELD SURFACES END J	GEOM STIF	TIME HIST	FEF PATTERNS DL LL	FEF SCALE FACTORS DL LL	INITIAL FORCES NO.	SCALE FAC.
1	3	4	4	2	0	2	2	NO	NO	0	0.00	0	0.00
2	7	8	4	2	0	2	2	NO	NO	0	0.00	0	0.00
3	11	12	4	2	0	2	2	NO	NO	0	0.00	0	0.00
4	15	16	4	2	0	2	2	NO	NO	0	0.00	0	0.00
5	19	20	4	2	0	2	2	NO	NO	0	0.00	0	0.00
6	23	24	4	2	0	2	2	NO	NO	0	0.00	0	0.00
7	27	28	4	2	0	2	2	NO	NO	0	0.00	0	0.00
8	31	32	4	2	0	2	2	NO	NO	0	0.00	0	0.00
9	35	36	4	2	0	2	2	NO	NO	0	0.00	0	0.00
10	39	40	4	2	0	2	2	NO	NO	0	0.00	0	0.00
11	43	44	4	2	0	2	2	NO	NO	0	0.00	0	0.00
12	47	48	4	2	0	2	2	NO	NO	0	0.00	0	0.00
13	51	52	4	2	0	2	2	NO	NO	0	0.00	0	0.00
14	55	56	4	2	0	2	2	NO	NO	0	0.00	0	0.00
15	59	60	4	2	0	2	2	NO	NO	0	0.00	0	0.00
16	63	64	4	2	0	2	2	NO	NO	0	0.00	0	0.00

APPENDIX A.4

INPUT DATA FOR LSB JOINT/TRUSS ELEMENT

Section E1(a), E1(c) and E1(d) remain the same as for the Truss Element of the main program. [82]

E1(b) STIFFNESS TYPES (I5, 6F10.0, 2F5.0 , I5). One card for each stiffness type.

Columns	1 - 5	Stiffness type number, in sequence beginning with 1.
	6 - 15	Young's Modulus of Elasticity. Use fictitious value for LSB joint as explained in para. 4.5.4
	16 - 25	Strain hardening modulus, as a proportion of Young's modulus. For LSB joint use a value of 0.00001 to correspond to the elasto-plastic behaviour.
	26 - 35	Average cross sectional area. Use fictitious area for LSB joint as explained in para. 4.5.4.
	36 - 45	Yield stress in tension. Use fictitious stress for LSB joint as explained in para. 4.5.4.
	46 - 55	Yield stress of elastic buckling stress in compression. For LSB joint use same value as above.
	56 - 65	Proportion of 3rd stage stiffness k_2 to initial stiffness k_0 of LSB joint. Leave blank in case the 3rd stage does not exist or Truss element.
	66 - 70	Maximum allowable slip length in joint in units of displacement. High number for Truss element.
	70 - 75	Maximum failure load of LSB joint. Use high number for Truss element.
	70 - 80	Punch 2 if element is LSB joint. Buckling code. Punch 1 if element buckles elastically in compression. Punch zero or leave blank if element yields in compression without buckling.

PRINTOUT OF LSB JOINT SPECIFICATIONS

ELEMENT SPECIFICATION, GROUP 1

TRUSS ELEMENTS (TYPE 1) OR LSB JOINTS

NO. OF ELEMENTS = 20
NO. OF STIFFNESS TYPES = 1
NO. OF F.E.F. PATTERNS = 0

LSB JOINT DATA

TYPE NO.	INITIAL STIFFNESS	STIFFNESS RATIO 1	STIFFNESS RATIO 2	SLIP LENGTH	SLIP LOAD	FAILURE LOAD
1	1200000.00	.00001	.5000000	-.00090	320.00	1200.00

ELEMENT SPECIFICATION

ELEM NO.	NODE I	NODE J	NODE DIFF	STIF TYPE	GEOM STIF	TIME HIST	FEF PATTERNS		FEF SCALE FACTORS		INITIAL FORCE
							DL	LL	DL	LL	
1	4	5	1	1	1	NO	0	0	0.00	0.00	0.00
2	6	9	1	1	1	YES	0	0	0.00	0.00	0.00
3	12	13	1	1	1	NO	0	0	0.00	0.00	0.00
4	16	17	1	1	1	NO	0	0	0.00	0.00	0.00
5	20	21	1	1	1	NO	0	0	0.00	0.00	0.00
6	24	25	1	1	1	YES	0	0	0.00	0.00	0.00
7	28	29	1	1	1	NO	0	0	0.00	0.00	0.00
8	32	33	1	1	1	NO	0	0	0.00	0.00	0.00
9	36	37	1	1	1	NO	0	0	0.00	0.00	0.00
10	40	41	1	1	1	NO	0	0	0.00	0.00	0.00
11	44	45	1	1	1	NO	0	0	0.00	0.00	0.00
12	48	49	1	1	1	NO	0	0	0.00	0.00	0.00
13	52	53	1	1	1	NO	0	0	0.00	0.00	0.00
14	56	57	1	1	1	NO	0	0	0.00	0.00	0.00
15	60	61	1	1	1	YES	0	0	0.00	0.00	0.00
16	64	65	1	1	1	NO	0	0	0.00	0.00	0.00
17	68	69	1	1	1	NO	0	0	0.00	0.00	0.00
18	72	73	1	1	1	YES	0	0	0.00	0.00	0.00
19	76	77	1	1	1	NO	0	0	0.00	0.00	0.00
20	80	81	1	1	1	YES	0	0	0.00	0.00	0.00

OUTPUT RESULTS OF LSB JOINT

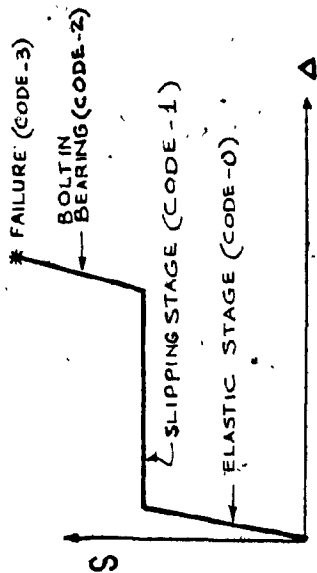
RESULTS ENVELOPES, ELEMENT GROUP 1 TIME = 9.010

TRUSS ELEMENTS (TYPE 1) OR LSB JOINTS

ELEM NO.	NODE I	NODE J	MAXIMUM AXIAL FORCES		MAXIMUM EXTENSIONS		ACCUM. PLASTIC EXTENSIONS				
			TENSION	TIME	POSITIVE	NEGATIVE	POSITIVE	NEGATIVE			
									(NOT FOR LSB JOINTS)		
1	4	5	320.00	4.35	-320.02	2.76	-.0059	4.35	-.00188	2.76	-.00464
2	8	9	320.01	4.35	-320.04	2.96	-.0080	4.35	-.00349	2.96	-.01167
3	12	13	320.01	4.36	-320.06	2.96	-.0086	4.36	-.00492	2.96	-.01382
4	16	17	320.00	1.57	-320.08	2.96	-.0042	1.57	-.00614	2.96	-.01594
5	20	21	320.00	1.58	-320.09	2.96	-.0038	1.58	-.00714	2.96	-.01651
6	24	25	320.00	1.58	-320.10	2.96	-.0033	1.58	-.00795	2.96	-.01566
7	28	29	320.00	1.58	-320.11	2.96	-.0027	1.58	-.00856	2.96	-.01354
8	32	33	319.98	2.40	-352.57	2.95	-.0023	1.14	-.00899	2.95	-.01049
9	36	37	319.97	2.41	-627.20	2.87	-.0022	1.16	-.00938	2.87	-.01247
10	40	41	319.97	4.46	-651.87	2.87	-.0022	1.17	-.00973	2.87	-.01392
11	44	45	319.98	4.46	-1006.74	2.87	-.0021	1.18	-.00997	2.87	-.01494
12	48	49	319.99	4.47	-1097.67	2.88	-.0020	1.18	-.01011	2.88	-.01560
13	52	53	320.00	4.47	-1125.51	2.88	-.0032	4.47	-.01016	2.88	-.01591
14	56	57	320.01	4.47	-1095.05	2.88	-.0070	4.47	-.01011	2.88	-.01577
15	60	61	320.01	4.47	-1014.01	2.88	-.0093	4.47	-.00990	2.88	-.01519
16	64	65	320.01	4.48	-893.41	2.88	-.0084	4.48	-.00980	2.88	-.01430
17	68	69	320.01	4.48	-748.25	2.88	-.0085	4.48	-.00957	2.88	-.01320
18	72	73	320.01	4.48	-597.97	2.88	-.0080	4.48	-.00933	2.88	-.01285
19	76	77	320.01	4.48	-466.82	2.88	-.0091	4.48	-.00913	2.88	-.01123
20	80	81	320.01	4.48	-384.07	2.88	-.0082	4.48	-.00980	2.88	-.01089

RESULTS FOR GROUP 1, TRUSS ELE. OR LSR JOINT NO: 14

TIME	NODE I	NODE J	YIELD CODE	AXIAL FORCE	TOTAL EXTENSION	ACCUM: PLASTIC EXTENSIONS POSITIVE NEGATIVE (NOT FOR LSR JOINTS)	
.020	56	57	0	.07	.00000	0.00000	0.00000
.040	56	57	0	.57	.00000	0.00000	0.00000
.060	56	57	0	1.20	.00000	0.00000	0.00000
.080	56	57	0	1.10	.00000	0.00000	0.00000
.100	56	57	0	1.20	.00000	0.00000	0.00000
.120	56	57	0	1.51	.00000	0.00000	0.00000
.140	56	57	0	1.10	.00000	0.00000	0.00000
.160	56	57	0	-.98	-.00000	0.00000	0.00000
.180	56	57	0	-4.60	-.00000	0.00000	0.00000
.200	56	57	0	-8.60	-.00001	0.00000	0.00000
.220	56	57	0	-11.33	-.00001	0.00000	0.00000
.240	56	57	0	-12.14	-.00001	0.00000	0.00000
.260	56	57	0	-12.05	-.00001	0.00000	0.00000
.280	56	57	0	-12.90	-.00001	0.00000	0.00000
.300	56	57	0	-15.33	-.00001	0.00000	0.00000
.320	56	57	0	-18.00	-.00001	0.00000	0.00000
.340	56	57	0	-20.81	-.00002	0.00000	0.00000
.360	56	57	0	-23.65	-.00002	0.00000	0.00000
.380	56	57	0	-24.92	-.00002	0.00000	0.00000
.400	56	57	0	-23.84	-.00002	0.00000	0.00000
.420	56	57	0	-22.74	-.00002	0.00000	0.00000
.440	56	57	0	-24.21	-.00002	0.00000	0.00000
.460	56	57	0	-27.55	-.00002	0.00000	0.00000
.480	56	57	0	-29.26	-.00002	0.00000	0.00000
.500	56	57	0	-26.80	-.00002	0.00000	0.00000
.520	56	57	0	-21.22	-.00002	0.00000	0.00000
.540	56	57	0	-13.93	-.00001	0.00000	0.00000
.560	56	57	0	-6.63	-.00001	0.00000	0.00000



1.880	56	57	1	-320.00	-0.0040	0.00000	-0.00015
1.900	56	57	1	-320.01	-0.00108	0.00000	-0.00083
1.920	56	57	1	-320.02	-0.00202	0.00000	-0.00177
1.940	56	57	1	-320.03	-0.00201	0.00000	-0.00256
1.960	56	57	1	-320.04	-0.00341	0.00000	-0.00316
1.980	56	57	1	-320.05	-0.00421	0.00000	-0.00396
2.000	56	57	1	-320.06	-0.00500	0.00000	-0.00483
2.020	56	57	1	-320.07	-0.00560	0.00000	-0.00543
2.040	56	57	1	-320.07	-0.00503	0.00003	-0.00550
2.060	56	57	0	-179.00	-0.00572	0.00000	-0.00550
2.080	56	57	0	-173.29	-0.00571	0.00000	-0.00550
2.100	56	57	0	-29.55	-0.00560	0.00000	-0.00550
2.120	56	57	0	121.03	-0.00548	0.00000	-0.00550
2.140	56	57	0	297.73	-0.00538	0.00000	-0.00550
2.160	56	57	1	319.93	-0.00529	0.00003	-0.00550
2.180	56	57	1	319.93	-0.00508	0.00025	-0.00550
2.200	56	57	1	319.94	-0.00475	0.00057	-0.00550
2.220	56	57	1	319.94	-0.00442	0.00091	-0.00550
2.240	56	57	1	319.95	-0.00404	0.00129	-0.00550
2.260	56	57	1	319.95	-0.00388	0.00145	-0.00550
2.280	56	57	0	272.39	-0.00392	0.00145	-0.00550
2.300	56	57	0	260.63	-0.00392	0.00145	-0.00550
2.320	56	57	0	226.72	-0.00395	0.00145	-0.00550
2.340	56	57	0	157.81	-0.00401	0.00145	-0.00550
2.360	56	57	0	85.22	-0.00406	0.00145	-0.00550
2.380	56	57	0	35.39	-0.00410	0.00145	-0.00550
2.400	56	57	0	22.84	-0.00411	0.00145	-0.00550
2.420	56	57	0	45.01	-0.00409	0.00145	-0.00550
2.440	56	57	0	120.45	-0.00404	0.00145	-0.00550
2.460	56	57	0	204.90	-0.00397	0.00145	-0.00550
2.480	56	57	0	277.60	-0.00391	0.00145	-0.00550

2.520	56	57	0	210.01	-0.0396	.00145	-0.00558
2.540	56	57	0	136.13	-0.0402	.00145	-0.00558
2.560	56	57	0	-4.63	-0.0413	.00145	-0.00558
2.580	56	57	0	-111.17	-0.0422	.00145	-0.00558
2.600	56	57	0	-174.05	-0.0427	.00145	-0.00558
2.620	56	57	0	-190.61	-0.0428	.00145	-0.00558
2.640	56	57	0	-170.46	-0.0427	.00145	-0.00558
2.660	56	57	0	-190.30	-0.0428	.00145	-0.00558
2.680	56	57	0	-267.47	-0.0434	.00145	-0.00558
2.700	56	57	1	-320.06	-0.0457	.00145	-0.00577
2.720	56	57	1	-320.06	-0.0502	.00145	-0.00622
2.740	56	57	1	-320.07	-0.0554	.00145	-0.00674
2.760	56	57	1	-320.07	-0.0607	.00145	-0.00726
2.780	56	57	1	-320.08	-0.0659	.00145	-0.00779
2.800	56	57	1	-320.09	-0.0720	.00145	-0.00840
2.820	56	57	1	-320.10	-0.0801	.00145	-0.00920
2.840	56	57	2	-522.10	-0.0912	.00145	-0.00975
2.860	56	57	2	-1044.92	-0.0993	.00145	-0.00975
2.880	56	57	2	-1159.05	-0.1011	.00145	-0.00975
2.900	56	57	2	-978.74	-0.0983	.00145	-0.00975
2.920	56	57	2	-779.03	-0.0952	.00145	-0.00975
2.940	56	57	2	-704.54	-0.0940	.00145	-0.00975
2.960	56	57	2	-610.10	-0.0925	.00145	-0.00975
2.980	56	57	2	-490.32	-0.0907	.00145	-0.00975
3.000	56	57	2	-414.95	-0.0895	.00145	-0.00975
3.020	56	57	2	-346.79	-0.0884	.00145	-0.00975
3.040	56	57	0	-274.03	-0.0876	.00145	-0.00975
3.060	56	57	0	-243.69	-0.0874	.00145	-0.00975
3.080	56	57	0	-195.13	-0.0870	.00145	-0.00975
3.100	56	57	0	-124.65	-0.0865	.00145	-0.00975
3.120	56	57	0	-54.72	-0.0859	.00145	-0.00975

3.803	56	57	0	-181.23	.00665	.01679	-.0075
3.820	56	57	0	-200.76	.00664	.01679	-.00575
3.840	56	57	0	-206.69	.00663	.01679	-.00575
3.860	56	57	0	-221.07	.00662	.01679	-.00575
3.880	56	57	0	-272.90	.00658	.01679	-.00575
3.900	56	57	1	-319.91	.00652	.01679	-.00570
3.920	56	57	1	-319.91	.00645	.01679	-.00504
3.940	56	57	1	-319.91	.00642	.01679	-.00587
3.960	56	57	0	-319.89	.00642	.01679	-.00508
3.980	56	57	0	-306.24	.00643	.01679	-.00508
4.000	56	57	0	-270.27	.00646	.01679	-.00508
4.020	56	57	0	-214.60	.00650	.01679	-.00508
4.040	56	57	0	-150.52	.00655	.01679	-.00508
4.060	56	57	0	-93.75	.00659	.01679	-.00508
4.080	56	57	0	-56.84	.00662	.01679	-.00508
4.100	56	57	0	-30.13	.00664	.01679	-.00508
4.120	56	57	0	-27.67	.00665	.01679	-.00508
4.140	56	57	0	-19.20	.00665	.01679	-.00508
4.160	56	57	0	-11.12	.00666	.01679	-.00508
4.180	56	57	0	-.80	.00667	.01679	-.00508
4.200	56	57	0	15.50	.00668	.01679	-.00508
4.220	56	57	0	44.34	.00670	.01679	-.00508
4.240	56	57	0	86.14	.00673	.01679	-.00508
4.260	56	57	0	129.50	.00677	.01679	-.00508
4.280	56	57	0	202.55	.00683	.01679	-.00508
4.300	56	57	1	320.09	.00697	.01684	-.00508
4.320	56	57	1	320.09	.00724	.01712	-.00508
4.340	56	57	1	320.09	.00762	.01749	-.00508
4.360	56	57	1	320.10	.00806	.01793	-.00508
4.380	56	57	1	320.11	.00855	.01842	-.00508
4.400	56	57	2	548.45	.00916	.01942	-.00508

4.440	56	57	3	0.00	.01446	.01842	-.00388
4.460	56	57	3	0.00	.03272	.01842	-.00388
4.480	56	57	3	0.00	.05215	.01842	-.00388
4.500	56	57	3	0.00	.05751	.01842	-.00388
4.520	56	57	3	0.00	.05211	.01842	-.00388
4.540	56	57	3	0.00	.04853	.01842	-.00388
4.560	56	57	3	0.00	.05188	.01842	-.00388
4.580	56	57	3	0.00	.05792	.01842	-.00388
4.600	56	57	3	0.00	.06062	.01842	-.00388
4.620	56	57	3	0.00	.05911	.01842	-.00388
4.640	56	57	3	0.00	.05663	.01842	-.00388
4.660	56	57	3	0.00	.05567	.01842	-.00388
4.680	56	57	3	0.00	.05604	.01842	-.00388
4.700	56	57	3	0.00	.05637	.01842	-.00388
4.720	56	57	3	0.00	.05629	.01842	-.00388
4.740	56	57	3	0.00	.05676	.01842	-.00388
4.760	56	57	3	0.00	.05843	.01842	-.00388
4.780	56	57	3	0.00	.06128	.01842	-.00388
4.800	56	57	3	0.00	.06478	.01842	-.00388
4.820	56	57	3	0.00	.06860	.01842	-.00388
4.840	56	57	3	0.00	.07271	.01842	-.00388
4.860	56	57	3	0.00	.07692	.01842	-.00388
4.880	56	57	3	0.00	.08110	.01842	-.00388
4.900	56	57	3	0.00	.08507	.01842	-.00388
4.920	56	57	3	0.00	.08872	.01842	-.00388
4.940	56	57	3	0.00	.09205	.01842	-.00388
4.960	56	57	3	0.00	.09512	.01842	-.00388
4.980	56	57	3	0.00	.09797	.01842	-.00388
5.000	56	57	3	0.00	.10067	.01842	-.00388
5.020	56	57	3	0.00	.10322	.01842	-.00388
5.040	56	57	3	0.00	.10565	.01842	-.00388

APPENDIX A.7

QUASI-STATIC ANALYSIS FOR SEISMIC FORCES

a) 10 Story Building

Seismic Force, $V = \text{ASKIFW}$

where $A = 0.08$ for seismic zone 3 for a probability of 1 in 100 years.

$$K = 1, I = 1, F = 1$$

$$T = \frac{0.09h_n}{\sqrt{D}} = \frac{0.09 \times 2.65 \times 10}{\sqrt{14.6}}$$

$$= 0.62 \text{ seconds}$$

$$S = \frac{0.5}{T^{1/3}} = \frac{0.5}{0.62^{1/3}} = 0.58636$$

$$W = 128 \times 9.8 \times 10 = 12500 \text{ kN.}$$

$$\text{Base shear, } V_{\max} = 0.08 \times 0.58636 \times 1 \times 1 \times 1 \times 12500 = 584 \text{ kN}$$

Since $H/D < 3$, no additional forces are induced at the top. The inertial forces are triangular in shape and is maximum at the base.

$$F_x = V_{\max} \left[\frac{(w_x \cdot h_x)}{\sum w_i h_i} \right]$$

QUASI-STATIC SEISMIC FORCES-10 STORY BUILDING

Floor	h_x (m)	w_x (kN)	$h_x \cdot w_x$ (kN.M)	$F_x = \frac{V_{max} h_x w_x}{\sum w_i h_i}$	$V = \sum F_x$ (shear above) (kN)
10	26.50	1245	32,992.50	106.18	0
9	23.85	1245	29,693.25	95.56	106.18
8	21.2	1245	26,394.00	84.94	201.74
7	18.55	1245	23,094.75	74.33	286.68
6	15.90	1245	19,795.50	63.71	361.01
5	13.25	1245	16,496.25	53.09	424.72
4	10.60	1245	13,197.00	42.47	477.81
3	7.95	1245	9,897.75	31.85	520.28
2	5.30	1245	6,598.50	21.24	552.13
1	2.65	1245	3,299.25	10.62	573.37
0	0	--	--	0	584.00

Σ 12450 181,458.75

b) 15 Story Building

$$T = \frac{0.09 \times 2.65 \times 15}{\sqrt{14.6}} = 0.931 \text{ seconds}$$

$$S = \frac{0.5}{T^{1/3}} = \frac{0.5}{0.931^{1/3}} = 0.512$$

$$W = 128 \times 9.8 \times 15 = 18750 \text{ kN}$$

$$\text{Base shear, } V_{\max} = 0.08 \times 0.512 \times 1 \times 1 \times 1 \times 18750 = 765 \text{ kN}$$

$$\text{Since } H/D = \frac{15 \times 2.65}{14.6} < 3, \text{ no additional whipping forces are}$$

induced at the top, i.e. $F_t = 0$.

F_x are in triangular shape having the apex at the base.

$$F_x = V_{\max} \frac{w_x \cdot h_x}{\sum_{i=1}^{i=n} w_i \cdot h_i}$$

$$\sum_{i=1}^{i=15} w_i \cdot h_i = 120 \times 1245 \times 2.65 = 395,910 \text{ kN}$$

$$F_{x=15\text{th floor}} = 765 \frac{(1245 \times 15 \times 2.65)}{395,910} = 95.62 \text{ kN}$$

QUASI-STATIC SEISMIC FORCES 15 STORY WALL

Floor	w_x (kN)	h_x (m)	F_x (kN)	$V_x = \Sigma F_x$ (kN)
15	1245	2.65	95.62	0
14	1245	2.65	89.25	95.62
13	1245	2.65	82.87	184.86
12	1245	2.65	76.50	267.74
11	1245	2.65	70.12	344.24
10	1245	2.65	63.75	414.36
9	1245	2.65	57.37	478.11
8	1245	2.65	51.00	535.48
7	1245	2.65	44.62	586.48
6	1245	2.65	38.25	631.10
5	1245	2.65	31.87	669.35
4	1245	2.65	25.50	701.22
3	1245	2.65	19.12	726.72
2	1245	2.65	12.75	745.84
1	1245	2.65	6.37	758.59
0	0	0	0	765.00

APPENDIX B.1

MAGNIFICATION FACTOR FOR WORK CAPACITY
OF A STORY IN RESERVE ENERGY TECHNIQUE

Lateral deformation of a wall due to shear at the top edge is:

$$\Delta_1 = \frac{1.2 Vh}{AG} + \frac{Vh^3}{3EI} \quad (B 1.1)$$

If a moment M is applied at top edge, additional deflection is:

$$\Delta_{11} = \frac{Mh^2}{2EI} \quad (B 1.2)$$

Hence total deflection is:

$$\Delta = \Delta_1 + \Delta_{11} \quad (B 1.3)$$

Total Energy in the system is:

$$U = \frac{1.2 V^2 h}{2AG} + \frac{(Vh + M)^2 h}{EI} \quad (B 1.4)$$

Substituting $G = 0.4E$ and $I = \frac{Ab^2}{12}$, we get

$$U = \frac{1.5 V^2 h}{2AE} + \frac{3 V^2 h^3}{AEb^2} + \frac{12 M^2 h}{AEb^2} + \frac{12 MVh^2}{AEb^2} \quad (B 1.5)$$

Work capacity of story W, as calculated from diagram of story shear plotted against total deformation:

$$W = \frac{V}{2} \left(\frac{1.2 Vh}{AG} + \frac{Vh^3}{3EI} + \frac{Mh^2}{2EI} \right) \quad (B 1.6)$$

Substituting $G = 0.4E$ and $I = \frac{Ab^2}{12}$, we get

$$W = \frac{1.5 V^2 h}{AE} + \frac{3 V^2 h^3}{AEb^2} + \frac{3 MVh^2}{AEb^2} \quad (B 1.7)$$

Magnification factor, $MF = \frac{V}{W}$

$$\begin{aligned} MF &= \frac{\frac{1.5V^2h}{2AE} + \frac{3V^2h^3}{AEb^2} + \frac{12M^2h}{AEb^2} + \frac{12MVh^2}{AEb^2}}{\frac{1.5V^2h}{AE} + \frac{3V^2h^3}{AEb^2} + \frac{3MVh^2}{AEb^2}} \\ &= 1 + \frac{V^2h^2 + 12M^2 + 9VMh}{1.5V^2b^2 + 2V^2h^2 + 3VMh} \quad (B 1.8) \end{aligned}$$

Hence the area of the load-deformation diagram when multiplied by the magnification factor will give the true work capacity of the story.

APPENDIX B.2

MEMBER STIFFNESS MATRICES

a) Column $[S_c]$

$$[S_c] = \begin{bmatrix} \frac{EA}{h} & 0 & 0 & 0 & 0 & 0 \\ 0 & \frac{12EI}{h^3(1+\phi)} & \frac{6EI}{h^2(1+\phi)} & 0 & -\frac{12EI}{h^3(1+\phi)} & \frac{6EI}{h^2(1+\phi)} \\ 0 & \frac{6EI}{h^2(1+\phi)} & \frac{(4+\phi)EI}{h(1+\phi)} & 0 & -\frac{6EI}{h^2(1+\phi)} & \frac{(2+\phi)EI}{h(1+\phi)} \\ -\frac{EA}{h} & 0 & 0 & \frac{EA}{h} & 0 & 0 \\ 0 & -\frac{12EI}{h^3(1+\phi)} & -\frac{6EI}{h^2(1+\phi)} & 0 & \frac{12EI}{h^3(1+\phi)} & -\frac{6EI}{h^2(1+\phi)} \\ 0 & \frac{6EI}{h^2(1+\phi)} & \frac{(2-\phi)EI}{h(1+\phi)} & 0 & -\frac{6EI}{h^2(1+\phi)} & \frac{(4+\phi)EI}{h(1+\phi)} \end{bmatrix} \quad \text{(Symmetric)}$$

where $\phi = \frac{12EI}{GA_s h^2}$, where A_s is effective shear area = $\frac{A}{1.2}$

b) Stiffness Matrix of Equivalent Beam $[S_b]$

This can be expressed as

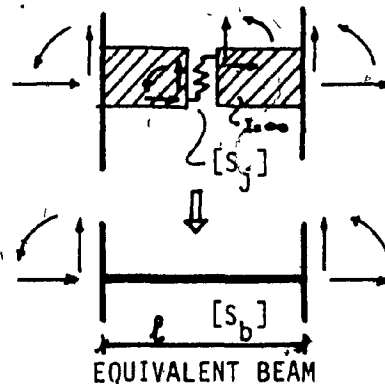
$$[S_b] = [H]^T [S_j] [H]$$

where $[H]$ is transformation matrix and

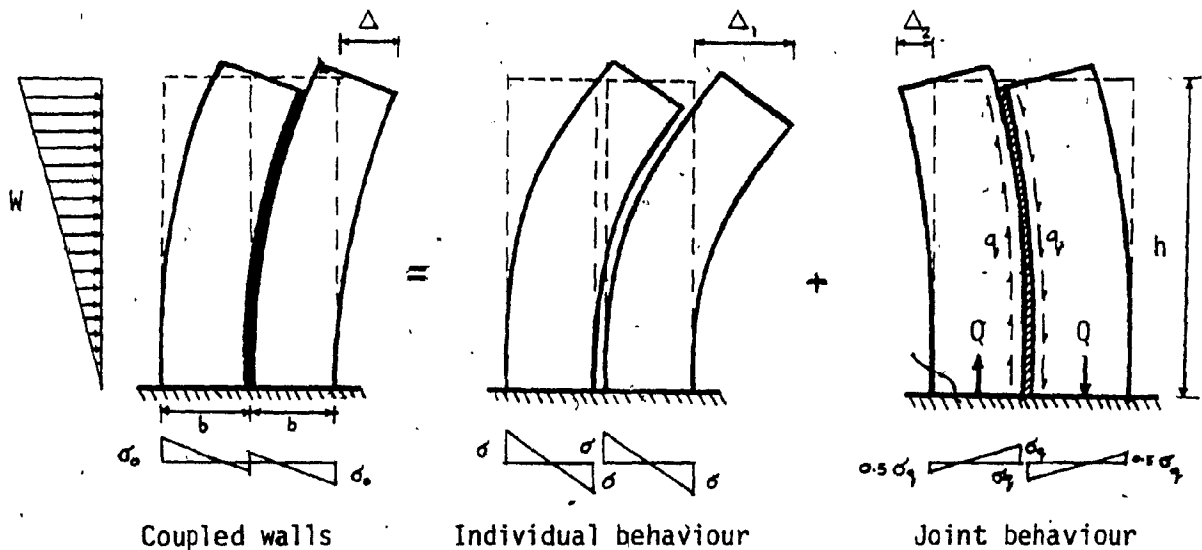
$[S_j]$ is joint stiffness matrix

where

$$[H] = \begin{bmatrix} 1 & 0 & 0 & 1 & 0 & 0 \\ 0 & 1 & l/2 & 0 & 0 & 0 \\ 0 & 0 & 1 & 0 & 0 & 0 \\ 1 & 0 & 0 & 0 & 0 & 0 \\ 0 & 0 & 0 & 0 & 1 & -l/2 \\ 0 & 0 & 0 & 0 & 0 & 1 \end{bmatrix} \quad \text{and } [S_j] = \begin{bmatrix} 0 & 0 & 0 & 0 & 0 & 0 \\ 0 & k & 0 & 0 & -k & 0 \\ 0 & 0 & 0 & 0 & 0 & 0 \\ 0 & 0 & 0 & 0 & 0 & 0 \\ 0 & -k & 0 & 0 & k & 0 \\ 0 & 0 & 0 & 0 & 0 & 0 \end{bmatrix}$$



EQUIVALENT DUCTILITY OF LSB JOINTED WALLS



a) Maximum Deflection for Maximum Permissible Stress at Base

i) Due to individual behaviour

$$\text{Maximum bending stress, } \sigma = W_a \cdot \frac{2h}{3} \cdot \frac{6}{2b^2t}$$

$$= \frac{2W_a h}{b^2t}$$

$$W_a = 0.5b^2t \sigma / h \quad (\text{B 3.1})$$

$$\text{Deflection due to bending, } \Delta_{a1} = \frac{0.183 W_a h^3}{EI_a} \quad (\text{B 3.2})$$

$$= \frac{0.183 \times 0.5b^2t\sigma h^3}{E \cdot h} \cdot \frac{12}{2b^3t}$$

$$= \frac{0.55\sigma h^2}{bE} \quad (\text{B 3.3})$$

ii) Due to Joint Forces

The joint exerts a moment equal to $\frac{Qb}{2}$ and axial force Q on each panel resulting in stresses of $\frac{\sigma_q}{2}$ and σ_q at the panel edges.

$$\text{Negative deflection, } \Delta_{a2} = \frac{0.5\sigma_q h^2}{bE} \quad (B 3.4)$$

Now knowing that $\sigma_o = \sigma - 0.5\sigma_q$

and $\sigma_q = 4\sigma_t$ where $\sigma_t = 0.15\sigma_o$, we get

$$\left. \begin{aligned} \sigma_q &= 0.60\sigma_o \\ \text{and } \sigma &= 1.30\sigma_o \end{aligned} \right\} \quad (B 3.5)$$

iii) Total deflection $\Delta_a = \Delta_{a1} - \Delta_{a2} \quad (B 3.6)$

$$\begin{aligned} &= \frac{0.55 \times 1.30 \sigma_o h^2}{bE} - \frac{0.5 \times 0.15 \sigma_o h^2}{bE} \\ &= \frac{0.41 \sigma_o h^2}{bE} \quad (B 3.7) \end{aligned}$$

b) Deflection at Top on the First Slip of a Joint

Assuming that the first joint to slip is at a height of about $h/4$ from the bottom, then

$$q = \frac{15}{16} \times \frac{1.5 W_b}{2b} = \frac{0.7 W_b}{b} \quad (B 3.8)$$

$$\therefore W_b = \frac{qb}{0.7}$$

Since $q = \sigma_t bt/h$ where $\sigma_t = 0.15\sigma_o$, we get

$$W_b = 0.214 \sigma_o b^2 t / h \quad (B 3.9)$$

In this stage the behaviour of the two walls is assumed monolithic,
then

$$\Delta_b = \frac{0.183 W_b h^3}{EI_b}$$

$$= \frac{0.183 \times 0.214 \sigma_o b^2 t h^2 \times 12}{E 8 b^3 t} \quad (B 3.10)$$

$$= \frac{0.059 \sigma_o h^2}{bE} \quad (B 3.11)$$

c) Deflection of Building on the last slip of joint

Assuming that no differential movement has taken place at
the top of wall, then

$$\frac{1}{2} \cdot \frac{W_c h^2}{EI} \cdot \frac{b}{2} - \frac{qhb}{4} \cdot \frac{bh}{2I} - \frac{qh^2}{2btE} = 0 \quad (B 3.12)$$

$$W_c = 2.66 \sigma_o b^2 t / h \quad (B 3.13)$$

$$\text{Deflection, } \Delta_c = \frac{0.183 W_c h^3}{2EI} - \frac{2 \sigma_t h^2}{bE} \quad (B 3.14)$$

$$= \frac{0.138 \sigma_o h^2}{bE} \quad (B 3.15)$$

d) Deflection at top when approximately half the joints slip

$$\Delta_d = \frac{1}{2} (\Delta_b + \Delta_c)$$

$$= \frac{0.0985 \sigma_o h^2}{bE} \quad (B 3.16)$$

e) Ductility Ratio, μ

$$= \frac{\Delta_a}{\Delta_d} = \frac{0.41 \sigma_o h^2}{bE} \cdot \frac{bE}{0.0985 \sigma_o h^2} \quad (B 3.17)$$

$$= 4.1, \text{ say } 4$$